METAL CATALYZED FORMATION OF ALIPHATIC POLYCARBONATES INVOLVING OXETANES AND CARBON DIOXIDE AS MONOMERS

A Dissertation

by

ADRIANA INEZ MONCADA

Submitted to the Office of Graduate Studies of
Texas A&M University
in partial fulfillment of the requirements for the degree of

DOCTOR OF PHILOSOPHY

May 2010

Major Subject: Chemistry

METAL CATALYZED FORMATION OF ALIPHATIC POLYCARBONATES INVOLVING OXETANES AND CARBON DIOXIDE AS MONOMERS

A Dissertation

by

ADRIANA INEZ MONCADA

Submitted to the Office of Graduate Studies of
Texas A&M University
in partial fulfillment of the requirements for the degree of

DOCTOR OF PHILOSOPHY

Approved by:

Chair of Committee,	Donald J. Darensbourg
Committee Members,	Michael B. Hall
	Timothy R. Hughbanks
	Hong Liang
Head of Department,	David H. Russell

May 2010

Major Subject: Chemistry

ABSTRACT

Metal Catalyzed Formation of Aliphatic Polycarbonates Involving Oxetanes and Carbon Dioxide as Monomers. (May 2010)

Adriana Inez Moncada, B.S., La Universidad del Zulia;

M.S., Oklahoma State University

Chair of Advisory Committee: Dr. Donald J. Darensbourg

Biodegradable aliphatic polycarbonates are important components of non-toxic thermoplastic elastomers, which have a variety of medical applications. Industrially, aliphatic polycarbonates derived from six-membered cyclic carbonates such as trimethylene carbonate (TMC or 1,3-dioxan-2-one) are produced via ring-opening polymerization (ROP) processes in the presence of a tin catalyst. It is worth mentioning that TMC is readily obtained by transesterification of 1,3-propanediol with various reagents including phosgene and its derivatives. Therefore, it has been of great interest to investigate greener routes for the production of this important class of polymers. Toward this goal, the synthesis of aliphatic polycarbonates via the metal catalyzed alternative coupling of oxetanes and carbon dioxide represents an attractive alternative. The use of an abundant, inexpensive, non-toxic, and biorenewable resource, *carbon dioxide,* makes this method very valuable. Furthermore, in this reaction, the six-membered cyclic carbonate byproduct, TMC, can also be ring-opened and transformed into the same polycarbonate. For over a decade, the Darensbourg research group has

successfully utilized metal salen complexes as catalysts for the epoxide/CO_2 copolymerization process. Hence, this dissertation focuses on the examination of these complexes as catalysts for the oxetane/CO_2 copolymerization reaction and the further elucidation of its mechanism.

Chromium(III) salen derivatives in the presence of an azide ion initiator were determined to be very effective catalysts for the coupling of oxetanes and carbon dioxide providing polycarbonates with minimal amounts of ether linkages. Kinetic and mechanistic investigations performed on this process suggested that copolymer formation proceeded by two routes. These are the direct enchainment of oxetane and CO_2, and the intermediacy of trimethylene carbonate, which was observed as a minor product of the coupling reaction. Anion initiators which are good leaving groups, e.g. bromide and iodide, are effective at affording TMC, and hence, more polycarbonate can be formed by the ROP of preformed trimethylene carbonate. Research efforts at tuning the selectivity of the oxetane/CO_2 coupling process for TMC and/or polycarbonate produced from the homopolymerization of preformed TMC have been performed using cobalt(II) salen derivatives along with anion initiators. Lastly, investigations of this process involving 3-methoxy-methyl-3-methyloxetane will be presented.

DEDICATION

I dedicate this dissertation to my mother and father, Emelida and Diego, and to my husband, Manuel. Mom and Dad, your love, guidance, unconditional support in everything I do, and your prayers have given me the strength needed to be where I am today reaching my goals and dreams. Manuel, you are an essential ingredient of my life. You are my love, my support, and my encouragement always. I love you all very much. I also dedicate this dissertation to my Lord Jesus Christ for always being by my side, giving me so much love, the strength, directions, and spiritual peace to accomplish what I have thus far in my life.

ACKNOWLEDGEMENTS

I first would like to thank my research advisor, Prof. Donald J. Darensbourg, for giving me the great opportunity and pleasure to work in his research laboratory. He is an excellent scientist, a great advisor and person. His guidance, support, and encouragement were very valuable during my graduate studies at Texas A&M University. He has contributed in many ways to my science career. More importantly, I have learned how to independently conduct scientific research and how to write up my research results and present them to other people. I would like to thank Professors Timothy R. Hughbanks, Michael B. Hall, Hong Liang, and Marcetta Y. Darensbourg for also being involved in my education, for their guidance and assistance when needed, and for serving on my dissertation committee. The Women in Science and Engineering and the Society of Plastics Engineers Organizations student chapters at Texas A&M University have influenced me in many ways to further develop my leadership and organizational skills. My sincere thanks also go to my undergraduate advisor Prof. Dora M. Finol who let me experience for the first time the conduction of scientific research. This knowledge was very precious and inspired me to look forward to a career in science. I also must thank my M.S advisor, Prof. Legrande M. Slaughter, who introduced me to the theory of organometallic chemistry of the transition metals and who has always supported and mentored me throughout the years.

I gratefully acknowledge the financial support of the research presented in this dissertation from the National Science Foundation (CHE-0543133) and the Robert A.

Welch Foundation (A-0923). I also would like to thank Dr. Joseph H. Reibenspies and Dr. Nattamai Bhuvanesh for their invaluable teachings on X-ray Crystallography and for their assistance in solving very complicated X-ray crystal structures. Thanks to Dr. Joseph H. Reibenspies who solved and finished material for publication for the crystal structures of complexes **II-5**, **II-6, III-7**, **VI-1**, and trimethylene carbonate presented in this dissertation.

My most sincere and special thanks should go to my friends Dr. Wonsook Choi, Osit "Pop" Karroonnirun, Roxanne Jenkins, and Dr. Elky Almaraz for the beautiful friendship that we have had and, I hope, will always keep through the years and for the countless times that we had discussions about our research. I want to also thank you all for celebrating many special occasions with me and my family and for letting me take part in many of yours with your families. I must also thank my other fellow members of the DJD and MJD research groups for their friendship and assistance in the lab: Dr. Eric Frantz, Dr. Shawn Fitch, Dr. Jeremy Andreatta, Dr. Liu Tianbiao, Dr. Kayla Green, Dr. Christine Thomas, Dr. Chung-Hung Hsieh, Susan Winters, Ethel Mejías, Ross Poland, Sheng Hsuan Wei, Stephanie Wilson, Bin Li, Scott Brothers, Mike Singleton, Tiffany Pinder, Jennifer Hess, William Foley, Jason Denny, and Ryan Bethel. Special thanks also go to three undergraduate students who worked with me at different stages of this journey: Curtis Boyd, Leah Salganik, and Viviana Salon.

With my Venezuelan background I have always been interested in diversity, and what I mean by that is meeting people from other countries and learning about their different cultures. This is something that I had the pleasure to experience in the DJD

group. I am so thankful to have met and worked with many Postdoctoral Fellows and visiting scholars from Brazil, Turkey, Hungary, China, and Italy: Dr. Carla Rodarte de Maura, Dr. Adolfo Horn Jr, Dr. Mamut Ulusoy, Dr. Attila, Dr. Xiao-Bing Lu, and Paolo Bottarelli.

Finally, I would like to thank my family: my Mom and Dad, Emelida and Diego, for their love, unconditional support, encouragement, and for their direction and teachings throughout my life; my sister and brother in law, Gloria and Dale, for their love, support, and for helping me proofread a lot of my letters, resumes, and CVs; my brother, Alejandro, for his love and unconditional support; my nephew, Lucas Daniel, for bringing so much happiness to my life and to all my family. From the bottom of my heart I want to thank my husband, Manuel, for being my strongest support, my love, my encouragement in many difficult and stressful times, for always being there for me, for believing in me, and for giving me the biggest happiness anyone could ever imagine. Thank you very much for being the most important part of my life; I love you so much. I also want to thank my political family for their support, love, and encouragement during this journey: my parents-in-law, Jose Prado "Chalo" and Nelly Prado; my brothers-in-law; Jose Prado "Chalingo," Chris Cooper, Rafael Suárez, and Carlos Luis Sánchez; my sisters-in-law; Mónica Prado, Diana Prado, Alicia Prado, and Mónica Carbonell; and my nephews and niece, José Rafael Suárez, José Miguel Prado, José Alonso Suárez, Victor Gonzalo Cooper, Luis Alejandro Sánchez, and Stephanie Prado.

TABLE OF CONTENTS

CHAPTER Page

LIST OF FIGURES

FIGURE Page

FIGURE Page

FIGURE Page

FIGURE Page

FIGURE Page

FIGURE Page

FIGURE Page

LIST OF TABLES

TABLE Page

CHAPTER I

INTRODUCTION

Utilization of Carbon Dioxide as a C1 Feedstock

The utilization of renewable resources is an important requirement for a sustainable society. One easily available example of a renewable resource is carbon dioxide (CO_2) (**Scheme I-1**), which has the advantages of being abundant, non-toxic, non-corrosive, non-flammable, inexpensive, and has an easily reachable supercritical point.[1] The critical point of carbon dioxide lies at 31.1ºC and 72.9 atm, where it behaves as a supercritical fluid.[2] Carbon dioxide has found uses as a fluid in refrigerators, dry-cleaning, air conditioners, fire-extinguishers, separation techniques, water treatments, and in the agro- and food-industries.[3] Recently, carbon dioxide also known as a greenhouse gas, has been receiving much attention from the scientific community as its atmospheric concentrations are rising, and the approaching threat of global warming.[3,4] For these reasons, there has been a great interest from multinational research laboratories in utilizing CO_2 for a variety of applications. However, few industrial processes utilize CO_2 as a raw chemical. This is in part due to the stability of carbon dioxide, which is in the most oxidized state of carbon, and hence, in a low energy level. In other words, in other to activate CO_2 a large energy input is required.[1]

This dissertation follows the style of *Journal of the American Chemical Society*.

Four ways to transform CO_2 into useful chemicals have been reported in the literature and these are:[1]

i) To use high-energy starting chemicals, e.g., hydrogen, unsaturated compounds such as acetylene and dienes, small-membered ring compounds such as epoxides and oxetanes, and organometallics.

ii) To shift the equilibrium of the reaction to the product side by removing a particular compound from the reaction mixture.

iii) To supply physical energy such as light or electricity.

iv) To choose oxidized low-energy synthetic targets such as organic carbonates.

Scheme I-1. CO_2 as a C1 Feedstock. Adapted From Reference 1.

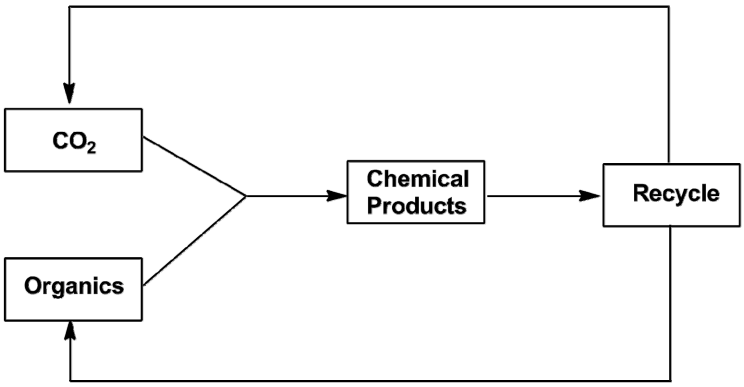

A significant amount of research has been devoted to the incorporation of CO_2 into organic molecules.[1, 3,4] For example, the synthesis of carboxylated products such as acids, esters, lactones, carbamates, and isocyanates, cyclic and linear carbonates, and

polycarbonates. One particular process that this dissertation will focus on is the production of useful polycarbonates obtained from renewable carbon dioxide and small-membered ring-compounds, oxetanes.

Industrial Route to Polycarbonates

Polycarbonates are a class of engineering thermoplastics of high quality with a unique combination of outstanding properties including strength, lightness, durability, high transparency, thermal stability, and good electrical insulation. Because of these excellent properties, polycarbonates are currently used in a variety of applications providing a wide range of benefits to consumers.[5,6] These can be found in numerous everyday products such as CDs, DVDs, cell phones, automotive interiors, plastic water bottles, food storage containers, household appliances, electronics, and optical instruments among others. Another important application of polycarbonates exists in biomedical areas due to their stability and biological inertness. Polycarbonates are both environmentally friendly and readily degradable.

The current industrial route for the production of polycarbonates involves the polycondensation of phosgene and diols (Bisphenol A in case of General Electric Lexan®) (**Scheme I-2A**). However, phosgene is highly toxic, large amounts of organic solvents are required for this process, and thus, a costly cleanup.[5,6] Another industrial route to polycarbonates involves the melt polymerization of diphenyl carbonate and diols such as Bisphenol A (**Scheme I-2B**). This process requires very high temperatures (180-300°C) in comparison with 40°C for the polycondensation process, which results in an increase in the probability of side reactions, along with the difficulty of removing phenol

byproduct completely. In addition, diphenyl carbonate is normally synthesized from highly toxic phosgene.[5,6] Hence, it has been of great importance to investigate alternative routes for the production of this important class of thermoplastics. Furthermore, understanding of the mechanistic aspects of such processes could greatly assist in improving the methodology employed for the production of these polymeric materials.

Scheme I-2. Industrial Routes to Polycarbonates[5,6]

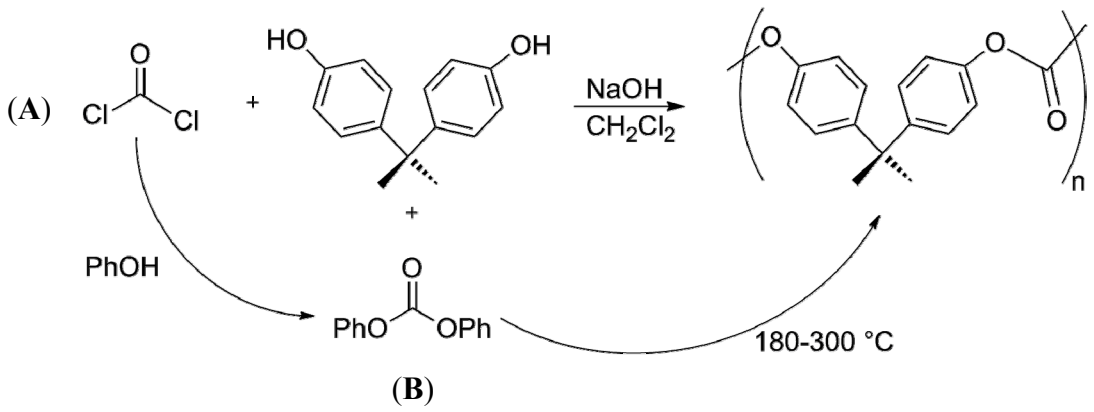

Polycarbonates from Epoxides and Carbon Dioxide

In 1969, Inoue and coworkers were the first to report a more environmentally benign route for the production of polycarbonates, which involved the copolymerization of carbon dioxide and epoxides in the presence of a heterogeneous catalyst made from the mixture of diethyl zinc and water.[7] This copolymerization process is illustrated in

eq. I-1, and in general, is accompanied by varying amounts of both ether linkages and the thermodynamically stable five-membered cyclic carbonate byproduct. Ether linkages have been shown to alter the thermal and physical properties of the polymers, and are the result of consecutive epoxide ring-opening by the catalyst. Additionally, five-membered cyclic carbonates are observable byproducts in these reactions, which are formed via a backbiting mechanism, thus shortening the polymer chain by one unit each occurrence. Cyclohexene oxide (CHO) and propylene oxide (PO) are the most widely utilized monomers to date with other epoxides investigated more sparingly.

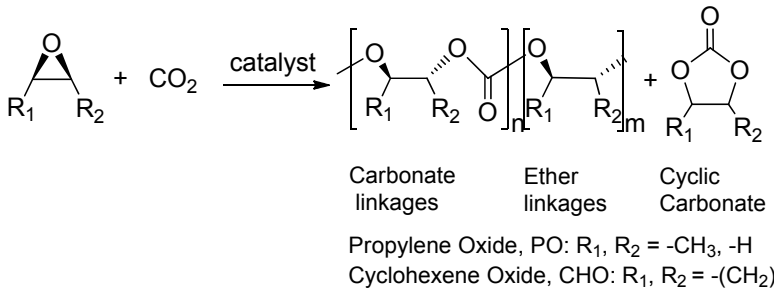

(I-1)

Subsequent to Inoue's early discovery significant advances have been made from multinational research programs in the design of a wide variety of well-defined metal catalysts for this important transformation.[8] Among the most effective, and importantly most robust, catalysts for these processes involve metal(III) salen complexes (where M = Cr, Co, or Al).[8a, b, 8f] These studies have led to greatly improved catalytic activity, selectivity, and importantly a better understanding of the mechanistic aspects of this process for both alicyclic and aliphatic epoxides. Nevertheless, the production of

polycarbonates from aliphatic epoxides and CO_2 has suffered from the tendency of this coupling reaction to generally favor production of the corresponding five-membered cyclic carbonate byproduct.[9] This general propensity of aliphatic epoxides and CO_2 for selectively affording cyclic carbonates is somewhat unfortunate because their corresponding copolymers are biodegradable materials which possess a wide variety of potential applications, including those in biomedical areas such as drug delivery devices and tissue engineering.[10] Notwithstanding, recent investigations of cobalt(III) and chromium(III) complexes have demonstrated these derivatives to greatly enhance the catalytic activity and selectivity for copolymer formation from the coupling of propylene oxide and CO_2 under mild reaction conditions.[8g, 8j, 11] Hopefully, in the future these catalysts will be useful for copolymer synthesis from a wide variety of functionalized aliphatic epoxides.

Aliphatic Polycarbonate Synthesis via Ring-Opening Polymerization

An optional synthetic methodology for the production of aliphatic polycarbonates involves the ring-opening polymerization of 6- and 7-membered cyclic carbonates. Six- and higher membered cyclic carbonates such as trimethylene carbonate can produce aliphatic polycarbonates with complete retention of their CO_2 contents under certain catalytic conditions (eq. I-2).[12] That is, the $\Delta H_p < 0$ and $\Delta S_p > 0$, and thus the polymerization process is thermodynamically allowed at all temperatures. Additionally, the increased ring-strain of six- and higher membered cyclic carbonates also promotes the ROP reaction.[13] On the other hand, the ROP of five-membered cyclic carbonates is

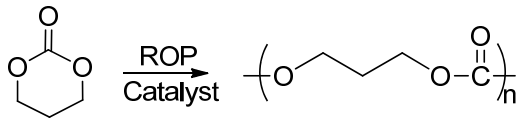

(I-2)

thermodynamically unfavored. Nevertheless, five-membered cyclic carbonates have undergone ROP processes at high temperatures (T > 100°C), resulting in the production of polycarbonates with significant amounts of ether linkages that are the consequence of CO_2 loss (eq. I-3). Researchers exploring this area have postulated that when the reactions are performed at these high temperatures the loss of carbon dioxide makes the $\Delta S_p > 0$, and hence the polymerization process becomes thermodynamically allowed.[14] The advantage however, of producing polycarbonates with none or at least reduced ether linkages is that the physical properties of the resulting polymers are greatly improved.

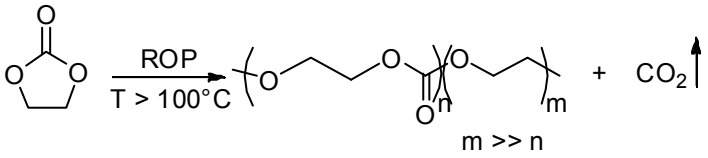

(I-3)

It is noteworthy that trimethylene carbonate is readily achieved by transesterification of 1,3-propanediol with various reagents including phosgene and its derivatives (di- and tri-phosgene), dialkylcarbonates, and ethylchloroformate.[15] Although, 1,3-propanediol is currently produced industrially from petroleum derivatives,

in the context of sustainability it can also be synthesized by microbiological or biochemical routes.[16]

Catalysts for Ring-Opening Polymerization of Six-Membered Cyclic Carbonates

Aliphatic polycarbonates are an interesting class of biodegradable polymers. In particular, poly(TMC) can be utilized to modify the properties of brittle and stiff biodegradable polyesters such as poly(glycolide) and poly(lactide).[17] Moreover, poly(TMC) can be hydrolyzed both in vivo and in vitro.[10a, 18] Hence, these resulting biodegradable thermoplastic elastomers have a variety of potential medical applications including sutures, drug delivery systems, body and dental implants, and tissue engineering.[10b, 19] The formation of aliphatic polycarbonates via ring-opening polymerization of six-membered cyclic carbonates has been investigated utilizing a variety of catalysts. This section will summarize the most widely used catalysts that have been reported in the literature for this process.

Prior to reviewing the most widely employed catalysts reported for ROP reactions of six-membered cyclic carbonates, it is beneficial to define two terms which will be referred to in further discussions throughout this dissertation, namely, turnover-frequency (TOF) and polydispersity (PDI). TOF is the moles of monomer consumed/(moles of catalyst-h). It is important to note that TOFs are highly dependent on the time period reactions are monitored. That is, the highest TOF values are obtained during the initial period of the polymerization process. The molecular weight distribution is referred to as polydispersity and is defined as $\overline{M}_w / \overline{M}_n$, where $\overline{M}_w$ is the weight-average molecular weight $\left(\frac{\Sigma N_i M_i^2}{\Sigma N_i M_i}\right)$ and $\overline{M}_n$ is the number average molecular

weight $\left(\frac{\Sigma N_i M_i}{\Sigma N_i}\right)$. N_i equals the number of chains containing mass M_i, and M_i equals the mass of the chain. The value of M_w is always > M_n .

Cationic and anionic initiators have both been shown to be effective for the ROP of six-membered cyclic carbonates. Strong Lewis acids such as methyl triflate and boron halogenides undergo cationic initiation providing the corresponding polycarbonates with ether linkages resulting from decarboxylation side reactions.[20] On the contrary, weaker Lewis acids such as alkoxide-, alkyllithium- and alcoholate-based initiators undergo anionic ROP processes providing in general the corresponding polycarbonates with 100% carbonate linkages.[21] Because of their Lewis acidic characteristics aluminum and tin salts have been widely employed for the ROP of trimethylene carbonate.

An alternative mechanism for the ROP of six-membered cyclic carbonates is the coordination-insertion pathway. When metal alkoxides containing catalysts having free p-, d- or f-orbitals of favorable energy are used a two step coordination-insertion mechanism takes place (eq. I-4).[13] The first step has been postulated to involve complexation of the monomer via the carbonyl oxygen of the cyclic carbonate. This complexation improves the electrophilicity of the monomer and is followed by cleavage of the acyl-oxygen bond of the cyclic carbonate monomer.[13]

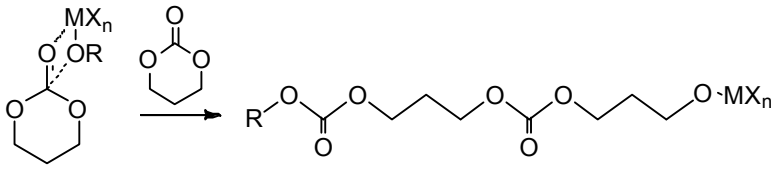

(I-4)

A very effective catalyst for the metal-catalyzed ROP of six-membered cyclic carbonates is tin(II)bis(2-ethyl-hexanoate) or tin(II)octoate (Figure I-1). For example, the ROP of TMC catalyzed by tin(II)octoate in bulk at 90, 120 and 150°C produced polycarbonates with no ether units and with M_w's up to approximately 22 000. Based on ^{1}H NMR mechanistic studies, the ring-opening mechanism was suggested to involve the cleavage of the acyl-O bond of the cyclic carbonate.[22] Aluminum-based complexes have also been effectively employed as catalysts for ROP of six-membered cyclic carbonates (Figure I-2). Early reports on the ROP of 2,2-dimethyltrimethylene carbonate (DTC) catalyzed by tetraphenylporphyrin-aluminum compounds, demonstrated that a halide (-Cl) or alkyl (-CH_3) groups attached to the aluminum center were inactive for polymerization. Only alkoxy nucleophile groups bound to the aluminum center proved effective. The polymerization reaction in methylene chloride was slow at ambient temperature (100 h) where only an 85% conversion was obtained.

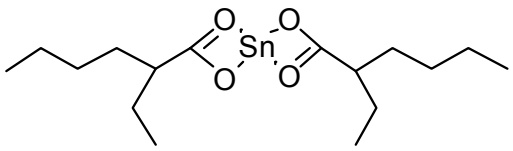

Figure I-1. Structure of tin(II)bis(2-ethyl-hexanoate), or tin(II)octoate.

As expected, in non- coordinating solvents such as toluene at 50°C, the reaction time was considerably reduced.[23] On the other hand, our group as well as Cao and coworkers reported on the use of aluminum complexes bearing salen ligands as very effective catalysts for the ROP of trimethylene carbonate. For example, Cao reported the ROP of TMC by a monomeric aluminum complex in anisole at 100°C for 3 h, which led to the formation of poly(TMC) with a PDI of 1.41, > 95% conversion and M_n = 13 400.[24] Similarly, an aluminum salen complex containing *tert*-butyl groups in the 3,5 positions of the phenolate rings, an ethylene backbone for the diimine, and an ethoxy initiator bound to the aluminum center was used by our group for the ROP of TMC, displaying an activity of TOF = 105 h^{-1}, M_w = 24 000 and PDI = 1.61.[25]

More recently, we have also demonstrated the effective application of biometal derivatives as catalysts for the ring-opening polymerization of TMC, showing a high control of the level of polymerization (Figure I-3). These catalytic systems are of particular importance because the use of biocompatible metals, such as calcium, magnesium, and zinc, eliminates the difficulty of removing trace amounts of metal residues from the produced polycarbonates.[26] Similarly, Guillaume and coworkers

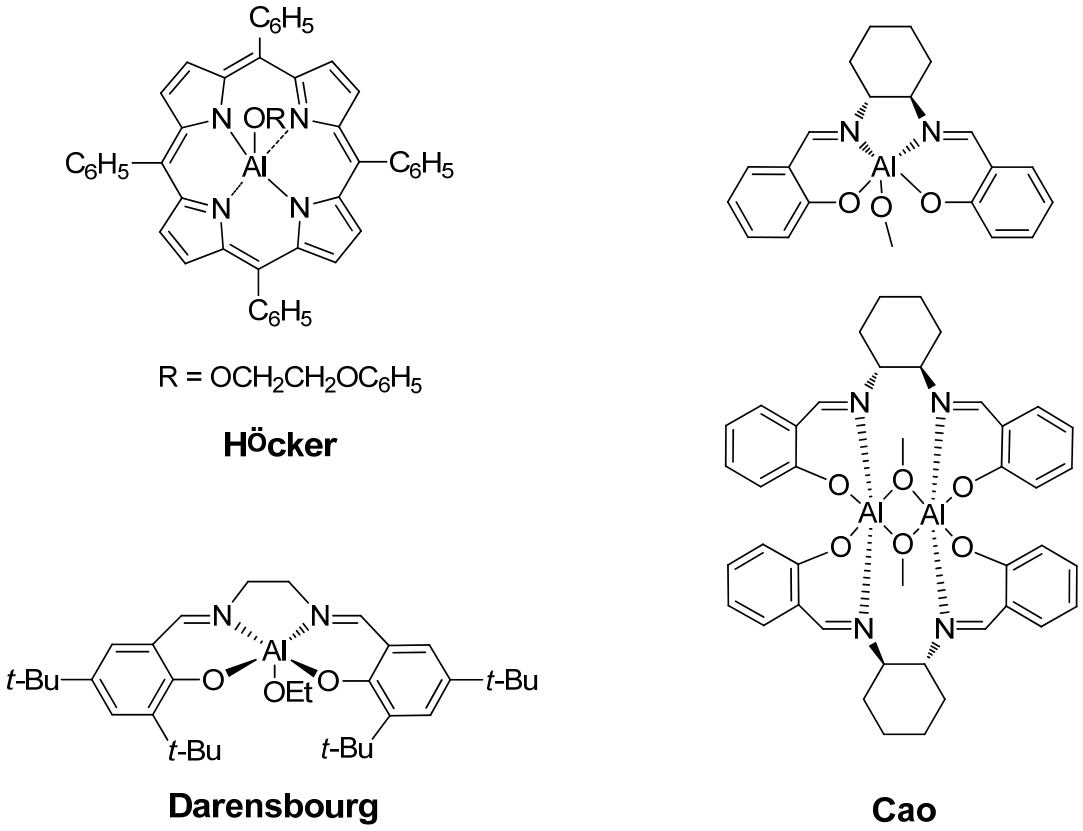

Figure I-2. Examples of Höcker's, Darensbourg's, and Cao's aluminum-based catalysts.

reported on the application of an "immortal" solvent-free polymerization process catalyzed by a zinc complex supported by a β-diiminate ligand in conjunction with benzyl alcohol as a transfer agent. This approach allows the growth of several polymer chains per metal center while keeping the control of the polymerization reaction through the presence of protic sources that acts as chain-transfer agents (Figure I-3).[27] With the same respect, the utilization of low toxic acetylacetonates of iron, zinc, and zirconium

have been reported as active catalysts for ROP of six-membered cyclic carbonates, where the zinc-based complex was found to be the more effective.[28] The attractiveness of acetylacetonates as ligands is attributed to their availability, low price, and stability.

Other catalysts such as homoleptic lanthanide amidinate complexes,[29] samarium borohydride complexes,[30] lanthanide aryloxide complexes,[31] and 2,2-dibutyl-2-stanna-1,3-oxepane[32] have also recently been investigated as catalysts for the ring-opening polymerization of trimethylene carbonate. In addition, organocatalysts in the presence of benzyl alcohol as initiator were reported by the Waymouth group as catalytic systems for the ROP of TMC, where high polymerization control, low polydispersities and high end group fidelity could be achieved.[33] Likewise, Bowden and coworkers have utilized 2-(dimethylamino)ethanol as an efficient catalyst for the ring-opening polymerization of TMC.[34]

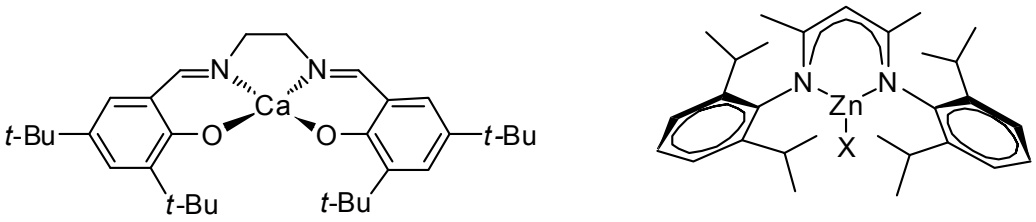

Figure I-3. Examples of biometal-based catalysts employed for the ROP of TMC.

A summary of the available catalysts for the ring-opening polymerization of six-membered cyclic carbonates cannot be completed without mentioning the available enzymatic-based catalysts. The use of enzymes as catalysts for the synthesis of biodegradable polymers is gaining increased attention in the last few years. In contrast to metal-based catalysis that often requires the use of pure monomers, anhydrous conditions, and the need of catalyst removal from the final polymer, enzymatic catalysis requires milder reaction conditions, and the enzyme catalysts are safe and often recyclable.[35]

As an example on the use on enzymes as catalysts for the production of aliphatic polycarbonates, the Gross research group reported a comprehensive study on the lipase-catalyzed ring-opening polymerization of TMC in bulk.[36] Commercially available lipases from different sources were screened for the ROP of TMC at 70°C. The lipase from *Candida Antarctica* gave the highest rate. After 120 h, 97% conversion, and poly(TMC) with M_n = 15 000 and a PDI = 2.2 with no ether linkages resulting from decarboxylation was achieved. Interestingly, increasing the water content in these lipases resulted in an enhancement in polymerization rates but decreased molecular weights. This is most likely due to an increase in the propagating chain ends as well as an improve in enzyme activity. Additionally, the molecular weights decreased as the reaction temperatures were increased from 55 to 85°C. This behavior was explained to be caused to the presence of side reactions such as hydrolysis, chain initiation, and depolymerizations. There is quite an extensive variety of lipases that have been tested for their catalytic efficiency for the ROP of six-membered cyclic carbonates including

immobilized lipases, which have the added advantage of having thermal activity and stability and can be recycled.[35, 37] However, current research efforts are concentrating on improving the yield of the polymer and molecular weights.

Aliphatic Polycarbonates from Oxetanes and Carbon Dioxide

Another alternative route to aliphatic polycarbonates involves the copolymerization of four-membered cyclic ethers, such as oxetane and carbon dioxide (eq. I-5). Surprisingly, this reaction has not been widely studied, but it is of particular interest, since in this case the cyclic carbonate byproduct, TMC, can be ring-opened and transformed into the same polycarbonate by means of the reaction defined in eq I-2. The

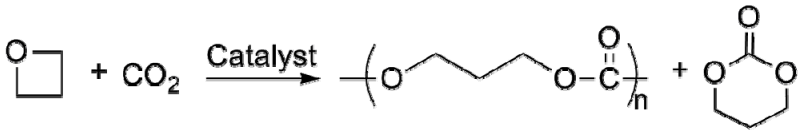

(I-5)

starting point of the metal catalyzed copolymerization of oxetane and carbon dioxide can be traced back to the early research efforts of Professors Koinuma and Hirai at the University of Tokyo, who were motivated by their earlier results on the copolymerization of oxiranes (epoxides) and CO_2 catalyzed by organoaluminum-based catalysts to produce polycarbonates.[38] Hence, they hypothesized that it might be possible to synthesize aliphatic polycarbonates not only from three-membered cyclic ethers, but also from four-membered cyclic ethers such as oxetane. Poly(trimethylene carbonate) was initially prepared employing a ternary catalyst system composed of

triethylaluminium, water, and acetylacetone in a ratio of 2:1:1. This catalytic system however, was plagued by poor yields of copolymers with significant quantities of ether linkages.[39] In this case, an anionic coordination mechanism was postulated for the formation of polycarbonate. In 1984, Baba at Osaka University reported the use of organotin halides (halides = Cl, Br, I) and Lewis bases e.g. phosphines and amines as catalytic systems, yielding low molecular weight polycarbonates from the coupling of oxetane and CO_2.[40] Additionally, tetraphenylstibonium iodide was also employed by Baba to selectively synthesize trimethylene carbonate from oxetane and carbon dioxide (Figure I-4).[41]

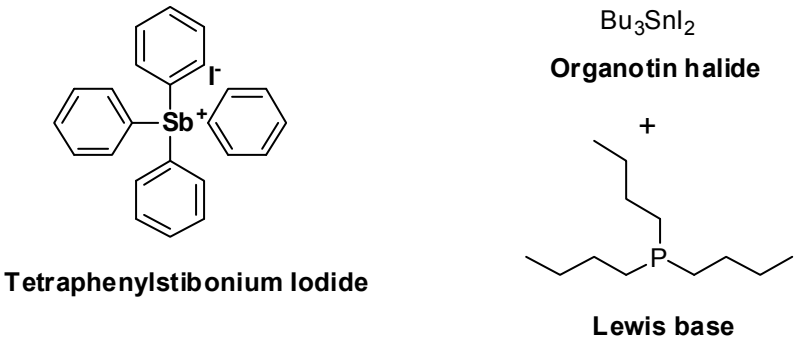

Figure I-4. Examples of catalytic systems employed by Baba for the coupling of oxetane and CO_2.

In 1985, Baba reported a more comprehensive study on the coupling reaction of oxetane and carbon dioxide catalyzed by organotin iodides with phosphines or phosphine oxides as catalytic systems.[42] It was demonstrated in this instance that the

choice of the ligand that coordinated to the organotin iodides was crucial, and affected the catalytic activity and selectivity of the reaction. For example, complexes formed by coordination of an organotin compound with Bu_3P produced polycarbonate exclusively. However, the combination of Bu_3SnI with $Bu_3P{=}O$ yielded only trimethylene carbonate in good yields. A reaction mechanism was proposed by Baba and coworkers and is illustrated in **Scheme I-3**.

Scheme I-3. Reaction Mechanism for Copolymer Formation Proposed by Baba. Adapted From Reference 42.

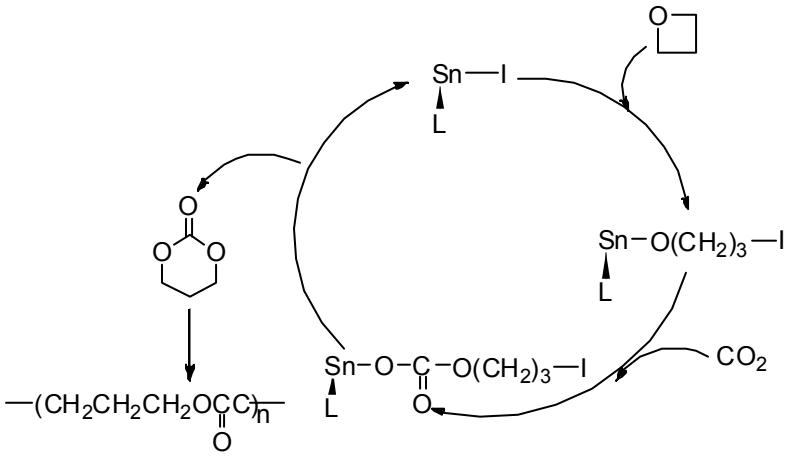

In the first step oxetane is ring-opened by an organotin iodide complex producing an organotin iodopropoxide intermediate, which undergoes CO_2 insertion into the Sn-O bond, generating an organotin carbonate adduct. Trimethylene carbonate was proposed to be formed by a backbiting reaction, regenerating the organotin complex. Coordination of phosphine or phosphine oxide ligands to organotin iodide compounds

was proposed to activate the Sn-I bond by enhancing the nucleophilicity of the halide-based initiator, allowing the oxetane ring to be opened. Polymerization of preformed TMC was proposed to occur by free organotin iodide complexes in solution. This conclusion was supported by the fact that in the presence of a large excess of $Bu_3P{=}O$, dissociation of this phosphine oxide from Bu_3SnI was suppressed and no polymerization reaction took place. On the contrary, complexes of Bu_3P and Bu_3SnI were found to be too unstable to suppress polymerization, even in the presence of a large excess of phosphine.

Of importance, these early reports on the coupling reaction of oxetane and carbon dioxide suggested that a full understanding of the mechanistic details of this process was lacking. Hence, the main objective of this dissertation will be to provide a strong chemical background for the following questions:

i) What would be a suitable catalytic system for this reaction?

ii) What are the mechanistic details of this process? In other words, does the copolymerization reaction proceed by the direct enchainment of oxetane and carbon dioxide or by the intermediate formation of TMC?

iii) Can the selectivity for one product over the other be tuned?

iv) Can this chemistry be extended to other oxetane derivatives that could afford copolymers with different properties?

Metal Salen Complexes as Catalysts

Metal salen complexes are one of the most popular and fundamental class of complexes in coordination chemistry today. The first salen complexes were synthesized

in 1933 by a condensation reaction of a salicylaldehyde and ethylene diamine with various metal-based salts.[43] Currently, there is an extensive array of metal salen complexes that have been synthesized and fully characterized. The most important advantage of the salen ligands is its ease of preparation, which involves the condensation of a salicylaldehyde and a diamine (Figure I-5). Moreover, the sterics and electronics of the ligand architecture can be fine tuned by varying the R_1, R_2 and R_3 groups. A fundamental reaction that intensified the use of metal salen complexes was the enantioselective epoxidation of unfunctionalized alkenes catalyzed by manganese salen complexes.[44] Metal salen complexes are utilized for a variety of catalytic reactions including asymmetric ring-opening of epoxides, enantioselective intramolecular openings of oxetanes, ring-expansions of epoxide and CO_2 to form five-membered cyclic carbonates, and epoxide/CO_2 copolymerization processes among others.

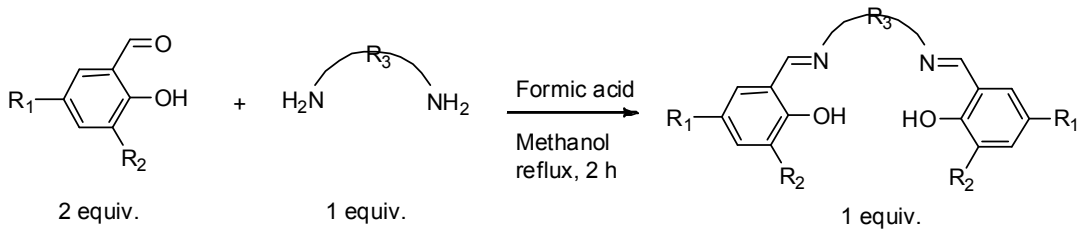

Figure I-5. Skeletal representation of the synthesis of salen ligands.

In particular, the Darensbourg research group has been investigating for a decade a variety of catalytic systems based on metal salen complexes in the presence of onium

salts as cocatalysts for the copolymerization of cyclohexene oxide or propylene oxide and carbon dioxide. An emphasis on chromium(III) salen complexes has been made due to their greater catalytic activity for these processes compared to main group elements containing salen complexes. Furthermore, the employment of chromium salen complexes in conjunction with anionic-based cocatalysts of the type *n*-Bu_4NX or PPNX

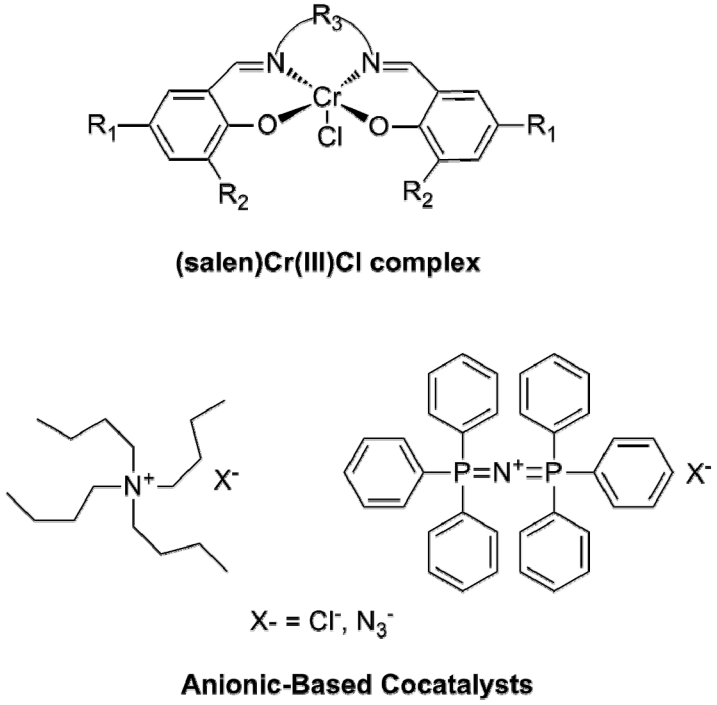

Figure I-6. Skeletal representation of (salen)Cr(III)Cl complex and anionic-based cocatalysts used in epoxide/CO_2 copolymerization processes.

(PPN^+ = $(Ph_3P)_2N^+$) have proved to increase their catalytic activity and selectivity towards copolymer formation from the epoxide (CHO or PO)/CO_2 copolymerization

processes (Figure I-6). That is, copolymers with greater than 99% carbonate linkages, low polydispersities and high molecular weights have been obtained.[8b, 8d] Additional benefits arising from the use of chromium salen complexes as catalysts is their stability, robustness, and ease of synthesis. The synthesis of chromium salen complexes have been fully described in the literature by two methods.[45] The treatment of the corresponding salen ligand with $CrCl_2$ in THF under an argon atmosphere, followed by oxidation in air (Figure I-7). Another methodology involves prior deprotonation of the salen ligand with NaH or KH, followed by treatment of the corresponding formed salt with $CrCl_3(THF)_3$ under an argon atmosphere.

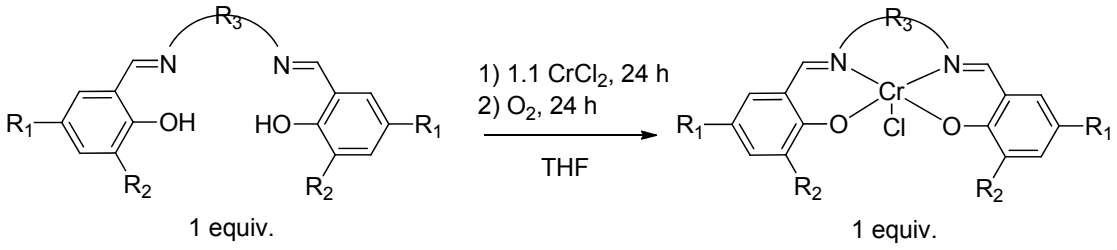

Figure I-7. Skeletal representation of the synthesis of chromium salen complexes from $CrCl_2$.

Given the success achieved by our group on the application of metal salen complexes as catalysts for the copolymerization of cyclohexene oxide or propylene oxide and carbon dioxide, a clear issue to investigate was the efficiency of these complexes as catalysts for the copolymerization of four-membered cyclic ethers such as oxetanes and CO_2. Because the ring-strain energy of propylene oxide and oxetane do

not differ significantly, 114.2 *vs* 106.7 kJ/mol, respectively, it would be expected that metal salen complexes in the presence of anionic-based cocatalysts would serve as effective catalytic systems for the oxetane and CO_2 coupling process. This is an issue that will be tackled in the following pages of this dissertation.

Physical Methods for the Characterization of the Coupling Reaction of Oxetane and CO_2

A detailed analysis of the products resulting from the copolymerization of oxetane and carbon dioxide can readily be done by ^{1}H NMR and IR spectroscopies. The molecular weights and polydispersities of the purified copolymers is generally performed by gel permeation chromatography in tetrahydrofuran solution. Purification of the copolymers is normally achieved by precipitation from a dichloromethane solution of the copolymer with 1 M HCl in methanol, followed by vacuum drying. As seen in Figure I-8, the presence of possible coupling products from the oxetane/CO_2 coupling reaction, namely, poly(TMC) and TMC, can easily be assigned using ^{1}H NMR spectroscopy. The percent conversion to polymer can be monitored based on the amount of oxetane monomer left in the reaction solution. Furthermore, the quantities of poly(TMC), TMC, and ether linkages in the copolymer can be determined by integrating the peak area of the corresponding resonances at 4.23, 4.43, and 3.50 ppm, respectively. Another spectroscopy technique that has been extremely useful for monitoring the copolymerization reactions of oxetane and CO_2 is *in situ* Attenuated Total Reflectance Infrared Spectroscopy (Figure I-9).[46] By utilizing a high-pressure stainless steel Parr

autoclave modified with a silicon composite ATR crystal located at the bottom of the reactor, high-pressure reaction kinetic measurements can be performed. We have been able to examine the growth of copolymer and cyclic carbonate as a function of time under the temperature and pressure conditions required. Infrared stretching bands of the carbonyl groups of poly(TMC) and TMC, in CH_2Cl_2 both appeared at 1750 cm^{-1}. On the other hand, in a mixture of toluene and oxetane they are separated by 20 cm^{-1}. That is, the carbonyl group of TMC is seen at 1770 cm^{-1} and that of poly(TMC) at 1750 cm^{-1} (Figure I-10). Due to the close proximity of the carbonyl stretching bands of copolymer and cyclic carbonate, deconvolution of selected IR spectra was carried out when necessary, in order to get accurate reaction profiles. Figure I-11 shows an example of a deconvoluted spectrum.

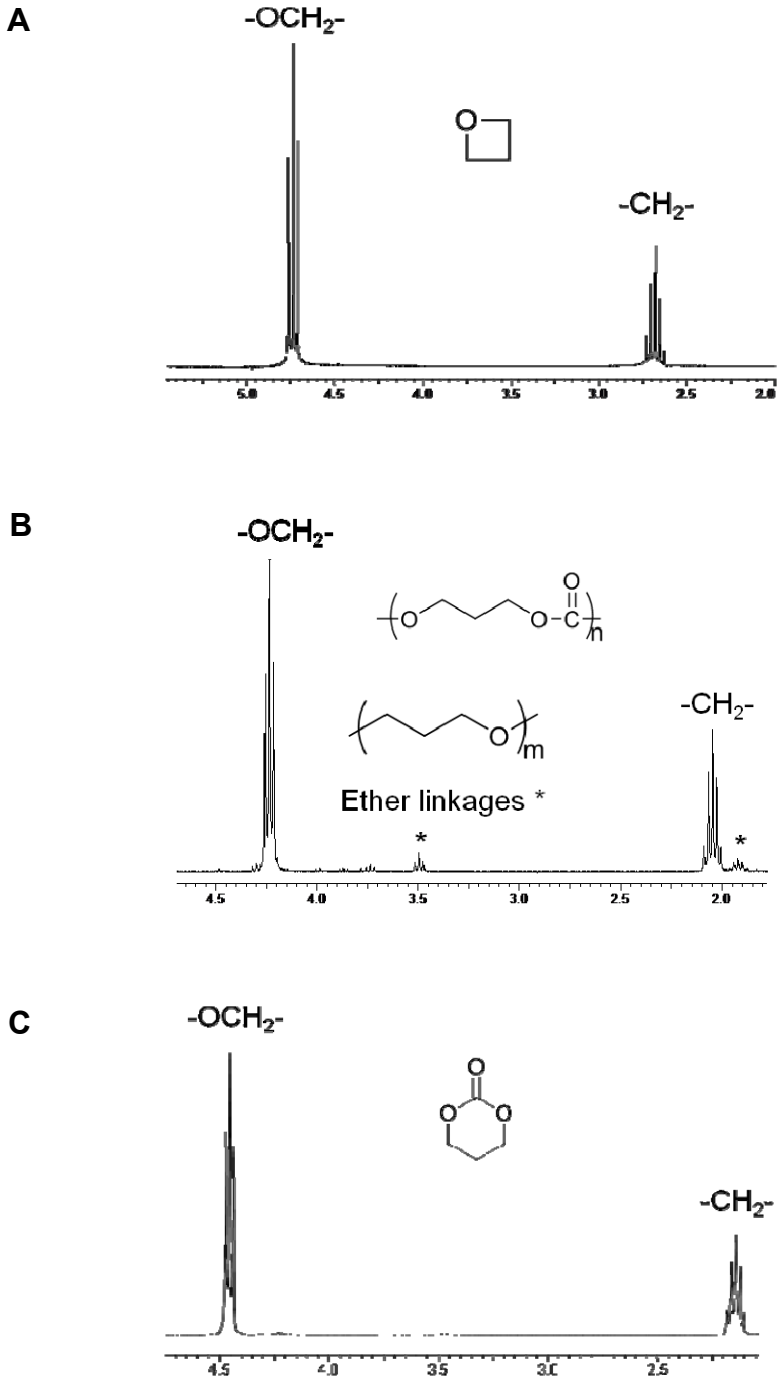

Figure I-8. ^{1}H NMR in $CDCl_3$ of (**A**) oxetane, (**B**) poly(TMC) obtained from oxetane and CO_2, and (**C**) trimethylene carbonate.

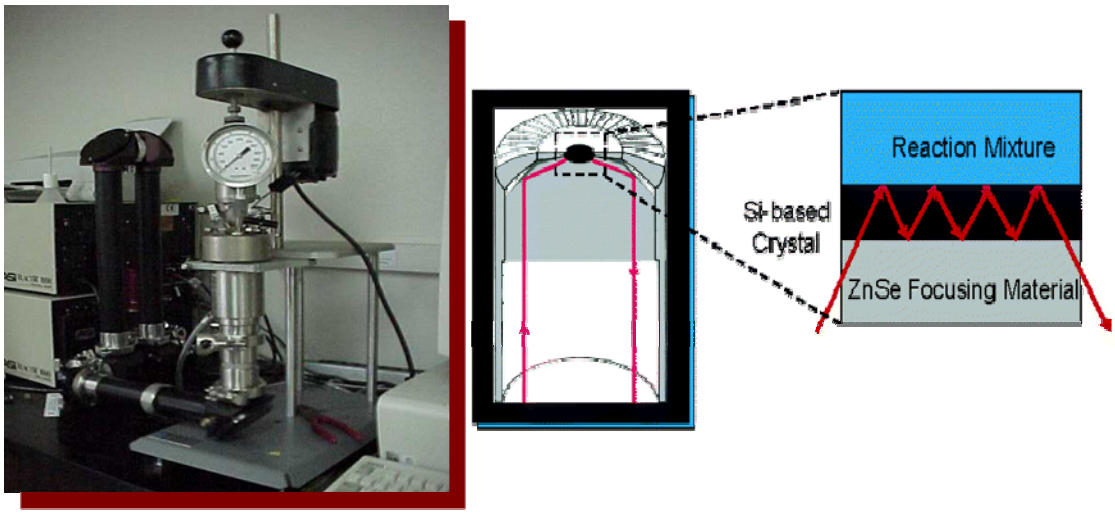

Figure I-9. ASI ReactIR 1000 system modified for ATR with a high-pressure Parr autoclave used for monitoring high-pressure reaction systems (left), and a diagram illustrating ATR-FTIR (right).

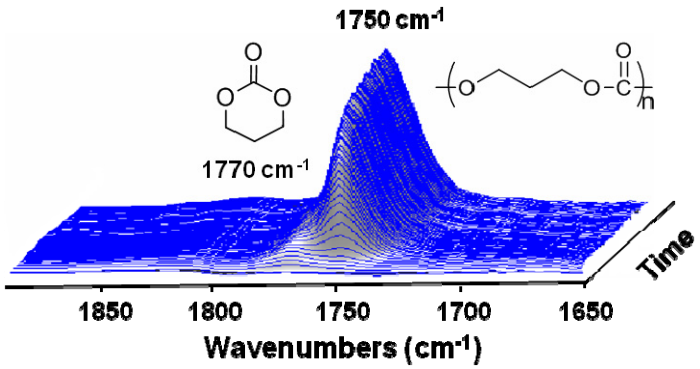

Figure I-10. Three-dimensional stack plot of the IR spectra collected every 3 min for the copolymerization reaction of oxetane and carbon dioxide, displaying the $\nu_{C=O}$ stretches for poly(TMC) at 1750 cm^{-1} and trimethylene carbonate at 1770 cm^{-1}.

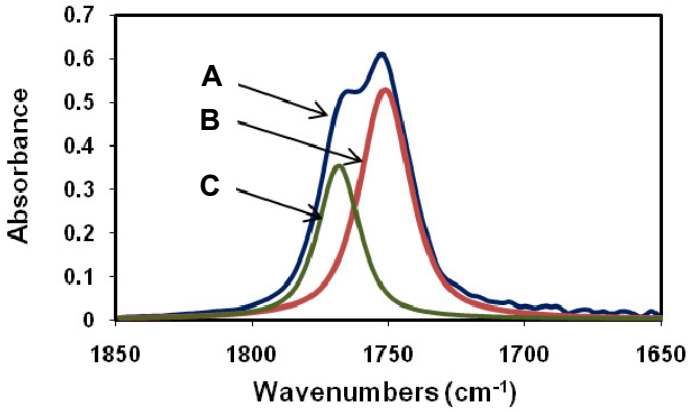

Figure I-11. Selected IR spectrum of a reaction solution obtained from the reaction between oxetane and CO_2. (**A**) Undeconvoluted IR spectrum, (**B**) Deconvoluted IR spectrum corresponding to poly(TMC), (**C**) Deconvoluted IR spectrum corresponding to TMC.

In the reminder of this dissertation, the application of metal salen complexes along with anionic-based cocatalysts for the copolymerization of oxetanes and CO_2 will be discussed. The topics covered will range from catalyst system optimization to detailed kinetic and mechanistic investigations on this transformation. Lastly, the exploration of the copolymerization of 3-methoxy-methyl-3-methyloxetane and CO_2 will be presented.

CHAPTER II

MECHANISTIC STUDIES OF THE COPOLYMERYZATION REACTION OF OXETANE AND CARBON DIOXIDE TO PROVIDE ALIPHATIC POLYCARBONATES CATALYZED BY (SALEN)CrX COMPLEXES*

Introduction

In 2006, the Darensbourg group began research efforts to examine the efficiency of metal salen complexes for the copolymerization of oxetane and carbon dioxide. Initially, the catalytic activity of the (salen)M(III)Cl derivatives (where M = Cr, Al) towards the copolymerization of oxetane and CO_2 in the presence of *n*-Bu_4NCl as cocatalyst was investigated. It was demonstrated that the (salen)Cr(III)Cl complex, was more active (TOF = 41.2 h^{-1}) than its aluminum salen analog (TOF = 8.59 h^{-1}) to catalyze this coupling reaction. In all the instances, high selectivity for copolymer formation was obtained even at high temperatures (110ºC). Based on circumstantial evidence, it was suggested that formation of copolymer did not proceed via the intermediacy of TMC which was observed as a minor product of the coupling reaction.[47]

Herein, we have extended these investigations by further optimizing the (salen)CrCl catalytic system for this reaction (Figure II-1). Efforts have been made to

---

*Reproduced in part with permission from: "Mechanistic Studies of the Copolymerization Reaction of Oxetane and Carbon Dioxide to Provide Aliphatic Polycarbonates Catalyzed by (Salen)CrX Complexes." Darensbourg, D. J.; Moncada, A. I.; Choi, W.; Reibenspies, J. H. *J. Am. Chem. Soc.* **2008**, *130,* 6523-6533. Copyright 2008 American Chemical Society.

gain a greater insight into the mechanistic aspects of this important reaction based on kinetic and copolymer end-group analysis studies performed utilizing *in situ* infrared and ^{1}H NMR spectroscopies.

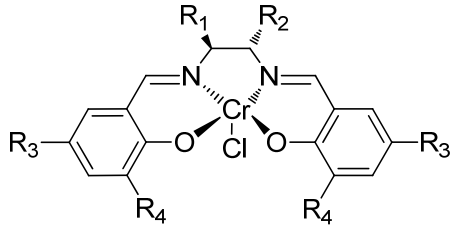

Complex II-1: $R_1 = R_2 = H$; $R_3 = R_4 = t$-Bu
II-2: $R_1, R_2 = -C_4H_4-$; $R_3 = R_4 = t$-Bu
II-3: $R_1, R_2 = -C_4H_4-$; $R_3 = OMe$; $R_4 = t$-Bu
II-4: $R_1, R_2 = (1R,2R)-C_4H_8-$; $R_3 = R_4 = t$-Bu

Figure II-1. Structures of the (salen)Cr(III) chloride complexes utilized as catalysts for the copolymerization of oxetane and CO_2.

Experimental Section

Reagents and Methods. Unless otherwise specified, all syntheses and manipulations were carried out on a double-manifold Schlenk vacuum line under an atmosphere of argon or in an argon filled glove box. Toluene and tetrahydrofuran were freshly distilled from sodium/benzophenone. Ethanol and methanol were freshly distilled from Mg/I_2. 1,1,2,2-tetrachloroethane (TCE) was freshly distilled over CaH_2. Diethyl ether, dichloromethane, and pentane, were purified by an MBraun Manual Solvent Purification System packed with Alcoa F200 activated alumina desiccant. Oxetane (Alfa Aesar) was freshly distilled over CaH_2 and stored in the freezer of the glove box. Trimethylene carbonate (Boehringer Ingelheim) was recrystallized from

tetrahydrofuran and diethyl ether, dried under vacuo and stored in the glove box. Tricyclohexylphosphine (Alfa Aesar) was recrystallized from distilled ethanol before use. PPNCl (PPN^+ = $(Ph_3P)_2N^+$) (Aldrich) was recrystallized from dichloromethane/ether before use, and $PPNN_3$ was synthesized according to a published procedure.[48] Tetra-*n*-butylammonium bromide (Aldrich) was recrystallized from acetone/diethyl ether before use. Tetra-*n*-butylammonium azide (TCI) was stored in the freezer of the glove box upon arrival. Ethylenediamine (Aldrich), 1,2-phenylenediamine (ACROS), chromium(II) chloride (Alfa Aesar) and sodium sulfate (EMD) were used as received. Bone-dry carbon dioxide supplied in a high-pressure cylinder and equipped with a liquid dip tube was purchased from Scott Speciality Gases. The corresponding salen ligands and chromium complexes were synthesized as previously described.[45]

^{1}H NMR spectra were acquired on Unity+ 300 MHz and VXR 300 MHz superconducting NMR spectrometers. IR spectra were recorded on a Mattson 6021 Fourier Transform (FT) IR spectrometer with a MCT detector. TGA measurements were performed with SDT Q600 V7.0 Build 84. Analytical elemental analysis was provided by Canadian Microanalytical Services Ltd. Molecular weight determinations (M_n and M_w) were carried out with a Viscotek Modular GPC apparatus equipped with ViscoGEL^{TM} I-series columns (H + L) and Model 270 dual detector comprised of Refractive Index and Light Scattering detectors. High-pressure reaction kinetic measurements were performed using an ASI ReactIR 1000 reaction analysis system with stainless steel Parr autoclave modified with a permanently mounted ATR crystal (SiComp) at the bottom of the reactor (purchased from Mettler Toledo).

Optimization of the Cocatalyst for the Copolymerization Reactions of Oxetane and Carbon Dioxide. In a typical experiment, 17 mg of catalyst (*N,N'*-bis(3,5-di-*tert*-butylsalicylidene)-1,2-ethylenediimine chromium(III) chloride), the appropriate amount of cocatalyst, and 1.15 g of oxetane were dissolved in 10 mL of toluene. This solution was then delivered via the injection port into a 300-mL stainless steel Parr autoclave reactor that was previously dried in vacuo overnight at 80°C. The autoclave was then pressurized with 35 bar of CO_2 and the temperature was increased to 110°C. The monomer:catalyst:cocatalyst ratio was maintained at 675:1:2, and the reaction was run for 24 hours. In the case of PPNCl and $PPNN_3$, the catalyst and cocatalyst were previously premixed in a 4:1 benzene:methanol solution, dried overnight and then dissolved into 1.15 g of oxetane and 10 mL of toluene. After the reaction was stopped, the autoclave was put into ice, cooled down to 10°C, and vented in a fume hood. The percent conversion to products was determined based on the amount of oxetane monomer left in the reaction solution. ^{1}H NMR (300 MHz, $CDCl_3$), oxetane: δ 4.75 (t, 4H, OCH_2) and 2.70 (quintet, 2H, CH_2). Furthermore, the quantities of poly(TMC), TMC, and ether linkages in the copolymer were determined by integrating the peak area of the corresponding resonances. ^{1}H NMR (300 MHz, $CDCl_3$), poly(TMC): δ 4.23 (t, 4H, OCH_2) and 2.05 (quintet, 2H, CH_2). ^{1}H NMR (300 MHz, $CDCl_3$), TMC: δ 4.45 (t, 4H, OCH_2) and 2.14 (quintet, 2H, CH_2). ^{1}H NMR (300 MHz, $CDCl_3$), ether linkages: δ 3.50 (t, 4H, OCH_2) and 1.90 (quintet, 2H, CH_2).

Optimization of the (salen)Cr(III)Cl Catalyst for the Copolymerization Reactions of Oxetane and Carbon Dioxide. In a typical experiment, 4 g of oxetane, and the appropriate amount of catalyst and cocatalyst (*n*-Bu_4NN_3), were delivered via the injection port into a 300-mL stainless steel Parr autoclave reactor that was previously dried in vacuo overnight at 80°C. The autoclave was pressurized with 35 bar of CO_2 and the temperature was increased to 110°C. The monomer:catalyst:cocatalyst ratio was maintained at 1292:1:2, and the reaction was run for 24 hours. After the reaction was stopped, the autoclave was put into ice, cooled down to 10°C, and vented in a fume hood. The reaction solution was analyzed by ^{1}H NMR spectroscopy in the same manner as above, to determine the percent conversion to products, and the percentages of poly(TMC), TMC, and ether linkages. The resulting polymer was purified by precipitation from dichloromethane and 1 M HCl solution in methanol and then dried in vacuo. Turnover frequencies (mol of oxetane consumed/mol of catalyst-h) were calculated following weight of the vacuum dried polymer.

Substrate Binding and Ring-Opening Steps Examined by Infrared Spectroscopy. Substrate binding and ring-opening step studies were examined by solution infrared spectroscopy. The catalytic system used in these studies was a (salen)Cr(III)Cl (50 mg) complex (*N,N'*-bis(3,5-di-*tert*-butylsalicylidene)-1,2-ethylenediimine chromium(III) chloride) in the presence of *n*-Bu_4NN_3 as cocatalyst and using TCE as the solvent (4 mL).

X-ray Structural Studies. Single crystals of a hydroxo-bridge **(salen)$_2$(Cr(III))$_2$Cl·OH·oxetane** (complex **II-5)** were obtained by layering pentane into a saturated dichloromethane solution of the corresponding (salen)Cr(III)Cl complex (*N,N'*-bis(3,5-di-*tert*-butylsalicylidene)-1,2-phenylenediimine chromium(III) chloride) containing 20 equivalents of oxetane. Anal. Calcd for $C_{80}H_{111}ClCr_2N_4O_6$: C, 70.43; H, 8.20; N, 4.10. Found: C, 68.50; H, 7.85; N, 4.06.

Single crystals of a **(salen)Cr(III)Cl·oxetane** (complex **II-6**) were obtained at 5°C by layering pentane into a saturated dichloromethane solution of the corresponding (salen)Cr(III)Cl complex (*N,N'*-bis(3,5-di-*tert*-butylsalicylidene)-1,2-phenylenediimine chromium(III) chloride) containing 20 equivalents of oxetane. Anal. Calcd for $C_{47}H_{70}Cl_7CrN_2O_3$: C, 55.82; H, 6.97; N, 2.77. Found: C, 57.21; H, 6.72; N, 3.84.

For both structures, a Bausch and Lomb 10× microscope was used to identify suitable crystals. Each crystal was coated in paratone, affixed to a nylon loop, and placed under streaming nitrogen (110K) in a Bruker - AXS Apex II three-circle X-ray diffractometer. Space group determinations were made on the basis of systematic absences and intensity statistics. Both crystal structures were solved by direct methods and were refined by full-matrix least-squares on F^2. All hydrogen atoms were placed in idealized positions and refined with fixed isotropic displacements parameters equal to 1.2 (1.5 for methyl protons), times the equivalent isotropic displacements parameters of the atoms to which they were attached. All non-hydrogen atoms were refined with anisotropic displacement parameters.

The following are the programs that were used: data collection and cell refinements; APEX II data collection software, data reduction; APEX II data reduction software, absorption correction; SADABS,[49] program used to solve structures; SHELXS-97,[50] program used to refine the structures; SHELXL-97,[51] molecular graphics and preparation of material for publication; SHELXTL, version 6.14,[52] X-Seed, version 1.5.[53]

Copolymerization Reactions Monitored by *in situ* IR Spectroscopy. In a typical experiment, the catalyst (*N,N'*-bis(3,5-di-*tert*-butylsalicylidene)-1,2-cyclohexelynediimine chromium(III) chloride), cocatalyst (*n*-Bu_4NN_3),and oxetane (4 g) were dissolved in 10 mL of toluene and delivered via the injection port into a 300-mL stainless steel Parr autoclave reactor that was previously dried in vacuo overnight at 80°C. The autoclave is modified with a 30 bounce SiComp window to allow for the use of an ASI ReactIR 1000 system equipped with a MCT detector. In this manner a 128-scan background spectrum was collected after the reaction mixture was heated to the temperature of the corresponding experiment, the autoclave was then pressurized to the appropriate CO_2 pressure, and the infrared spectrometer was set to collect one spectrum every 3 min over a 12 or 24 h period. Profiles of the absorbance at 1750 cm^{-1} (polymer) with time were recorded after base line correction, and analyzed to provide initial reaction rates. In some cases, after the reaction was stopped the autoclave was cooled down to room temperature, and a ^1H NMR spectrum in $CDCl_3$ of the reaction mixture was taken to determine the percent conversion to polymer. (Note: catalyst loading,

cocatalyst loading, and temperature varied within each experiment and are described in the Results and Discussion section).

Kinetic Studies for the Ring-Opening Polymerization of Trimethylene Carbonate. For kinetic studies of the ring-opening polymerization of TMC, the catalyst (*N,N'*-bis(3,5-di-*tert*-butylsalicylidene)-1,2-cyclohexelynediimine chromium(III) chloride) and the cocatalyst (*n*-Bu_4NN_3) were weighed out in a Schlenk flask in the desired monomer:catalyst:cocatalyst ratio followed by the addition of dry TCE (5 mL). The reaction vessel was placed into a preheated oil bath. The percent conversion of the monomer with time was calculated by manually sampling a small aliquot of the solution, quenching it, and analyzing it by ^{1}H NMR spectroscopy. (Note, catalyst loading, cocatalyst loading, and temperature varied within each experiment and are described in the Results and Discussion section).

Copolymerization Reaction of Oxetane and Carbon Dioxide Monitored by ^{1}H NMR Spectroscopy. 12 g of oxetane, 373 mg of catalyst (*N,N'*-bis(3,5-di-*tert*-butylsalicylidene)-1,2-cyclohexelynediimine chromium(III) chloride), and 335 mg of cocatalyst (*n*-Bu_4NN_3) were dissolved in 30 mL of toluene and delivered via the injection port into a 300-mL stainless steel Parr autoclave reactor that was previously dried in vacuo overnight at 80°C. The reactor was pressurized with 35 bar of CO_2 and the temperature was increased to 110°C. The monomer:catalyst:cocatalyst ratio used was 350:1:2, and the reaction was run for 28 hours. The percent conversion to polymer, the percentages of TMC, and polycarbonate were calculated with time, by manually

sampling a small aliquot of the reaction mixture, which was first cooled down to 10°C and then analyzed by ^{1}H NMR spectroscopy.

Results and Discussion

Initially we chose to employ the (salen)CrCl catalyst, complex **II-1** in Figure II-1, in the presence of various cocatalysts to optimize the selectivity for copolymer formation from the coupling of oxetane and carbon dioxide. The copolymerization reactions were performed under identical reaction conditions, i.e., 110ºC and 35 bar CO_2 pressure. The results are summarized in Table II-1, where the counterions of the anionic initiators were either $PPN^+[(Ph_3P)_2N^+]$ or *n*-Bu_4N^+. The product mixtures were analyzed by ^{1}H NMR spectroscopy, with the quantities of poly(TMC), TMC, and ether linkages in the poly(TMC) determined by integrating the resonances at 4.23, 4.43, and 3.50 ppm, respectively. As is readily seen in Table II-1, the yield of poly(TMC) is much greater than the cyclic product, TMC, at the end of a 24 h reaction period in all instances. Of importance here, the azide salts are slightly better than their chloride analogs, with little difference between the PPN^+ and *n*-Bu_4N^+ salts being observed. The bromide anion was shown to be significant less selective for copolymer formation than the chloride anion, and tricyclohexylphosphine displayed the lowest selectivity towards copolymer formation of the cocatalysts studied.[54]

Table II-1. Selectivity for Copolymer Formation using Complex **II-1** in the Presence of Various Cocatalysts.[a]

Entry	Cocatalyst	% TMC[b]	% Poly(TMC)[b]	% Ether Linkages[b]
1	*n*-Bu_4NCl[c]	0	100	3.0
2	*n*-Bu_4NN_3[c]	0	100	2.9
3	*n*-Bu_4NBr	11.7	88.2	7.2
4	PPNCl	5.9	94	3.6
5	$PPNN_3$	2.3	97.6	1.4
6	$P(Cy)_3$	21.1	79	21.5

[a] Copolymerization conditions: 17 mg of catalyst (0.15 mol%), 1.15 g of oxetane, M:I = 675:1, 2 equiv. of cocatalyst, 10 mL of toluene, 35 bar of CO_2, at 110°C for 24 h. [b] Product distributions were determined by ^{1}H NMR spectroscopy. [c] Previous published results.[25] Note for the first entry in Table II-1 in reference 47, the % TMC is incorrectly reported due to missassigned ^{1}H NMR resonances.

Subsequent studies were carried out to interrogate the effects of changing the nature of (i) the substituents on the phenolate rings, and (ii) the diimine backbone of the salen ligand in the (salen)CrCl derivative. In this instance the copolymerization reactions were performed at a monomer:catalyst:cocatalyst ratio of 1292:1:2, with a CO_2 pressure of 35 bar at 110ºC for 24 h. The results of this inquiry are provided in Table II-2, where the TOFs (mol of oxetane consumed/mol of initiator-h) were determined from the *isolated copolymer* obtained upon precipitation from dichloromethane with a 1 M HCl solution in methanol. It is important to note here that a minimal quantity of ether linkages were observed in the copolymer samples resulting from consecutive oxetane ring-opening processes, however, in all cases the CO_2 content was very high (> 95%). Note that 100% carbon dioxide incorporation defines a *completely alternating* copolymer of oxetane and CO_2. The molecular weights of the copolymers were

determined in THF solution by gel permeation chromatography using RI and light scattering detectors and polystyrene standards. In general, the observed M_n values were found to be much lower than the theoretical values, e.g., in entry 4 of Table II-2 the observed M_n of 11 050 is considerably lower than the theoretical value of 85 000. This is most likely due to a chain transfer mechanism arising from the presence of trace quantities of water in the system.[11b, 55] The PDI was in general about 1.5, and a copolymer with M_n of 11 050 was found to be stable up to 260ºC by TGA. A more comprehensive compilation of molecular weights as a function of the monomer:initiator ratio, along with polydispersities, can be found in Table II-3. Included in Table II-3 is a catalytic run done under super anhydrous conditions, i.e., no solvent and in the presence

Table II-2. Copolymerization of Oxetane and CO_2 Catalyzed by (salen)Cr(III)Cl Complexes.[a]

Entry	Complex	R_1	R_2	R_3	R_4	TON[b]	TOF[c]	% CO_2 content[d]	% Conversion[d]
1	**II-2**	-C_4H_4-		*tert*-butyl	*tert*-butyl	588	24.5	97.1	54.6
2	**II-3**	-C_4H_4-		OCH_3	*tert*-butyl	382	15.9	97.5	33.3
3	**II-1**	H	H	*tert*-butyl	*tert*-butyl	775	32.3	95.5	67.9
4	**II-4**	(1*R*,2*R*)-C_4H_8-		*tert*-butyl	*tert*-butyl	835	34.8	95.9	71.6

[a] Copolymerization conditions: Catalyst loading = 0.077 mol %, 4 g of oxetane, 2 equiv. of *n*-Bu_4NN_3, M/I =1292, 35 bar of CO_2, at 110°C for 24 h. [b] mol of oxetane consumed/mol of initiator. [c] mol of oxetane consumed/(mol of catalyst-h). [d] Estimated by ^{1}H NMR spectroscopy.

of the less hydroscopic $PPNN_3$ salt. As is evident under these conditions the molecular weight more closely tracks the predicted value.

Table II-3. Molecular Weights and Polydispersities of Poly(TMC).[a]

Entry	M/I	% Conversion[b]	M_n (GPC)	M_n (Theoretical)[c]	M_w/M_n (GPC)
1	150	99.5	11 200	15 200	1.26
2	275	90.7	9 500	25 500	1.45
3	350	48.5	6 700	17 300	1.43
4	475	29.7	7 050	14 400	1.60
5[d]	150	100.0	14 500	15 300	1.30

[a] Copolymerization conditions: Reactions carried out in toluene at 110°C using (salen)Cr(III)Cl catalyst, 2 equivalents of *n*-Bu_4NN_3 as cocatalyst at 35 bar CO_2 pressure. [b] Estimated by ^{1}H NMR spectroscopy. [c] M_n(theoretical) = M/I×mol.wt.(oxetane + CO_2) × % conversion. [d] Done in the absence of solvent using $PPNN_3$ as cocatalyst.

Retaining the salen ligand with the phenylene backbone while changing the substituents in the 3,5-positions of the phenolate rings (entries 1 and 2, Table II-2) reveals the Cr(III) salen derivative containing the bulky di-*tert*-butyl groups to be the more active. This is consistent with previous observations reported for the ROP of TMC catalyzed by aluminum and calcium salen complexes.[25-26, 56] On the other hand, for the copolymerization of cyclohexene oxide and CO_2 catalyzed by chromium salen complexes, higher catalytic activity was obtained in complexes containing methoxy and *tert*-butyl groups in the 3 and 5 positions of the phenolate rings.[45] We have also studied the effects of altering the diimine backbone of the Cr(III) salen complex while maintaining the di-*tert*-butyl groups in the 3,5-positions of the phenolate moiety (entries 3 and 4, Table II-2). As can be seen in Table II-2, the catalytic behavior of the chromium salen complexes is not much affected by changing the diimine backbone from ethylene to cyclohexylene, with the chromium salen complex with the cyclohexylene backbone displaying slightly higher catalytic activity.

Substrate Binding and Ring-Opening Steps Examined by Infrared Spectroscopy. Fundamental to a better understanding of the mechanism of the coupling reaction of oxetane and carbon dioxide is an investigation of the initiation step of this process. Since it is known that oxetane has less ring strain compared to epoxides, e.g., the heat of polymerization of ethylene oxide ($-\Delta H_p$ = 104 kJ/mol) differ from that of oxetane by 23 kJ/mol,[57] its ease of ring-opening should depart significantly from that of epoxides. In order to address this issue we have conducted cocatalyst, oxetane binding, and subsequent ring-opening studies via infrared spectroscopy using the (salen)CrN_3 complex containing di-*tert*-butyl substituents in the 3,5-positions of the phenolate rings, and an ethylene backbone for the diimine. We have employed the azide derivatives for these studies because the ν_{N_3} stretching vibration provides accessible probes for both cocatalyst binding and anion ring-opening steps. The results of these studies are depicted in **Scheme II-1** and Figure II-2.

Scheme II-1. Ring-Opening Step of Oxetane Catalyzed by (Salen)$Cr(N_3)_2^-$.

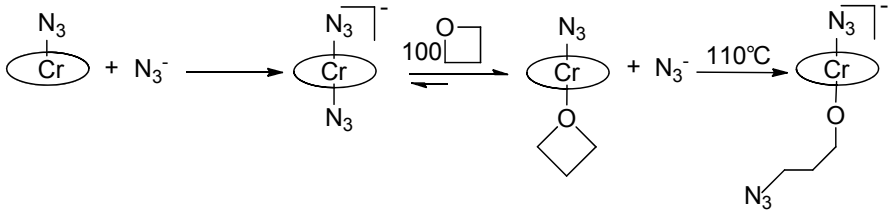

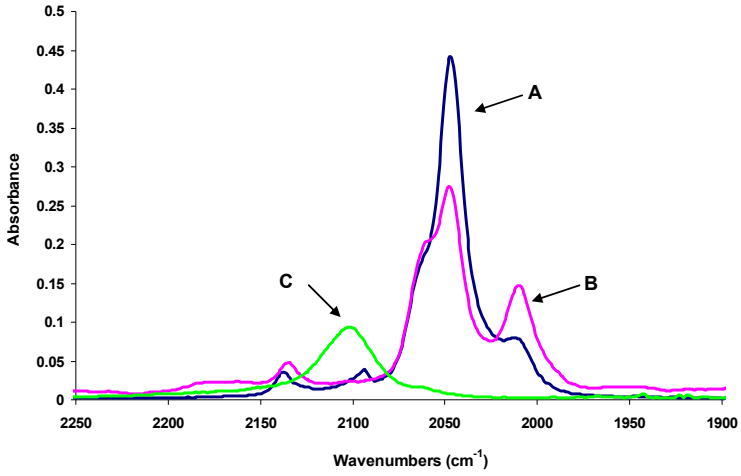

Figure II-2. Spectra of TCE solutions of chromium salen azide complex with 1 equivalent of *n*-Bu_4NN_3 (**A**), after addition of 100 equivalents of oxetane at room temperature (**B**), after heating the reaction solution at 110°C for 3 h (**C**).

As indicated in **Scheme II-1**, upon addition of one equivalent of *n*-Bu_4NN_3 to (salen)CrN_3, the anionic six-coordinate *bis*-azide species (salen)$Cr(N_3)_2^-$ readily forms at ambient temperature. This is apparent in the ν_{N_3} stretching region where the infrared band of (salen)CrN_3 shifts from 2083 cm^{-1} to a band at 2047 cm^{-1} with a shoulder at 2057 cm^{-1} upon addition of *n*-Bu_4NN_3. It should be noted here that the *n*-Bu_4N^+ salts of numerous (salen)CrX_2^- anions have been fully characterized by X-ray crystallography and these studies will be reported in Chapter III. For example, Figure II-3 illustrates the solid-state structure of the *bis*-azide anion of one such derivative. Addition of 100-fold excess of oxetane to the *bis*-azide complexes displaces some of the azide ligand as can be seen by an increase in the free azide ion concentration by its ν_{N_3} band at 2009 cm^{-1} with a concomitant decrease in the concentration of (salen)$Cr(N_3)_2^-$ (spectrum **B**). Moreover, a new ν_{N_3} stretching band appears at 2061 cm^{-1} which is assigned to (salen)Cr(N_3)•oxetane. Upon stirring this reaction mixture for 24 h at ambient

temperature no changes in the infrared spectrum resulted, indicative of the ring-opening process of oxetane requiring higher temperatures. Indeed, heating the reaction mixture for three hours at 110ºC led to oxetane ring-opening by azide as indicated by the organic azide band at 2100 cm^{-1}. It should be recalled that an analogous experiment carried out with cyclohexene oxide results in epoxide ring-opening by azide at ambient temperature, although the equilibrium between (salen)$Cr(N_3)_2^-$ and cyclohexene oxide lies much farther to the left.[45] That is, cyclohexene oxide has less of a penchant for displacing the azide from the chromium(III) center than the more basic oxetane monomer.

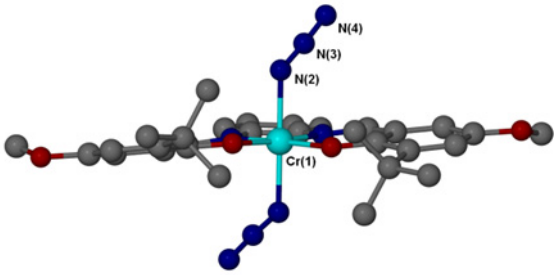

Figure II-3. Ball-and-stick representation of the X-ray defined structure of the anion of the [*n*-Bu_4N][(salen)$Cr(N_3)_2$] complex, where the salen ligand contains –OMe and –*t*-Bu substituents in the 3,5-positions of the phenolates respectively, with a phenylene diimine backbone.

X-ray crystallography was utilized in conjunction with the ν_{N_3} infrared spectral data (*vide supra*) to verify that oxetane binding to the chromium center occurs without ring-opening at ambient temperature. Two (salen)CrCl complexes with oxetane bound to the chromium centers were successfully characterized by X-ray crystallography. To

the best of our knowledge these represent the only crystal structures of oxetane bound to a metal center thus far reported in the literature. Crystallographic data pertaining to these two crystal structures are provided in Table II-4.

In our first attempt at isolating single crystals of a (salen)CrCl complex with an axially coordinated oxetane, the presence of trace quantities of water led to hydrolysis of the Cr–Cl bond. Nevertheless, crystals of a hydroxo-bridged structure with oxetane bound to one of the chromium centers were obtained which were suitable for X-ray analysis (Figure II-4 and Table II-5). Similar solid-state structures of hydroxo-bridged

Table II-4. Crystallographic Data for Complexes **II-5** and **II-6**.

	II-5	**II-6**
empirical formula	$C_{80}H_{110}ClCr_2N_4O_6$	$C_{34.40}H_{48.80}Cl_{3.20}Cr_{0.80}N_{1.60}O_{2.40}$
fw	1364.17	678.19
temperature (K)	110(2) K	110(2) K
crystal system	triclinic	triclinic
space group	*P*-1	*P*-1
a (Å)	12.266(5)	16.175(5)
b (Å)	14.702(5)	16.394(5)
c (Å)	21.630(5)	17.126(5)
α (deg)	102.839(5)	89.781(4)
β (deg)	95.784(5)	88.053(4)
γ (deg)	100.245(5)	79.249(4)
V (Å^3)	3702(2)	4459(2)
D_c (Mg/m^3)	1.223	1.263
Z	2	5
abs coeff (mm^{-1})	0.384	0.535
reflections collected	10087	41341
independent reflections	10392 [R(int) = 0.0755]	15610 [R(int) = 0.0612]
restrains/parameters	51/856	48/979
GOF on F^2	1.029	1.077
final *R* indices [$I > 2\sigma(I)$]	$^a R_1 = 0.0755$ $^b R_w = 0.1995$	$^a R_1 = 0.0579$ $^b R_w = 0.1433$
final *R* indices (all data)	$^a R_1 = 0.1239$ $^b R_w = 0.2321$	$^a R_1 = 0.0908$ $^b R_w = 0.1643$

$^a R = \sum||F_o| - |F_c||/\sum|F_o|$. $^b R_w = \{[\sum w(F_o^2 - F_c^2)^2]/[\sum w(F_o^2)^2]\}^{1/2}$
$w = 1/[\sigma^2(F_o^2) + (aP)^2 + bP]$, where $P = [(\max(F_o^2), 0) + 2(F_c^2)]/3$

chromium(III) derivatives have been reported by us resulting from the complete hydrolysis of (acacen)CrCl or (salen)CrOMe derivatives.[58] Complex **II-5** clearly shows that oxetane is capable of binding to the (salen)Cr(III) center without undergoing ring-

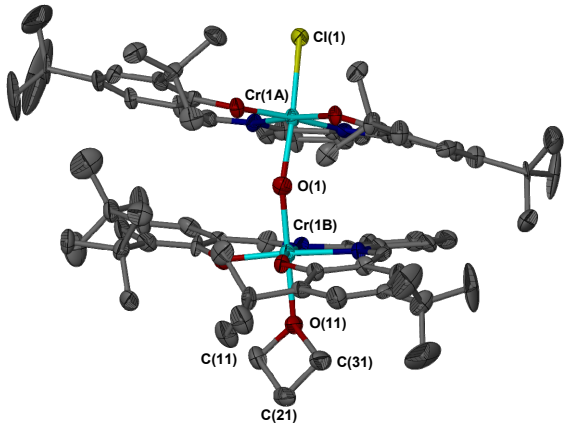

Figure II-4. Thermal ellipsoid plot of complex **II-5**. Ellipsoids are at the 50 % level. H atoms are omitted for clarity. One pentane molecule was crystallized in the unit cell and is omitted for clarity.

Table II-5. Selected Bond Distances and Angles for Complex **II-5**.[a]

Cr(1A)-Cl(1)	2.342(3)
Cr(1A)-O(1)	2.007(6)
Cr(1B)-O(1)	1.949(6)
Cr(1B)-O(11)	2.054(9)
O(11)-C(11)-C(21)	90.5(8)
O(11)-C(31)-C(21)	90.5(8)
C(11)-O(11)-C(31)	91.1(7)
C(31)-C(21)-C(11)	87.6(8)

[a] Units of bond angles and bond distances are (º) and (Å), respectively.

opening at ambient temperature. The oxetane molecule is disordered in complex **II-5**. Upon modeling the disorder two different positions for the oxetane ligand were found, where the dihedral angles of the plane C–O–C and C–C–C were determined to be 4.5º and 10.8º at 110K. That is, the oxetane molecule is not planar, which is in good agreement with the structure of free oxetane reported by Luger and Buschmann where the dihedral angle was found to be 10.7º at 90K and 8.7º at 140K.[59]

A successful isolation of single crystals of an oxetane adduct as depicted in **Scheme II-1** was achieved upon utilizing super dry conditions and low temperature. Complex **II-6** was fully characterized by X-ray crystallography and a thermal ellipsoid representation of this derivative is shown in Figure II-5, with selected bond distances and bond angles listed in Table II-6. Two molecules crystallized in the unit cell, where the sum of the angles in the oxetane ligands is 359.6º and 357.4º, respectively. The dihedral angles of the planes C–O–C and C–C–C in the oxetane ligands were found to be 10.5º and 11.8º at 110K, which clearly demonstrates that the oxetane molecule when bound to the metal center maintains its degree of nonplanarity. Metric parameters for free oxetane and bound oxetane in complex **II-6** are quite comparable as seen in Table II-7.

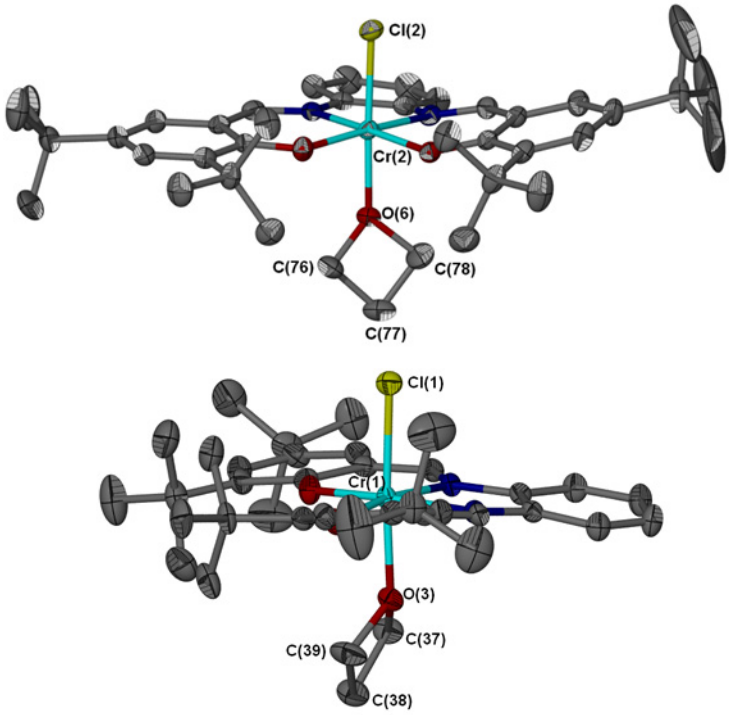

Figure II-5. Thermal ellipsoid plot of complex **II-6**. Ellipsoids are at the 50 % level. H atoms are omitted for clarity. Three dichloromethane and one pentane molecules were crystallized in the unit cell and are omitted for clarity.

Table II-6. Selected Bond Distances and Angles for Complex **II-6**.[a]

Cr(1)-Cl(1)	2.3167(6)
Cr(2)-Cl(2)	2.3036(7)
Cr(1)-O(3)	2.0456(10)
Cr(2)-O(6)	2.0528(11)
O(6)-C(76)-C(77)	90.75(11)
O(6)-C(78)-C(77)	90.88(12)
C(78)-C(77)-C(76)	85.72(12)
C(78)-O(6)-C(76)	90.08(11)

[a] Units for bond distances and bond angles are (Å) and (º), respectively.

Table II-7. Selected Bond Distances and Angles for Oxetane Molecules.[a]

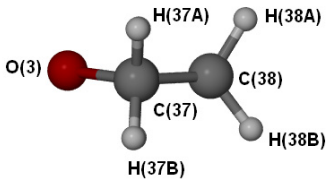

Oxetane molecule(1) from complex **II-6**.

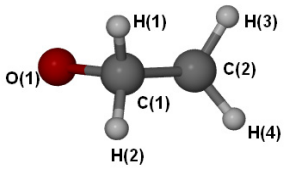

Free oxetane molecule from reference 59.

C(39)-O(3)	1.458(17)	O(3)-C(37)-C(38)	90.54(11)	C(1)-O(1)	1.433(2)	O(1)-C(1)-C(2)	91.89(9)
C(37)-O(3)	1.482(18)	O(3)-C(39)-C(38)	91.55(11)	C(3)-O(1)	1.433(2)	O(1)-C(3)-C(2)	91.89(9)
C(37)-C(38)	1.516(2)	C(39)-O(3)-C(37)	90.13(10)	C(1)-C(2)	1.517(2)	C(1)-O(1)-C(3)	90.5(1)
C(38)-C(39)	1.514(2)	C(39)-C(38)-C(37)	86.79(11)	C(2)-C(3)	1.517(2)	C(1)-C(2)-C(3)	85.0(1)
C(37)-H(37B)	0.99			C(1)-H(2)	0.99(2)		
C(38)-H(38B)	0.99			C(2)-H(4)	0.97(3)		
Dihedral angle of the plane C-O-C and C-C-C: 10.5				Dihedral angle of the plane C-O-C and C-C-C: 10.7			

[a]Units for bond distances and bond angles are (Å) and (º), respectively.

Kinetic Studies of the Copolymerization of Oxetane and Carbon Dioxide. Kinetic measurements of the coupling reaction of oxetane and carbon dioxide were performed in toluene solution in the presence of complex **II-4** along with two equivalents of *n*-Bu_4NN_3. These reactions were monitored by *in situ* infrared spectroscopy by observing the growth of the copolymer's $\nu_{C=O}$ band at 1750 cm^{-1} as a function of time. A typical reaction profile of the absorbance of the 1750 cm^{-1} infrared band with time is illustrated in Figure II-6. It should be noted as well in Figure II-6 that at the early stages of the coupling reaction a $\nu_{C=O}$ band at ~1770 cm^{-1} assigned to TMC was observed which subsequently disappeared. Furthermore, the presence of the induction period seen in Figure II-6 can be attributed to the drop in temperature of ~20ºC

observed following the addition of carbon dioxide to the 110ºC reaction mixture, as well as a slow initiation step.

The copolymerization reactions were demonstrated to be first-order in oxetane and catalyst (complex **II-4**) concentrations in the presence of two equivalents of *n*-Bu_4NN_3. This is shown in a representative case in Figure II-7 where a plot of $\ln[(A_\infty - A_t)/(A_\infty - A_o)]$ *vs.* time for the formation of copolymer is found to be linear, for A_∞ and A_t being the absorbance of the $\nu_{C=O}$ band of the copolymer at $t = \infty$ and t = time. It is important to note here that the data plotted in Figure II-7 is for the early portion of the reaction because at higher levels of conversion (>65%) the reaction solution becomes more viscous.[55] Similarly, the order of the reaction with regard to complex **II-4** was observed to be first-order based on the linear relationship between initial rate *vs.* complex **II-4** concentration (Figure II-8). As is readily seen in Figure II-8, the linear plot has a non- zero intercept of the x-axis of ~0.005 M, suggesting that a small quantity of the catalyst is degraded in the copolymerization process. Relevant to this latter point, when the copolymerization reaction is carried out under identical conditions except in neat oxetane at a catalyst concentration of 0.005 M the system is active for copolymer formation.

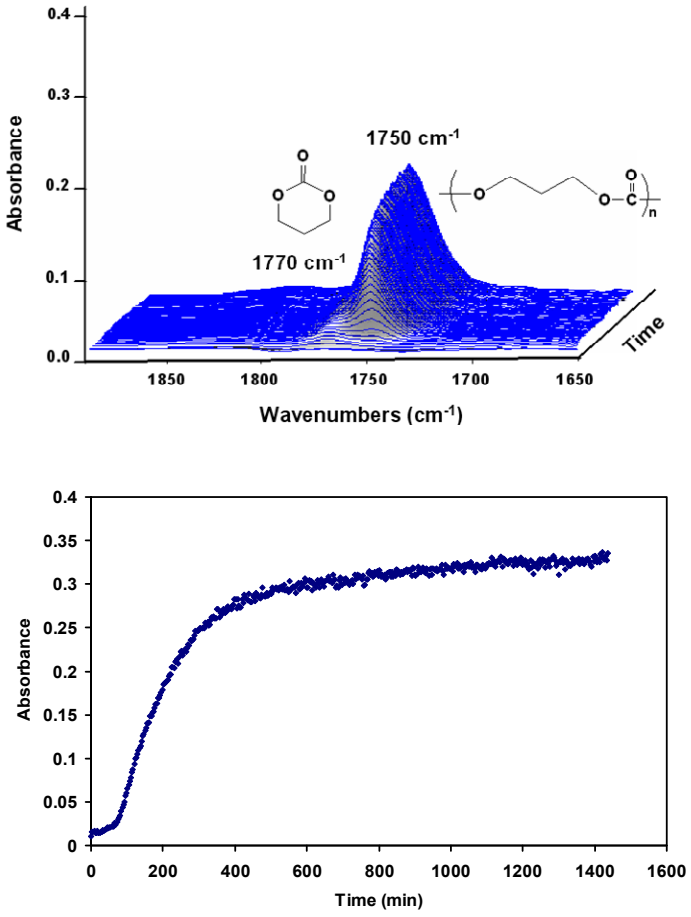

Figure II-6. Three-dimensional stack plot and reaction profile of the IR spectra collected every 3 min during the copolymerization reaction of oxetane and carbon dioxide. Reaction carried out at 110ºC in toluene at 35 bar CO_2 pressure, in the presence of complex **II-4** and 2 equiv. of *n*-Bu_4NN_3.

The dependence of the coupling of oxetane and carbon dioxide on the concentration of the anionic initiator (cocatalyst) was examined in the instance of *n*-Bu_4NN_3. As is evident in Figure II-9 the copolymerization rate was found to be first-order in [cocatalyst] up to approximately two equivalents of *n*-Bu_4NN_3. Hence, in the range of [*n*-Bu_4NN_3] investigated between 0.5 and 2.0 equivalents the copolymerization

process can be described as being first-order in oxetane, (salen)CrX, and cocatalyst concentrations, with zero-order dependence on [cocatalyst] greater than 8-10 equivalents. This latter behavior is to be expected for a reaction where the initiation step is not significantly faster than the propagation step.

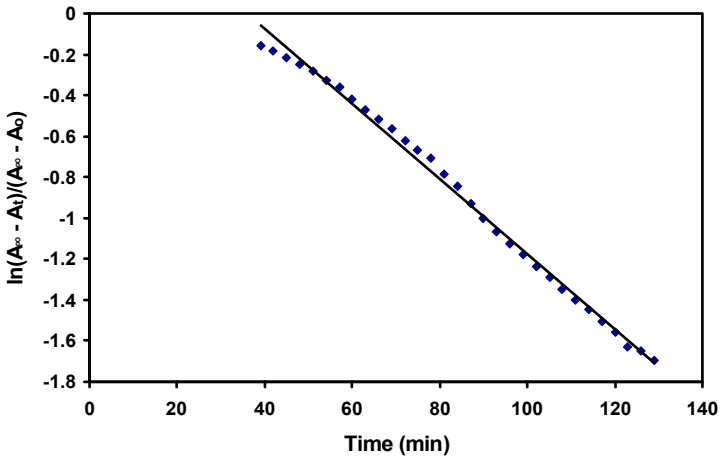

Figure II-7. First-order plot of the conversion of oxetane and CO_2 to poly(TMC). Reaction carried out in toluene at 110°C with complex **II-4** (0.0327 M), 2 equivalents of *n*-Bu_4NN_3 at 35 bar CO_2 pressure. Oxetane concentration = 4.92 M. Slope = -0.0183, y intercept = 0.6525 with $R^2 = 0.9946$.

The copolymerization of oxetane and CO_2 was performed at several temperatures between 80-110ºC and the rate constants for the process k_p, where rate = k_p[oxetane][catalyst][cocatalyst], were determined. These k_p values as a function of temperature are listed in Table II-8, with the corresponding Eyring plot depicted in Figure II-10. The calculated activation parameters, $\Delta H^{\ddagger}$ and $\Delta S^{\ddagger}$, were 45.6 ± 3 kJ/mol and -161.9 ± 8.2 J/mol-deg, respectively. In this instance the enthalpy of activation ($\Delta H^{\ddagger}$) is very similar to that observed for the copolymerization of cyclohexene oxide and

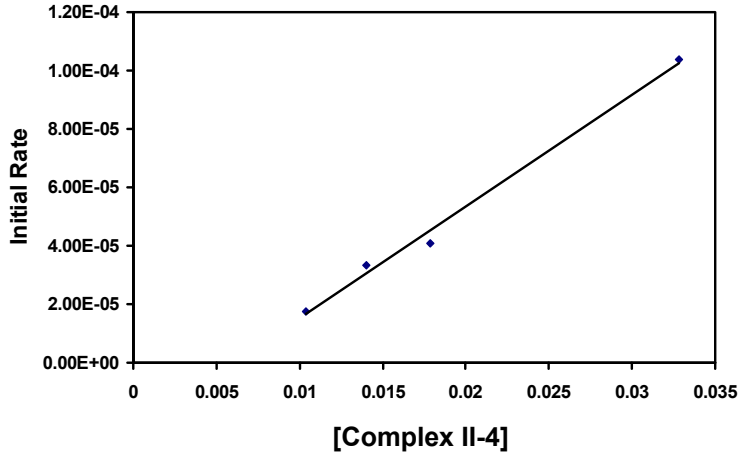

Figure II-8. Dependence of copolymerization reaction on [catalyst]. Reactions carried out in toluene at 110°C with complex **II-4**, 2 equivalents of *n*-Bu_4NN_3 at 35 bar CO_2 pressure. Oxetane concentration = 4.92 M. Initial rate *vs.* [complex **II-4**] provided a y intercept of -2.10^{-5} with $R^2 = 0.9931$.

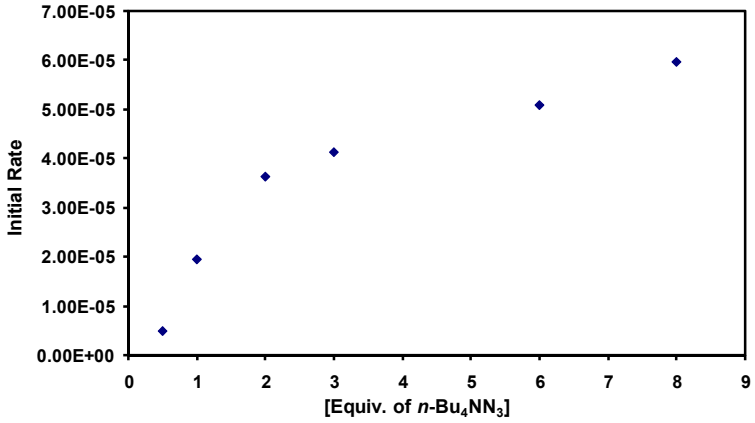

Figure II-9. Initial rates for production of poly(TMC) as a function of number of equivalents of cocatalyst. Reactions carried out in toluene at 110°C with complex **II-4** (0.014 M) and *n*-Bu_4NN_3 as cocatalyst, at 35 bar CO_2 pressure, oxetane concentration = 4.92 M.

Table II-8. Variable Temperature Rate Constants for the Copolymerization Reaction.[a]

T(K)	k_p (L^2/mol^2-s)
353	0.00449
363	0.00741
373	0.0103
383	0.0171

[a] Each experiment was performed in toluene with 0.014 M of complex **II-4** and 2 equivalents of *n*-Bu_4NN_3 at 35 bar CO_2 pressure. Oxetane concentration = 4.92 M.

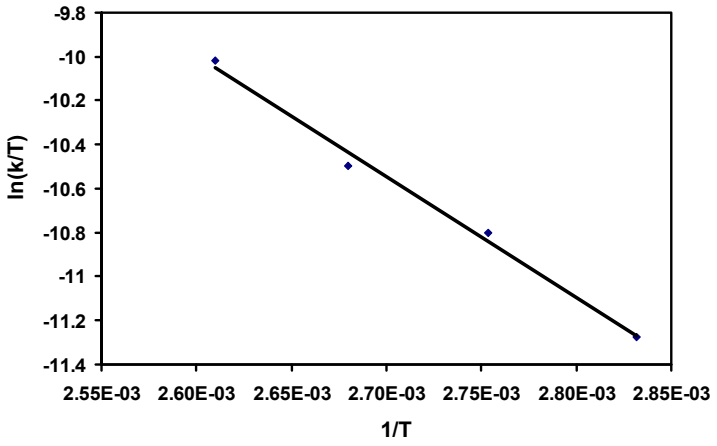

Figure II-10. Eyring plot for the formation of poly(TMC) in the presence of complex **II-4**/*n*-Bu_4NN_3 catalyst system in toluene. Slope = -5502.5 with R^2 = 0.992.

CO_2 (45.5 kJ/mol), and lower than that for the process involving the monomers propylene oxide and CO_2 (66.2 kJ/mol) employing a similar catalyst system.[60]

Solution Kinetic Studies of the Ring-Opening Polymerization of Trimethylene Carbonate. Herein we wish to describe in detail kinetic measurements for the ring-opening polymerization of trimethylene carbonate to poly(TMC), equation (I-2), under comparable conditions to that reported above for the copolymerization of

oxetane and CO_2 leading to poly(TMC). In this instance the use of 1,1,2,2-tetrachloroethane was found to be advantageous because of its high boiling point, and the high solubility of both monomer and polymer in a chlorinated solvent. These reactions were monitored by ^1H NMR spectroscopy. Figure II-11a displays a typical monomer consumption *vs.* time plot, whereas the semilogarithmic plot of $-\ln([monomer]_0/[monomer]_t)$ *vs.* time is displayed in Figure II-11b, and as might be expected the polymerization reaction was found to be first-order with respect to [TMC]. Table II-9 summarizes the determined rate constants (k_{obsd}) for the ROP of TMC as a function of [catalyst] and [cocatalyst]. Log-log plots of the rate constants (k_{obsd}) *vs.* [catalyst] and [cocatalyst] reveal relationships between $\ln k_{obsd}$ *vs.* ln[catalyst] or ln[cocatalyst] with slopes close to unity, thus, indicative of the polymerization reaction being first-order in [catalyst] and first-order with respect to [cocatalyst] up to 1 equivalent of cocatalyst.

Figures II-12 and II-13 illustrate the effect of excess quantities of cocatalyst (*n*-Bu_4NN_3) on the rate constant of the ring-opening polymerization process. As can be readily seen, the ROP reaction ultimately becomes independent of [cocatalyst] loadings as would be expected. A double reciprocal plot of these data reveals a linear relationship with a limiting rate constant (k_{obsd}) of 0.059 h^{-1} at 120ºC.

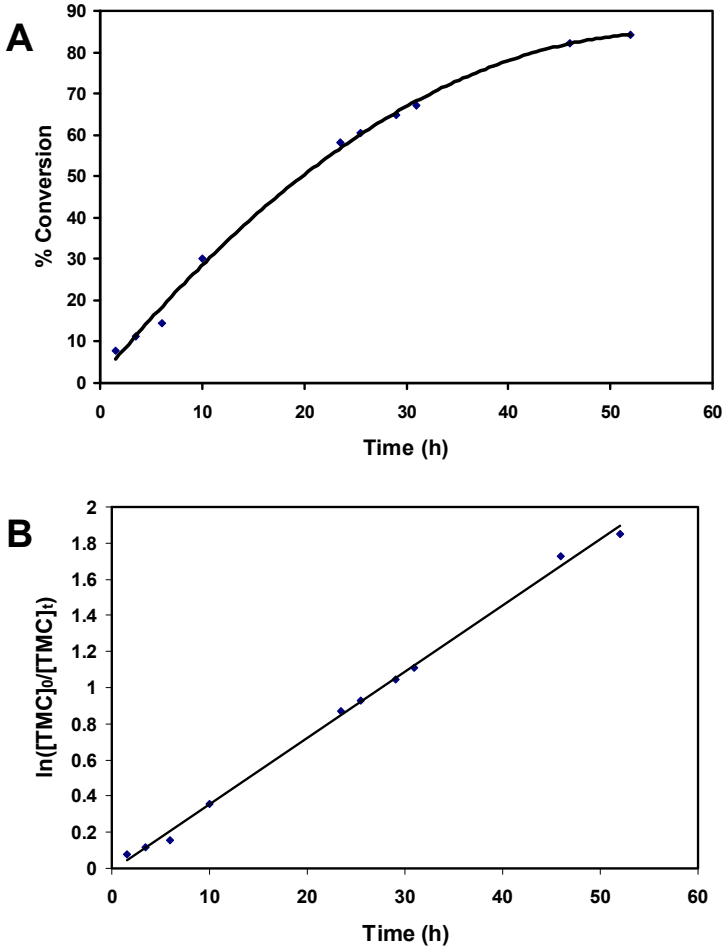

Figure II-11. (**A**) Plot of monomer conversion *vs.* time. (**B**) First-order plot of the conversion of TMC to poly(TMC). Reaction carried out in TCE at 120°C with complex **II-4** (0.00506 M) and 2 equivalents of *n*-Bu_4NN_3 (0.0098 M). TMC concentration = 0.98 M. Slope = 0.0366, y intercept = -0.0092 with R^2 = 0.9975.

Table II-9. Rate Constant Dependence on the Concentrations of Catalyst and Cocatalyst for the ROP of TMC.[a]

Entry	[catalyst](mol/L)	Equiv. of *n*-Bu_4NN_3	Temperature (°C)	k_{obsd} (h^{-1})
1	0.00253	2	120	0.0169
2	0.00380	2	120	0.0295
3	0.00506	2	120	0.0366
4	0.01010	2	120	0.071
5	0.00506	0	120	0.0055
6	0.00506	0.5	120	0.0168
7	0.00506	0.75	120	0.0225
8	0.00506	1	120	0.0275
9	0.00506	2	120	0.0366
11	0.00506	3	120	0.0414
12	0.00506	6	120	0.0473
13	0.00506	8	120	0.0530

[a] Monomer concentration held at 0.98 M. Reactions carried out in 1,1,2,2,-tetrachloroethane.

The ring-opening polymerization of TMC was carried out over the temperature range of 105-130ºC in order to obtain the activation parameters for this process. The rate constants of the ring-opening reaction, k_p, are listed in Table II-10. The activation parameters $\Delta H^{\ddagger}$ and $\Delta S^{\ddagger}$ calculated from the Erying plot shown in Figure II-14 were determined to be 74.1 ± 3.0 kJ/mol and -72.3 ± 8.3 J/mol-K, respectively. These parameters are consistent with a reaction pathway involving the attack of a nucleophilic center (polymer chain end) to a metal-bound cyclic carbonate (*vide infra*). The $\Delta G^{\ddagger}$ value of 101.9 kJ/mol at 110ºC for the ROP of TMC is quite similar to the comparable $\Delta G^{\ddagger}$ found for the copolymerization of oxetane and CO_2 of 107.6 kJ/mol. This small difference in $\Delta G^{\neq}$ for oxetane/CO_2 copolymerization and ring-opening polymerization of TMC clearly demonstrates that the two processes are energetically quite similar. Hence, the formation of polycarbonate from the oxetane and CO_2 coupling reaction could be occurring via two different or concurrent pathways, i.e., the intermediacy of TMC

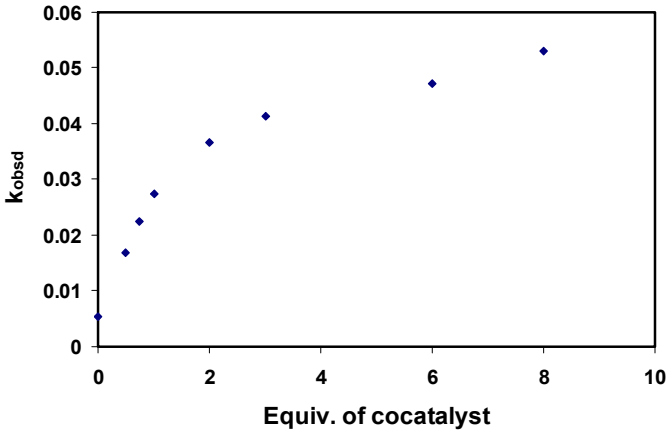

Figure II-12. Rate constant for production of poly(TMC) as a function of number of equivalents of cocatalyst (n-Bu_4NN_3). Data taken from Table II-9.

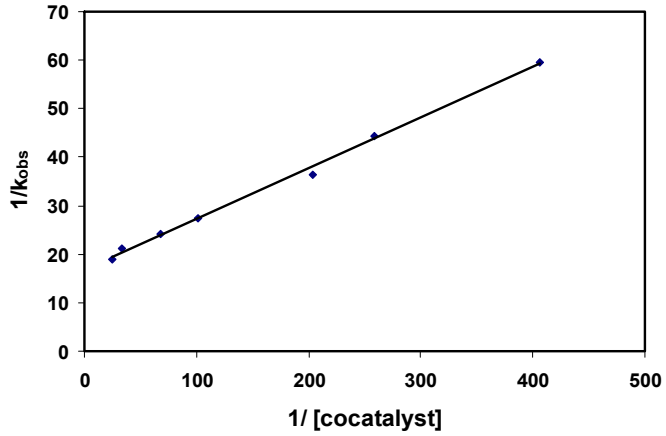

Figure II-13. Double reciprocal plot of the rate constant dependence of the ROP process with [cocatalyst]. Data taken from Table II-9. Slope = 0.1044 and y intercept = 16.792 with $R^2 = 0.9966$.

formation and subsequent polymerization and/or the direct enchainment of oxetane and CO_2. Indeed, *in situ* infrared spectroscopic monitoring of the copolymerization reaction suggest both pathways are operative (*vide supra*). Further studies detailed below based

on monitoring of the coupling of oxetane and CO_2 by ^1H NMR spectroscopy, accompanied by end-group analysis of the low molecular weight copolymers produced, are designed to more definitively address this issue.

Table II-10. Variable Temperature Rate Constants for the Polymerization Reaction.[a]

T(K)	$k_p(L^2/mol^2\text{-}s)$
378	0.07621
383	0.10469
393	0.19854
403	0.34825

[a] Each experiment was performed in TCE with complex **II-4** (0.00506 M) and *n*-Bu_4NN_3 as cocatalyst (0.0098 M), TMC concentration = 0.98 M.

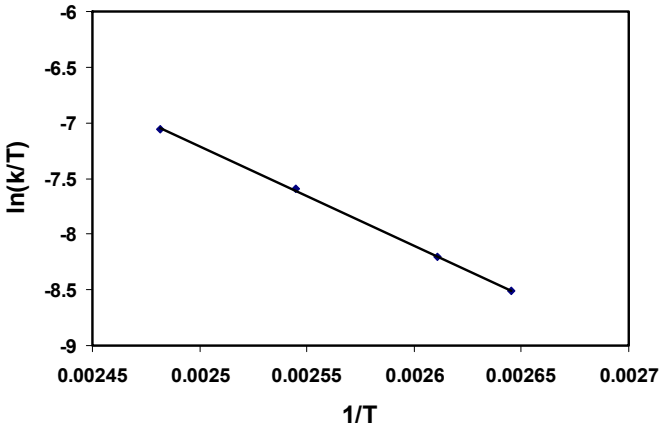

Figure II-14. Eyring plot for the formation of poly(TMC) in the presence of complex **II-4**/*n*-Bu_4NN_3 catalyst system in TCE. Slope = -8910.7 with $R^2 = 0.9997$.

Further Mechanistic Insight into the Oxetane and Carbon Dioxide Coupling Process. As mentioned above, an inquiry of the mechanistic aspects of the oxetane and carbon dioxide coupling reaction was undertaken utilizing ^{1}H NMR spectroscopy studies which should provide a better assessment of the role of trimethylene carbonate in this process. The copolymerization reactions were performed under identical conditions as previously described herein, i.e., complex **II-4**/2 equivalents of *n*-Bu_4NN_3, 35 bar CO_2, 110ºC and catalyst loading of 0.28 mol%. For these investigations, analysis of the reaction mixture was done by manually sampling a small aliquot withdrawn from the stainless steel reactor with subsequent quenching of the reaction's progress by cooling the solution to 10ºC. As was observed during this process by *in situ* infrared spectroscopic monitoring, formation of TMC was detected prior to poly(TMC) formation. That is, the initial formation of TMC was detected within 30 min by the appearance of a triplet at 4.43 ppm and a quintet at 1.98 ppm, with its consequent consumption to produce polycarbonate. After four hours of reaction no TMC was observed in the reaction mixture. Hence, it is apparent that in the early stages of the reaction a portion of the polycarbonate results from the ring-opening of trimethylene carbonate. This observation, coupled with the presence of some ether linkages in the copolymer, strongly supports the conclusions that both oxetane/CO_2 enchainment and TMC ring-opening are occurring simultaneously. End-group analyses of the polycarbonates produced from oxetane/CO_2 copolymerization and ROP of TMC were carried out in an effort to further corroborate these claims.

Figure II-15 illustrates the ^{1}H NMR spectrum of a purified polycarbonate sample obtained from the copolymerization of oxetane and carbon dioxide. *Purification of the copolymer was achieved by precipitation from a dichloromethane solution with 1 M HCl in methanol, followed by vacuum drying.* In $CDCl_3$ the copolymer exhibits two major signals at 4.23 ppm (t, 4H, $^{3}J_{HH}$ = 6.3 Hz, –OC*H*$_2$) and 2.05 ppm (quint, 2H, $^{3}J_{HH}$ = 5.9 Hz, –C*H*$_2$). Ether linkages were observed in the copolymer at 3.50 ppm (t, 4H, $^{3}J_{HH}$ = 5.9 Hz, –OC*H*$_2$) and 1.90 ppm (quint, 2H, $^{3}J_{HH}$ = 5.9 Hz, –C*H*$_2$). A –CH_2OH end group was observed before and after purification of the copolymer sample. These latter proton resonances appeared at 4.29 ppm (t, 2H, $^{3}J_{HH}$ = 6.0 Hz, –C*H*$_2$), 3.73 ppm (t, 2H, $^{3}J_{HH}$ = 6.3 Hz, –C*H*$_2$), and 1.90 ppm (quint, 2H, $^{3}J_{HH}$ = 5.9 Hz, –C*H*$_2$).[30, 34, 61] The presence of an organic azide end group (–CH_2N_3) was also seen in the ^{1}H NMR spectrum of the copolymer at 3.43 ppm (t, 2H, $^{3}J_{HH}$ = 6.3 Hz, –C*H*$_2$), with the other two resonances being obscured by the intense polymer signals at 4.23 and 2.05 ppm. This assignment was made based on the ^{1}H NMR spectrum in $CDCl_3$ of a model compound (3-azido-propan-1-ol), which showed signals at 3.74 ppm (t, 2H, $^{3}J_{HH}$ = 6.0 Hz, –C*H*$_2$OH), 3.47 ppm (t, 2H, $^{3}J_{HH}$ = 6.6 Hz, –C*H*$_2$N$_3$), 1.83 ppm (quint, 2H, $^{3}J_{HH}$ = 5.9 Hz, –CH_2C*H*$_2$$CH_2$), and 1.77 ppm (s, 1H, –O*H*). In addition, the infrared spectrum of this copolymer exhibited an organic azide ν_{N_3} mode at 2100 cm^{-1} in TCE. Finally, the polycarbonate displayed a ^{1}H NMR resonance a 3.79 ppm (s, 3H) attributed to the –OC(O)OC*H*$_3$ end group resulting from methanolysis of the original –OC(O)N_3 end group following copolymer purification from MeOH.[61]

Based on the above observations we can conclude that two initiation pathways are operative following the initial generation of some trimethylene carbonate via a back-biting process involving the carbonate species afforded from Pathway 1 (**Scheme II-2**).

In a similar fashion, a low molecular weight polycarbonate obtained from the ring-opening polymerization of trimethylene carbonate was analyzed by ^{1}H NMR spectroscopy. Figure II-16 illustrates the ^{1}H NMR spectrum of the resulting poly(TMC)

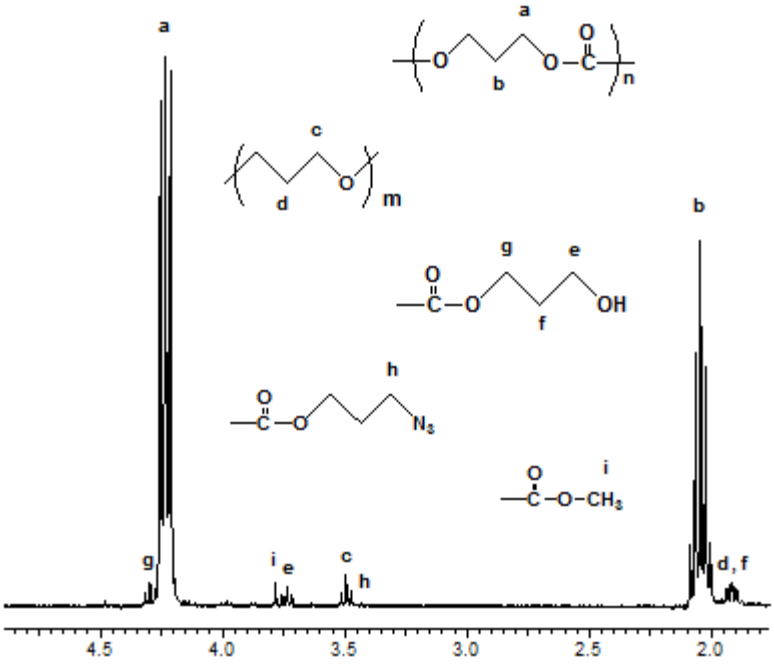

Figure II-15. ^{1}H NMR spectrum in $CDCl_3$ of poly(TMC) obtained by way of oxetane/CO_2, in the presence of (salen)Cr(III)Cl /*n*-Bu_4NN_3 as the catalytic system. Polymer was purified from dichloromethane and 1 M HCl solution in methanol.

Scheme II-2. Proposed Initiation Pathways.

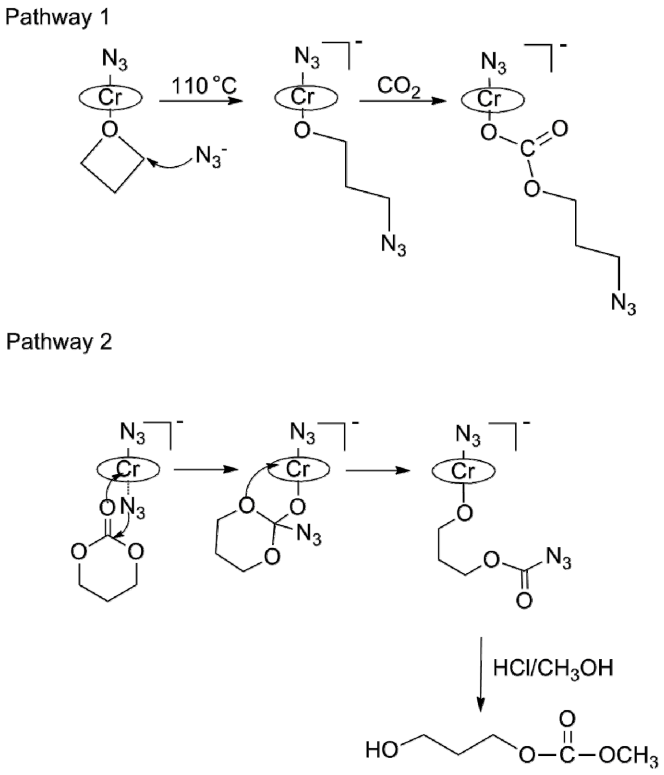

sample in $CDCl_3$, which exhibits as expected, two major resonances at 4.23 ppm (t, 4H, $^3J_{HH}$ = 6.0 Hz, –OCH_2) and 2.05 ppm (quint, 2H, $^3J_{HH}$ = 6.3 Hz, –CH_2). *Importantly, no ether linkages were observed in this polycarbonate.* A $–CH_2OH$ end group was observed before and after polymer purification, with ^{1}H NMR resonances appearing at 4.29 ppm (t, 2H, $^3J_{HH}$ = 6.0 Hz, –CH_2), 3.73 ppm (t, 2H, $^3J_{HH}$ = 6.0 Hz, –CH_2), and 1.90 ppm (quint, 2H, $^3J_{HH}$ = 6.3 Hz, –CH_2). The presence of an organic azide end group was also seen in the polymer sample at 3.43 ppm (t, 2H, $^3J_{HH}$ = 6.3 Hz, –CH_2N_3) and 2100 cm^{-1} in the ^{1}H NMR and infrared spectra, respectively. Similarly, the presence of an

–OC(O)OCH_3 end group at 3.79 ppm (s, 3H) was observed following polymer purification from methanol. The latter observations, i.e., the presence of –CH_2N_3 and –OC(O)OCH_3 end groups in the polymer produced from TMC, established that the ring-opening of TMC under these catalytic conditions occurs via both acyl-oxygen and alkyl-oxygen bond cleavage modes (**Scheme II-3**). Previously, we and others have reported that the mechanism for ring-opening polymerization of TMC occurs exclusively by acyl-oxygen bond cleavage.[25, 29, 62] However, the presence of an organic azide end group in the poly(TMC) sample obtained by this route utilizing the (salen)CrCl/*n*-Bu_4NN_3 catalytic system, suggests that under these higher temperatures the ring-opening polymerization of TMC could also be initiated by an alkyl-oxygen bond cleavage.

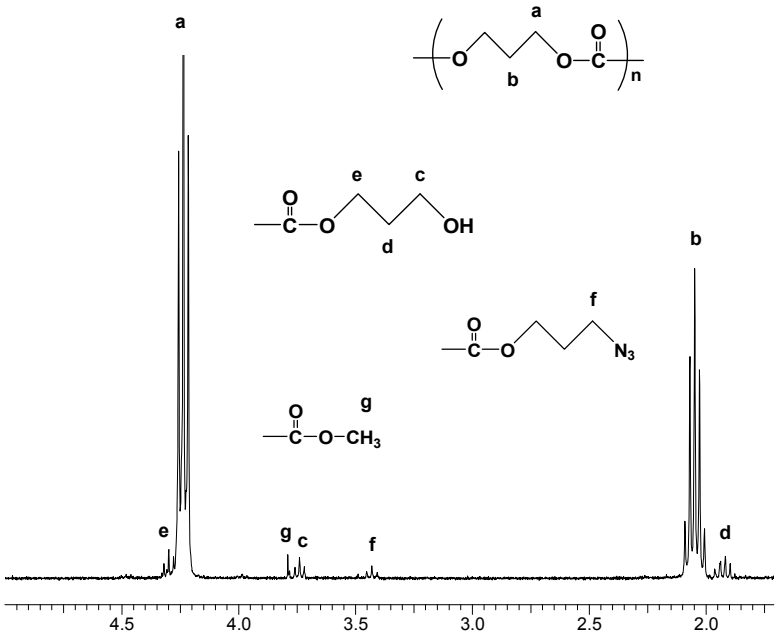

Figure II-16. ^{1}H NMR spectrum in $CDCl_3$ of poly(TMC) sample obtained by ROP of TMC in the presence of (salen)Cr(III)Cl/*n*-Bu_4NN_3 as the catalytic system. Polymer was purified from dichloromethane and 1 M HCl solution in methanol.

Scheme II-3. Proposed Initial TMC Ring-Opening Pathways.

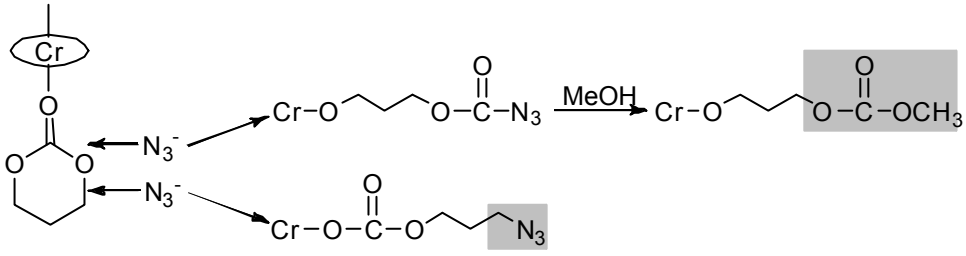

Scheme II-4 summarizes the proposed mechanistic aspects for the copolymerization of oxetane and carbon dioxide based on our current experimental findings. Although we have indicated only one of the chromium bound azide ligands taking part in the reaction, both are most likely involved. It is felt that only one copolymer chain grows from a single chromium center. In other words, the second azide ligand in the anionic chromium species is probably displaced by oxetane following the ring-opening process, with subsequent incorporation into the copolymer as an end group. Evidence for this is seen in Figure II-2, where upon complete ring-opening of oxetane (spectrum **C**) there is not metal bound or free azide present in the spectrum. As pointed out in the transition state illustrated in **Scheme II-4** of the initiation step, the azide ion has some association with the chromium center during the ring-opening process, as would be expected for the growing copolymer chain. Following the initial ring-opening step and CO_2 insertion into the resultant chromium-oxygen bond, two pathways are open for the intermediate. Route (1) involves consecutive additions of oxetane and CO_2 to yield the alternating copolymer, where route (2) leads to TMC formation by a back-biting proce ss with ring closure. Once TMC is formed it can enter the copolymer chain.

Scheme II-4. Proposed Reaction Mechanism.

Initiation Step

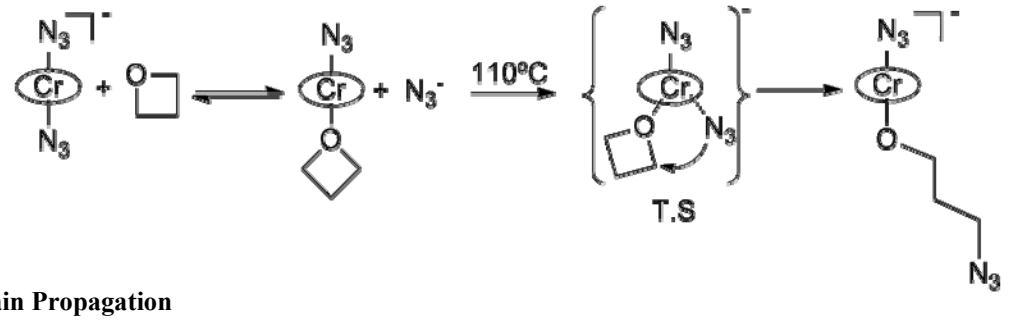

Chain Propagation

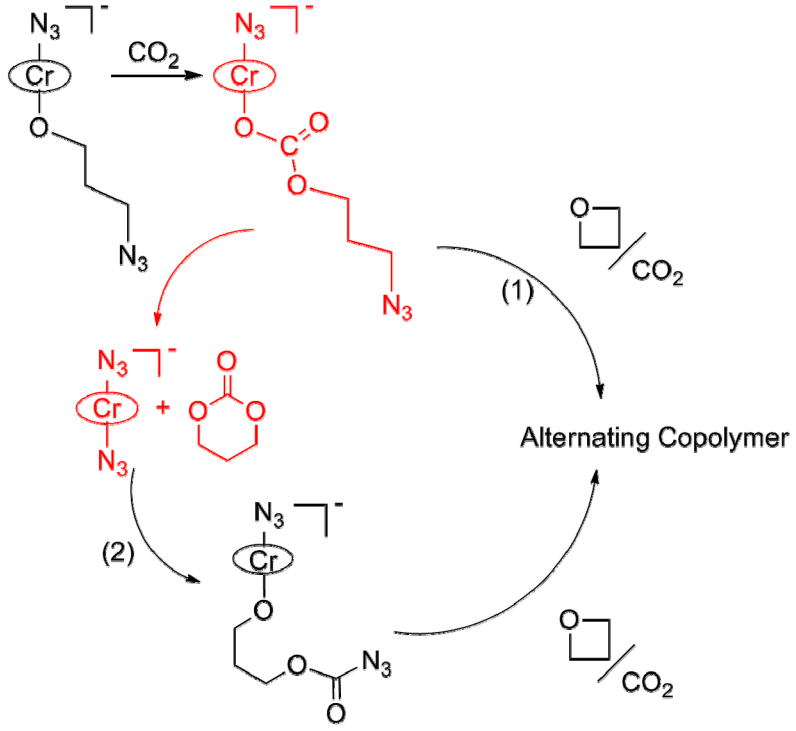

Chain Termination

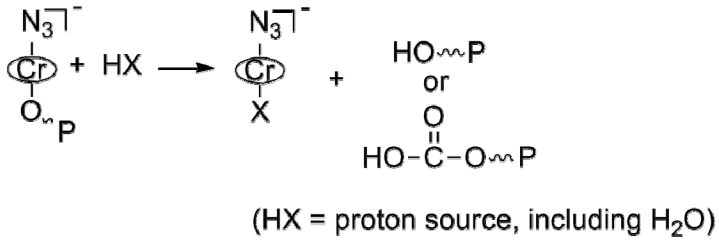

by a coordination-insertion mechanism. The portion of route (2) shown in red should be highly dependent on the nature of the anionic leaving group. *Indeed, we have noted for the bromide ion that this pathway is competitive with oxetane enchainment, and may provide a means for tuning the selectivity of the two pathways for poly(TMC) formation.* An advantage of proceeding exclusively via route (2) is the absence of ether linkages in the afforded polycarbonate.

Concluding Remarks

In summary, we have shown that chromium(III) salen complexes along with anionic initiators are effective catalysts for the copolymerization of oxetane and carbon dioxide. Optimization of the chromium catalyst was achieved utilizing a salen ligand with *tert*-butyl substituents in the 3,5-positions of the phenolate rings and a cyclohexylene backbone in the diimine, along with an azide ion as an initiator. Structural studies showed that oxetane binding to the chromium center occurred with little changes in its metric parameters as compared with the free cyclic ether. In particular, it remained nonplanar with the dihedral angle of the planes C–O–C and C–C–C being 10.5º at 110K. Kinetic measurements performed employing *in situ* infrared monitoring showed the oxetane/CO_2 coupling reaction to be first-order in oxetane, metal catalyst, and anionic initiator; with the latter exhibiting zero-order dependence at high concentrations. Furthermore, both infrared and ^{1}H NMR spectroscopy demonstrated the production of trimethylene carbonate in the early stages of the copolymerization process. Nevertheless, the presence of ether linkages in the copolymer clearly revealed that direct enchainment of oxetane and CO_2 into the growing

polymer chain occurs. The similarity of the free energy of activation of the copolymerization reaction of CO_2 and oxetane and the ring-opening polymerization of trimethylene carbonate supports these findings. In the following Chapers studies focused at tuning the selectivity of the oxetane and CO_2 coupling process for cyclic carbonate or copolymer by altering the anionic initiator or by using metal salen derivatives in oxidation state +2 will be presented.

CHAPTER III

MECHANISTIC INSIGHT INTO THE INITIATION STEP OF THE COUPLING REACTION OF OXETANE OR EPOXIDES AND CO_2 CATALYZED BY (SALEN)CrX COMPLEXES*

Introduction

As previously discussed in Chapter I, metal(III) salen complexes (where M = Cr, Co, or Al) have demonstrated to be the most effective and importantly most robust catalysts for the epoxide/CO_2 copolymerization process.[8a, b, 8f] Jacobsen and coworkers have clearly shown that an intermolecular bimetallic pathway for asymmetric nucleophilic ring-opening of epoxides catalyzed by (salen)CrX derivatives is operative (**Scheme III-1**).[63] However, in the absence of an added or endogenous source of cocatalyst these five-coordinate complexes are not effective catalysts for the copolymerization of CO_2 and epoxides. This is presumably a consequence of the metal center being too electrophilic to facilitate the CO_2 insertion reaction.[64] Relevant to this latter point, the Darensbourg group has recently demonstrated the ring-opening reaction of epoxides to be second-order in the five- coordinate Schiff base complex of manganese(III), (tfacacen)MnN_3 (tfacacen = *N,N*'-bis(trifluoroacetylacetone)-1,2-

---

*Reproduced in part with permission from "Mechanistic Insight into the Initiation Step of the Coupling Reaction of Oxetane or Epoxides and CO_2 Catalyzed by (Salen)CrX Complexes." Darensbourg, D. J.; Moncada, A. I. *Inorg. Chem.* **2008**, *47*, 10000-10008. Copyright 2008 American Chemical Society.

ethylenediamine), and at the same time to be ineffective at catalyzing the copolymerization of epoxide and CO_2.[65]

In the presence of various cocatalysts, e.g., heterocyclic amines and anionic nucleophiles, however, (salen)M(III)X (M = Cr and Co) are very reactive catalysts for the coupling of epoxides and CO_2.[8b] As shown in the previous Chapter, the chromium catalytic system has demonstrated to be active for the copolymerization of oxetane and CO_2 via a closely related mechanistic pathway to that of epoxides and CO_2. Anions derived from PPN^+($(Ph_3P)_2N^+$) and tetraalkylammonium$^+$ salts are the most active cocatalysts discovered to date.

Scheme III-1. Bimetallic Pathway for Asymmetric Nucleophilic Ring-Opening of Epoxides.

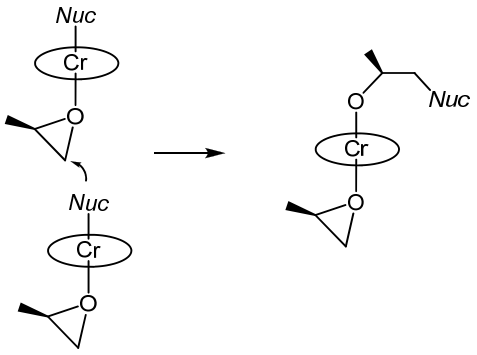

Herein, we wish to report on the structural characterization of complexes resulting from the reaction of (salen)CrX complexes with PPNX or *n*-Bu_4NX salts which serve as catalysts for the copolymerization processes described in equations I-1 and I-5.

In addition, comparative monomer binding to the chromium center and subsequent ring-opening steps of epoxides and oxetanes will be discussed.

Experimental Section

Reagents and Methods. Unless otherwise specified, all syntheses and manipulations were carried out on a double-manifold Schlenk vacuum line under an atmosphere of argon or in an argon filled glove box. Toluene and tetrahydrofuran were freshly distilled from sodium/benzophenone. Ethanol and methanol were freshly distilled from Mg/I_2. 1,1,2,2-tetrachloroethane was freshly distilled over CaH_2. Diethyl ether, dichloromethane, pentane, and hexanes, were purified by an MBraun Manual Solvent Purification System packed with Alcoa F200 activated alumina desiccant. Other chemicals employed in these studies, and their origin in parentheses, are provided below. Oxetane (Alfa Aesar) was freshly distilled over CaH_2 and stored in the freezer of the glove box. Cyclohexene oxide (TCI) and propylene oxide (Aldrich) were freshly distilled over CaH_2 before use. $PPNN_3$, PPNCN, and PPNNCO ($PPN^+ = (Ph_3P)_2N^+$) were synthesized according to a published procedure for the synthesis of $PPNN_3$.[48] Tetra-*n*-butylammonium bromide (Aldrich), tetra-*n*-butylammonium iodide (Eastman) and tetra-*n*-butylammonium chloride (TCI) were recrystallized from acetone/diethyl ether before use. Tetra-*n*-butylammonium azide (TCI) was stored in the freezer of the glove box upon arrival. Ethylenediamine (Aldrich), 1,2-phenylenediamine (ACROS), chromium(II) chloride (Alfa Aesar), and sodium sulfate (EMD) were used as received. Bone-dry carbon dioxide supplied in a high-pressure cylinder and equipped with a liquid

dip tube was purchased from Scott Speciality Gases. The corresponding salen ligands and chromium complexes were synthesized as previously described.[45]

IR spectra were recorded on a Mattson 6021 Fourier Transform (FT) IR spectrometer with a MCT detector. Analytical elemental analysis was provided by Canadian Microanalytical Services Ltd. High-pressure reaction measurements were performed using an ASI ReactIR 1000 reaction analysis system with a stainless steel Parr autoclave modified with a permanently mounted ATR crystal (SiComp) at the bottom of the reactor (purchased from Mettler Toledo).

Cocatalyst, Substrate Binding, and Ring-Opening Steps Examined by Infrared Spectroscopy. Cocatalyst, substrate binding, and ring-opening step studies were examined by solution infrared spectroscopy. The catalytic system used in these studies was a (salen)CrCl complex **III-1** (*N,N*'-bis(3,5-di-*tert*-butylsalicylidene)-1,2-ethylenediamino chromium(III) chloride) (50 mg) or a (salen)CrN_3 complex **III-2** (*N,N*'-bis(3,5-di-*tert*-butylsalicylidene)-1,2-ethylenediamino chromium(III) azide) (50 mg) in the presence of *n*-Bu_4NN_3 or *n*-Bu_4NCl as cocatalysts, and using TCE as the solvent (4 mL).

Statistical Deconvolution of FTIR Spectra. Where noted FTIR spectra were deconvoluted using Peakfit, version 4.12 (*Peakfit for Windows*, v. 4.12; SYSTAT Software Inc: San Jose, CA, 2003). Statistical treatment was a residuals method utilizing a combination Gaussian-Lorentzian summation of amplitudes with a linear baseline and Savitsky-Golay smoothing.

X-ray Structural Studies. Single crystals of (salen)$Cr(Cl)_2^-$*n*-Bu_4N^+ (complex **III-3**) were obtained by layering hexanes into a saturated dichloromethane solution of the corresponding (salen)CrCl complex (*N,N*'-bis(3-*tert*-butyl-5-methoxysalicylidene)-1,2-phenylenediamino chromium(III) chloride) containing two equivalents of *n*-Bu_4NCl. Anal. Calcd for $C_{47}H_{72}Cl_4CrN_3O_4$: C, 60.25; H, 7.15; N, 4.49. Found: C, 60.73; H, 7.91; N, 4.45.

Single crystals of (salen)$Cr(N_3)_2^-$*n*-Bu_4N^+ (complex **III-4**) were obtained in a similar manner as above employing 2 equivalents of *n*-Bu_4NN_3. Anal. Calcd for $C_{46}H_{70}CrN_9O_4$: C, 63.86; H, 8.16; N, 14.57. Found: C, 61.84; H, 7.96; N, 12.20. IR (TCE, cm^{-1}): 2057 (sh) and 2047 (s, N_3^-). Single crystals of (salen)$Cr(CN)_2^-PPN^+$ (complex **III-5**) were obtained in a similar manner as above employing 2 equivalents of PPNCN. Anal. Calcd for $C_{68}H_{64}CrN_5O_4P_2$: C, 72.33; H, 5.71; N, 6.20. Found: C, 70.31; H, 6.01; N, 5.80. IR (TCE, cm^{-1}): 2118 (w, CN^-). Single crystals of (salen)$Cr(NCO)_2^-PPN^+$ (complex **III-6**) were obtained in a similar manner as above employing 2 equivalents of PPNNCO. Anal. Calcd for $C_{70}H_{68}Cl_4CrN_5O_6P_2$: C, 63.16; H, 5.15; N, 5.26. Found: C, 63.12; H, 5.14; N, 5.20. IR (TCE, cm^{-1}): 2211 (s, NCO^-). Single crystals of (salen)$Cr(Cl)_x(N_3)_y^-PPN^+$ (complex **III-7**) were obtained in a similar manner as above employing 1 equivalent of $PPNN_3$. ESI-MS: *m/z* 608.18 [(salen)$Cr(Cl_2)^-$], 615.23 [(salen)Cr(Cl)$(N_3)^-$], 622.2 [(salen)$Cr(N_3)_2^-$] and 632.23 ([(salen)Cr(Cl)$(OAc)^-$]. IR (TCE, cm^{-1}): 2051 (b, N_3^-).

For all crystal structures, a Bausch and Lomb 10× microscope was used to identify suitable crystals. Each crystal was coated in paratone, affixed to a nylon loop, and placed under streaming nitrogen (110K) on a Bruker - AXS Apex II three-circle, a Bruker-D8 Adv GADDS or on a Bruker SMART 1000 CCD X-ray diffractometer. Space group determinations were made on the basis of systematic absences and intensity statistics. All crystal structures were solved by direct methods and were refined by full-matrix least-squares on F^2. All hydrogen atoms were placed in idealized positions and refined with fixed isotropic displacements parameters equal to 1.2 (1.5 for methyl protons), times the equivalent isotropic displacements parameters of the atoms to which they were attached. All non-hydrogen atoms were refined with anisotropic displacement parameters.

The following are the programs that were used: data collection and cell refinements; APEX II data collection software, FRAMBO Version 4.1.05 (GADDS)[66] or SMART WNT/2000 Version 5.632,[67] data reductions; APEX II data reduction software or SAINTPLUS Version 6.63,[68] absorption correction; SADABS,[49] structural solutions; SHELXS-97,[50] structural refinement; SHELXL-97;[51] molecular graphics and preparation of material for publication; SHELXTL, version 6.14,[52] and X-Seed, version 1.5.[53]

Copolymerization reactions monitored by *in situ* IR Spectroscopy. In a typical experiment, the catalyst (*N,N*'-bis(3,5-di-*tert*-butylsalicylidene)-1,2-cyclohexylenediamino chromium(III) chloride), (complex **III-8**), (124.4 mg), cocatalyst, and oxetane (4 g) were dissolved in 10 mL of toluene and delivered via the injection port into a 300-mL stainless steel Parr autoclave reactor that was previously dried in vacuo

overnight at 80°C. The autoclave is modified with a 30 bounce SiComp window to allow for the use of an ASI ReactIR 1000 system equipped with a MCT detector. In this manner a 128-scan background spectrum was collected after the reaction mixture was heated to the temperature of the corresponding experiment, the autoclave was then pressurized with 35 bar of CO_2, and the infrared spectrometer was set to collect one spectrum every 3 min over a 12 or 24 h period. Profiles of the absorbance at 1750 cm^{-1} (polymer) with time were recorded after base line correction. (*Note:* cocatalyst, cocatalyst loading, and temperature varied within each experiment and are described in the Result and Discussion section).

Results and Discussion

Our first concern was to examine in detail the nature of the soluble catalytic species resulting from the addition of the salt containing the anionic initiator to the (salen)CrX complex. In a typical copolymerization experiment the (salen)CrCl complex is dissolved in neat epoxide or oxetane in the presence of 1-2 equivalents of a salt cocatalyst. Anions derived from either the very bulky and less interacting PPN^+ cation or the more interacting *n*-Bu_4N^+ cation have been shown to be very effective initiators for these copolymerization processes.[54] Although, the PPNX salts have the added desirable feature of being readily available in an anhydrous form, these salts are generally insoluble or very sparingly soluble in low polarity cyclic ethers. Hence, in these instances *pretreatment* of the (salen)CrX complex with PPNX is required to assure maximum catalytic activity. This is achieved by dissolving the (salen)CrX complex and

PPNX salt in a compatible solvent such as methylene chloride, followed by vacuum removal of the solvent prior to introducing the cyclic ether monomer.

The identity of the chromium derivative resulting from the addition of *n*-Bu_4NX to (salen)CrX was initially investigated by solution infrared spectroscopy for X = azide ion, where azide is strongly absorbing in the infrared region around 2000 cm^{-1}. The titration of (salen)CrCl (complex **III-1**) with *n*-Bu_4NN_3 proceeded in a stepwise fashion as illustrated in **Scheme III-2** via monitoring the ν_{N_3} stretching vibration as depicted in Figure III-1. As noted the reaction proceeds all the way to the right, eventually forming an anionic *bis*-azide complex, (salen)$Cr(N_3)_2^-$. That is, the chloride ligand is easily displaced by an azide ligand in tetrachloroethane solution.[55a] Furthermore, the process is irreversible upon subsequent addition of excess *n*-Bu_4NCl. It should also be pointed out that, as expected, the identical diazide complex can be prepared by the reaction of (salen)CrN_3 with one equivalent of *n*-Bu_4NN_3.

Scheme III-2. Treatment of (salen)CrCl with *n*-Bu_4NN_3.

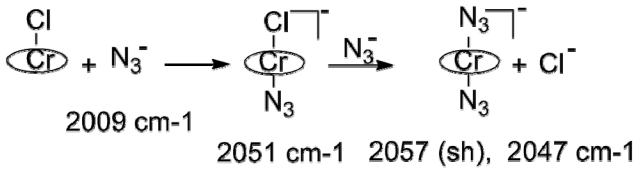

The generality of **Scheme III-2** involving the reaction of (salen)CrCl in the presence of two equivalents of X^- ligands other than azide (eq. III-1) was also noted as

revealed by infrared spectral data, and more importantly X-ray crystallography. Four such six- coordinate anionic chromium(III) complexes have been isolated and characterized as their PPN^+ or $n\text{-}Bu_4N^+$ salts, where X^- = Cl^-, N_3^-, CN^-, and NCO^-

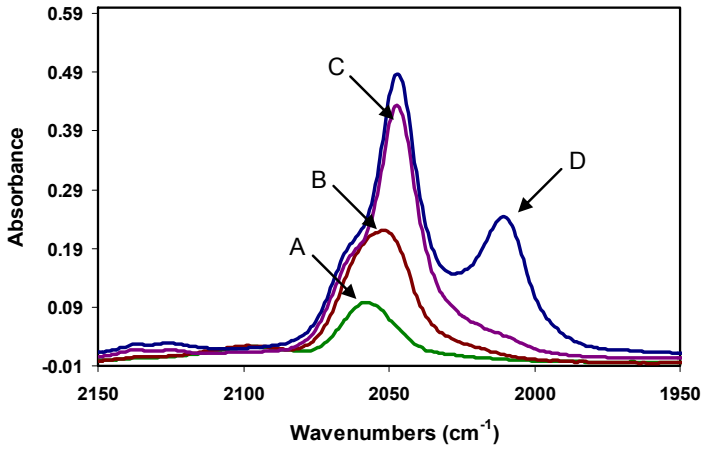

Figure III-1. Overlay of infrared spectra illustrating azide based cocatalyst dependence. 0.5 equivalents of $n\text{-}Bu_4NN_3$ (**A**), 1 equivalent of $n\text{-}Bu_4NN_3$ (**B**), 2 equivalents of $n\text{-}Bu_4NN_3$, (**C**) 3 equivalents of $n\text{-}Bu_4NN_3$ (**D**).

(Figure III-2).[54] Crystallographic data pertaining to these crystal structures are provided in Table III-1, with selected bond distances listed in Table III-2. As anticipated, strong field ligands such as N_3^-, CN^-, and NCO^- easily displace chloride at ambient temperature due to their greater trans effect.

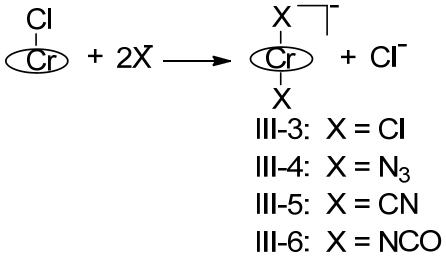

(III-1)

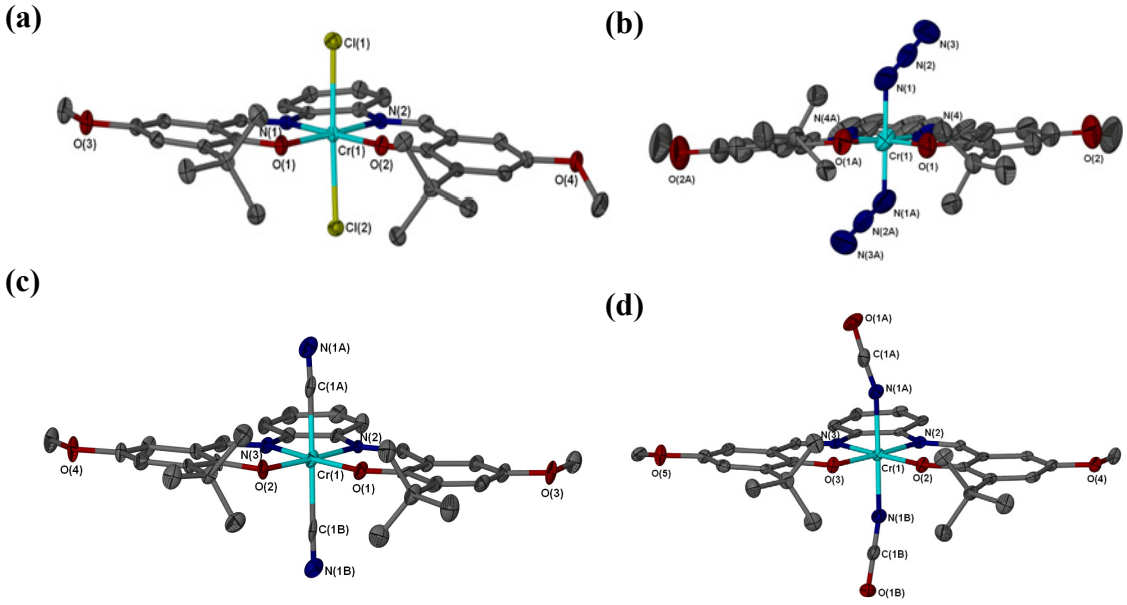

Figure III-2. Thermal ellipsoid representations of (salen)CrX_2^- anions, where the salen ligand contains –OMe and –*t*-Bu substituents in the 3,5-positions of the phenolates, respectively, with a phenylene diamino-backbone. H atoms omitted for clarity. Ellipsoids are at the 50% level. (a) *n*-Bu_4N^+ salt, X = Cl. One molecule of dichloromethane was crystallized in the unit cell. (b) *n*-Bu_4N^+ salt, X = N_3. (c) PPN^+ salt, X = CN. Three molecules of dichloromethane were crystallized in the unit cell. (d) PPN^+ salt, X = NCO. Two molecules of dichloromethane were crystallized in the unit cell.

Pertinent to the copolymerization reaction it was of interest to determine the characteristics of the anionic species which forms upon treating (salen)CrCl with only

one equivalent of $PPNN_3$. That is, we have demonstrated for cyclohexene oxide/CO_2 copolymerization processes that the rate of copolymer formation is the same whether we employ (salen)CrCl and one equivalent of $PPNN_3$ or (salen)CrN_3 and one equivalent of PPNCl as catalysts. This observation suggests the differently derived catalyst systems are equivalent. To more definitively address this issue we first examined the infrared data observed in the ν_{N_3} region upon treating (salen)CrCl with one equivalent of *n*-Bu_4N_3. As seen in Figure III-1, a broad absorption at 2051 cm^{-1} was observed which shifts to lower frequency upon addition of another equivalent of azide. At this point it is also noted that there is *no* free azide in solution as evident by the lack of a band at 2009

Table III-1. Crystallographic Data for Complexes **III-3**, **III-4**, **III-5**, **III-6**, and **III-7**.

	III-3·(CH_2Cl_2)	**III-4**	**III-5·[3(CH_2Cl_2)]**	**III-6·[2(CH_2Cl_2)]**	**III-7·[2(CH_2Cl_2)]**
empirical formula	$C_{47}H_{72}Cl_4CrN_3O_4$	$C_{46}H_{70}CrN_9O_4$	$C_{71}H_{70}Cl_6CrN_5O_4P_2$	$C_{70}H_{68}Cl_4CrN_5O_6P_2$	$C_{67.50}H_{67}Cl_3CrN_6O_4P_2$
fw	936.88	865.11	1383.96	1331.03	1215.59
temperature (K)	110(2) K	110(2) K	110(2) K	110(2) K	110(2) K
crystal system	Triclinic	Orthorhombic	Triclinic	Triclinic	Triclinic
space group	P-1	Pnna	P-1	P-1	P-1
a (Å)	13.039(3)	10.622(10)	12.104(3)	11.961(2)	12.447(2)
b(Å)	13.372(3)	25.105(2)	16.019(4)	15.876(3)	15.076(2)
c(Å)	14.703(3)	17.256(17)	19.970(7)	18.842(4)	18.509(3)
α(deg)	93.050(3)	90	66.377(15)	68.179(10)	70.026(8)
β(deg)	101.587(3)	90	80.31(2)	79.346(12)	82.558(9)
γ(deg)	104.698(3)	90	79.034(17)	88.643(11)	79.978(9)
V(Å)^3	2414.4(9)	4602.0(7)	3464.4(18)	3260.5	3205.3(9)
D_c(Mg/m^3)	1.289	1.249	1.327	1.356	1.260
Z	2	4	2	2	2
abs coeff(mm^{-1})	0.502	0.301	4.33	3.867	3.261
reflections collected	28288	42139	24726	25681	21367
independent reflections	11323 [R(int) = 0.0454]	5632 [R(int) = 0.0986]	9069 [R(int) = 0.0606]	9249 [R(int) = 0.0409]	8449 [R(int) = 0.0965]
Data/restrains/ parameters	11323/0/544	5632/0/278	9069/0/810	9249/0/801	8449/565/821
GOF on F^2	1.001	1.000	1.000	1.000	1.001
final *R* indices [I>2σ(I)]	$^aR_1$ = 0.0452 ^bR_w = 0.1152	$^aR_1$ = 0.0822 ^bR_w = 0.2018	$^aR_1$ = 0.0843 ^bR_w = 0.2478	$^aR_1$ = 0.0504 ^bR_w = 0.1663	$^aR_1$ = 0.0894 ^bR_w = 0.2131
final R indices (all data)	$^aR_1$ = 0.0706 ^bR_w = 0.1311	$^aR_1$ = 0.2139 ^bR_w = 0.2536	$^aR_1$ = 0.1344 ^bR_w = 0.3210	$^aR_1$ = 0.0657 ^bR_w = 0.2110	$^aR_1$ = 0.1747 ^bR_w = 0.2716

cm^{-1}. X-ray quality crystals were grown upon layering a concentrated dichloromethane solution of (salen)CrCl and one equivalent of $PPNN_3$ with hexanes. Surprisingly, four different anionic species were detected by X-ray crystallography, i.e., (salen)$CrCl_2^-$, (salen)$Cr(N_3)_2^-$, and two different forms of (salen)$Cr(N_3)Cl^-$ (see Table III-1, and Figure

Table III-2. Selected Bond Lengths for Complexes **III-3**, **III-4**, **III-5, and III-6.**[a]

	III-3	**III-4**	**III-5**	**III-6**
$Cr\text{-}O_{salen\ ligand}$	1.9245(15) 1.9220(15)	1.915(3)	1.907(5) 1.919(4)	1.926(3) 1.928(3)
$Cr\text{-}N_{salen\ ligand}$	2.0016(17) 2.0189(17)	2.007(4)	2.017(6) 2.026(5)	2.020(3) 2.023(3)
$Cr\text{-}N_{apical\ ligand}$		2.050(4)		2.016(4) 2.025(3)
$N\text{-}N_{apical\ ligand}$		1.174(5) 1.168(6)		
$Cr\text{-}Cl_{apical\ ligand}$	2.3236(7) 2.3959(7)			
$Cr\text{-}C_{apical\ ligand}$			2.104(9) 2.126(10)	
$C\text{-}N_{apical\ ligand}$			1.155(10) 1.144(10)	
$C\text{-}O_{apical\ ligand}$				1.210(5) 1.206(5)

III-3). The two forms of the mixed ligand complex results from the fact that the salen ligand is not completely planar. These crystals were further analyzed by electron-spray ionization mass spectrometry. The parent ions of (salen)$CrCl_2^-$, (salen)$Cr(N_3)Cl^-$, and (salen)$Cr(N_3)_2^-$ were observed in the negative mode of the ESI-mass spectrum at 608.18, 615.23, and 622.20 m/z, respectively. In addition the parent ion of (salen)Cr(Cl)$(OAc)^-$ was also detected which resulted from the reaction of (salen)$CrCl_2^-$ with acetic acid which is used in the mass spectral analysis experiment. These results from infrared spectroscopy, X-ray crystallography, and mass spectral analysis all suggest that when

(salen)CrCl is treated with one equivalent of azide a Schlenk (ligand redistribution) equilibrium as shown in equation III-2 is most likely formed.

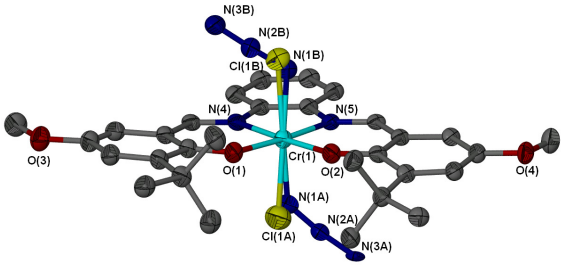

Figure III-3. Thermal ellipsoid plot of complex **III-7**. Ellipsoids are at the 50 % level. The salen ligand contains –OMe and -*t*-Bu substituents in the 3,5 positions of the phenolates respectively, with a phenylene diamino backbone. H atoms and PPN^+ cation are omitted for clarity. Two dichloromethane molecules were crystallized in the unit cell and are omitted for clarity. Selected bond lengths (Å): Cr(1)-Cl(1A) = 2.319(8); Cr(1)-Cl(1B) = 2.363(7); Cr(1)-N(1A) = 2.01(2), Cr(1)-N(1B) = 2.04(3); N(1A)-N(2A) = 1.212(15); N(2A)-N(3A) = 1.218(12); N(1B)-N(2B) = 1.232(15); N(2B)-N(3B) = 1.201(13).

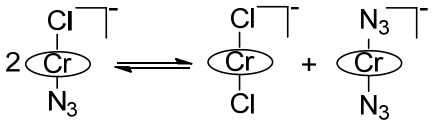

(III-2)

Substrate Binding and Ring-Opening Step Studies as Examined by Solution Infrared Spectroscopy and *in situ* Infrared Techniques. Subsequent to examining the nature of the catalyst system employed in these copolymerization reactions, our next challenge was to investigate in depth the monomer binding to the metal center and its consequent ring-opening *via* the anionic initiator. This was accomplished by adding X^-

to the five-coordinate chromium(III) complex in TCE to yield *trans*-(salen)CrX_2^-. Upon adding an excess of the cyclic ether monomers an equilibrium process was established as depicted in **Scheme III-3**.

Scheme III-3. Equilibrium Process Between Chromium Salen Catalyst and Monomer at Room Temperature.

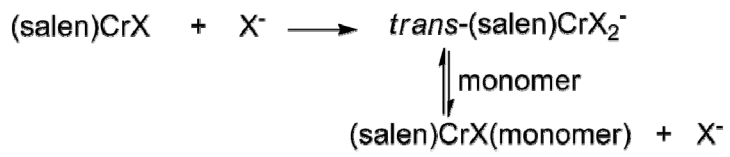

The equilibrium position and subsequent ring-opening reaction differ significantly with the nature of the monomer. For example, comparing propylene oxide and oxetane, these monomers have similar steric requirements, but the ring-strain energies of propylene oxide and oxetane have been calculated to be 27.3 and 25.5 kcal/mol, and their pK_b values are 6.94 and 3.13, respectively.[69] To illustrate how these differences affect the binding of these monomers to the metal center and subsequent ring-opening step, we have examined cyclohexene oxide, propylene oxide, and oxetane as substrates for these processes by solution infrared spectroscopy and by *in situ* infrared techniques.

For the solution infrared spectroscopy studies we utilized the (salen)CrX complexes (X = Cl or N_3), where the salen ligand contained di-*tert*-butyl substituents in the 3,5-positions of the phenolate rings and an ethylene backbone for the diamine

(complexes **III-1** and **III-2**). The azide anion derived from the very soluble *n*-Bu_4NN_3 was employed in these studies since the ν_{N_3} stretching vibration provides accessible probes for both anion binding and ring-opening steps. The results of studies involving oxetane as the monomer are presented first as depicted in **Scheme III-4** and Figure III-4.

Scheme III-4. Ring-Opening Step of Oxetane Catalyzed by (salen)$Cr(N_3)_2^-$.

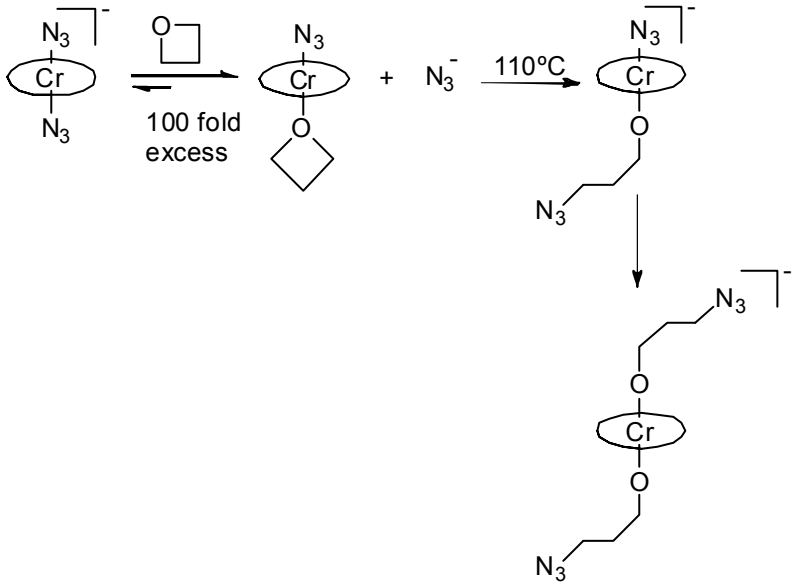

As indicated in **Scheme III-4** and revealed by the infrared spectrum **A** in Figure III-4, upon addition of slightly more than one equivalent of *n*-Bu_4NN_3 to (salen)CrN_3, the six-coordinate *bis*-azide complex (salen)$Cr(N_3)_2^-$ forms at ambient temperature. Subsequent addition of 100-fold excess of oxetane displaces some of the azide ligand as seen by an increase in the absorption at 2009 cm^{-1} due to free azide with a concomitant

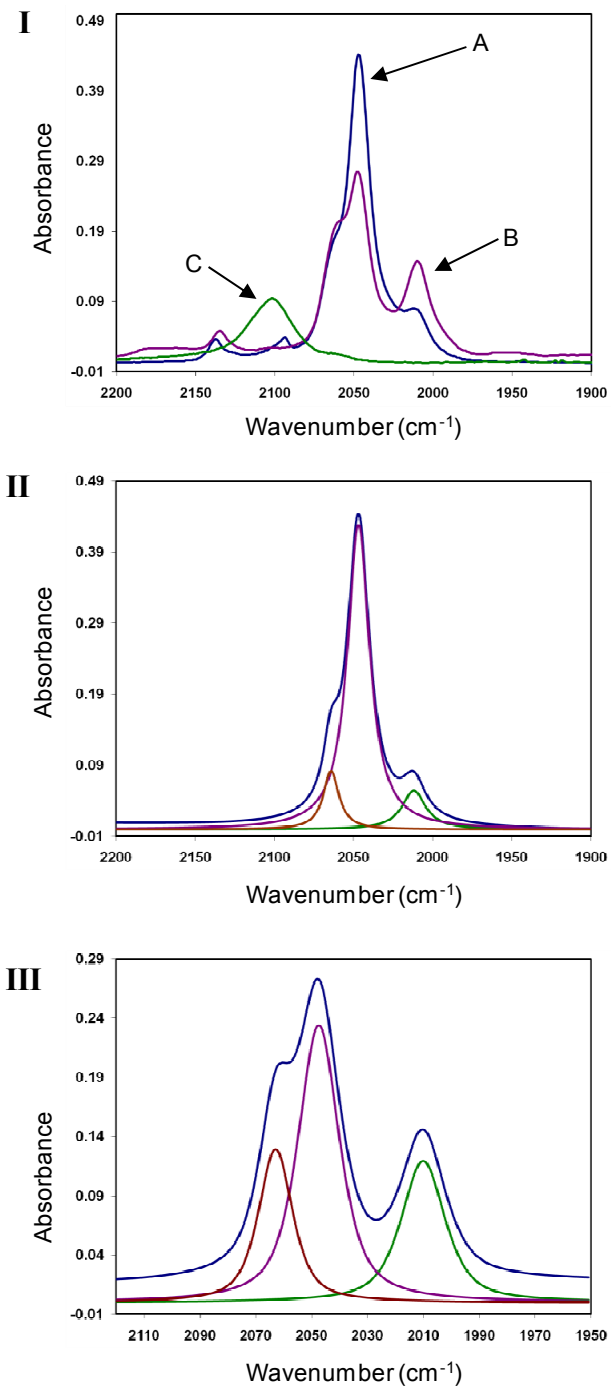

Figure III-4. I. Spectra of TCE solutions of chromium salen azide complex with 1 equivalent of *n*-Bu_4NN_3 (**A**), after addition of 100 equivalents of oxetane at ambient temperature (**B**), after heating the reaction solution at 110°C for 3 h (**C**). Data taken from Chapter II. **II.** Deconvoluted spectrum of **A**. **III.** Deconvoluted spectrum of **B**.

decrease in the infrared band at 2047 cm^{-1} of the (salen)$Cr(N_3)_2^-$ species. In addition, a new ν_{N_3} stretching band appears at 2061 cm^{-1} which was assigned to (salen)$Cr(N_3)$•oxetane, spectrum **B** in Figure III-4. Confirmation of this assignment was made by the isolation of single crystals of the oxetane adduct suitable for analysis by X-ray crystallography (Figure III-5). The ring-opening of the metal bound oxetane

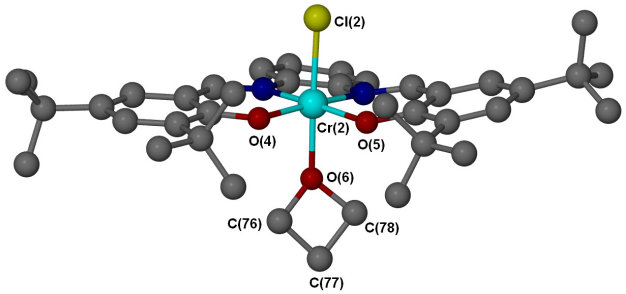

Figure III-5. Ball and stick representation of the X-ray defined structure of (salen)CrCl·oxetane adduct, where the salen ligand contains -*t*-Bu substituents in the 3,5 positions of the phenolates respectively, with a phenylene diimine backbone. Data taken from Chapter II.

monomer by azide was not observed at ambient temperature. Indeed, only after heating the reaction solution for 3 hrs at 110ºC did the metal azide species disappear accompanied by the appearance of an organic azide infrared band at 2100 cm^{-1} (spectrum **C** in Figure III-4). That is, following the oxetane ring-opening process, the only ν_{N_3} band present in the infrared spectrum **C** is that of the organic azide, with *no* observable free or metal bound azide ν_{N_3} vibrations.

A similar series of experiments were carried out to further investigate the initial ring-opening step of oxetane employing the (salen)CrN_3 complex in the presence of one equivalent of *n*-Bu_4NCl. The results of this inquiry are shown in **Scheme III-5** and Figure III-6. Consistent with our earlier observations, upon addition of *n*-Bu_4NCl to (salen)CrN_3, a mixed anionic six-coordinate species is formed at ambient temperature which displays a ν_{N_3} absorption at 2051 cm^{-1}. Further addition of 100-fold excess of oxetane leads to displacement of the chloride ligand as revealed by the appearance of a ν_{N_3} band at 2061 cm^{-1} corresponding to the (salen)$Cr(N_3)$•oxetane adduct, as well as no ν_{N_3} vibration for the free azide ion. Hence, the chloride ligand is selectively and quantitatively displaced by oxetane at an oxetane concentration where the azide ligand is only partially displaced in the (salen)$Cr(N_3)_2^-$ species (see Figure III-4, spectrum **B**). Oxetane ring-opening was detected in this instance after heating the reaction solution for 3 h at 110ºC, which lead to the appearance of an organic azide band at 2100 cm^{-1} (Figure III-6, spectrum **D**). Of importance to note here, is that oxetane ring-opening occurs by the azide ligand, which as stated before supports the fact that the azide ligand in (salen)$Cr(N_3)(O\text{-}(CH_2)_3\text{-}N_3)^-$ also ring-opens an oxetane monomer.

Scheme III-5. Ring-Opening of Oxetane Catalyzed by (salen)$Cr(N_3)(Cl)^-$.

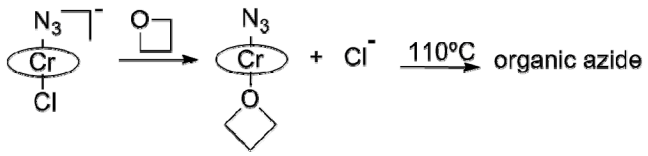

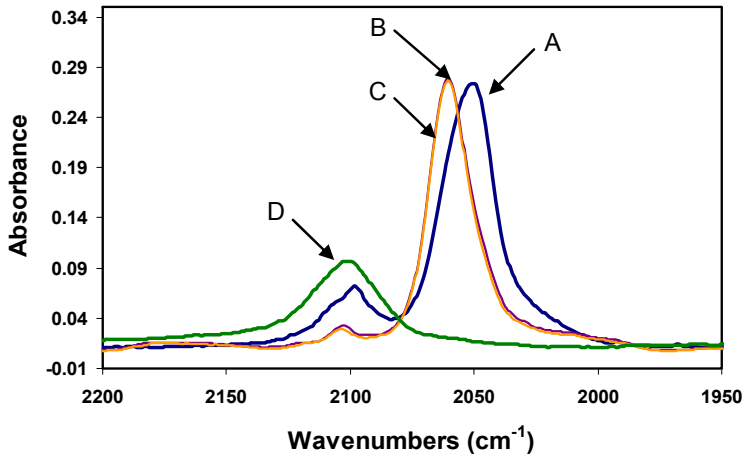

Figure III-6. Spectra of TCE solutions of chromium salen azide complex with 1 equivalent of *n*-Bu_4NCl (**A**), after addition of 100 equivalents of oxetane at ambient temperature (**B**), after stirring the reaction solution for 24 h at ambient temperature (**C**), and after heating the reaction solution for 3 h at 110ºC (**D**).

Additional studies of the initiation step for the coupling reaction of oxetane and carbon dioxide were undertaken using *in situ* infrared techniques.[46] In these studies a slightly modified (salen)CrCl complex was employed, that is one, containing di-*tert*-butyl substituents in the 3,5-positions of the phenolates with a cyclohexylenediamino backbone, along with *n*-Bu_4NN_3 as anion source. We have previously shown this to be the most active catalyst system we have thus far investigated for this copolymerization process. As evident in Figure III-4, upon the addition of 100-fold excess of oxetane to the catalyst system in solution an equilibrium is established between the *bis*-azide complex, (salen)$Cr(N_3)_2^-$, and the oxetane adduct, (salen)$Cr(N_3)$•oxetane. This equilibrium process greatly favors the neutral oxetane adduct in pure oxetane solution. On the other hand, in the presence of a large excess of azide ion initiator it favors the *bis*-azide species, and hence should retard the initial ring-opening step of the

copolymerization process. Figure III-7 depicts the reaction profiles for copolymer formation during the copolymerization of oxetane and CO_2 utilizing (salen)CrCl in the presence of varying quantities of *n*-Bu_4NN_3. As is readily observed in Figure III-7, an induction period is evident for the copolymerization process which increases as the numbers of equivalents of *n*-Bu_4NN_3 increases (see insert). This induction period is

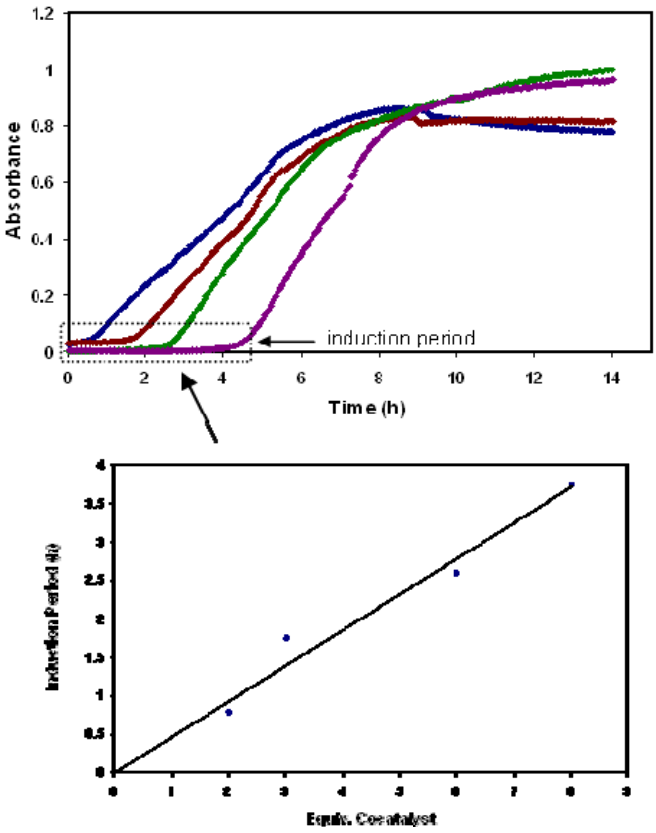

Figure III-7. Cocatalyst dependent reaction profiles depicting the growth of the copolymer at 1750 cm^{-1} with time for the copolymerization of oxetane and CO_2, utilizing (salen)CrCl with different equivalents of *n*-Bu_4NN_3 at 110ºC: 2 equivalents of *n*-Bu_4NN_3 (blue line), 3 equivalents of *n*-Bu_4NN_3 (red line), 6 equivalents of *n*-Bu_4NN_3 (green line), 8 equivalents of *n*-Bu_4NN_3 (purple line).

attributed to an inhibition of oxetane binding in the presence of excess azide ions which preferentially coordinate to the chromium(III) center thereby retarding the ring-opening process.

A brief induction period of several minutes is generally observed for the copolymerization of oxetane and CO_2 carried out at 110ºC during the addition of carbon dioxide where the temperature temporarily drops by 20ºC. This would be anticipated since we have demonstrated earlier that the oxetane ring-opening step is relatively slow at 110ºC (Figure III-4). We have further investigated the temperature dependence of this initial oxetane ring-opening step during the copolymerization reaction employing (salen)CrCl and two equivalents of *n*-Bu_4NN_3 in the temperature range 80-110ºC. As observed in Figure III-8, the induction period is lengthened as the reaction temperature is lowered, being most significant in the 80-90º temperature range. The induction period is not greatly different in the temperature range 100-110ºC. Nevertheless, it *must* be pointed out at this time that the selectivity for cyclic carbonate *vs* copolymer formation is also temperature dependent; hence, the difference noted in Figure III-8 cannot be ascribed to temperature alone.

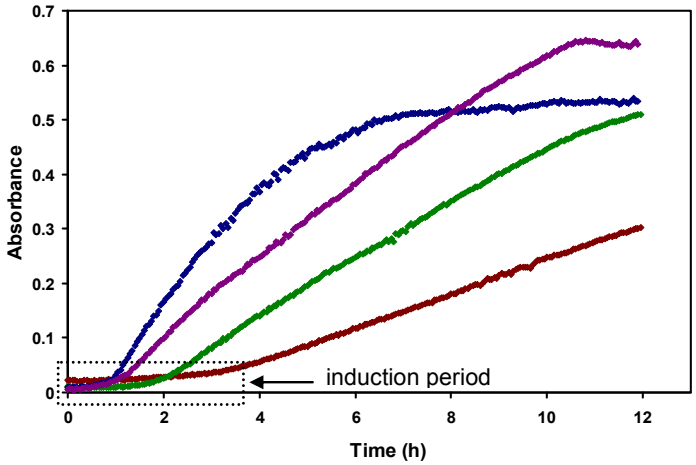

Figure III-8. Temperature dependent reaction profiles depicting the growth of the copolymer at 1750 cm^{-1} with time for the copolymerization of oxetane and CO_2, utilizing (salen)CrCl with 2 equivalents of *n*-Bu_4NN_3: Reaction temperature = 80°C (red line), reaction temperature = 90°C (green line), reaction temperature = 100°C (purple line), reaction temperature = 110°C (blue line).

In an analogous manner we have examined the initial ring-opening steps for cyclohexene oxide and propylene oxide in the presence of the (salen)CrCl/*n*-Bu_4NN_3 catalyst system. This study was designed to provide a semi-quantitative comparison of processes involving three- and four-membered cyclic ethers. **Scheme III-6**, along with Figures III-9 and III-10 summarize our findings. As expected, based on their relative ring strain energies the three-membered cyclic ethers, cyclohexene oxide and propylene oxide, undergo ring-opening under much milder conditions than their four-membered counterpart, oxetane. A bit more unanticipated was the significantly greater ease with which propylene oxide was ring-opened by azide compared to cyclohexene oxide.

Scheme III-6. Ring-Opening of Cyclohexene Oxide Catalyzed by (salen)$Cr(N_3)_2^-$.

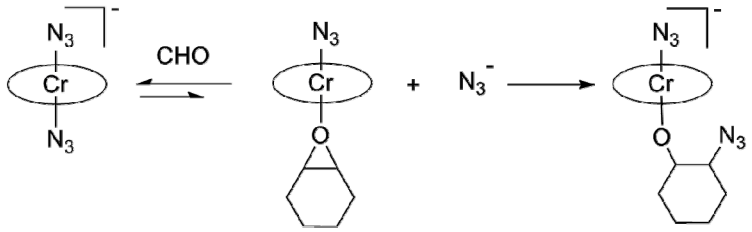

Other information apparent from these experiments (Figures III-4 and III-9) is that the equilibrium reaction between (salen)$Cr(N_3)_2^-$ and 100-fold excess of oxetane proceeded further to completion than the comparable process involving cyclohexene oxide with formation of (salen)$Cr(N_3)$•cyclohexene oxide (ν_{N_3} at 2058 cm^{-1}). That is, the

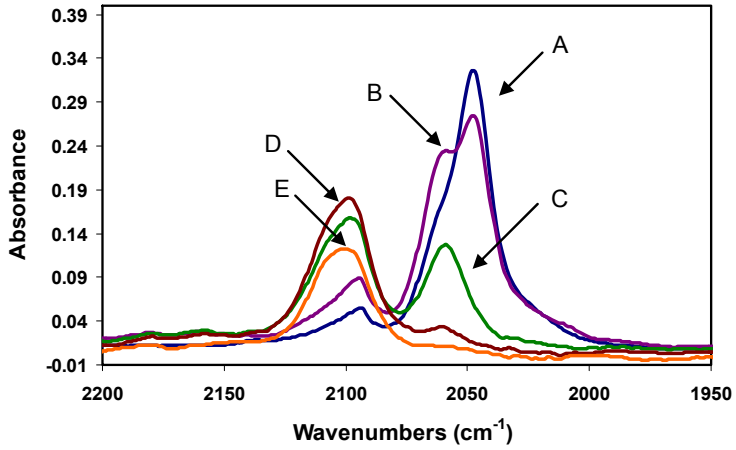

Figure III-9. Spectra of TCE solutions of chromium salen chloride complex with 2 equivalents of *n*-Bu_4NN_3 (**A**), after addition of 100 equivalents of cyclohexene oxide at ambient temperature (**B**), after stirring the reaction solution for 2 h at ambient temperature (**C**), after stirring the reaction solution for 4 h at ambient temperature (**D**), and after stirring the reaction solution for 24 h at ambient temperature (**E**).

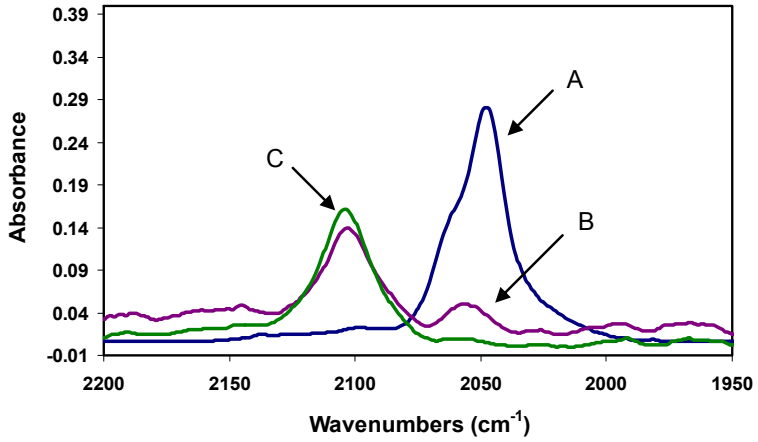

Figure III-10. Spectra of TCE solutions of (salen)CrCl with 2 equivalent of *n*-Bu_4NN_3 (**A**). Immediately after addition of 100 equivalents of propylene oxide at ambient temperature (**B**). Reaction solution stirred for 15 min at ambient temperature (**C**).

infrared spectra in Figure III-9 reveal a smaller decrease in the *bis*-azide complex at 2047 cm^{-1} than seen in Figure III-4, as well as a lack of initial formation of free azide ions at 2009 cm^{-1}. This is consistent with the lower basicity of three-membered *vs* four-membered cyclic ethers. As previously noted for the oxetane ring-opening process, both inorganic azide ligands are converted to organic azides.

In a similar manner the initial ring-opening step of the cyclohexene oxide/CO_2 copolymerization process was investigated employing a (salen)CrN_3 complex and one equivalent of *n*-Bu_4NCl. The results of this study are quite comparable to that for the oxetane/CO_2 process as seen in **Scheme III-7**, with the only difference being that ring-opening of cyclohexene oxide occurs at ambient temperature.

Scheme III-7. Ring-Opening of Cyclohexene Oxide Catalyzed by (salen)Cr(N_3)(Cl)$^-$.

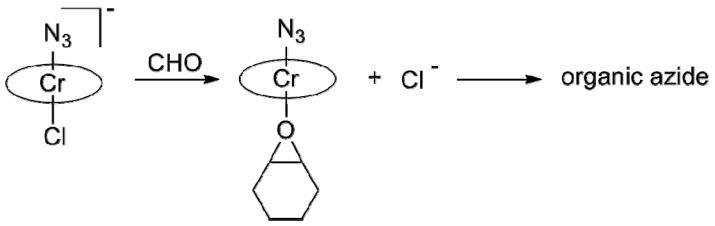

Nature of Anionic Initiator (Cocatalyst) on the Initial Ring-Opening Step of the Copolymerization Process. As previously noted, the formation of the anionic six-coordinate species of the form *trans*-(salen)CrX_2^- readily occurs upon treating (salen)CrCl with two equivalents of a salt of X^- (equation III-1). The next step in the process involves binding and subsequent ring-opening of the cyclic ether monomer, which in the case of oxetane is highly energetic process. Hence, based on the nature of the anion X^-, there should be a significant variation in the initiation step which is a function of both its binding ability to chromium(III) and propensity for ring-opening monomer. In order to investigate this dependence the copolymerization of oxetane/CO_2 was examined by *in situ* infrared spectroscopy utilizing (salen)CrCl and two equivalents of *n*-Bu_4NX. Figure III-11 depicts the reaction profiles for the formation of poly(trimethylene carbonate) involving either two equivalents of *n*-Bu_4NN_3 or *n*-Bu_4NCl. As evident in Figure III-11 a short induction period is seen when using *n*-Bu_4NN_3, and *no* induction period was detected when employing *n*-Bu_4NCl as cocatalyst. This observation is consistent with our earlier findings where oxetane more easily replaces a chloride ligand from chromium(III) than an azide ligand. The following

copolymerization reaction (monomer enchainment) processes as expected are not affected.

The initiation step for the copolymerization of oxetane and carbon dioxide was also examined in the presence of (salen)CrCl and other anions containing intense absorptions in infrared, namely, CN^- and NCO^-. These anions, like azide, exhibit induction periods for copolymer formation (see Figure III-11). This is consistent with the observation that CN^- and NCO^- readily displace Cl^- from (salen)CrCl, and at the same time are more difficult to be replaced by oxetane. Finally, it should be noted here that because of the ease of cyclohexene oxide ring-opening, *no* induction period is observed for the copolymerization reaction of cyclohexene oxide and CO_2 employing either PPNX or *n*-Bu_4NX (X = Cl or N_3) as cocatalyst along with (salen)CrX complexes.

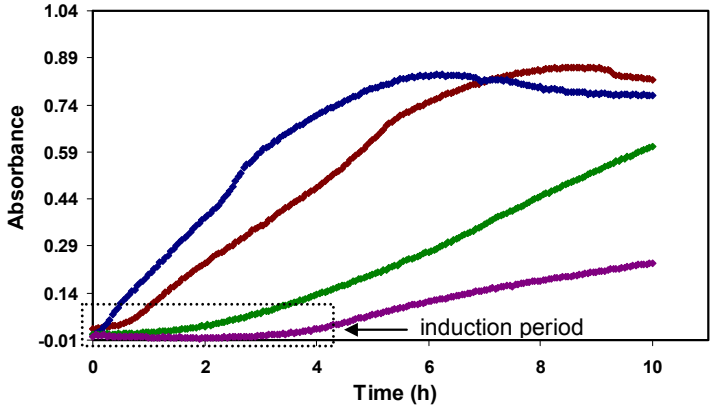

Figure III-11. Reaction profiles depicting the growth of the copolymer at 1750 cm^{-1} with time for the copolymerization of oxetane and CO_2 at 110ºC, utilizing (salen)CrCl with 2 equiv of *n*-Bu_4NN_3 (red line), 2 equiv of *n*-Bu_4NCl (blue line), 2 equiv of *n*-Bu_4NNCO (green line) and 2 equiv of *n*-Bu_4NCN (purple line).

Concluding Remarks

The addition of salts of PPNX or *n*-Bu_4NX to (salen)CrX complexes yield [*trans*-(salen)CrX_2][PPN or *n*-Bu_4N] complexes which have been crystallographically defined for salen = *N,N′*-bis(3-*tert*-butyl-5-methoxysalicylidene)-1,2-phenylenediamino) and X = Cl, N_3, CN, and NCO. The latter three derivatives are readily synthesized by the addition of two-equivalents of PPN^+ or *n*-Bu_4N^+ salts of N_3^-, CN^-, and NCO^- to (salen)CrCl. On the other hand, the addition of one-equivalent of *n*-Bu_4NN_3 to (salen)CrCl leads initially to *trans*-(salen)Cr(N_3)Cl^- which exists in TCE solution in a Schlenk equilibrium with the corresponding symmetric *trans*-(salen)CrX_2^- anions as revealed by X-ray crystallography and ESI-mass spectrometry. For all anions examined the displacement of X in *trans*-(salen)CrX_2^- with the cyclic ethers (propylene oxide, cyclohexene oxide, or oxetane) to provide *trans*-(salen)CrX•cyclic ether adducts in TCE solution greatly favored the anionic complexes. The ring-opening of bound epoxides by X^- readily occurred at ambient temperature, with propylene oxide being ring-opened by azide at a significantly faster rate than the corresponding process involving cyclohexene oxide. On the contrary the ring-opening of bound oxetane occurred readily at temperatures near 100ºC and greater, with this process being retarded in the presence of excess X^- anions such as N_3^-, CN^-, or NCO^- which strongly bind to the chromium(III) center. It was further shown that both inorganic azides are involved in epoxide or oxetane ring-opening leading to formation of the similar organic azides.

CHAPTER IV

(SALEN)Co(II)/*n*-Bu_4NX CATALYSTS FOR THE COUPLING OF CO_2 AND OXETANE: SELECTIVITY FOR CYCLIC CARBONATE FORMATION IN THE PRODUCTION OF POLY(TRIMETHYLENE CARBONATE)*

Introduction

As discussed in Chapter I, the copolymerization of epoxides and CO_2 process is often accompanied by the formation of varying amounts of ether linkages, which are the result of consecutive epoxide ring-opening. Additionally, five-membered cyclic carbonates are observable byproducts in these reactions, which are formed by a backbiting mechanism, thus shortening the polymer chain by one unit each occurrence. This latter event can be a major reaction pathway when utilizing aliphatic epoxides such as ethylene oxide, propylene oxide, and styrene oxide. Both polymeric and monomeric products obtained from the coupling of epoxides and carbon dioxide have important industrial applications. Polycarbonates as previously discussed have wide-scale uses in electronics, optical media, automotive, and medical industry. On the other hand, five-membered cyclic carbonates have numerous applications as high boiling and flash point solvents, and also as reactive intermediates.[12]

---

*Reproduced in part with permission from "(Salen)Co(II)/*n*-Bu_4NX Catalysts for the Coupling of CO_2 and Oxetane: Selectivity for Cyclic Carbonate Formation in the Production of Poly(trimethylene carbonate)." Darensbourg, D. J.; Moncada, A. I. *Macromolecules* **2009**, *42*, 4063-4070. Copyright 2009 American Chemical Society.

The formation of five-membered cyclic carbonates derived from the coupling reaction of epoxides and CO_2 has been extensively investigated using various types of catalysts. Homogeneous metal salen based catalysts of aluminum,[70] chromium,[71] cobalt,[72] zinc,[72d] manganese,[73] and tin,[74] have shown to have high catalytic activities. Similarly, aluminum complexes of phthalocyanines and porphyrins are also highly active catalysts.[75] Ionic liquids such as imidazolium salts have also been reported as catalysts for the formation of cyclic carbonates from epoxides and carbon dioxide.[76] Moreover, the reaction of epoxides and CO_2 in molten quaternary ammonium bromide has been shown to afford cyclic carbonates.[77] Furthermore, other metal complexes of nickel,[78] ruthenium,[79] zinc,[80] and copper[73b] have been similarly reported to be active catalysts for this transformation. Organic based catalysts such as phenols,[81] and 4-(*N,N*-dialkylamino)pyridines[82] have also been investigated. Recently, CO_2 adducts of *N*-heterocyclic carbenes were also demonstrated to be effective organic catalysts for these processes.[83] In addition, heterogeneous based materials such as Al-Mg mixed oxides,[84] magnesium oxide,[85] and Cs-modified zeolites,[86] have been shown to be interesting catalysts for this reaction, not only because of their high activity but also because these catalysts can be easily separated from the reaction solution, and in most cases recycled.

As previously mentioned in Chapter I, five-membered cyclic carbonates are thermodynamically stable toward polycarbonate formation without loss of carbon dioxide. However, six-membered cyclic carbonates such as trimethylene carbonate can under certain catalytic conditions undergo ring-opening polymerization to provide the corresponding polycarbonate, in this case poly(TMC), with complete retention of its CO_2

contents (eq. I-2).[12] Of Importance, this strategy is industrially desirable because it can be performed as a melt process.

As mentioned in Chapter I, trimethylene carbonate can be readily obtained via transesterification of 1,3-propanediol with various reagents including phosgene and its derivatives (di- and tri-phosgene), dialkylcarbonates, and ethylchloroformate.[15] Therefore, it is of great interest to investigate greener routes for the production of this six-membered cyclic carbonate monomer. Conforming to this objective, the coupling of oxetane and carbon dioxide represents an attractive alternative (eq I-5).

In Chapter II, mechanistic and kinetic studies on this reaction as catalyzed by (salen)Cr(III)Cl/*n*-Bu_4NN_3 demonstrated that the formation of copolymer proceeded in part by way of the intermediacy of trimethylene carbonate, and by the direct enchainment of oxetane and CO_2. As a consequence of our findings with the (salen)Cr(III)Cl derivatives, we surmised that a decrease in the electrophilicity of the metal center, in conjunction with the appropriate anionic initiator should tune the selectivity of the oxetane and CO_2 coupling process for cyclic carbonate formation and/or for polycarbonate produced directly from the homopolymerization of preformed TMC (**Scheme IV-1**). To examine this hypothesis the commercially available catalyst, (salen)Co(II)[87] ((1*R*, 2*R*)-(-)-1,2-cyclohexanediamino-*N,N'*-bis(3,5-di-*tert*-butyl-salicylidene)cobalt(II)) (Figure IV-1) was employed in the presence of anionic based cocatalysts derived from *n*-Bu_4NX (X = Cl, N_3, Br, I) salts. Included in this investigation is a mechanistic study of this process as monitored by *in situ* infrared

spectroscopy. This correspondence encompasses an examination of cocatalyst dependence, substrate binding, and oxetane ring-opening.

Scheme IV-1. General Reaction Scheme of the Coupling of Oxetane and CO_2.

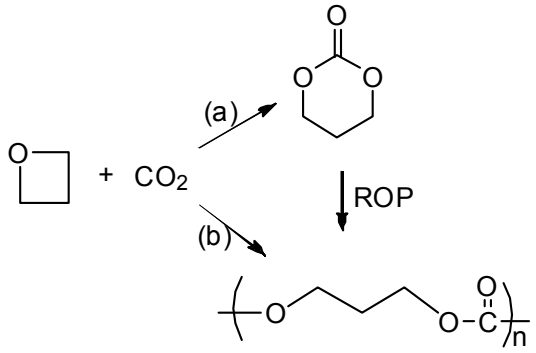

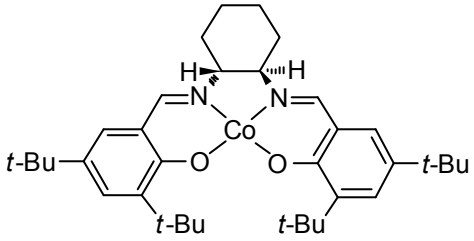

Figure IV-1. The (salen)Co(II) complex **IV-1** employed in the present studies, (1*R*, 2*R*)-(-)-1,2-cyclohexanediamino-*N,N′*-bis(3,5-di-*tert*-butyl-salicylidene)cobalt(II).

Experimental Section

Reagents and Methods. Unless otherwise specified, all manipulations were carried out on a double-manifold Schlenk vacuum line under an atmosphere of argon or in an argon filled glove box. (1*R*, 2*R*)-(-)-1,2-cyclohexanediamino-*N,N′*-bis(3,5-di-*tert*-

butyl-salicylidene)cobalt(II) was purchased from Strem Chemical. (Salen)CoBr was synthesized following the procedure published for the preparation of (salen)CoCl by Jacobsen and coworkers.[88] Toluene was freshly distilled from sodium/benzophenone. 1,1,2,2-tetrachloroethane was freshly distilled over CaH_2. Oxetane (Alfa Aesar) was freshly distilled over CaH_2 and stored in the freezer of the glove box. Tetra-*n*-butylammonium bromide (Aldrich), tetra-*n*-butylammonium iodide (Eastman), and tetra-*n*-butylammonium chloride (TCI) were recrystallized from acetone/diethyl ether before use. Tetra-*n*-butylammonium azide (TCI) was stored in the freezer of the glove box upon arrival. 4-(dimethylamino)pyridine (DMAP, Aldrich) was recrystallized from ethanol/diethyl ether, and triethylamine (Fisher Scientific) was freshly distilled over CaH_2 before use. Bone-dry carbon dioxide supplied in a high-pressure cylinder and equipped with a liquid dip tube was purchased from Scott Specialty Gases.

^{1}H NMR spectra were acquired on Unity+ 300 MHz and VXR 300 MHz superconducting NMR spectrometers. IR spectra were recorded on a Mattson 6021 Fourier Transform (FT) IR spectrometer with a MCT detector. Molecular weight determinations (M_n and M_w) were carried out with a Viscotek Modular GPC apparatus equipped with ViscoGEL^{TM} I-series columns (H + L) and Model 270 dual detector comprised of Refractive Index and Light Scattering detectors. High-pressure reaction measurements were performed using an ASI ReactIR 1000 reaction analysis system with stainless steel Parr autoclave modified with a permanently mounted ATR crystal (SiComp) at the bottom of the reactor (purchased from Mettler Toledo).

Optimization of the Cocatalyst for the Copolymerization Reactions of Oxetane and Carbon Dioxide. In a typical experiment, 119 mg of complex **IV-1**, the appropriate amount of cocatalyst, and 4 g of oxetane, were delivered via the injection port into a 300-mL stainless steel Parr autoclave reactor that was previously dried in vacuo overnight at 80°C. The autoclave was then pressurized with 35 bar of CO_2 and the temperature was increased to 110°C. The monomer:catalyst:cocatalyst ratio was maintained at 350:1:2, and the reaction was run for 24 hours. After the reaction was stopped, the autoclave was put into ice, cooled down to 10°C, and vented in a fume hood. The percent converion to products was determined based on the amount of oxetane monomer left in the reaction solution. ^{1}H NMR (300 MHz, $CDCl_3$), oxetane: δ 4.75 (t, 4H, OCH_2) and 2.70 (quintet, 2H, CH_2). Furthermore, the quantities of poly(TMC), TMC, and ether linkages in the copolymer were determined by integrating the peak area of the corresponding resonances. ^{1}H NMR (300 MHz, $CDCl_3$), poly(TMC): δ 4.23 (t, 4H, OCH_2) and 2.05 (quintet, 2H, CH_2). ^{1}H NMR (300 MHz, $CDCl_3$), TMC: δ 4.45 (t, 4H, OCH_2) and 2.14 (quintet, 2H, CH_2). ^{1}H NMR (300 MHz, $CDCl_3$), ether linkages: δ 3.50 (t, 4H, OCH_2) and 1.90 (quintet, 2H, CH_2).

Copolymerization Reactions Monitored by *in situ* IR Spectroscopy. In a typical experiment, complex **IV-1** (277 mg), the appropriate amount of *n*-Bu_4NBr, and oxetane (4 g) were dissolved in 10 mL of toluene and delivered via the injection port into a 300-mL stainless steel Parr autoclave reactor that was previously dried in vacuo overnight at 80°C. The autoclave is modified with a 30 bounce SiComp window to allow for the use of an ASI ReactIR 1000 system equipped with a MCT detector. In this manner a 128-

scan background spectrum was collected after the reaction mixture was heated to 110°C. The autoclave was pressurized with 35 bar of CO_2 and the infrared spectrometer was set to collect one spectrum every 3 min over a 24 h period. Profiles of the absorbance at 1750 cm^{-1} (polymer) and at 1770 cm^{-1}(TMC) with time were recorded after base line correction. After the reaction was stopped, the autoclave was cooled down to room temperature, and vented in a fume hood. The reaction solution was analyzed by ^1H NMR spectroscopy in the same manner as above, to determine the percent conversion to products, and the percentages of poly(TMC), TMC, and ether linkages.

Cocatalyst, Substrate Binding, and Ring-Opening Step Examined by Infrared Spectroscopy. Cocatalyst, substrate binding, and ring-opening step studies were examined by solution infrared spectroscopy. The catalytic system used in these studies was complex **IV-1** (50 mg) in the presence of *n*-Bu_4NN_3 as cocatalyst, and using TCE as the solvent (4 mL).

Statistical Deconvolution of FTIR Spectra. Where noted FTIR spectra were deconvoluted using Peakfit, version 4.12 (*Peakfit for Windows*, v. 4.12; SYSTAT Software Inc: San Jose, CA, 2003). Statistical treatment was a residuals method utilizing a combination Gaussian-Lorentzian summation of amplitudes with a linear baseline and Savitsky-Golay smoothing.

Control Experiments for the Ring-Opening Polymerization of Trimethylene Carbonate. In a typical experiment, the appropriate amounts of TMC, complex **IV-1**, and/or *n*-Bu_4NBr were weighted out in a Schlenk flask in a monomer:catalyst:cocatalyst ratio of 300:1:2 followed by the addition of 30 mL of toluene. The reaction vessel was

placed into a preheated oil bath at 110ºC and stirred for the corresponding reaction time. The percent conversion to polymer was obtained by analyzing the reaction solution by ^{1}H NMR spectroscopy.

X-ray Structural Study. Single crystals of trimethylene carbonate were grown and isolated from a reaction solution as it will be explained later in the Results and Discussion section, and these were analyzed by ESI mass spectral analysis and X-ray crystallography. For the crystal structure a Bausch and Lomb 10× microscope was used to identify suitable crystals. Each crystal was coated in paratone, affixed to a nylon loop, and placed under streaming nitrogen (110K) in a Bruker - AXS Apex II three-circle X-ray diffractometer. The space group determination was made on the basis of systematic absences and intensity statistics. The crystal structure was solved by direct methods and was refined by full-matrix least-squares on F^2. All hydrogen atoms were placed in idealized positions and refined with fixed isotropic displacements parameters equal to 1.2 (1.5 for methyl protons), times the equivalent isotropic displacements parameters of the atoms to which they were attached. All non-hydrogen atoms were refined with anisotropic displacement parameters.

The following are the programs that were used: data collection and cell refinements; APEX II data collection software, data reduction; APEX II data reduction software, absorption correction; SADABS,[49] program used to solve the structure; SHELXS-97,[50] program used to refine the structure; SHELXL-97,[51] molecular graphics and preparation of material for publication; SHELXTL, version 6.14,[52] X-Seed, version 1.5.[53]

Results and Discussion

Our initial study was to employ the (salen)Co(II) catalyst, complex **IV-1**, in the presence of various cocatalysts to investigate the catalytic activity and selectivity for cyclic carbonate *vs* copolymer formation from the coupling of oxetane and carbon dioxide. The chiral version of complex **IV-1** was employed in this study because of its commercial availability. Since there is not an opportunity for asymmetry in the copolymer produced, a racemic catalyst would suffice. The copolymerization reactions were performed under identical reaction conditions, i.e., 110°C and 35 bar of CO_2 pressure, and the monomer:catalyst:cocatalyst ratio was maintained at 350:1:2. The results are summarized in Table IV-1. The product mixtures were analyzed by ^{1}H NMR spectroscopy, with the quantities of poly(TMC), TMC, and ether linkages in poly(TMC) determined by integrating the resonances at 4.23, 4.43, and 3.50 ppm, respectively. As is readily seen in Table IV-1, both products poly(TMC) and TMC were obtained with the use of bromide and iodide based cocatalysts, and the yield of poly(TMC) was much greater than that of the cyclic product (entries 1 and 2, Table IV-1). Among the ionic based cocatalysts examined, the bromide anion displayed the highest catalytic activity (entry 1, Table IV-1). The iodide, chloride, and azide anions were found to be significantly less effective (entries 2-4, Table IV-1). The catalytic activity of this system largely depended on the counter anion of the cocatalyst used, and the order of decreasing activity was $Br^- > I^- > Cl^- > N_3^-$. A similar trend has been observed by Endo for the coupling of carbon dioxide or carbon disulfide and aziridines, employing alkali metal halides or tetraalkylammonium halides as catalysts.[89] In addition, Caló reported the

coupling of oxiranes and CO_2 to produce cyclic carbonates in the presence of molten tetra-*n*-butylammonium bromide as catalyst.[77]

Table IV-1. Copolymerization of Oxetane and CO_2 Catalyzed by Complex **IV-1** in the Presence of Various Cocatalysts.[a]

Entry	Cocatalyst	% Conversion[b]	% Poly(TMC)[b]	% TMC[b]	% CO_2 Content[b]
1	*n*-Bu_4NBr[c]	68.4	93.3	6.7	98.4
2	*n*-Bu_4NI	13.9	93.0	7.0	97.6
3	*n*-Bu_4NCl	6.4	100	0	>99
4	*n*-Bu_4NN_3	1.4	100	0	>99
5	DMAP	0.44	0	100	>99
6	Triethylamine	1.06	0	100	>99

[a]Copolymerization conditions: 119 mg of catalyst, 4 g of oxetane, M/I = 350:1, 2 equivalents of cocatalyst, 35 bar of CO_2, at 110 °C for 24 h. [b]% Conversion to products, product distributions, and % of CO_2 content were determined by ^{1}H NMR spectroscopy. [c]M_n (GPC) = 7 560, PDI = 1.56, M_n(theoretical) = 22 852.

It was also of interest to investigate the catalytic activity of amine-based cocatalysts such as DMAP and triethylamine for this process. It has been reported in the literature that these types of initiators in the presence of cobalt, zinc, copper, chromium and tin based catalysts, are active for the formation of cyclic carbonates from the coupling of propylene oxides and CO_2.[71b, 72c, 74, 90] In contrast, triethylamine and DMAP were found to be ineffective for the coupling of oxetane and CO_2 in the presence of complex **IV-1** (entries 5 and 6, Table IV-1), most likely due to the difficulty of these amine-based cocatalysts to ring-open oxetane.

In Chapter III, we showed that oxetane ring-opening is a higher energy process than the corresponding reaction involving epoxides as catalyzed by (salen)CrX complexes along with anionic-based cocatalysts. Thus, a good nucleophile would be

required for this step. On the other hand, the formation of TMC, which is most likely caused by a backbiting mechanism, needs a good leaving group (**Scheme IV-2**). It is worth mentioning at this point that in the case of the tetraalkylammonium halide-based cocatalysts studied, the tetraalkylammonium cation is weakly interacting, and hence the anions are freer for ring-opening the monomer. The order of decreasing nucleophilicity of the anions, in a polar aprotic media (neat oxetane) and in a nonpolar solvent (such as toluene, as it will be shown later) is $N_3^- \sim Cl^- > Br^- > I^-$. The bromide anion, being in the middle of the series, is promoting the formation of the cyclic product better than the iodide, chloride and azide ions. The iodide anion is the best leaving group among the series, but at the same time it is a poorer nucleophile and does not as readily facilitate the ring-opening reaction. On the contrary, the azide and chloride anions are the better nucleophiles but are the poorer leaving groups of the series, and as a result they do not drive the reaction to the formation of the cyclic carbonate product. Of importance to point out at this time, is that the formation of copolymer is evident with the use of the bromide anion, and its mechanism of formation will be discussed *vide infra*.

Scheme IV-2. General Proposed Reaction Pathway for the Coupling of Oxetane and CO_2 Catalyzed by (salen)Co(II) Along with an Anion X^-.

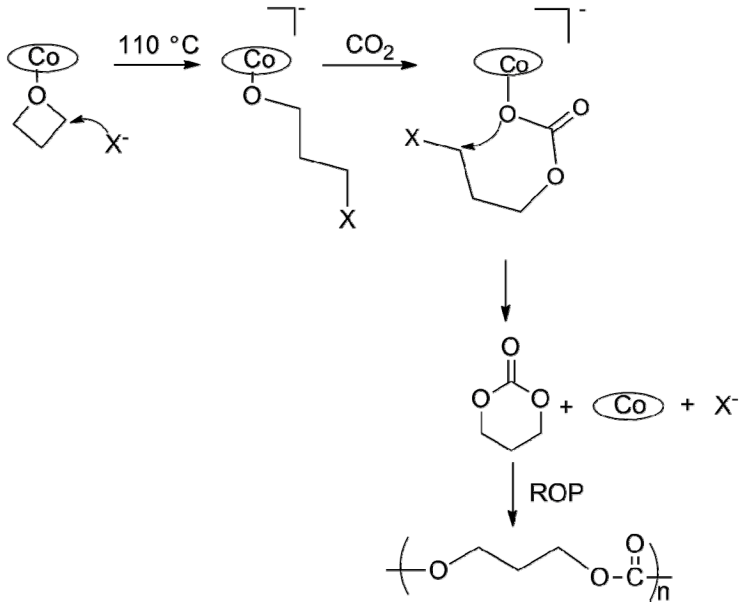

Cocatalyst, Substrate Binding, and Ring-Opening Step Examined by Solution Infrared Spectroscopy. Fundamental to a better understanding of the mechanism of the coupling reaction of oxetane and carbon dioxide catalyzed by (salen)Co(II)/*n*-Bu_4NBr, is an investigation of the initiation step of this process. For this purpose, cocatalyst/substrate binding, and ring-opening step studies carried out using solution infrared spectroscopy in TCE were designed to address this issue. For the solution infrared spectroscopy studies we utilized (salen)Co(II), complex **IV-1**, along with the azide anion derived from the very soluble *n*-Bu_4NN_3, since the ν_{N_3} stretching vibration provides accessible probes for both anion metal binding and ring-opening steps.

The infrared spectrum of complex **IV-1** in the presence of two equivalents of *n*-Bu_4NN_3 revealed that most of the azide anion remained uncoordinated to the metal center. That is, a large absorbance of free N_3^- at 2009 cm^{-1} was observed with only a weak absorbance at 2052 cm^{-1} assignable to (salen)CoN_3^- being seen. Similarly, upon addition of three equivalents of *n*-Bu_4NN_3, there was an increase in the extent of azide binding to cobalt(II) as indicated by an increase in the absorbance at 2052 cm^{-1} with a concomitant decrease in the ν_{N_3} mode at 2009 cm^{-1} due to free azide. Subsequent addition of an 100-fold excess of oxetane to the solution resulted in an increase intensity of the metal bound azide vibrational mode at ~2052 cm^{-1}, presumably due to (salen)CoN_3•oxetane$^-$. Upon heating the solution at 110ºC an organic azide vibration was noted at 2100 cm^{-1} which grew in intensity as the free and metal bound azide frequencies decreased in intensity. These observations are best summarized in **Scheme IV-3**.

Scheme IV-3. Ring-Opening of Oxetane Catalyzed by (salen)Co(II)/*n*-Bu_4NN_3.

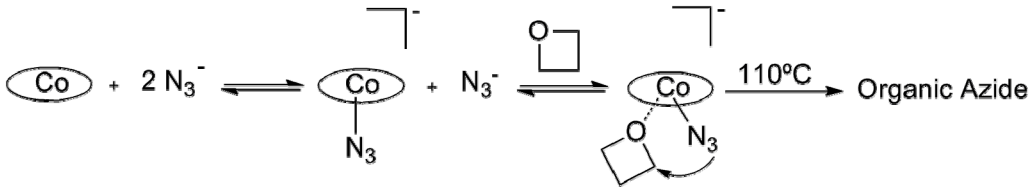

On the other hand, upon changing the cyclic ether to tetrahydrofuran, at an 100-fold excess to (salen)Co, the extent of formation of (salen)CoN_3•THF^- was seen to be

significantly lower than in the oxetane analogous process. This is consistent with the lower basicity of tetrahydrofuran compared to that of oxetane (pK_b of tetrahydrofuran = 5.00, pK_b of oxetane = 3.13).[69b] That is, in the presence of a less basic ether ligand, the formation of a stable octahedral (salen)Co(II)(N_3)(THF)$^-$ adduct is diminished.

Cocatalyst Dependence on the Copolymerization of Oxetane and CO_2 Catalyzed by (salen)Co(II)/*n*-Bu_4NBr. After examining the initiation step of the copolymerization process, we have undertaken an investigation into the cocatalyst (anion) concentration dependence of the copolymerization process in order to further optimize the catalytic system. These reactions were performed in toluene solution in the presence of complex **IV-1** along with varying amounts of *n*-Bu_4NBr. The reactions were monitored by *in situ* infrared spectroscopy by observing the growth of the copolymer's $\nu_{C=O}$ band at 1750 cm^{-1}, as well as the growth and/or consumption of the TMC's $\nu_{C=O}$ band at 1770 cm^{-1}. The three dimensional plots for poly(TMC) formation, and TMC formation and consumption, along with their corresponding reaction profiles are shown in Figures IV-2-4. It can be seen that the rate for the production of poly(TMC) is the highest when two equivalents of *n*-Bu_4NBr are utilized (Figure IV-2). The product distributions for the copolymerization reactions performed using varying amounts of *n*-Bu_4NBr are shown in Table IV-2. Consistent with the *in situ* IR data, the best catalytic activity is obtained when two equivalents of *n*-Bu_4NBr are employed (entry 2, Table IV-2). The use of one equivalent of cocatalyst was found to be detrimental to the overall process (entry 1, Table IV-2), where just an 8.2% conversion was obtained. The use of more than two equivalents of cocatalyst enhanced the production of TMC over that of

poly(TMC), but the catalytic activity is decreased. (entries 3 and 4, Table IV-2). The decrease in rate of oxetane conversion upon increasing the bromide ion concentration is

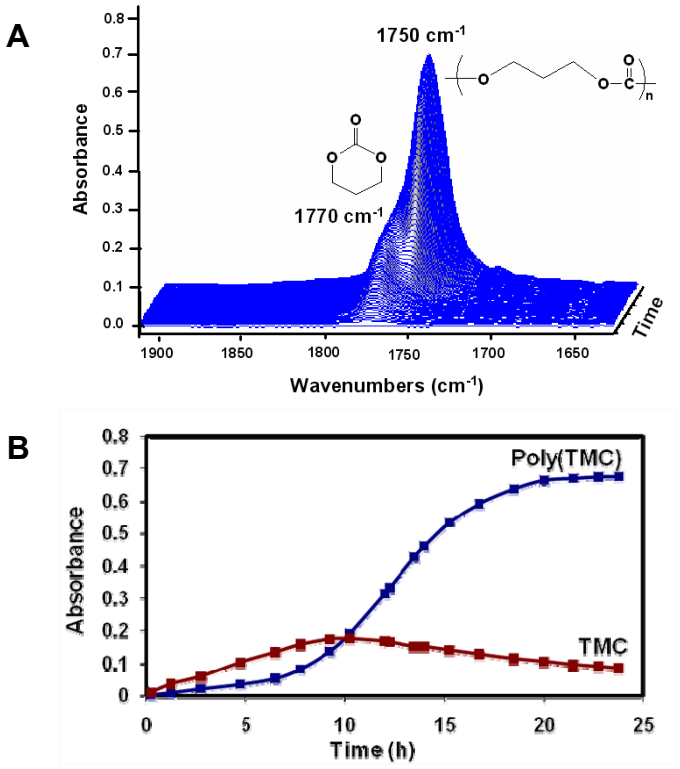

Figure IV-2. (**A**) Three dimensional stack plot of the IR spectra collected every 3 min during the copolymerization reaction of oxetane and CO_2. Reaction carried out at 110°C in toluene at 35 bar CO_2 pressure, in the presence of complex **IV-1** along with 2 equiv. of *n*-Bu_4NBr. (**B**) Reaction profiles obtained after deconvolution of selected IR spectra, indicating poly(TMC) and TMC formation with time.

likely due to competitive binding of bromide *vs* the oxetane monomer to the cobalt center. At this time it is not clear why five equivalents of bromide ion result in higher conversion as compared to three equivalents. Further studies, including attempts to kinetically model these consecutive reactions will be explored. Unfortunately, this

process is complicated by difficulties in measuring the disappearance of oxetane at high pressures and hydrolysis of bromide end groups in the polymer resulting from ROP of TMC by adventitious water. The reactions depicted in Figures IV-3 and IV-4 with 3 and 5 equivalents of *n*-Bu_4NBr, respectively, were carried out for an additional 24 hours resulting in an increase in the ratio of poly(TMC) to TMC as would be anticipated.

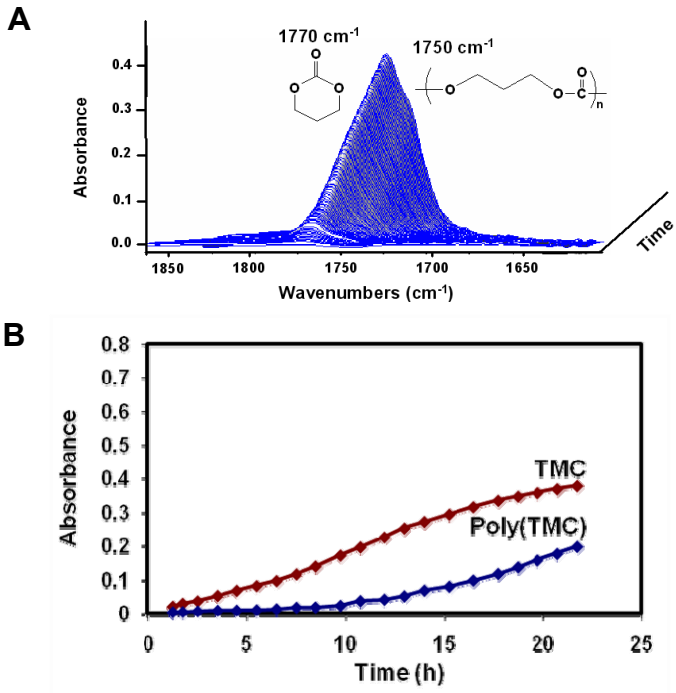

Figure IV-3. (**A**) Three dimensional stack plot of the IR spectra collected every 3 min during the copolymerization reaction of oxetane and CO_2. Reaction carried out at 110°C in toluene at 35 bar CO_2 pressure, in the presence of complex **IV-1** along with 3 equiv. of *n*-Bu_4NBr. (**B**) Reaction profiles obtained after deconvolution of selected IR spectra, indicating poly(TMC) and TMC formation with time.

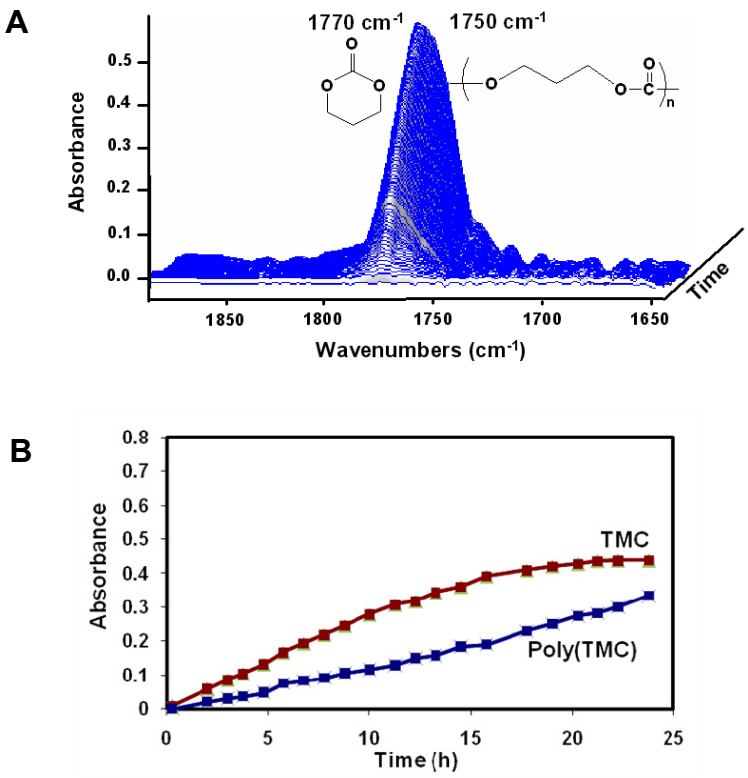

Figure IV-4. (**A**) Three dimensional stack plot reaction profile of the IR spectra collected every 3 min during the copolymerization reaction of oxetane and CO_2. Reaction carried out at 110°C in toluene at 35 bar CO_2 pressure, in the presence of complex **IV-1** along with 5 equiv. of *n*-Bu_4NBr. (**B**) Reaction profiles obtained after deconvolution of selected IR spectra, indicating poly(TMC) and TMC formation with time.

Table IV-2. Copolymerization of Oxetane and CO_2 Catalyzed by Complex **IV-1** in the Presence of Varying Quantities of *n*-Bu_4NBr[a]

Equiv. of Cocatalyst	% Conversion[b]	% Poly(TMC)[b]	% TMC[b]	% CO_2 Content[b]
1	8.2	53.5	46.5	>99
2[c]	64.0	95.2	4.8	97.3
3	28.8	32.2	67.8	>99
5	46.7	20.9	79.1	>99

[a]Copolymerization conditions: 277 mg of catalyst, 4 g of oxetane, 10 mLs of toluene, M/I = 150:1, 35 bar of CO_2, at 110 °C for 24 h. [b] % Conversion to products, product distributions, and % of CO_2 content were determined by ^1H NMR spectroscopy. [c]M_n (GPC) = 4 215, PDI = 1.64, M_n(Theoretical) = 9 344.

The reaction solution obtained from the experiment performed employing (salen)Co(II) with 5 equivalents of *n*-Bu_4NBr was further analyzed by electron-spray ionization mass spectrometry. The parent ions of $(TMC + Li)^+$ and $(2TMC + Li)^+$ (Figure IV-5) were observed in the positive mode of the ESI-mass spectrum at 109.04 and 211.07 m/z, respectively. This result strongly suggests that larger size cyclic backbiting products are possible during the reaction. Pertinent to this point, single crystals of trimethylene carbonate were isolated from the reaction solution and characterized by X-ray crystallography (Figure IV-6). The structure of trimethylene carbonate has been reported by Kataeva and coworkers in the gas phase by electron diffraction, and in solution using the Kerr effect and dipole moments.[91] The metric parameters for TMC are similar to those previously reported but are of greater accuracy with $R_1 = 0.0277$, $R_w = 0.0753$ and a goodness-of-fit of 1.017. Crystallographic data pertaining to this crystal structure are provided in Table IV-3, with selected bond distances and angles provided in Table IV-4.

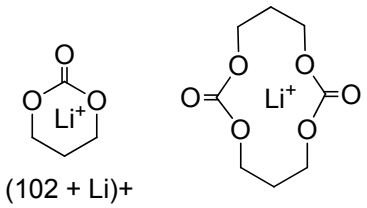

Figure IV-5. Lithium adducts of TMC and dimeric TMC.

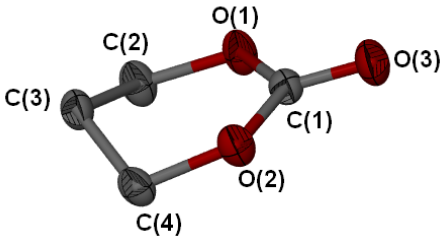

Figure IV-6. Thermal ellipsoid plot of trimethylene carbonate. Ellipsoids are at the 50 % level. H atoms are omitted for clarity.

Table IV-3. Crystallographic Data for Trimethylene Carbonate.

empirical formula	$C_4H_6O_3$
fw	102.09
temperature (K)	110(2) K
crystal system	Monoclinic
space group	P21/n
a (Å)	6.097(6)
b (Å)	11.306(11)
c (Å)	6.734(7)
α (deg)	90.0
β (deg)	102.259(11)
γ (deg)	90.0
V (Å^3)	453.6(8)
D_c (Mg/m^3)	1.495
Z	4
abs coeff (mm^{-1})	0.130
reflections collected	3668
independent reflections	708 [R(int) = 0.0277]
restrains/parameters	0/64
GOF on F^2	1.017
final *R* indices [$I > 2\sigma(I)$]	$^aR_1 = 0.0277$ $^bR_w = 0.0753$
final *R* indices (all data)	$^aR_1 = 0.0286$ $^bR_w = 0.0762$

Table IV-4. Selected Bond Distances and Angles for Trimethylene Carbonate.[a]

O(1)-C(1)	1.3296(18)
O(1)-C(2)	1.4545(17)
O(3)-C(1)	1.2056(15)
C(2)-C(3)	1.4910(19)
C(1)-O(2)-C(4)	120.97(10)
O(3)-C(1)-O(2)	119.73(12)
O(1)-C(1)-O(2)	120.44(9)
O(1)-C(2)-C(3)	110.91(11)
C(2)-C(3)-C(4)	107.47(10)

[a] Units of bond angles and bond distances are (º) and (Å), respectively.

Polymer Characterization. Relevant to our mechanistic studies for copolymer formation was the characterization of the polymers by ^{1}H NMR spectroscopy, and their molecular weight determinations by gel permeation chromatography. In general, the observed M_n values of the copolymers obtained from the coupling of oxetane and CO_2 in the presence of (salen)Co(II)/*n*-Bu_4NBr were found to be much lower than the expected theoretical values. This is most likely due to a chain transfer mechanism arising from the presence of trace quantities of water in the system.[11b, 55a]

It was of interest to carefully analyze the copolymers obtained from oxetane/CO_2 by ^{1}H NMR spectroscopy to determine if the copolymers contained ether linkages. We have previously shown that polycarbonates obtained from the ring-opening polymerization of TMC catalyzed by (salen)CrCl complexes in the presence of *n*-Bu_4NN_3 contained no ether linkages. On the other hand, by utilizing the same catalyst

system copolymers obtained from oxetane/CO_2 showed minimal amounts of ether linkages (Chapter II). Figure IV-7 illustrates the ^1H NMR spectrum of a purified polycarbonate sample obtained from the copolymerization of oxetane and carbon dioxide. Purification of the copolymer was achieved by precipitation from a dichloromethane solution with 1 M HCl in methanol, followed by vacuum drying. In general, a small amount of ether linkages are observed in the copolymers (~1.1%), which strongly suggests, that oxetane is ring-opened during polymer chain growth.

The presence of ether linkages was further confirmed by treatment of the polymer with trifluoroacetic anhydride in $CDCl_3$ (Figure IV-8). Trifluoroacetic anhydride reacts rapidly with –OH end groups of the polymers, with the signal of the resulting $–CH_2O-C(O)CF_3$ end groups showing up around 0.5 ppm downfield relative to the $–CH_2OH$ end groups. In a similar manner, a downfield shift of about 0.1-0.15 ppm of the ether linkages is expected, and indeed, it was observed after addition of trifluoroacetic anhydride. Kricheldorf has reported this method as a way to identify $–CH_2OH$ end groups, and ether linkages in poly(TMC) samples. The downfield shift of the ether linkages was attributed to hydrogen bonding between the oxygen of ether linkages and the liberated trifluroacetic acid byproduct. In good accordance with this interpretation was the increase of the downfield shift of the ether linkages with higher concentrations of trifluoroacetic acid observed by Kricheldorf.[61] Ether linkages which are observed at 3.50 ppm may be overlapping with $–CH_2Br$ end groups in the copolymer

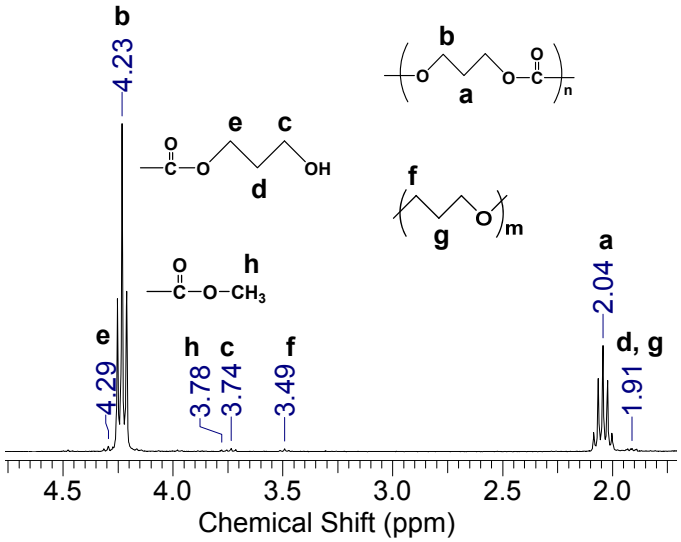

Figure IV-7. ^{1}H NMR spectrum in $CDCl_3$ of poly(TMC) obtained by way of oxetane/CO_2, in the presence of (salen)Co(II)/*n*-Bu_4NBr as the catalytic system. Polymer was purified from dichloromethane and 1 M HCl solution in methanol.

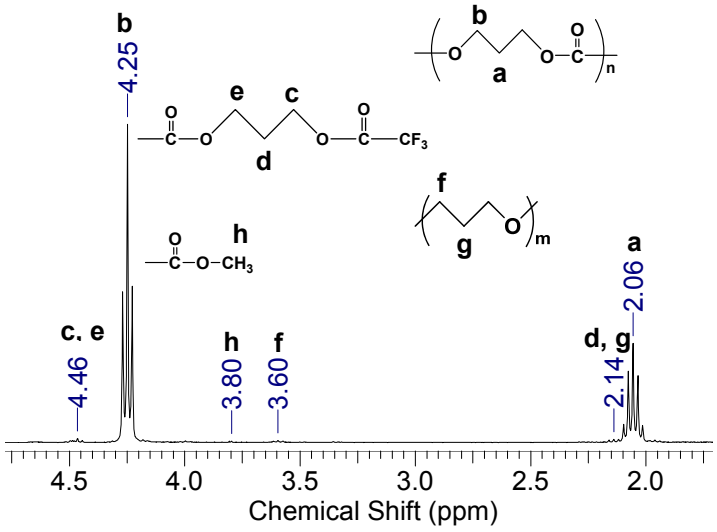

Figure IV-8. ^{1}H NMR spectrum in $CDCl_3$ of poly(TMC) obtained by way of oxetane/CO_2, in the presence of (salen)Co(II)/*n*-Bu_4NBr as the catalytic system. Polymer was purified from dichloromethane and 1 M HCl solution in methanol, and treated with trifluoroacetic anhydride.

which are expected to show at 3.5 ppm as well. However, $–CH_2Br$ end groups were not detectable by ^1H NMR.

Mechanistic Insight into the Oxetane and Carbon Dioxide Coupling Process. At this point it is beneficial to summarize our findings on the copolymerization reaction. Firstly, trimethylene carbonate production via a backbiting mechanism is evident as definitively shown by *in situ* infrared spectroscopy. Furthermore, although ring-opening polymerization of *preformed* trimethylene carbonate accounts for much of the copolymer production under certain conditions, at least some copolymer formation results from direct oxetane incorporation into the growing polymer chain. Prior to putting forth a complete mechanistic scheme for copolymer formation it remains for us to assess the conditions for trimethylene carbonate ring-opening to polycarbonate. A series of control experiments were designed to address this issue, and these are found in Table IV-5.

Initially, a copolymerization run was performed under identical conditions as described before but in the absence of the (salen)Co(II) complex, i.e., 4 g of oxetane, 35 bars of CO_2, 110°C, and *n*-Bu_4NBr as the catalyst. Under these conditions no copolymer was produced after a 24 h period (entry 1, Table IV-5). In addition, two control experiments were performed for the ring-opening polymerization of TMC, utilizing 0.5 g of TMC, 2 equiv. of *n*-Bu_4NBr, in the presence and absence of complex **IV-1**, and reaction temperature 110°C (Table IV-5, entries 2 and 3). As readily seen on Table IV-5, the percent conversion to polymer obtained from the reaction where complex **IV-1**/*n*-Bu_4NBr was employed as the catalyst system was slightly higher than that where *n*-

Bu_4NBr was employed alone (entries 2 and 3). Similarly, longer reaction times (4 h) produced closer percent conversion to polymer (entries 4 and 5). Importantly, after only 4 hours of reaction TMC is converted to polymer in high percent conversions in both instances. On the other hand, the coupling of oxetane and CO_2 catalyzed by (salen)Co(II)/*n*-Bu_4NBr requires a much longer reaction time (24 h) under similar reaction conditions to obtain around 64% conversion to polymer. This reaction time difference further supports the role of (salen)Co(II) on the coupling reaction. Therefore, (salen)Co(II) complex catalyzes the formation of TMC by a backbiting mechanism, and the resultant TMC undergoes ring-opening polymerization by an anionic mechanism with the bromide anions in solution.

Table IV-5. Control Experiments to Examine Copolymer Formation.[a]

Entry	Monomer	% Conversion[b]	M_n (GPC)	M_n (Theoretical)	PDI
1	Oxetane/CO_2	-	-	-	-
2	TMC[c]	78.11	29 512	23 902	1.68
3	TMC[c]	87.23	28 917	26 692	1.68
4	TMC[d]	89.78	25 025	27 473	1.63
5	TMC[d]	88.14	22 053	26 971	1.66

[a]Reaction conditions: Oxetane/CO_2 run: 4 g of oxetane, M/I = 350:1, 2 equiv of *n*-Bu_4NBr, 35 bar of CO_2, at 110°C for 24 h. TMC runs (entries 2 and 4): 0.5 g TMC, M/I = 300:1, 2 equiv. of *n*-Bu_4NBr, 30 mLs of toluene, at 110 °C. TMC runs (entries 3 and 5): 0.5 g TMC, M/I = 300:1, 10 mg of complex **IV-1**, 2 equiv. *n*-Bu_4NBr, 30 mLs of toluene, at 110°C. [b]% Conversion to polymer was determined by ^1H NMR spectroscopy. [c]Reaction time = 1 h. [d]Reaction time = 4 h.

Scheme IV-4 summarizes the proposed mechanistic aspects for the coupling reaction of oxetane and carbon dioxide catalyzed by (salen)Co(II)/*n*-Bu_4NBr catalyst,

Scheme IV-4. Proposed Mechanism for the Coupling of Oxetane and CO_2 Catalyzed by (salen)Co(II)/*n*-Bu_4NBr.

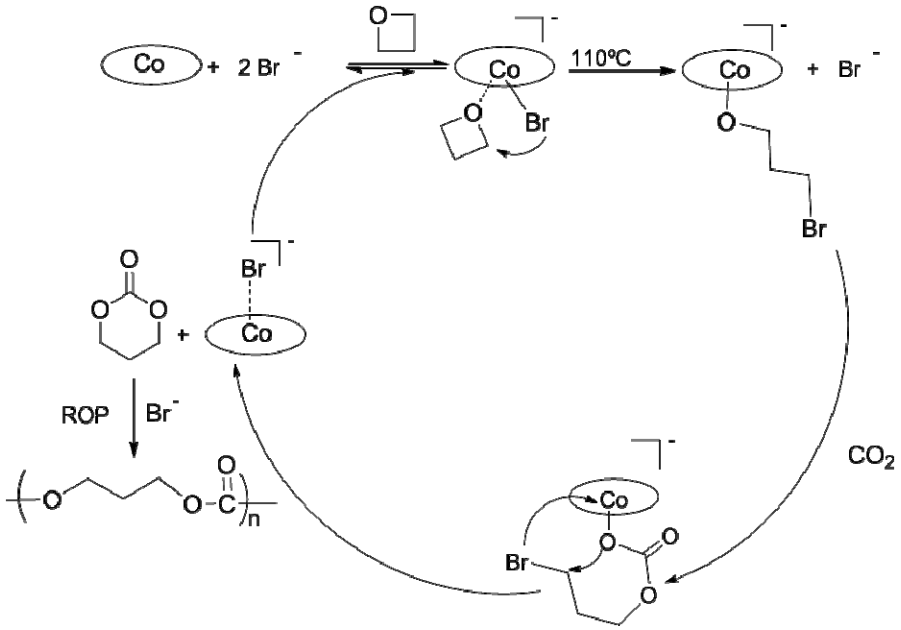

based on our current experimental findings. In the initiation step, treatment of (salen)Co(II) with two equivalents of *n*-Bu_4NBr, and in the presence of oxetane monomer, a (salen)Co(II)Br·(oxetane)$^-$ adduct is formed. Following the initial ring-opening of oxetane by bromide and CO_2 insertion into the resultant cobalt-oxygen bond, the formation of TMC by a backbiting process with ring closure is evident. Regeneration of a (salen)$CoBr^-$ species is then followed by oxetane binding to the cobalt center and the catalytic cycle starts over. Moreover, ring-opening polymerization of preformed TMC may be carried out by an anionic mechanism in the presence of bromide anion in solution, to yield poly(TMC). Furthermore, it is important to note that oxetane

insertion into the polymer chain occurs, which generates small amounts of ether linkages in the copolymer.

Since (salen)CoX complexes in the presence of quaternary organic salts have been shown to be effective catalyst systems under mild reaction conditions for the epoxide/CO_2 coupling process, it was of interest to examine this catalyst for the copolymerization of oxetane and CO_2.[8b, 11a, 11d] For this study the (salen)Co(III)Cl complex along with anionic initiators from *n*-Bu_4NX or PPNX (X = Cl or N_3) was utilized. The polymerization reactions were performed under identical reaction conditions to those employed in the (salen)Co(II) investigation, i.e., 110ºC and 35 bar CO_2 pressure. Under these conditions no copolymer was obtained after 24 h, and upon lowering the reaction temperature to 50ºC no improvement in catalytic activity was noted. However, upon changing to (salen)Co(III)Br in the presence of *n*-Bu_4NBr catalytic activity was observed, with the results indicated in Table IV-6.

Table IV-6. Selectivity for Poly(TMC) and TMC Formation Using (Salen)CoBr Complex in the Presence of *n*-Bu_4NBr as Cocatalyst.[a]

Salen Cobalt(III)Complex	Cocatalyst (Equivalents)	% Conversion[b]	% Poly(TMC)[b]	% TMC[b]	% CO_2 Content[b]
(salen)CoBr	*n*-Bu_4NBr (1 equiv.)	34.37	32.93	67.02	>99
(salen)CoBr[c]	*n*-Bu_4NBr (2 equiv.)	62.28	41.52	58.47	>99

[a]Copolymerization conditions: 157 mg of catalyst, 2 g of oxetane, M/I = 150:1, 35 bar of CO_2, at 110°C for 24 h. [b]% Conversion to products, product distributions, and % of CO_2 content were determined by ^{1}H NMR spectroscopy. [c]M_n (GPC) = 6 284, PDI = 1.68, M_n(Theoretical) = 3 960.

As noted in Table IV-6, the percent conversion to products, poly(TMC) and TMC, increases upon increasing the number of equivalents of *n*-Bu_4NBr from one to two equivalents. This observation, coupled with the lack of catalytic activity seen for the chloride and azide catalyst analogs, is consistent with what is observed when utilizing (salen)Co(II) complexes as catalysts. Indeed, upon quenching the copolymerization process, a red solid precipitates which was identified as (salen)Co(II). Recall, (salen)CoX complexes are a deep green in color. This behavior of (salen)CoX complexes operating at elevated temperatures has been previously observed numerous times.[2c] Hence, copolymerization reactions of oxetane and CO_2 at 110ºC employing (salen)CoX/*n*-Bu_4NX catalyst systems proceed via the mechanism described in **Scheme IV-4** for the (salen)Co(II) complex.

Concluding Remarks

We initially chose the (salen)Co(II) catalyst for the coupling of oxetanes and carbon dioxide because of its reduced electrophilicity and substitutional lability relative to (salen)CrX complexes. That is, (salen)Co(II) should have less of a tendency to bind the growing polymer chain, thus leading to an enhanced rate of cyclization of the free anionic CO_2 inserted ring-opened monomer or oligomer. As has been documented, the metal center in (salen)CoX is also less electrophilic than that in (salen)CrX, however noted herein and elsewhere, (salen)CoX complexes are unstable with regard to reduction to (salen)Co under the required reaction conditions of elevated temperatures. An unanswered issue in this study is whether the metal's only involvement is to activate the oxetane for ring-opening. In other words, does CO_2 insertion occur at the metal center

or does CO_2 simply react with the dissociated alkoxide resulting from ring-opened oxetane?

CHAPTER V

TUNING THE SELECTIVITY OF THE OXETANE AND CO_2 COUPLING PROCESS CATALYZED BY (SALEN)CrCl/*n*-Bu_4NX: CYCLIC CARBONATE FORMATION VS ALIPHATIC POLYCARBONATE PRODUCTION

Introduction

In Chapter II, detailed mechanistic and kinetic studies on the copolymerization of oxetane and CO_2 catalyzed by a (salen)Cr(III)Cl complex, namely, 1,2-cyclohexanediamino-*N,N'*-bis-(3,5-di-*tert*-butylsalicylidene)chromium(III) chloride, (complex **II-4**), along with an anionic-based cocatalyst, *n*-Bu_4NN_3, were presented (Figure V-1). Our studies have demonstrated that this catalytic system allows for two operative pathways responsible for polycarbonate formation. These are the direct enchainment of oxetane and CO_2, and the ring-opening polymerization of preformed trimethylene carbonate via a coordination-insertion mechanism (**Scheme V-1**). Complex **II-4** was employed in this investigation because it was found to be the more active towards copolymer formation, among a series of (salen)CrCl catalysts screened for this reaction. As a consequence of our experimental findings with the (salen)CrCl/*n*-Bu_4NN_3 catalytic system, we first hypothesized that by reducing the electrophilicity of the metal salen complex in conjunction with the appropriate anionic-based cocatalyst, should modulate the selectivity of the oxetane/CO_2 coupling reaction. Indeed, in Chapter IV we showed that a (salen)Co(II) complex in the presence of anions that are

good leaving groups such as bromide, forms a very active catalyst system for the ring expansion of oxetane with CO_2 forming trimethylene carbonate. Subsequently, TMC is polymerized by an anionic ring-opening polymerization mechanism in the presence of bromide ions in the reaction solution.

These results inspired us to further explore the activity and selectivity of the (salen)Cr(III)Cl catalyst in the presence of anions that are better leaving groups than the azide anion, i.e., bromide and iodide. We surmised that this catalytic system should more effectively tune the selectivity of the oxetane/CO_2 coupling process for cyclic carbonate formation, and/or for polycarbonate produced from the homopolymerization of preformed TMC (**Scheme V-1**, route (2)). The isolation of trimethylene carbonate from this process is also of interest because it could be used in melt polymerization processes with other monomers such as lactides or caprolactones, for the production of important copolymers. In addition, the polycarbonate obtained from the ROP of preformed TMC would have no ether linkages, as we have previously demonstrated for the ROP of TMC in the presence of the (salen)CrCl catalyst, along with an anionic-based cocatalyst (Chapter II). This would result in a polycarbonate with better physical properties.

Herein, we wish to report further studies on this transformation as it pertains to the effects of a variety of anionic-based cocatalysts on the selectivity of the oxetane and CO_2 coupling reaction catalyzed by complex **II-4**. An investigation of the nature of the catalytic species involved in the reaction will be described. Additionally, the

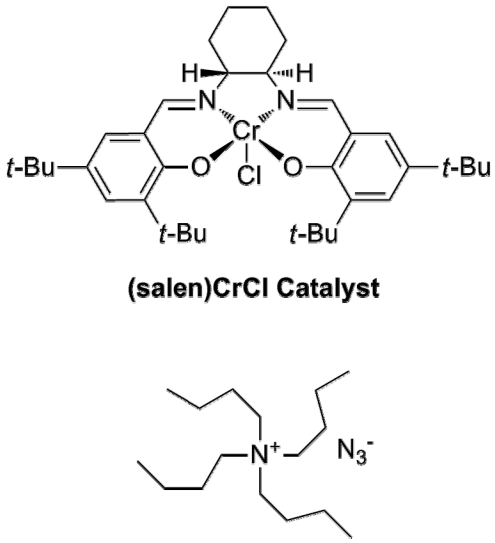

Figure V-1. The (salen)CrCl complex **II-4**, and anionic-based cocatalyst employed in mechanistic and kinetic studies performed on the copolymerization of oxetane and CO_2 (Chapter II).

Scheme V-1. Proposed Reaction Mechanism (Chapter II).

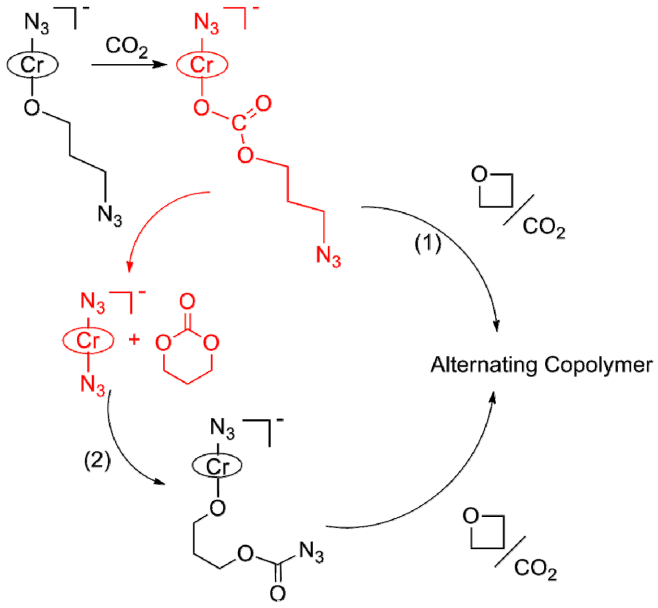

dependence of reaction temperature on the selectivity of the coupling of oxetane and CO_2 as monitored by high-pressure *in situ* IR spectroscopy will be presented. Lastly, the effects of temperature and pressure on the selective synthesis of TMC from the coupling of oxetane and CO_2 will be discussed.

Experimental Section

Reagents and Methods. Unless otherwise specified, all syntheses and manipulations were carried out on a double-manifold Schlenk vacuum line under an atmosphere of argon or in an argon filled glove box. Toluene and tetrahydrofuran were freshly distilled from sodium/benzophenone. Ethanol was freshly distilled from Mg/I_2. Diethyl ether, dichloromethane, and hexanes were purified by an MBraun Manual Solvent Purification System packed with Alcoa F200 activated alumina desiccant. Oxetane (Alfa Aesar) was freshly distilled over CaH_2 and stored in the freezer of the glove box. Tetra-*n*-butylammonium bromide (Eastman), tetra-*n*-butylammonium iodide (Eastman), and tetra-*n*-butylammonium chloride (TCI) were recrystallized from acetone/diethyl ether before use. Tetra-*n*-butylammonium azide (TCI), and tetra-*n*-butylammonium cyanate (Fluka) were stored in the freezer of the glove box upon arrival. Chromium(II) chloride (Alfa Aesar) and sodium sulfate (EMD) were used as received. Bone-dry carbon dioxide supplied in a high-pressure cylinder and equipped with a liquid dip tube was purchased from Scott Specialty Gases. PPNBr ($PPN^+ = (Ph_3P)_2N^+$) was synthesized following the procedure reported in the literature for the synthesis of $PPNN_3$.[48] The syntheses of *N,N'*-bis(3,5-di-*tert*-butylsalicylidene)-1,2-cyclohexanediimine, *N,N*'-bis(3-*tert*-butyl-5-methoxysalicylidene)-1,2-phenylene

diimine, 1,2-cyclohexanediamino-*N,N'*-bis-(3,5-di-*tert*-butylsalicylidene)chromium(III) chloride (complex **II-4**), and 1,2-phenylenediamino-*N,N*'-bis(3-*tert*-butyl-5-methoxysalicylidene)chromium(III) chloride (complex **V-1**) were performed as described in the literature.[45] Single crystals of (salen)Cr(Cl)$_x$(Br)$_y^-$PPN$^+$ (complex **V-2**) were obtained by layering hexanes into a saturated dichloromethane solution of the corresponding (salen)CrCl complex (1,2-phenylenediamino-*N,N*'-bis(3-*tert*-butyl-5-methoxysalicylidene)chromium(III) chloride) containing two equivalents of PPNBr. ESI-MS: *m/z* 608.05 [(salen)Cr(Cl$_2$)$^-$], 698.04 [(salen)Cr(Br$_2$)$^-$], 653.99, [(salen)Cr(Cl)(Br)$^-$], 632.09 [(salen)Cr(Cl)(OAc)$^-$], and 678.03 ([(salen)Cr(Br)(OAc)$^-$].

^{1}H NMR spectra were acquired on Unity+ 300 MHz and VXR 300 MHz superconducting NMR spectrometers. Molecular weight determinations (M_n and M_w) were carried out with Viscotek Modular GPC apparatus equipped with ViscoGEL^{TM} I-series columns (H + L), and Model 270 dual detector comprised of RI and Light Scattering detectors. High-pressure reactions were performed using an ASI ReactIR 1000 reaction analysis system with stainless steel Parr autoclave modified with a permanently mounted ATR crystal (SiComp) at the bottom of the reactor (purchased from Mettler Toledo).

Copolymerization Reactions Monitored by *in situ* IR Spectroscopy. In a typical experiment, complex **II-4 (**124.4 mg**)**, the appropriate amount of cocatalyst, *n*-Bu$_4$NX, (X = Br, I, Cl, N$_3$, NCO), and oxetane (4 g) were dissolved in 10 mL of toluene and delivered via the injection port into a 300-mL stainless steel Parr autoclave reactor that was previously dried in vacuo overnight at 80°C. The monomer:catalyst:cocatalyst

ratio was maintained at 350:1:2. The autoclave is modified with a 30 bounce SiComp window to allow for the use of an ASI ReactIR 1000 system equipped with a MCT detector. In this manner a 128-scan background spectrum was collected after the reaction mixture was heated to the temperature of the corresponding experiment. The autoclave was pressurized with the appropiate CO_2 pressure, and the infrared spectrometer was set to collect one spectrum every 3 min over a 24 h period. Profiles of the absorbance at 1750 cm^{-1} (polymer) and at 1770 cm^{-1} (TMC) with time were recorded after base line correction. After the reaction was stopped, the autoclave was cooled down to room temperature, and vented in a fume hood. The percent conversion to products was determined based on the amount of oxetane monomer left in the reaction solution. ^{1}H NMR (300 MHz, $CDCl_3$), oxetane: δ 4.75 (t, 4H, OC*H*$_2$) and 2.70 (quintet, 2H, *C*H_2). Furthermore, the quantities of poly(TMC), TMC, and ether linkages in the copolymer were determined by integrating the peak area of the corresponding resonances. ^{1}H NMR (300 MHz, $CDCl_3$), poly(TMC): δ 4.23 (t, 4H, OC*H*$_2$) and 2.05 (quintet, 2H, *C*H_2). ^{1}H NMR (300 MHz, $CDCl_3$), TMC: δ 4.45 (t, 4H, OC*H*$_2$) and 2.14 (quintet, 2H, *C*H_2). ^{1}H NMR (300 MHz, $CDCl_3$), ether linkages: δ 3.50 (t, 4H, OC*H*$_2$) and 1.90 (quintet, 2H, *C*H_2). (Note: cocatalyst, temperature, and pressure varied within each experiment, and are described in the Results and Discussion section).

Statistical Deconvolution of FTIR Spectra. When noted FTIR spectra were deconvoluted using Peakfit, version 4.12 (Peakfit for Windows, v. 4.12; SYSTAT Software Inc., San Jose, CA, 2003). Statistical treatment was a residuals method utilizing a combination Gaussian-Lorentzian summation of amplitudes with a linear baseline and Savitsky-Golay smoothing.

Results and Discussion

Effects of Various Anionic-Based Cocatalysts on the Coupling of Oxetane and CO_2. Our initial efforts were directed at employing complex **II-4**, along with various *n*-Bu_4NX (X = Br, I, Cl, N_3, NCO) salts as cocatalysts, to examine the catalytic activity and selectivity for cyclic carbonate *vs* copolymer formation from the oxetane and CO_2 coupling reaction. The copolymerization reactions were all carried out under identical reaction conditions. i.e., 110ºC, 35 bar of CO_2 pressure in toluene solution, and were monitored by *in situ* IR spectroscopy. The growth of the copolymer was monitored by observing its $\nu_{C=O}$ band at 1750 cm^{-1}, and the growth and/or consumption of the cyclic product, TMC, by observing its $\nu_{C=O}$ band at 1770 cm^{-1}. Due to the close proximity of the carbonyl stretching bands of copolymer and cyclic carbonate, it was necessary to deconvolute selected IR spectra employing the band parameters for the pure components, in order to get accurate reaction profiles. The reaction profiles for copolymer formation as a function of various *n*-Bu_4NX cocatalysts present in two equivalents relative to complex **II-4** are shown in Figure V-2. It can be readily seen that the rates for copolymer formation differ slightly from each other, and the order of decreasing reaction rate was Br^-, $I^- > Cl^-$, $N_3^- > NCO^-$. As we have previously noted in

Chapter III, a more remarkable induction period is observed when utilizing the anion NCO^- as cocatalyst. This is consistent with this anion being a stronger field ligand, and thus displacing the Cl^- from (salen)CrCl more easily forming the corresponding [*trans*-(salen)CrX_2][*n*-Bu_4N^+] (X = NCO) complex. Concomitantly, this ligand is more difficult to be displaced by the oxetane monomer, hence retarding the initial stage of the ring-opening reaction.

Relative to the initiation step of the copolymerization process, in Chapter III we showed that the ring-opening of oxetane in the presence of (salen)Cr(III)Cl complexes by *n*-Bu_4NX (X = Cl, N_3) salts, is a higher energy process compared to the corresponding reaction involving epoxides. Recently, Jacobsen and coworkers have reported the enantioselective intramolecular openings of oxetanes-containing *O*-centered nucleophiles catalyzed by (salen)Co(III) complexes, producing good yields of enantioenriched tetrahydrofurans under mild reaction conditions.[92] However, under the catalytic conditions utilized for the copolymerization reaction of oxetane and CO_2 a good nucleophile (X) is required for the ring-opening step (**Scheme V-2**). On the contrary, the formation of trimethylene carbonate which is due to a backbiting process would need a good leaving group (X) (**Scheme V-2**). Figure V-3 illustrates the reaction profiles for the series of reactions performed at 110ºC utilizing complex **II-4**, in the presence of the various anionic-based cocatalysts. Among the cocatalysts examined, the bromide anion displayed the highest catalytic activity towards trimethylene carbonate formation at the early stages of the coupling reaction, followed by the iodide, chloride, azide, and cyanate anions. The bromide anion under these catalytic conditions

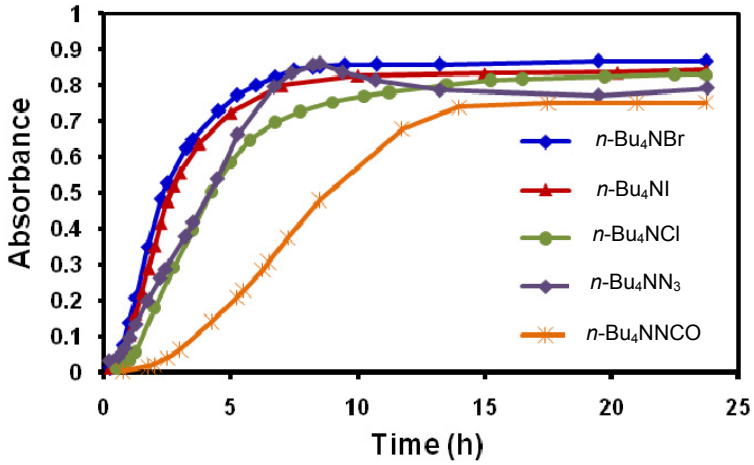

Figure V-2. Reaction profiles obtained after deconvolution of selected IR spectra, indicating copolymer formation with time for the copolymerization of oxetane and CO_2 in the presence of complex **II-4** and 35 bar of CO_2 at 110ºC employing various *n*-Bu_4NX salts as cocatalysts.

Scheme V-2. Initial Ring-Opening of Oxetane and Formation of TMC via a Backbiting Pathway.

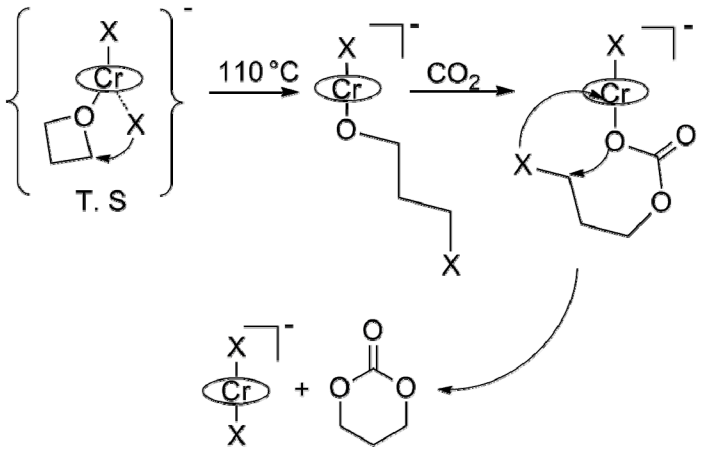

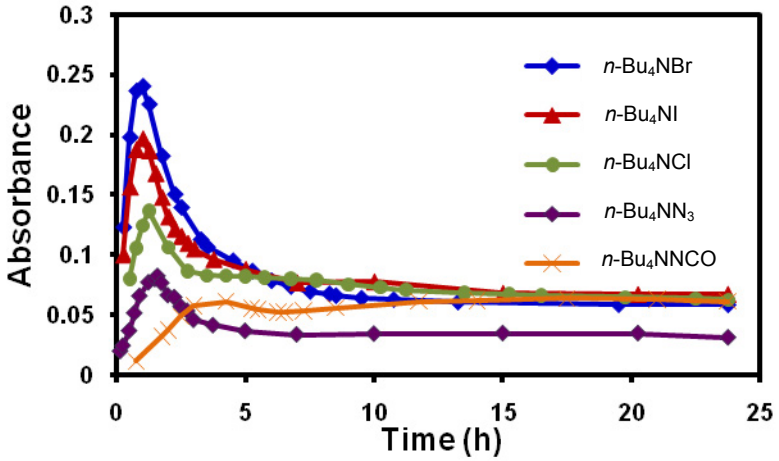

Figure V-3. Reaction profiles obtained after deconvolution of selected IR spectra, indicating trimethylene carbonate formation with time for the copolymerization of oxetane and CO_2 in the presence of complex **II-4** and 35 bar of CO_2 at 110ºC employing various *n*-Bu_4NX salts as cocatalysts.

is better promoting the formation of TMC by a backbiting mechanism. In Chapter IV, we observed a similar catalytic tendency for the formation of TMC from the coupling of oxetane and CO_2 utilizing a (salen)Co(II) complex along with anionic-based cocatalysts of the type described here, *n*-Bu_4NX (X = N_3, Cl, Br, I). Subsequently, TMC polymerizes by an anionic pathway. Others have reported analogous trends for the coupling of CO_2 or CS_2 and aziridines employing alkali metal halides or tetraalkylammonium halides as catalysts.[89] Moreover, Caló reported the formation of five-membered cyclic carbonates from the coupling of oxiranes and CO_2 utilizing molten *n*-Bu_4NBr as catalyst.[77] More recently, North and coworkers reported a detailed mechanistic study on the formation of five-membered cyclic carbonates from the

coupling of epoxides and CO_2 catalyzed by a bimetallic aluminum salen complex along with *n*-Bu_4NBr as cocatalyst.[93]

Figure V-4 shows the reaction profiles of both, copolymer and TMC formation for the copolymerization reaction of oxetane and CO_2 carried out in the presence of complex **II-4** along with 2 equivalents of *n*-Bu_4NBr as cocatalyst. It is clearly observed that when using this catalytic system and conditions the formation of TMC is enhanced at the early stages of the coupling reaction and its concentration is rapidly decreased over time. On the other hand, the concentration of poly(TMC) is initially inhibited followed by rapidly increasing over the course of the reaction. The product distribution for the copolymerization reactions carried out using various anionic-based cocatalysts is shown in Table V-1, as determined by ^1H NMR spectroscopy. All the cocatalysts examined displayed good to high activity for copolymer formation, and the percentages of poly(TMC) were found to be $\geq$ 98% with trace quantities of TMC detected after 24 h of reaction. Consistent with the *in situ* IR data, these results strongly suggest that there is an equilibrium process between the cyclic carbonate byproduct and the polycarbonate, as the percentages of poly(TMC) did not reach 100% after a 24 h reaction period. Relevant to this point, anionic equilibrium polymerizations of six-membered cyclic carbonates have been documented in the literature.[21a, 94] In this respect, monomers that undergo equilibrium polymerization processes are very useful, because this property of reversibility can be utilized in the recycling of polymeric materials.[95] It should be pointed out that we have noted more remarkable equilibrium processes between the cyclic carbonate byproduct and the corresponding polycarbonate, upon using four-

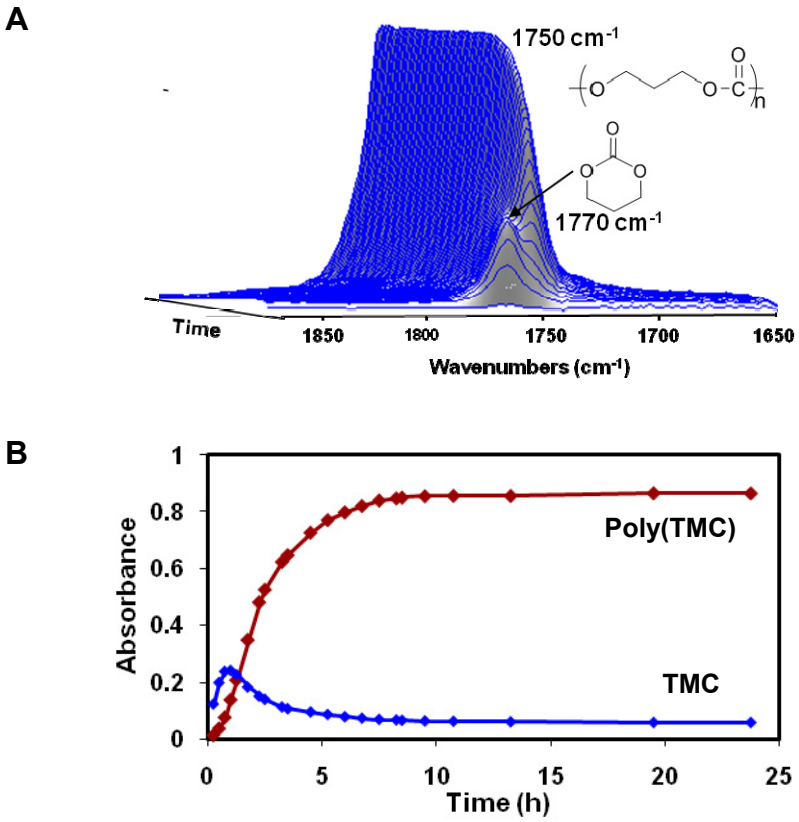

Figure V-4. (**A**) Three-dimensional stack plot of IR spectra collected every 3 min during the copolymerization reaction of oxetane and CO_2. (**B**) Reaction profiles obtained after deconvolution of selected IR spectra, indicating copolymer and trimethylene carbonate formation with time. Reaction carried out at 110ºC in toluene, at 35 bar of CO_2 pressure, in the presence of complex **II-4** and 2 equiv. of *n*-Bu_4NBr.

Table V-1. Copolymerization of Oxetane and CO_2 Catalyzed by Complex **II-4** in the Presence of Various *n*-Bu_4NX Salts as Cocatalysts.[a]

Cocatalyst	% Conversion[b]	% Poly(TMC)[b]	% TMC[b]	% CO_2 Content[b]	M_n (GPC)	PDI
n-Bu_4NBr	100	98.2	1.8	99	7 100	1.42
n-Bu_4NI	100	98.3	1.7	99	7 000	1.43
n-Bu_4NCl	75.4	>99	<1.0	97.9	7 600	1.20
n-Bu_4NN_3	74.4	>99	<1.0	97.6	5 800	1.48
n-Bu_4NNCO	67.6	>99	<1.0	98.2	4 700	1.41

[a]Reaction conditions: 124.4 mg of complex **II-4**, 2 equiv. of cocatalyst, 4 g of oxetane, 10 mL of toluene, M/I = 350:1, 35 bar of CO_2 at 110 ºC for 24 h. [b]Percent conversion to products, product distributions, and % of CO_2 content were determined by ^1H NMR spectroscopy.

membered cyclic ethers containing two substituents in the 3-position of trimethylene oxide, i.e., 3-methoxy-methyl-3-methyloxetane, and these studies will be reported in the following Chapter.

Importantly, the highest percentages of CO_2 incorporation were observed for the reactions where *n*-Bu_4NBr and *n*-Bu_4NI were used as cocatalysts. This result is consistent with the observation that in these reactions there was more TMC formed and thus, more polycarbonate produced by the ring-opening polymerization of preformed trimethylene carbonate via a coordination-insertion pathway. *It should be recalled that we have independently shown that the ROP of TMC by these catalytic systems occurs with no CO_2 loss during the copolymerization reaction (Chapter II).*

The molecular weight and polydispersities of the polycarbonates were measured in THF by gel permeation chromatography. Under these reaction conditions the typical M_n value ranged from 4 700 to 7 100 with polydispersities of 1.20 to 1.60 (Table V-1). A more detailed presentation of M_n as a function of the [monomer]/[initiator] ratio on this catalytic process may be found in Chapter II.

Examination of the Catalytic Species Involved in the Copolymerization Reaction. Subsequent studies were focused on determining the characteristics of the catalytic species formed upon treating a (salen)CrCl with two equivalents of a bromide-based cocatalyst. This catalytic system was demonstrated to have the highest activity towards TMC formation at the initial stages of the reaction at 110°C. Additionally, the polycarbonate produced displayed a high fixation of carbon dioxide (>99%). To investigate the nature of the initial catalytic species involved in the reaction a (salen)CrCl

complex, 1,2-phenylenediamino-*N,N'*-bis(3-*tert*-butyl-5-methoxysalicylidene)-chromium(III) chloride, (complex **V-1)**, was treated with two equivalents of PPNBr, and analyzed by electron-spray ionization mass spectrometry. The parent ions of (salen)$CrCl_2^-$, (salen)$CrClBr^-$, and (salen)$CrBr_2^-$ were observed in the negative mode of the ESI-MS spectrum at 608.05, 653.99, and 698.04 *m/z*, respectively. Moreover, the parent ions of (salen)Cr(Cl)$(OAc)^-$ and (salen)Cr(Br)$(OAc)^-$ were also detected, which resulted from the reaction of (salen)$CrCl_2^-$ and (salen)$CrBr_2^-$ with acetic acid, which is used during the mass spectral analysis experiment. Because of the presence of excess bromide, the complexes (salen)$CrBr_2^-$ and (salen)$CrClBr^-$ are expected to be the most abundant in solution. These results suggested that when (salen)CrCl is treated with two equivalents of bromide, a Schlenk equilibrium is produced (eq V-1.) Pertinent to this point, we have isolated and fully characterized the *n*-Bu_4N^+ salt of the (salen)$CrCl_2^-$ anion by X-ray crystallography (Figure V-5).

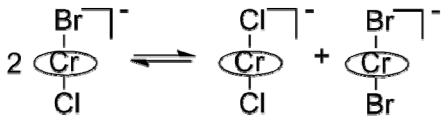

(V-1)

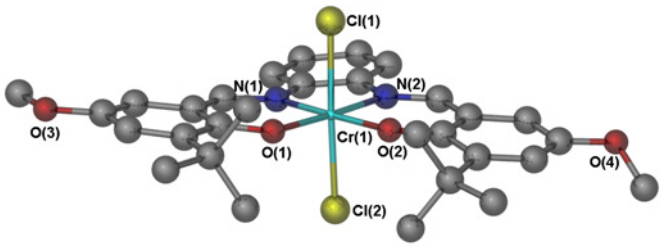

Figure V-5. Ball and stick representation of the X-ray defined structure of (salen)$CrCl_2^-$ anion, where the salen ligand contains –OMe and –*t*-Bu substituents in the 3,5 positions of the phenolates respectively, with a phenylene diimine backbone. Tetrabutylammonium cation omitted for clarity. Data taken from Chapter III.

Temperature Dependence on the Coupling of Oxetane and CO_2 Catalyzed by (salen)CrCl/*n*-Bu_4NBr. Subsequently, temperature dependence studies were performed in order to examine the selectivity of the oxetane and CO_2 coupling process utilizing the (salen)CrCl/*n*-Bu_4NBr catalytic system. We previously showed that in the presence of *n*-Bu_4NBr as cocatalyst a higher catalytic activity towards trimethylene carbonate formation is obtained at the early stages of the coupling reaction performed at 110ºC. It would be anticipated that lowering the reaction temperature would enhance the formation of TMC throughout the course of the reaction. The coupling reactions were carried out under identical reaction conditions. i.e., 35 bar of CO_2 pressure, utilizing complex **II-4** and 2 equiv. of *n*-Bu_4NBr as cocatalyst, at various reaction temperatures.

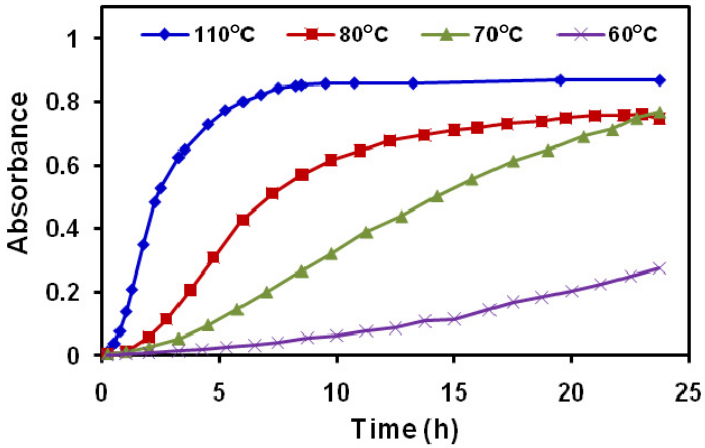

Figure V-6. Reaction profiles obtained after deconvolution of selected IR spectra, indicating poly(TMC) formation with time for the copolymerization of oxetane and CO_2 in the presence of complex **II-4**, 2 equiv. of *n*-Bu_4NBr, and 35 bar of CO_2 at various reaction temperatures.

Figure V-6 depicts the reaction profiles for copolymer formation with time for a series of reactions performed at various reaction temperatures. As anticipated the reaction rate for copolymer formation is decreased as the reaction temperature is lowered from 110 to 60ºC. Figure V-7 illustrates the reaction profiles for trimethylene carbonate formation for the series of reactions carried out at this same temperature range of 110 to 60ºC. It can be clearly observed that upon lowering the temperature from 110 to 60ºC the selectivity for the formation of trimethylene carbonate by a backbiting mechanism is enhanced during the course of the coupling reaction. This is the result of the higher temperatures needed to ROP TMC than those required to couple oxetane and CO_2 to form TMC in the presence of bromide ions. The product distribution for the copolymerization reactions is presented in Table V-2 as determined by ^1H NMR spectroscopy.

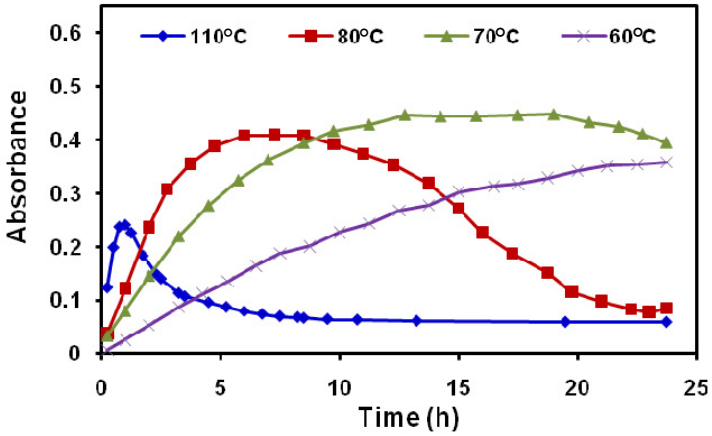

Figure V-7. Reaction profiles obtained after deconvolution of selected IR spectra, indicating TMC formation with time for the copolymerization of oxetane and CO_2 in the presence of complex **II-4**, 2 equiv. of *n*-Bu_4NBr, and 35 bar of CO_2 at various reaction temperatures.

Table V-2 clearly illustrates that lowering the reaction temperature from 110 to 60ºC drives the selectivity of the oxetane and CO_2 coupling reaction for TMC production in the presence of complex **II-4**/*n*-Bu_4NBr. As it was expected a decrease in catalytic activity is observed as the temperature is decreased, where the ring-opening of oxetane is more difficult. Nevertheless, under these catalytic conditions the formation of TMC and the production of polycarbonate through the ROP of preformed TMC via a coordination-insertion mechanism are favored. Furthermore, the highest percentages of CO_2 fixation are observed in the thus produced polycarbonates (Table V-2). It is important to note that although ring-opening polymerization of preformed trimethylene carbonate accounts for most of the polycarbonate production at lower reaction temperatures (< 80°C), we cannot rule out that at least some polycarbonate formation results from the direct enchainment of oxetane and CO_2.

Table V-2. Copolymerization of Oxetane and CO_2 Catalyzed by Complex **II-4**/*n*-Bu_4NBr at Various Reaction Temperatures.[a]

Temperature (°C)	% Conversion[b]	% Poly(TMC)[b]	% TMC[b]	% CO_2 Content[b]
110	100	98.2	1.8	99
80	100	93.3	6.7	99.3
70	73.7	62.6	37.4	>99
60	33.9	13.3	86.7	>99

[a]Reaction conditions: 124.4 mg of complex **II-4**, 2 equiv. of *n*-Bu_4NBr, 4 g of oxetane, 10 mL of toluene, M/I = 350:1, 35 bar of CO_2 at 110 ºC for 24 h. [b]Percent conversion to products, product distributions, and % of CO_2 content were determined by ^1H NMR spectroscopy.

It is evident from our recent experimental results that the formation of trimethylene carbonate is enhanced with the employment of the (salen)CrCl catalyst along with a bromide-based cocatalyst. Additionally, it is suggested that formation of TMC by a backbiting process occurring via a metal-carbonate intermediate is favored at lower reaction temperatures (< 80°C) (**Scheme V-3A)**. By way of contrast, in the chain propagation step the ring-opening of oxetane by a metal-carbonate intermediate is favored at higher reaction temperatures (≥ 80°C) (**Scheme V-3B**). As a result, enhancing the process shown in **Scheme V-3B** minimizes the ability of backbiting via a terminal bromide anion (**Scheme V-3A**) forming TMC. Although a dimer of TMC has been observed by us in a related process catalyzed by (salen)Co(II)/*n*-Bu_4NBr (Chapter IV), larger carbonate rings have not been observed thus far utilizing the (salen)CrCl/*n*-Bu_4NBr catalytic system.

Scheme V-3. (**A**) Formation of TMC by a Backbiting Mechanism Through a Metal Carbonate Intermediate. (**B**) Ring-Opening of Oxetane by a Metal Carbonate Intermediate.

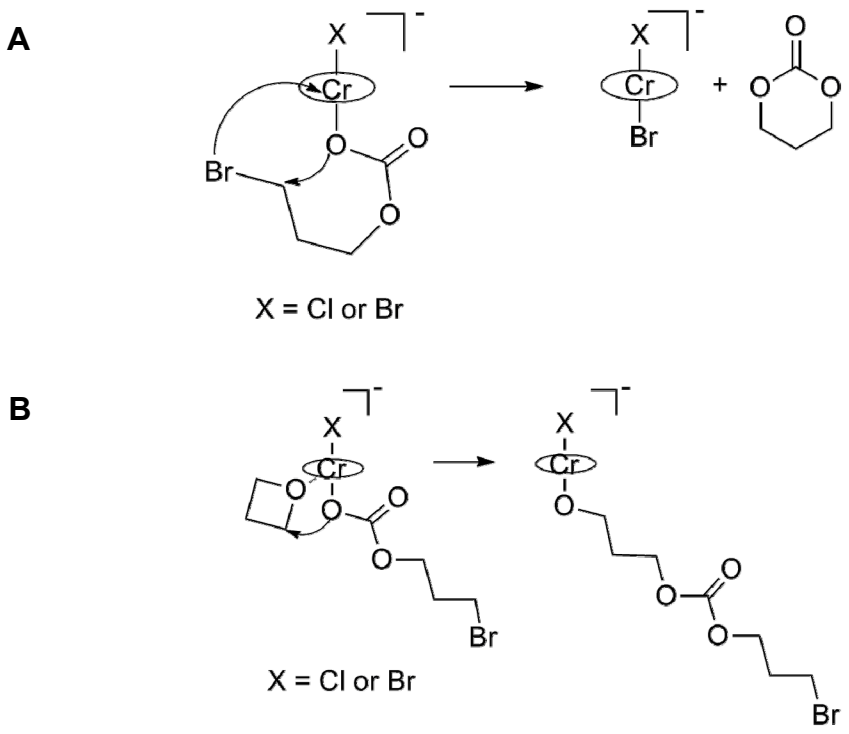

It is important to mention that we have performed a cocatalyst dependence study on the coupling reaction using complex **II-4**/*n*-Bu_4NBr as catalytic system at 110°C. As expected the initial formation of TMC was found to be increased as the number of equivalents of cocatalyst utilized increased. This was consistent with the formation of cyclic carbonate by a backbiting mechanism not only aided but the metal catalyst, but also but the free anionic polymer chain. The latter process is thought to have a lower barrier and to be assisted in the presence of excess of ionic-based cocatalysts, which serve to displace the growing polymer chain from the metal catalyst.[96]

Further Optimization of the Oxetane and CO_2 Coupling Process for Trimethylene Carbonate Formation. In an effort to tune the selectivity of the oxetane and CO_2 coupling process exclusively for trimethylene carbonate formation, we have designed a series of experiments where the temperature was kept at 60 or 50°C, and the CO_2 pressure was varied between 35 and 10 bar as shown in Table V-3 and Figures V-8 and V-9.

The ring expansion of oxetane with CO_2 catalyzed by complex **II-4** along with *n*-Bu_4NBr as cocatalyst was found to be most favored at lower reaction temperatures and CO_2 pressures (50°C, 10 bar of CO_2), even though a low conversion could only be achieved under these reaction conditions (Table V-3, Figure V-8). This result is consistent with the formation of cyclic carbonate occurring mostly via a metal-alkoxide

Table V-3. Coupling of Oxetane and CO_2 to Afford Trimethylene Carbonate.[a]

T(°C)	CO_2 Pressure (bar)	% Conversion[b]	% Poly(TMC)[b]	% TMC[b]
50	35	9.4	0	100
50	10	20.3	0	100
60	35	33.9	13.3	86.7
60	10	46.6	46.5	53.5

[a]Reaction conditions: complex **II-4** (124.4 mg), 2 equiv. of *n*-Bu_4NBr, 4 g of oxetane, 10 mL of toluene, M/I = 350:1 for 24 h. [b]Percent conversion to products and product distributions were determined by ^1H NMR spectroscopy.

intermediate (**Scheme V-4A**) rather than by a metal-carbonate intermediate (**Scheme V-4B**). Previously, we have determined an $E^{\ddagger}_{act}$ of 105 kJ/mol for the formation of *trans*-cyclohexylene carbonate in the absence of comonomers from the metal bound polymer chain.[97] On the contrary, the activation barrier for the formation of cyclic carbonate

during the copolymerization of cyclohexene oxide and CO_2 at 55 bar, was found to be 133 kJ/mol. In this case, cyclic carbonate formation was suggested to occur by way of a metal-carbonate (polymer chain) intermediate.[98] Interestingly, the effect of lowering the reaction pressure from 35 to 10 bar is slightly different when the coupling reaction is performed at 60°C (Table V-3, Figure V-9). In this instance, a higher conversion to products was achieved, and the product distribution differed significantly, with almost equivalent quantities of poly(TMC) and TMC obtained after 24 h of reaction. This is most likely due to an enhancement on the formation of TMC via a backbiting mechanism through a metal-alkoxide intermediate (**Scheme V-4A**). However, TMC produced could undergo ring-opening polymerization by a coordination-insertion pathway more readily at 60°C than at 50°C.

Scheme V-4. Formation of Trimethylene Carbonate via Backbiting Pathways.

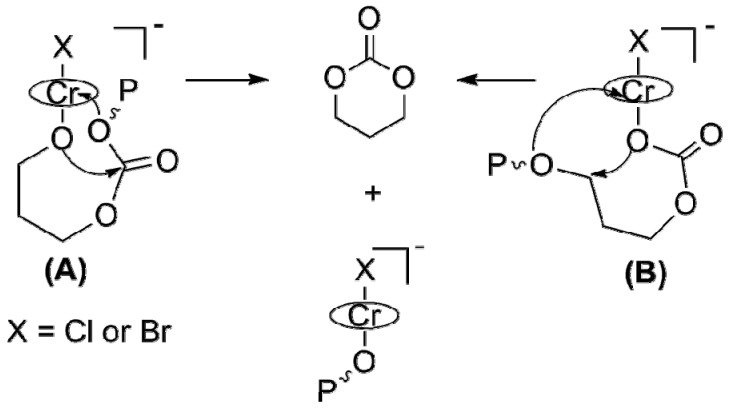

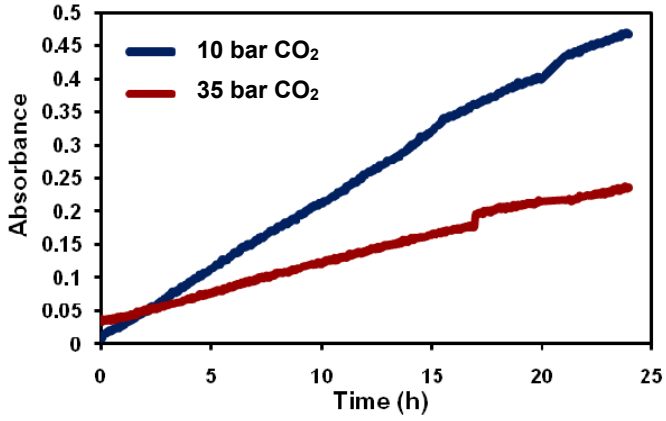

Figure V-8. Reaction profiles indicating trimethylene carbonate formation with time for the coupling of oxetane and CO_2. Reactions carried out at 50ºC in toluene in the presence of complex **II-4** and 2 equiv. of *n*-Bu_4NBr at the indicated CO_2 pressures.

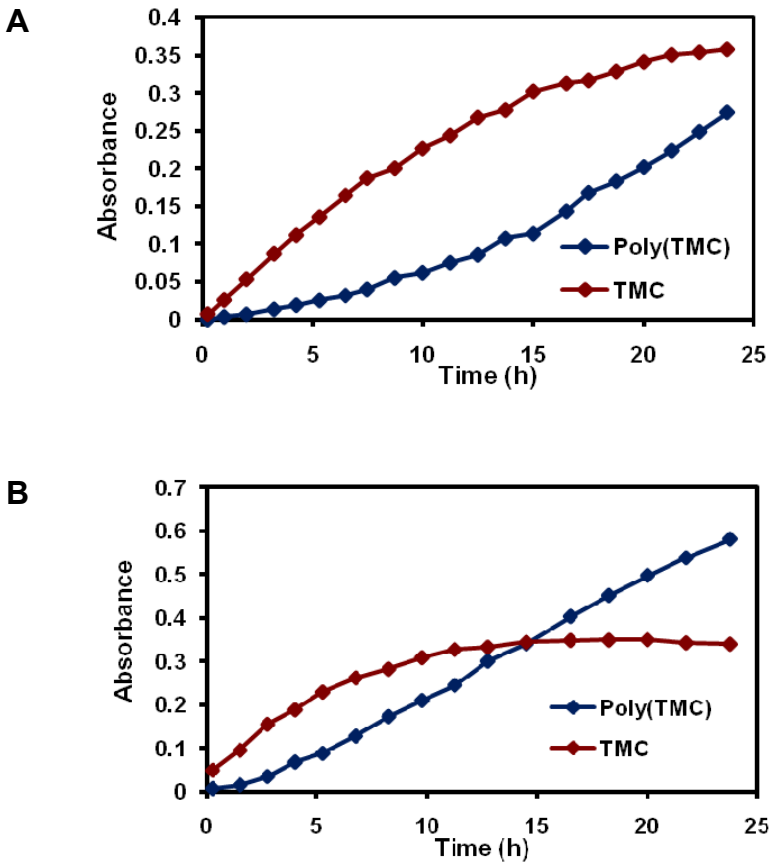

Figure V-9. Reaction profiles obtained after deconvolution of selected IR spectra, indicating poly(TMC) and TMC formation with time for the copolymerization of oxetane and CO_2. (**A**) Reaction carried out at 60ºC in toluene, at 35 bar of CO_2 pressure, in the presence of complex **II-4** and 2 equiv. of *n*-Bu_4NBr. (**B**) Reaction carried out at 60ºC in toluene, at 10 bar of CO_2 pressure, in the presence of complex **II-4** and 2 equiv. of *n*-Bu_4NBr.

Concluding Remarks

We have shown that the (salen)CrCl complex along with *n*-Bu_4NX (X = Br, I) is an effective catalyst system for the selective coupling of oxetane and CO_2, providing the corresponding polycarbonate with minimal amounts of ether linkages at 110°C. The

selectivity of the oxetane and CO_2 coupling process can be tuned by altering the nature of the anionic-based cocatalyst. Anions that are good leaving groups such as bromide and iodide are more effective at yielding trimethylene carbonate by a backbiting process at the early stages of the coupling reaction. Furthermore, at lower reaction temperatures ($T < 80°C$) the catalyst system (salen)CrCl/*n*-Bu_4NBr is capable of producing polycarbonate directly from the ROP of preformed TMC via a coordination-insertion pathway. Treatment of the (salen)CrCl with two equivalents of *n*-Bu_4NBr forms [*trans*-(salen)$CrClBr^-$] which exits in solution in a Schlenk equilibrium with the corresponding symmetric [*trans*-(salen)CrX_2^-] complexes as demonstrated by ESI-MS. Additional attempts at tuning the selectivity of the coupling reaction for trimethylene carbonate formation were achieved by utilizing the aforementioned catalytic system under lower reaction temperatures and CO_2 pressures, where the formation of TMC by a backbiting mechanism is enhanced via a metal-alkoxide intermediate. Fundamental studies of the type described in this Chapter should provide us with the knowledge to develop catalyzed methods to synthesize trimethylene carbonate via the ring-expansion of oxetane and carbon dioxide under mild reaction conditions.

CHAPTER VI

EXPLORATION OF THE COPOLYMERIZATION OF 3-METHOXY-METHYL-3-METHYLOXETANE AND CO_2 TO AFFORD ALIPHATIC POLYCARBONATES CATALYZED BY (SALEN)CrCl COMPLEXES

Introduction

A continuing theme in this research area is the exploration of other monomers that can be activated in a similar manner to oxetane and thus, the generation of new aliphatic polycarbonates with different and hopefully improved properties. One of the drawbacks about this chemistry is the availability of the oxetane monomers. There are few commercially available and these are in general expensive. Our initial interest was to explore monomers with substituents in the 3-position of trimethylene oxide such as 3-methoxy-methyl-3-methyloxetane (MMO). This monomer can be easily synthesized from 3-methyl-3-oxetanemethanol, which is a relatively inexpensive and commercially existing oxetane derivative.

Herein, we wish to report preliminary investigations on the copolymerization of 3-methoxy-methyl-3-methyloxetane and CO_2 catalyzed by the (salen)CrCl catalytic system (Figure II-1), along with *n*-Bu_4NN_3 as cocatalyst.

Experimental Section

Reagents and Methods. Unless otherwise specified, all syntheses and manipulations were carried out on a double-manifold Schlenk vacuum line under an

atmosphere of argon or in an argon filled glove box. Toluene and tetrahydrofuran were freshly distilled from sodium/benzophenone. Ethanol and methanol were freshly distilled from Mg/I_2. Diethyl ether, dichloromethane, and hexanes were purified by an MBraun Manual Solvent Purification System packed with Alcoa F200 activated alumina desiccant. 1,1,2,2-tetrachlotoethane (TCI) was freshly distilled over CaH_2. 3-methyl-3-oxetanemethanol (Alfa Aesar) was used as received. Triethylamine was freshly distilled over CaH_2 before use. Ethyl chloroformate (Aldrich), diethyl methylmalonate (Alfa Aesar), *n*-butyllithium (Aldrich), lithium aluminum hydride (Alfa Aesar), chloromethyl methyl ether (Aldrich), sodium hydride (60% in mineral oil) (Alfa Aesar), dimethyl sulfate (Alfa Aesar), potassium hydroxide (EMD), ethylenediamine (Aldrich), 1,2-phenylenediamine (ACROS), chromium(II) chloride (Alfa Aesar), sodium hydroxide (EMD), sodium sulfate (EMD), and magnesium sulfate (EMD) were used as received. Tetra-*n*-butylammonium azide was stored in the freezer of the glove box upon arrival. Bone-dry carbon dioxide supplied in a high-pressure cylinder and equipped with a liquid dip tube was purchased from Scott Specialty Gases. The corresponding salen ligands and chromium complexes were synthesized as described in the literature.[45]

^1H NMR spectra were acquired on Unity+ 300 MHz and VXR 300 MHz superconducting NMR spectrometers. Molecular weight determinations (M_n and M_w) were carried out with Viscotek Modular GPC apparatus equipped with ViscoGEL^{TM} I-series columns (H + L), and Model 270 dual detector comprised of RI and Light Scattering detectors. High-pressure reaction measurements were performed using an ASI ReactIR 1000 reaction analysis system with stainless steel Parr autoclave modified

with a permanently mounted ATR crystal (SiComp) at the bottom of the reactor (purchased from Mettler Toledo).

Synthesis of 3-methoxy-methyl-3-methyloxetane. It was prepared according to the procedure reported by McAlees with some modifications.[99] Sodium hydride (23.5 g, 60% in mineral oil) was added to a solution of 3-methyl-3-oxetanemethanol (50 g, 0.489 mol) in THF (1 L), and the resulting mixture was stirred for 24 h. Dimethyl sulfate (86.4 g, 0.685 mol) was then added dropwise (exothermic reaction), and the mixture was stirred for 24 h at room temperature. A solution of sodium hydroxide (30 g in 50 mL of water) was added, and most of the THF was disttiled out. The residue was extracted with ether, and the ether extract was dried over Na_2SO_4 and vacuum distilled to give 3-methoxy-methyl-3-methyloxetane (36 g, 63.3%). ^{1}H NMR (300 MHz, $CDCl_3$): δ 4.45 (d, 2H, J = 6.8 Hz, OCH_2), 4.30 (d, 2H, J = 6.8 Hz, OCH_2), 3.40 (s, 2H, CH_2), 3.35 (s, 3H, OCH_3), 1.26 (s, 3H, CH_3).

Synthesis of 2-methoxy-methyl-2-methyl malonic acid diethyl ester. It was prepared according to the procedure reported by Doherty.[100] A tetrahydrofuran solution (40 mL) of diethyl methylmalonate (5 g, 0.0287 mol) was cooled to -78°C and treated with a 1.64 M solution of *n*-butyllithium in hexanes (17.5 mL, 0.0287 mol). The resulting mixture was stirred rapidly and after warming to room temperature, was transferred dropwise a tetrahydrofuran solution (30 mL) of chloromethyl methyl ether (2.9 g, 0.0287 mol). After stirring the reaction solution overnight the solvent was removed under vacuum and the residue extracted into diethyl ether (2 × 30 mL), washed with water (2 × 30 mL), dried over $MgSO_4$, and filtered, and the solvent was removed to

afford the desired ester as a pale yellow/colorless oil in 80% yield (5.02 g). ^{1}H NMR (300 MHz, $CDCl_3$): δ 4.13 (quart, 4H, J = 6.9 Hz CH_2CH$_3$), 3.66 (s, 2H, CH_2), 3.28 (s, 3H, OCH_3), 1.42 (s, 3H, CH_3), 1.19 (t, 6H, J = 7.1 Hz CH$_2$CH_3).

Synthesis of 2-methoxy-methyl-2-methyl-1,3-propanediol. It was prepared according to the procedure reported by Doherty.[100] A solution of 2-methoxy-methyl-2-methyl malonic acid diethyl ester (5 g, 0.0229 mol) in tetrahydrofuran (20 mL) was added dropwise via canula to a stirred suspension of $LiAlH_4$ (4.36 g, 0.115 mol) in tetrahydrofuran (80 mL), at 0°C. The reaction mixture was allowed to warm to room temperature and stirred for a further 4 h. After cooling to 0°C, the resulting suspension was diluted with diethyl ether (100 mL) and quenched by addition of water (10 mL), followed by KOH (2.8 g in 10 mL of water), and finally water (10 mL), and stirred for a further 1 h. After hydrolysis was complete, the resulting mixture was filtered and the solids were washed with diethyl ether (2 × 25 mL). The organic fractions were combined, and dried over $MgSO_4$, and the solvent was removed to afford 2-methoxy-methyl-2-methyl-1,3-propanediol as a colorless oil in 90% yield. ^{1}H NMR (300 MHz, $CDCl_3$): δ 3.65 (d, 2H, J = 10.7 Hz, OCH_2), 3.54 (d, 2H, J = 10.7 Hz, OCH_2), 3.37 (s, 2H, CH_2), 3.33 (s, 3H, OCH_3), 0.79 (s, 3H, CH_3).

Synthesis of 5-methoxy-methyl-5-methyl-1,3-dioxan-2-one. It was synthesized according to the procedure reported by Endo for the synthesis of trimethylene carbonate with a slight modification.[15a] Triethylamine (21.4 g, 0.211 mol) was added dropwise to a solution of 2-methoxy-methyl-2-methyl-1,3-propanediol (13.5 g, 0.100 mol) and ethyl chloroformate (21.7 g, 0.201 mol) in 700 mL of THF at 0°C over

a period of 30 min. The reaction mixture was stirred overnight at room temperature. Precipitated triethylamine hydrochloride salt was filtered off, and the filtrate was concentrated under vacuum. The oily residue was vacuum distilled to afford 5-methoxy-methyl-5-methyl-1,3-dioxan-2-one as colorless oil. After a period of several months colorless crystals grew and were successfully analyzed by X-ray crystallography. ^{1}H NMR (300 MHz, $CDCl_3$): δ 4.27 (d, 2H, J = 10.7 Hz OCH_2), 4.02 (d, 2H, J = 10.7 Hz OCH_2), 3.31 (s, 3H, OCH_3), 3.28 (s, 2H, CH_2), 1.03 (s, 3H, CH_3).

Substrate Binding and Ring-Opening Step Examined by Infrared Spectroscopy. 3-methoxy-methyl-3-methyloxetane binding and ring-opening step studies were examined by solution infrared spectroscopy. The catalytic system used in these studies was a (salen)Cr(III)Cl (50 mg) complex (*N,N'*-bis(3,5-di-*tert*-butylsalicylidene)-1,2-ethylenediimine chromium(III) chloride) in the presence of *n*-Bu_4NN_3 as cocatalyst and using TCE as the solvent (4 mL).

X-ray Structural Studies. Single crystals of (salen)Cr(III)Cl·oxetane (complex **VI-1**) were obtained by layering hexanes into a saturated dichloromethane solution of the corresponding (salen)Cr(III)Cl complex (*N,N'*-bis(3-methoxy-5-*tert*-butylsalicylidene)-1,2-phenylenediimine chromium(III) chloride) containing 20 equivalents of MMO.

Single crystals of 5-methoxymethyl-5-methyl-1,3-dioxan-2-one were grown after several months.

For both structures, a Bausch and Lomb 10× microscope was used to identify suitable crystals. Each crystal was coated in paratone, affixed to a nylon loop, and

placed under streaming nitrogen (110K) in a Bruker-D8 Adv GADDS X-ray diffractometer. Space group determinations were made on the basis of systematic absences and intensity statistics. Both crystal structures were solved by direct methods and were refined by full-matrix least-squares on F^2. All hydrogen atoms were placed in idealized positions and refined with fixed isotropic displacements parameters equal to 1.2 (1.5 for methyl protons), times the equivalent isotropic displacements parameters of the atoms to which they were attached. All non-hydrogen atoms were refined with anisotropic displacement parameters.

The following are the programs that were used: data collection and cell refinements; FRAMBO Version 4.1.05 (GADDS),[66] data reductions; SAINTPLUS Version 6.63,[68] absorption correction; SADABS,[49] structural solutions; SHELXS-97,[50] structural refinement; SHELXL-97;[51] molecular graphics and preparation of material for publication; SHELXTL, version 6.14,[52] and X-Seed, version 1.5.[53]

General Procedure for Copolymerization Reactions of 3-methoxy-methyl-3-methyloxetane and CO_2. In a typical experiment, the appropiate amount of catalyst, cocatalyst (*n*-Bu_4NN_3), and 4 g of MMO were delivered via the injection port into a 300-mL stainless steel Parr autoclave reactor that was previously dried in vacuo overnight at 80°C. The autoclave was then pressurized with 35 bar of CO_2 and the temperature was increased to 110°C. The monomer:catalyst:cocatalyst ratio was maintained at 275:1:2, and the reaction was run for the corresponding reaction time. After the reaction was stopped, the autoclave was put into ice, cooled down to 10°C, and vented in a fume hood. The percent conversion to products was determined based on the amount of

oxetane monomer left in the reaction solution. ^{1}H NMR (300 MHz, $CDCl_3$), MMO: δ 4.45 (d, 2H, OC*H*$_2$), 4.30 (d, 2H, OC*H*$_2$), 3.40 (s, 2H, C*H*$_2$), 3.35 (s, 3H, OC*H*$_3$), 1.26 (s, 3H, C*H*$_3$). Furthermore, the quantities of 5-methoxy-methyl-5-methyl-1,3-dioxan-2one (MTC), poly(MTC), and ether linkages in the copolymer were determined by integrating the peak area of the corresponding resonances. ^{1}H NMR (300 MHz, $CDCl_3$), poly(MTC): δ 4.07 (s, 4H, OC*H*$_2$), 3.31 (s, 3H, OC*H*$_3$), 3.26 (s, 2H, C*H*$_2$), 1.0 (s, 3H, C*H*$_3$). ^{1}H NMR (300 MHz, $CDCl_3$), MTC: δ 4.27 (d, 2H, OC*H*$_2$), 4.02 (d, 2H, OC*H*$_2$), 3.31 (s, 3H, OC*H*$_3$), 3.28 (s, 2H, C*H*$_2$), 1.03 (s, 3H, C*H*$_3$). ^{1}H NMR (300 MHz, $CDCl_3$), ether linkages: δ 0.9 (s, 3H, C*H*$_3$), other resonances corresponding to ether linkages are overlapping with the more intense polymer signals.

Copolymerization Reaction Monitored by *in situ* IR Spectroscopy. In a typical experiment, the appropiate amount of complex **II-1**, cocatalyst, (*n*-Bu_4NN_3), and oxetane monomer (8 g) were dissolved in 6 mL of toluene and delivered via the injection port into a 300-mL stainless steel Parr autoclave reactor that was previously dried in vacuo overnight at 80°C. The monomer:catalyst:cocatalyst ratio was maintained at 150:1:2. The autoclave is modified with a 30 bounce SiComp window to allow for the use of an ASI ReactIR 1000 system equipped with a MCT detector. In this manner a 128-scan background spectrum was collected after the reaction mixture was heated to 110°C. The autoclave was pressurized with 35 bar of CO_2, and the infrared spectrometer was set to collect one spectrum every 3 min over a 48 h period. Profiles of the absorbance at 1750 cm^{-1} (polymer) and at 1770 cm^{-1} (cyclic carbonate) with time were recorded after base line correction. After the reaction was stopped, the autoclave was

cooled down to room temperature and vented in a fume hood. The reaction solution was analyzed by ^{1}H NMR spectroscopy in the same manner as above, to determine the percent conversion to products, and the percentages of polycarbonate, cyclic carbonate and ether linkages.

Statistical Deconvolution of FTIR Spectra. FTIR spectra were deconvoluted using Peakfit, version 4.12 (Peakfit for Windows, v. 4.12; SYSTAT Software Inc., San Jose, CA, 2003). Statistical treatment was a residuals method utilizing a combination Gaussian-Lorentzian summation of amplitudes with a linear baseline and Savitsky-Golay smoothing.

Results and Discussion

The monomer, 3-methoxy-methyl-3-methyloxetane, was prepared according to the published procedure reported by McAlees.[99] The synthesis involves the prior deprotonation of 3-methyl-3-oxetanemethanol with NaH in mineral oil, followed by treatment with dimethyl sulfate to generate 3-methoxy-methyl-3-methyloxetane in 63% yield. The corresponding cyclic carbonate, 5-methoxy-methyl-5-methyl-1,3-dioxan-2-one, was prepared according to the published procedure reported by Endo for the synthesis of trimethylene carbonate.[15a] The synthesis involves the treatment of 5-methoxy-methyl-5-methyl-1,3-propanediol with ethylchloroformate in the presence of stoichiometric amounts of triethylamine. The crystal structure of MTC was successfully confirmed by X-ray crystallography (Figure VI-1 and Table VI-1). Prior to a discussion

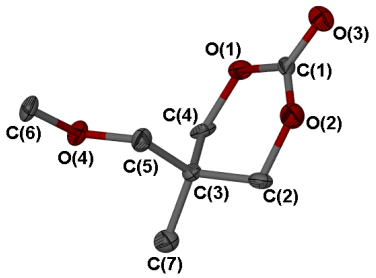

Figure VI-1. Thermal ellipsoid plot of 5-methoxy-methyl-5-methyl-1,3-dioxan-2-one. Ellipsoids are at the 50 % level. H atoms are omitted for clarity.

Table VI-1. Selected Bond Distances and Angles for 5-Methoxy-methyl-5-methyl-1,3-dioxan-2-one.[a]

O(1)-C(1)	1.357(12)
O(3)-C(1)	1.187(12)
O(1)-C(4)	1.460(12)
O(4)-C(6)	1.418(13)
O(3)-C(1)-O(1)	118.3(10)
O(2)-C(1)-O(1)	119.7(9)
C(2)-C(3)-C(4)	105.6(8)
C(5)-O(4)-C(6)	111.4(8)

[a] Units of bond angles and bond distances are (º) and (Å), respectively.

on the copolymerization of 3-methoxy-methyl-3-methyloxetane and CO_2 as catalyzed by the (salen)CrCl catalytic system, it is beneficial to mention how the product distributions of the copolymerization reactions are analyzed by ^{1}H NMR and IR spectroscopies. As seen in Figure VI-2, the presence of possible coupling products from the MMO/CO_2 coupling reaction, namely, poly(MTC) and MTC, can easily be assigned using ^{1}H NMR

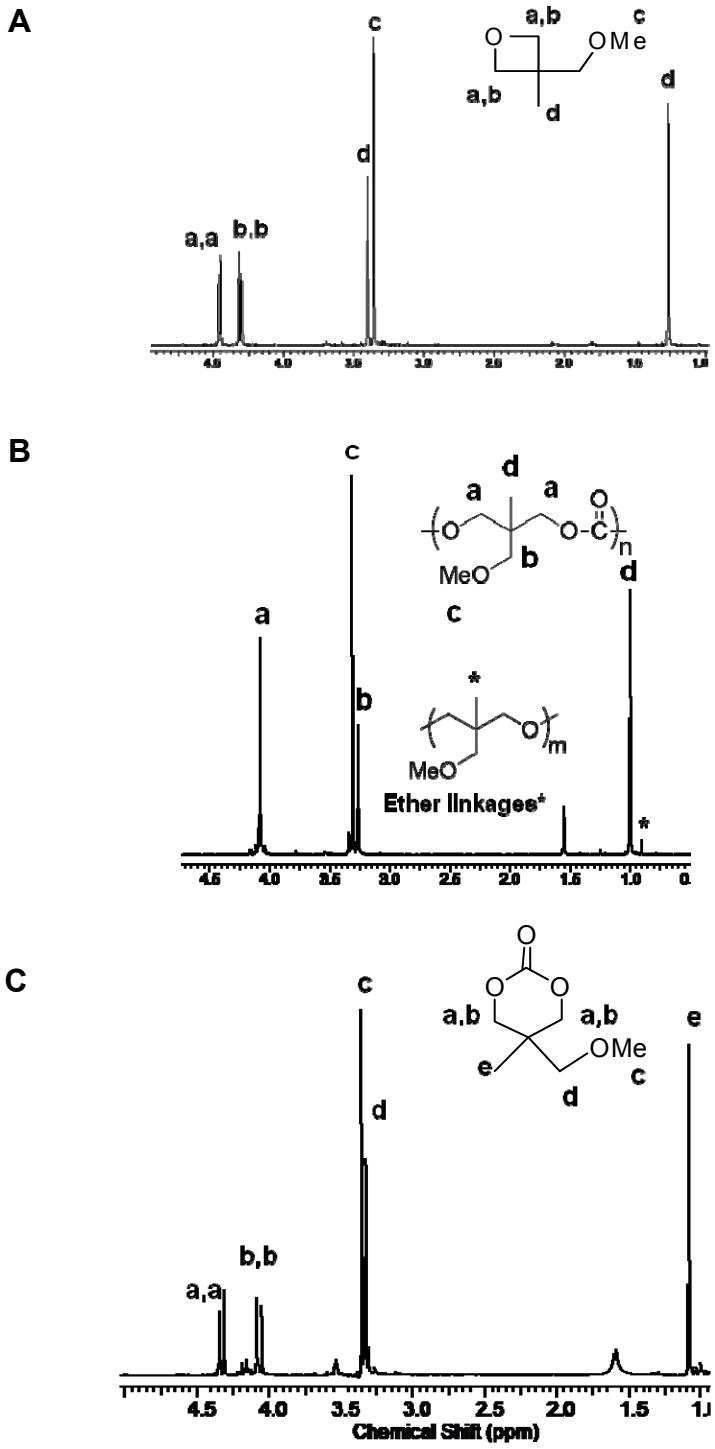

Figure VI-2. ^{1}H NMR in $CDCl_3$ of (**A**) MMO, (**B**) poly(MTC) obtained from MMO and CO_2, and (**C**) MTC.

spectroscopy. The percent conversion to polymer can be monitored based on the amount of oxetane monomer left in the reaction solution. Furthermore, the quantities of poly(MTC), MTC, and ether linkages in the copolymer can be determined by integrating the peak area of the corresponding resonances at 1.0, 1.03, and 0.9 ppm, respectively. Infrared stretching bands of the carbonyl groups of the corresponding copolymer and cyclic carbonate in a mixture of toluene and oxetane monomer are observed at 1750 cm^{-1} and 1770 cm^{-1}, respectively.

Studies Related to the Copolymerization of 3-methoxy-methyl-3-methyloxetane and CO_2 Catalyzed by (salen)CrCl Complexes. Initially we chose to employ the (salen)CrCl catalyst, complex **II-1** in Figure II-1, in the presence of *n*-Bu_4NN_3 to examine the selectivity and catalytic activity for copolymer formation from the coupling of MMO and carbon dioxide. The copolymerization reactions were performed under identical reaction conditions, i.e., 110ºC, 35 bar CO_2 pressure, at various reaction times, and the monomer:catalyst:cocatalyst ratio was maintained at 275:1:2. The results are summarized in Table VI-2. The product mixtures were analyzed by ^1H NMR spectroscopy, with the quantities of poly(MTC), MTC, and ether linkages in the poly(MTC) determined by integrating the resonances at 1.0, 1.03, and 0.9 ppm, respectively. As is readily seen in Table VI-2, the yield of poly(MTC) is greater than the cyclic product, MTC, in all instances. It can be noted that the copolymerization

Table VI-2. Copolymerization of 3-Methoxy-methyl-3-methyloxetane and CO_2 Catalyzed by Complex **II-1** in the Presence of *n*-Bu_4NN_3 at Various Reaction Times.[a]

Time (days)	% Poly(MTC)	% (MTC)	% CO_2 content	% Conversion
1	77.6	22.4	75.4	23.3
2	85.4	14.5	73.6	52.7
3	85.7	14.2	87.6	76.7

[a]Copolymerization conditions: Catalyst loading = 0.012 mol %, 4 g of MMO, 2 equiv. of *n*-Bu_4NN_3, M/I = 275, 35 bar of CO_2, at 110°C. [b]Percent conversion to products, product distributions, and % of CO_2 content were determined by ^{1}H NMR spectroscopy.

reactions undergo considerably slower compared to those employing oxetane as monomer. Only a percent conversion to products of 76.7 was obtained after 3 days of reaction time. Additionally, a greater amount of cyclic carbonate was detected after a period of 3 days.

Subsequent studies were carried out to interrogate the effects of changing the nature of (i) the substituents on the phenolate rings, and (ii) the diimine backbone of the salen ligand in the (salen)CrCl derivative. The copolymerization reactions were performed at a monomer:catalyst:cocatalyst ratio of 275:1:2, with a CO_2 pressure of 35 bar at 110ºC for 3 days. The results of this inquiry are provided in Table VI-3. Retaining the salen ligand with the phenylene backbone while changing the substituents in the 3,5-positions of the phenolate rings (entries 1 and 2, Table VI-3) reveals the Cr(III) salen derivative containing the bulky di-*tert*-butyl groups to be the more active. This is consistent with previous observations reported for the copolymerization of oxetane and CO_2 catalyzed by the (salen)CrCl catalyst system (Chapter II). On the other hand, for the copolymerization of cyclohexene oxide and CO_2 catalyzed by chromium salen complexes, higher catalytic activity was obtained in complexes containing

methoxy and *tert*-butyl groups in the 3 and 5 positions of the phenolate rings.[45] We have also studied the effects of altering the diimine backbone of the Cr(III) salen complex while maintaining the di-*tert*-butyl groups in the 3,5-positions of the phenolate moiety (entries 3 and 4, Table VI-3). As can be seen in Table VI-3, the catalytic behavior of the chromium salen complexes is greatly affected by changing the diimine backbone from cyclohexylene to ethylene, with the chromium salen complex with the ethylene backbone displaying higher catalytic activity. This is most likely due to the flexibility imparted to the chromium salen complex by the ethylene backbone compared to the cyclohexylene backbone. Hence, binding of a bulkier oxetane to the chromium center

Table VI-3. Copolymerization of 3-Methoxy-methyl-3-methyl oxetane and CO_2 Catalyzed by (salen)Cr(III)Cl Complexes.[a]

Entry	Complex	R_1	R_2	R_3	R_4	% Poly (MTC)[b]	% MTC[b]	% CO_2 content[b]	% Conversion[b]
1	**II-2**	-C_4H_4-		*tert*-butyl	*tert*-butyl	87.3	12.7	80.5	42.4
2	**II-3**	-C_4H_4-		OCH_3	*tert*-butyl	85.1	14.9	64.3	38.3
3	**II-1**	H	H	*tert*-butyl	*tert*-butyl	85.7	14.2	87.6	76.7
4	**II-4**	(1*R*,2*R*)-C_4H_8-		*tert*-butyl	*tert*-butyl	84.1	15.9	81.6	37.2

[a]Copolymerization conditions: Catalyst loading = 0.012 mol %, 4 g of MMO, 2 equiv. of *n*-Bu_4NN_3, M/I = 275, 35 bar of CO_2, at 110°C for 3 days. [b]Percent conversion to products, product distributions, and % of CO_2 content were determined by ^{1}H NMR spectroscopy.

would be more feasible. It is important to point out that the percentage of CO_2 incorporation in the copolymers was lower than the typical CO_2 fixation observed in polycarbonates obtained from oxetane and CO_2 catalyzed by the (salen)CrCl catalytic system.

In general, the observed M_n values were found to be much lower than the theoretical values, e.g., M_n of 11 370 is considerably lower than the theoretical value of 58 650. This is most likely due to a chain transfer mechanism arising from the presence of trace quantities of water in the system.[11b, 55] The PDI was in general about 1.3.

Substrate Binding and Ring-Opening Steps Examined by Infrared Spectroscopy. Fundamental to a better understanding of the mechanism of the coupling reaction of 3-methoxy-methyl-3-methyloxetane and carbon dioxide is an investigation of the initiation step of this process. In order to address this issue we have conducted cocatalyst, oxetane monomer binding, and subsequent ring-opening studies via infrared spectroscopy using the (salen)CrCl complex containing di-*tert*-butyl substituents in the 3,5-positions of the phenolate rings, and an ethylene backbone for the diimine, along with *n*-Bu_4NN_3 as cocatalyst. We have employed an azide-based cocatalyst for these studies because the ν_{N_3} stretching vibration provides accessible probes for both cocatalyst binding and anion ring-opening steps. The results of these studies are depicted in **Scheme VI-1** and Figure VI-3.

As indicated in **Scheme VI-1**, upon addition of two equivalents of *n*-Bu_4NN_3 to (salen)CrCl, the anionic six-coordinate *bis*-azide species (salen)$Cr(N_3)_2^-$ readily forms at ambient temperature. This is apparent in the ν_{N_3} stretching region with the appearance of

Scheme VI-1. Ring-Opening Step of MMO Catalyzed by (Salen)Cr$(N_3)_2^-$.

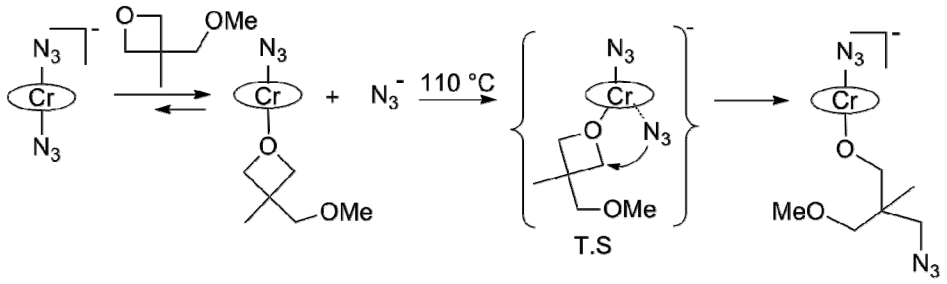

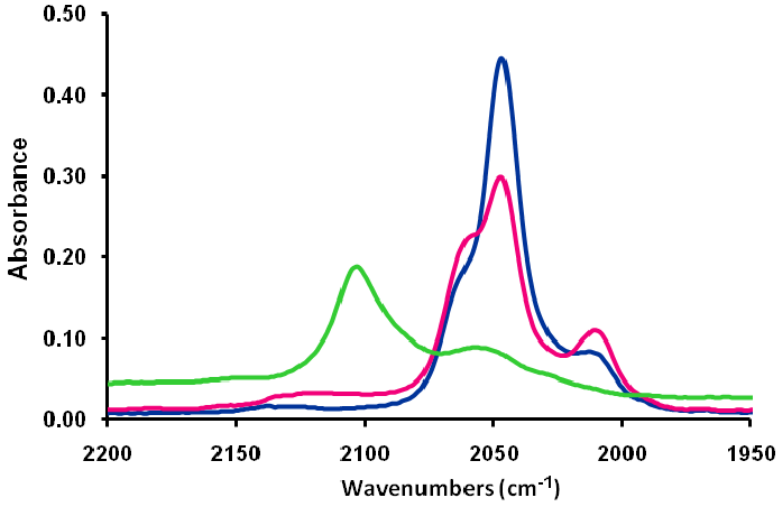

Figure VI-3. Spectra of TCE solutions of chromium salen chloride complex with 2 equivalents of *n*-Bu_4NN_3 (blue line), after addition of 100 equivalents of MMO at ambient temperature and stirred for 3 h (pink line), and after stirring the reaction solution at 110°C for 24 h (green line).

an infrared band at 2047 cm^{-1} with a shoulder at 2057 cm^{-1} upon addition of *n*-Bu_4NN_3. It should be noted here that the *n*-Bu_4N^+ salt of (salen)Cr$(N_3)_2^-$ anion has been fully characterized by X-ray crystallography and these studies are reported in Chapter III. Addition of 100-fold excess of 3-methoxy-methyl-3-methyloxetane to the *bis*-azide

complexes displaces some of the azide ligand as can be seen by an increase in the free azide ion concentration by its ν_{N_3} band at 2009 cm^{-1} with a concomitant decrease in the concentration of (salen)$Cr(N_3)_2^-$ (yellow line, Figure VI-3). Moreover, a new ν_{N_3} stretching band appears at 2061 cm^{-1} which is assigned to (salen)$Cr(N_3)$•oxetane. Upon stirring this reaction mixture for 24 h at ambient temperature no significant changes in the infrared spectrum resulted, indicative of the ring-opening process of MMO requiring higher temperatures. Indeed, heating the reaction mixture at 110ºC led to oxetane ring-opening by azide as indicated by the organic azide band at 2100 cm^{-1}. After heating the reaction solution for 24 h at 110°C, the main infrared stretching band observed was that of organic azide. It should be noted that an analogous experiment employing oxetane as monomer, led to oxetane ring-opening by azide at 110°C after only 3 h (Chapters II and III). Hence, these results suggest that the ring-opening of MMO by azide requires longer reaction times. This is consistent with 3-methoxy-methyl-3-methyloxetane being more sterically hindered than oxetane. Additionally, the presence of electron donating substituents on the 3-position of trimethylene oxide could drive the ring-opening step to undergo slower.

X-ray crystallography was utilized in conjunction with the ν_{N_3} infrared spectral data (*vide supra*) to verify that MMO binding to the chromium center occurs without ring-opening at ambient temperature, in an analogous manner to oxetane. A successful isolation of single crystals of an oxetane adduct as depicted in **Scheme VI-1** was achieved. Complex **VI-1** was fully characterized by X-ray crystallography and a thermal ellipsoid representation of this derivative is shown in Figure VI-4, with selected bond

distances and bond angles listed in Table VI-4. Complex **VI-1** clearly shows that 3-methoxy-methyl-3-methyloxetane is capable of binding to the (salen)Cr(III) center without undergoing ring-opening at ambient temperature.

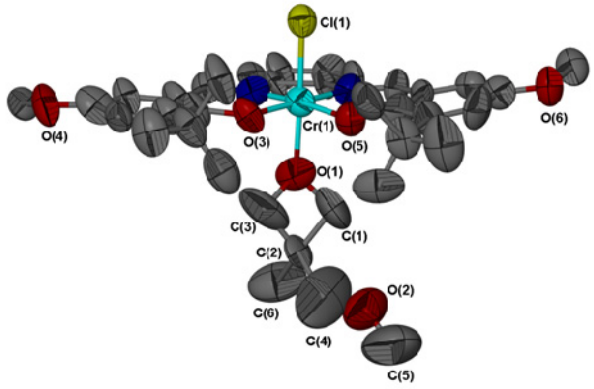

Figure VI-4. Thermal ellipsoid plot of complex **VI-1**. Ellipsoids are at the 50 % level. H atoms are omitted for clarity.

Table VI-4. Selected Bond Distances and Angles for Complex **VI-1**.[a]

Cr(1)-Cl(1)	2.297(3)
Cr(1)-O(1)	2.056(8)
Cr(1)-O(5)	1.920(6)
O(1)-C(1)-C(2)	94.5(8)
O(1)-C(3)-C(2)	94.4(8)
C(3)-C(2)-C(1)	78.9(9)
C(3)-O(1)-C(1)	89.6(10)

[a] Units for bond distances and bond angles are (Å) and (º), respectively.

Copolymerization Reaction Monitored by *in situ* IR Spectroscopy. Figure VI-5 shows the reaction profiles of both, copolymer and cyclic carbonate formation for the copolymerization reaction of MMO and CO_2 carried out at 110°C in the presence of complex **II-1** along with 2 equivalents of *n*-Bu_4NN_3 as cocatalyst. It is clearly observed that when using this catalytic system and conditions the formation of MTC is enhanced

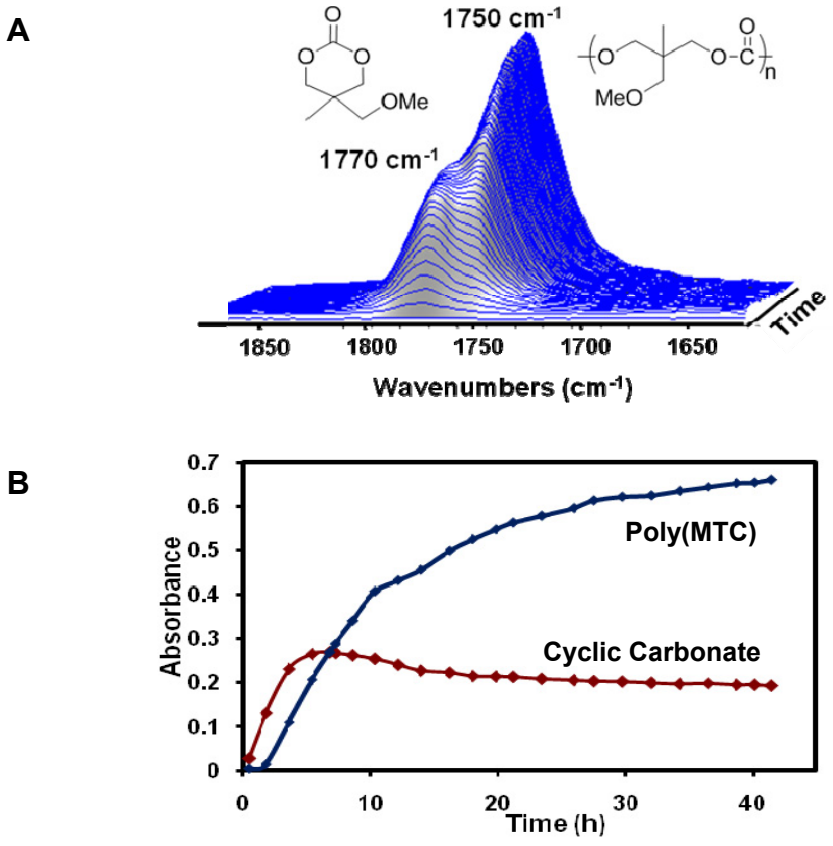

Figure VI-5. (**A**) Three-dimensional stack plot of IR spectra collected every 3 min during the copolymerization reaction of MMO and CO_2. (**B**) Reaction profiles obtained after deconvolution of selected IR spectra, indicating copolymer and cyclic carbonate formation with time. Reaction carried out at 110ºC in toluene, at 35 bar of CO_2 pressure, in the presence of complex **II-1** and 2 equiv. of *n*-Bu_4NN_3.

at the early stages of the coupling reaction and its concentration is slowly decreased over time. On the other hand, the concentration of poly(MTC) is initially inhibited followed by rapidly increasing over the course of the reaction. These results are consistent with the presence of an equilibrium between the cyclic carbonate byproduct and the polycarbonate, as the percentages of poly(MTC) did not reach 100% after a 3 days of reaction period. It is important to point out that the polycarbonate produced from the ring-opening polymerization of preformed MTC, might be a more difficult process compared to that involving TMC. Hence, the higher percentages of ether linkages observed could also be the result of decarboxylation from the thus produced polycarbonates.

Concluding Remarks

In summary, we have demonstrated that chromium(III) salen complexes along with *n*-Bu_4NN_3 have moderate activity for the copolymerization of 3-methoxy-methyl-3-methyloxetane and carbon dioxide. Optimization of the chromium catalyst was achieved utilizing a salen ligand with *tert*-butyl substituents in the 3,5-positions of the phenolate rings and an ethylene backbone in the diimine, along with an azide ion as an initiator. This catalytic system provided the corresponding polycarbonate with ~13% of ether linkages. In general, the copolymerization reactions catalyzed by the (salen)CrCl/*n*-Bu_4NN_3 catalytic system undergo slower than those involving oxetane as monomer. This is most likely due to the steric hindrance imparted by 3-methoxy-methyl-3-methyloxetane monomer. Solution IR spectroscopy in conjunction with X-ray crystallography showed that MMO binds to the chromium center at ambient temperature

without undergoing ring-opening. Instead, the ring-opening step of MMO by azide ion was found to be a high energy process requiring high temperatures (110°C). Additionally, the ring-opening step took longer reaction times than the analogous process employing oxetane as monomer. A copolymerization reaction monitored by *in situ* IR spectroscopy suggested that there is an equilibrium process between the cyclic carbonate, MTC, and the polycarbonate produced. However, further investigations on the mechanism involved in this case are needed. Of importance here, is that the copolymerization of a bulkier oxetane and CO_2 catalyzed by the (salen)CrCl/*n*-Bu_4NN_3 was successfully performed. This in turn should establish a foundation for a multitude of applications of this methodology for the synthesis of polycarbonates with different properties.

CHAPTER VII

SUMMARY AND CONCLUSIONS

Due to the many advantages on utilizing CO_2 as a chemical feedstock, there is quite an extensive interest for the scientific community in investigating a variety of chemical transformations involving carbon dioxide as a reagent. One such process that has received a lot of attention is the production of polycarbonates from the copolymerization of epoxides and CO_2 in the presence of a metal based catalyst, a field pioneered by Inoue in 1969. Inspired by the early efforts of Inoue and others, our research group has been investigating a variety of catalytic systems based on metal salen complexes as catalysts for this reaction. Research efforts have focused on understanding and developing the mechanism for copolymer formation involving the aforementioned catalytic systems. A related process for the production of useful polycarbonates involves the copolymerization of oxetane and CO_2, a transformation that has received little attention, most likely due to the lower reactivity and commercial availability of oxetane monomers. Of importance, in this case the cyclic carbonate byproduct obtained in this reaction, namely, trimethylene carbonate, is thermodynamically unstable relative to the copolymer. Thus, it can be ring-opened and transformed into the same polycarbonate. Importantly, the copolymers produced by this methodology are biodegradable and are important components of thermoplastic elastomers, which have a variety of potential applications in the medical industry.

This dissertation has covered detailed mechanistic investigations on the copolymerization of oxetanes and CO_2 catalyzed by metal salen complexes of chromium(III) and cobalt(II) along with anionic-based cocatalysts. Efforts have been made to understand and elucidate a mechanism for this important process.

In Chapter II, optimization of the catalytic system was first carried out. Chromium salen derivatives in the presence of anionic initiators were shown to be very effective catalytic systems for the selective coupling of oxetane and carbon dioxide to provide the corresponding polycarbonate with minimal amount of ether linkages. Molecular weights of the copolymers produced were as high as 14 500, with polydispersities ranging from 1.2 to 1.6. Optimization of the chromium(III) system was achieved utilizing a salen ligand with *tert*-butyl groups in the 3,5-positions of the phenolate rings, and a cyclohexylene backbone for the diimine along with an azide ion initiator. The mechanism for the coupling reaction of oxetane and carbon dioxide was studied by means of infrared spectroscopy, ^{1}H NMR spectroscopy, and X-ray crystallography, utilizing the optimized (salen)CrCl/*n*-Bu_4NN_3 catalytic system. The copolymerization reaction was found to be first-order in oxetane, catalyst, and cocatalyst, with the latter exhibiting zero-order dependence at high concentrations. The formation of copolymer was shown to proceed in part by way of the intermediacy of trimethylene carbonate, which was observed as a minor product of the coupling reaction, and by the direct enchainment of oxetane and CO_2. The parity of the determined free energies of activation for these two processes, namely 101.9 kJ-mol^{-1} for ring-opening

polymerization of trimethylene carbonate and 107.6 kJ-mol^{-1} for copolymerization of oxetane and carbon dioxide supported this conclusion.

In Chapter III, a detailed investigation of the initiation step of the coupling of oxetane and CO_2 catalyzed by (salen)CrX/(*n*-Bu_4NX or PPNX) was done by means of solution infrared spectroscopy and X-ray crystallography. These studies were compared to the related process involving epoxides (cyclohexene oxide or propylene oxide) as monomers. The species formed upon treatment of (salen)CrX with PPNX (PPN^+ = $(Ph_3P)_2N^+$) or *n*-Bu_4NX (X = Cl, N_3, CN, NCO) cocatalysts was fully investigated both in solution by infrared spectroscopy, and in the solid state by X-ray crystallography. All anions (X) afford six-coordinate chromium(III) PPN^+ or *n*-Bu_4N^+ salts composed of *trans*-(salen)CrX_2^- species. Of the X groups investigated in (salen)CrX, chloride is easily displaced by the others, that is, the reaction of (salen)CrCl with two-equivalents of N_3^-, CN^- or NCO^- quantitatively provide (salen)$Cr(N_3)_2^-$, (salen)$Cr(CN)_2^-$, and (salen)$Cr(NCO)_2^-$, respectively. On the other hand, addition of less than two-equivalents of azide to (salen)CrCl leads to a Schlenk equilibrium of the three possible anions both in solution and in the solid-state as shown by X-ray crystallography and ESI mass spectrometry. It was further demonstrated that all *trans*-(salen)CrX_2^- anions react with the epoxide or oxetane monomers in TCE solution to afford an equilibrium mixture containing (salen)CrX•monomer, with the oxetane adduct being thermodynamically more favored. The ring-opening steps of the bound cyclic ether monomers by X^- was examined, revealing the rate of ring-opening of the epoxides (cyclohexene oxide and propylene oxide) to be much faster than oxetane, with propylene oxide faster than

cyclohexene oxide. Furthermore, both X anions in (salen)CrX_2^- were shown to be directly involved in the monomer ring-opening step.

Based on the results obtained in Chapter II, it was of interest to investigate how the selectivity of the oxetane and CO_2 coupling process could be tuned for trimethylene carbonate formation and/or for polycarbonate obtained from the homopolymerization of preformed trimethylene carbonate. The advantage of proceeding exclusively via ring-opening polymerization of TMC is the complete absence of ether linkages in the afforded polycarbonates, which would result in a polymer with improved physical properties. We first surmised that a decrease in the electrophilicity of the metal center, in conjunction with the appropriate anionic initiator should modulate the selectivity of coupling process for TMC or polycarbonate produced via ROP of preformed TMC. In Chapter IV, the commercially available (salen)Co(II) complex ((1R, 2R)-(-)-1,2-cyclohexanediamino-*N,N′*-bis(3,5-di-*tert*-butyl-salicylidene)cobalt(II)) in the presence of anion initiators was employed as catalytic system for the oxetane and CO_2 coupling process. This catalyst system in the presence of an anion initiator, e.g. bromide, was shown to be very effective for the coupling of oxetane and carbon dioxide, providing the corresponding polycarbonate with minimal amount of ether linkages. The mechanism of the coupling of oxetane and carbon dioxide was studied by *in situ* infrared spectroscopy, where the first formed product was demostrated to be trimethylene carbonate. TMC was proposed to be formed by a backbiting mechanism following ring-opening of oxetane by the anion initiator, subsequent to CO_2 insertion into the cobalt-oxygen bond. The formation of the copolymer was suggested to proceed mostly by way of the anionic ring-

opening polymerization of preformed trimethylene carbonate in the presence of an anion in the reaction solution. Anions which are good leaving groups, i.e., bromide and iodide were most effective at affording polycarbonate via this route. In the presence of greater than two equivalents of anions the overall rate of copolymer production was decreased, presumably due to inhibition of oxetane monomer binding to the cobalt center. However, under these conditions copolymer formation through ROP of TMC was enhanced, with mass spectral evidence found for the formation of a dimer of TMC.

Inspired by the same idea of tuning the selectivity of the oxetane and CO_2 coupling process for TMC formation and/or polycarbonate produced from the ROP of preformed TMC, we further explored the activity and selectivity of the (salen)Cr(III)Cl catalyst in the presence of anions that are better leaving groups than the azide anion, i.e., bromide and iodide. The isolation of trimethylene carbonate from this process is also of interest because it could be used in melt polymerization processes with lactides or caprolactones, for the production of important thermoplastic elastomers. In Chapter V, the (salen)Cr(III)Cl complex (1,2-cyclohexanediamino-*N,N'*-bis-(3,5-di-*tert*-butylsalicylidene)chromium(III) chloride), in the presence of *n*-Bu_4NX (X = Br, I, Cl, N_3, NCO) as cocatalyst was revealed to be an effective catalytic system for the coupling of oxetane and CO_2 to provide the corresponding aliphatic polycarbonate with small quantities of ether linkages at 110°C. The selectivity of the oxetane and CO_2 coupling process was effectively tuned for the formation of copolymer produced directly from the homopolymerization of preformed trimethylene carbonate, by employing the previously mentioned (salen)CrCl complex along with *n*-Bu_4NBr as cocatalyst, at reaction

temperatures lower than 80°C. Notably, under these conditions the amount of carbonate linkages obtained was remarkably high (>99%). An investigation of the initial catalytic species involved in the coupling reaction was performed by ESI mass spectral analysis, revealing a Schlenk equilibrium of the three possible anions formed after treatment of the (salen)CrCl with two equivalents of *n*-Bu_4NBr cocatalyst. Remarkably, this catalytic system afforded trimethylene carbonate exclusively from the coupling of oxetane and CO_2 at mild reaction conditions (50°C and 10 bar of CO_2) via a backbiting process involving mostly a metal-alkoxide intermediate.

In Chapter VI, the exploration of the copolymerization of 3-methoxy-methyl-3-methyloxetane and carbon dioxide catalyzed by the (salen)CrCl catalytic system was examined. In general, chromium(III) salen complexes along with *n*-Bu_4NN_3 as cocatalyst revealed moderate activity for this process. Optimization of the chromium catalyst was achieved utilizing a salen ligand with *tert*-butyl substituents in the 3,5-positions of the phenolate rings and an ethylene backbone in the diimine, along with an azide ion as an initiator. This catalytic system provided the corresponding polycarbonate with ~13% of ether linkages. Molecular weights of the copolymers produced were as high as 11 370, with polydispersities around 1.3. In general, the copolymerization reactions catalyzed by the (salen)CrCl/*n*-Bu_4NN_3 catalytic system were slower than those involving oxetane as monomer. This is most likely due to the steric hindrance offered by 3-methoxy-methyl-3-methyloxetane monomer. *In situ* IR spectroscopy suggested the presence of an equilibrium process between the cyclic carbonate byproduct and the polycarbonate formed. Nevertheless, investigations to further clarify

these preliminary experimental findings will be needed. However, it could be shown from these studies that the application of this strategy could provide a way to synthesize a variety of aliphatic polycarbonates with different and hopefully improved properties.

In summary, it is with hope that the studies presented in this dissertation has demonstrated the mechanistic details and understanding into the copolymerization of oxetanes and CO_2 catalyzed by (salen)CrX complexes to afford aliphatic polycarbonates. The field of the metal catalyzed copolymerization of oxetanes and carbon dioxide has and will continue to flourish, not only because of the versatility of the reaction but also because the afforded aliphatic polycarbonates are important components of biodegradable thermoplastic elastomers. The exploration of other oxetane monomers opens the door to a multitude of applications of this method for the production of aliphatic polycarbonates with diverse properties and/or aliphatic polycarbonates that can be post-polymerization modified.

REFERENCES

(1) Sakakura, T.; Choi, J.-C.; Yasuda, H. *Chem. Rev.* **2007**, *107*, 2365-2387.

(2) Jacobs, M., *Supercritical Fluid*; Wikimedia Foundation, Inc., 2008. (Accessed October 2008)

(3) Aresta, M.; Dibenedetto, A. *Dalton Trans.* **2007**, 2975-2992.

(4) (a) Song, C. *Catal. Today* **2006**, *115*, 2-32; (b) Vansant, J. In *Carbon Dioxide Recovery and Utilization*; Aresta, M., Ed.; Klumer Academic Publishers: Dordrecht, The Netherlands, 2003; pp 3-50.

(5) Bottenbruch, L. *Engineering Thermoplastics: Polycarbonates, Polyacetals, Polyesters, Cellulose Esters*; Hanser Publishers: New York, 1996; p 112.

(6) Brunelle, D. J.; Korn, M. R. In *Adavances in Polycarbonates*, American Chemical Society: Washington, DC, 2003; pp 1-21.

(7) (a) Inoue, S.; Koinuma, H.; Tsuruta, T., *J. Polym. Sci., Part B: Polym. Lett.* **1969,** *7*, 287-292; (b) Inoue, S.; Koinuma, H.; Tsuruta, T., *Makromol. Chem.* **1969,** *130*, 210-220.

(8) (a) Chisholm, M. H.; Zhou, Z. *J. Mater. Chem.* **2004***, 14*, 3081-3092; (b) Darensbourg, D. J. *Chem. Rev.* **2007**, *107*, 2388-2410; (c) Darensbourg, D. J.; Holtcamp, M. W. *Coord. Chem. Rev.* **1996**, *153*, 155-174; (d) Darensbourg, D. J.; Mackiewicz, R. M.; Phelps, A. L.; Billodeaux, D. R. *Acc. Chem. Res.* **2004**, *37*, 836-844; (e) Kuran, W. *Prog. Polym. Sci.* **1998**, *23*, 919-992; (f) Coates, G. W.; Moore, D. R. *Angew. Chem., Int. Ed.* **2004**, *43*, 6618-6639; (g) Paddock, R. L.; Nguyen, S. T. *Macromolecules* **2005**, *38*, 6251-6253; (h) Sugimoto, H.; Inoue, S. *J. Polym. Sci., Part A: Polym. Chem.* **2004**, *42*, 5561-5573; (i) Super, M. S.; Beckman, E. J. *Trends Polym. Sci.* **1997**, *5*, 236-240; (j) Cohen, C. T.; Chu, T.; Coates, G. W. *J. Am. Chem. Soc.* **2005**, *127*, 10869-10878.

(9) (a) Kruper, W. J.; Dellar, D. V. *J. Org. Chem.* **1995**, *60*, 725-727; (b) Kuran, W.; Listos, T. *Macromol. Chem. Phys.* **1994**, *195*, 1011-1015.

(10) (a) Albertsson, A. C.; Eklund, M. *J. Polym. Sci., Part A: Polym. Chem.* **1994**, *32*, 265-279; (b) Pêgo, A. P.; Siebum, B.; Van Luyn, M. J. A.; Gallego y Van Seijen, X. J.; Poot, A. A.; Grijpma, D. W.; Feijen, J. *Tissue Eng.* **2003**, *9*, 981-994.

(11) (a) Lu, X. B.; Shi, L.; Wang, Y. M.; Zhang, R.; Zhang, Y. J.; Peng, X. J.; Zhang, Z. C.; Bo, Li. *J. Am. Chem. Soc.* **2006**, *128*, 1664-1674; (b) Nakano, K.; Kamada, T.; Nozaki, K. *Angew. Chem., Int. Ed.* **2006**, *45*, 7274-7277; (c) Noh, E. K.; Na, S. J.; S, S.; Kim, S. W.; Lee, B. Y. *J. Am. Chem. Soc.* **2007**, *129*, 8082-8083; (d) Cohen, C. T.; Coates, G. W. *J. Polym. Sci., Part A: Polym. Chem.* **2006**, *44*, 5182-5191; (e) S, S.; Min, J. K.; Seong, J. E.; Na, S. J.; Lee, B. Y. *Angew. Chem., Int. Ed.* **2008**, *47*, 7306-7309; (f) Ren, W. M.; Liu, Z. W.; Wen, Y. Q.; Zhang, R.; Lu, X. B. *J. Am. Chem. Soc.* **2009**, *131*, 11509-11518; (g) Bo, Li.; Wu, G. P.; Ren, W. M.; Wang, Y. M.; Rao, D. Y.; Lu, X. B. *J. Polym. Sci., Part A: Polym. Chem.* **2008**, *46*, 6102-6113; (h) Darensbourg, D. J.; Ulusoy, M.; Karroonnirun, O.; Poland, R. R.; Reibenspies, J. H.; Çetinkaya, B. *Macromolecules* **2009**, *42*, 6992-6998.

(12) Clements, J. H. *Ind. Eng. Chem. Res* **2003**, *42*, 663-674.

(13) Rokicki, G. *Prog. Polym. Sci.* **2000**, *25*, 259-342.

(14) (a) Harris, R. F. *J. Appl. Polym. Sci.* **1989**, *37*, 183-200; (b) Kéki, S.; Török, J.; Deák, G.; Zsuga, M. *Macromolecules* **2001**, *34*, 6850-6857; (c) Lee, J. C.; Litt, M. H. *Macromolecules* **2000**, *33*, 1618-1627; (d) Storey, R. F.; Hoffman, D. C. *Macromolecules* **1992**, *25*, 5369-5382.

(15) (a) Ariga, T.; Takata, T.; Endo, T. *Macromolecules* **1997**, *30*, 737-744; (b) Carothers, W. H.; Van Natta, F. J. *J. Am. Chem. Soc.* **1930**, *52*, 314-326.

(16) (a) Tong, I. T.; Cameron, D. C. *Appl. Biochem. Biotechnol.* **1992**, *34/35*, 149-159; (b) Haynie, S.; Wagner, L.; Winoma, L. (i.e Dupont de Nemours and Co.) Patent WO/035799, 1996.

(17) (a) Kricheldorf, H. R.; Jenssen, J. *J. Macromol. Sci., Pure Appl. Chem.* **1989**, *A26*, 631-644; (b) Ariga, T.; Takata, T.; Endo, T. *J. Polym. Sci., Part A: Polym. Chem.* **1993**, *31*, 581-584; (c) Matsumura, S.; Tsukada, K.; Toshima, K. *Macromolecules* **1997**, *30*, 3122-3124.

(18) (a) Cai, J.; Zhu, K. J.; Yang, S. L. *Polymer* **1988**, *39*, 4409-4415; (b) Hori, Y.; Gonda, Y.; Takahashi, Y.; Hagiwara, T. *Macromolecules* **1996**, *29*, 804-806.

(19) (a) Penco, M.; Donetti, R.; Mendichi, R.; Ferruty, P. *Macromol. Chem. Phys.* **1998**, *199*, 1737-1745; (b) Smith, A.; Hunneyball, I. M. *Int. J. Pharm.* **1986**, *30*, 215-220; (c) Pêgo, A. P.; Van Luyn, M. J. A.; Brouwer, L. A.; van Wachem, P. B.; Poot, A. A.; Grijpma, D. W.; Feijen, J. *J. Biom. Mater. Res-A* **2003**, *67*, 1044-1054.

(20) (a) Kricheldorf, H. R.; Dunsing, R.; Serra i Albet, A. *Makromol. Chem.* **1987**, *188*, 2453-2466; (b) Kricheldorf, H. R.; Jenssen, J. *J. Macromol. Sci., Chem.* **1989**, *A26*, 631-644; (c) Kricheldorf, H. R.; Weegen-Schulz, B. *Macromolecules* **1993**, *26*, 5991-5998.

(21) (a) Matsuo, J.; Aoki, K.; Sanda, F.; Endo, T. *Macromolecules* **1998**, *31*, 4432-4438; (b) Hovestadt, W.; Muller, A. J.; Keul, H.; Höcker, H. *Makromol. Chem. Rapid. Commun.* **1990**, *11*, 271-278; (c) Takata, T.; Sanda, F.; Ariga, T.; Nemoto, H.; Endo, T. *Macromol. Rapid. Commun.* **1997**, *18*, 461-469; (d) Weilandt, K. D.; Keul, H.; Höcker, H. *Macromol. Chem. Phys.* **1996**, *197*, 3851-3868.

(22) Kricheldorf, H. R.; Jenssen, J.; Kreiser-Saunders, I. *Makromol. Chem.* **1991**, *192*, 2391-2399.

(23) Hovestadt, W.; Keul, H.; Höcker, H. *Polymer* **1992**, *33*, 1941-1948.

(24) Yang, J.; Yu, Y.; Li, Q.; Li, Y.; Cao, A. *J. Polym. Sci., Part A: Polym. Chem.* **2005**, *43*, 373-384.

(25) Darensbourg, D. J.; Ganguly, P.; Billodeaux, D. R *Macromolecules* **2005**, *38*, 5406-5410.

(26) Darensbourg, D. J.; Choi, W.; Ganguly, P.; Richers, C. P. *Macromolecules* **2006**, *39*, 4374-4379.

(27) Helou, M.; Miserque, O.; Brusson, J. M.; Carpentier, J. F.; Guillaume, S. M. *Chem. Eur. J.* **2008**, *14*, 8772-8775.

(28) Dobrzynski, P.; Pastusiak, M.; Bero, M. *J. Polym. Sci., Part A: Polym. Chem.* **2005**, *43*, 1913-1922.

(29) Li, C.; Wang, Y.; Zhou, L.; Sun, H.; Shen, Q. *J. Appl. Polym. Sci.* **2006**, *102*, 22-28.

(30) Palard, I.; Schappacher, M.; Belloncle, B.; Soum, A.; Guillaume, S. M. *Chem. Eur. J.* **2007**, *13*, 1511-1521.

(31) Zhao, B.; Lu, C. R.; Shen, Q. *J. Appl. Polym. Sci.* **2007**, *106*, 1383-1389.

(32) Pospiech, D.; Komber, H.; Jehnichen, D.; Häussler, L.; Eckstein, K.; Scheibner, H.; Janke, A.; Kricheldorf, H. R.; Petermann, O. *Biomacromolecules* **2005**, *6*, 439-446.

(33) Nederberg, F.; Lohmeijer, B. G. G.; Leibfarth, F.; Pratt, R. C.; Choi, J.; Dove, A. P.; Waymouth, R. M.; Hedrick, J. L. *Biomacromolecules* **2007**, *8*, 153-160.

(34) Mindermark, J.; Hilborn, J.; Bowden, T. *Macromolecules* **2007**, *40*, 3515-3517.

(35) Feng, J.; He, F.; Zhuo R. *Macromolecules* **2002**, *35*, 7175-7177.

(36) Bisht, K. S.; Svirkin, Y. Y.; Henderson, L. A.; Gross, R. A.; Kaplan, D. L.; Swift, G. *Macromolecules* **1997**, *30*, 7735-7742.

(37) He, F.; Wang, Y.; Feng, J.; Zhuo, R.; Wang, X. *Polymer* **2003**, *44*, 3215-3219.

(38) Koinuma, H.; Hirai, H. *Makromol. Chem.* **1977**, *178*, 1283-1294.

(39) Koinuma, H.; Hirai, H. *Makromol. Chem.* **1977**, *178*, 241-246.

(40) Baba, A.; Meishou, H.; Matsuda, H. *Makromol. Chem. Rapid. Commun.* **1984**, *5*, 665-668.

(41) Baba, A.; Kashiwagi, H.; Matsuda, H. *Tetrahedron Lett.* **1985**, *26*, 1323-1324.

(42) Baba, A.; Kashiwagi, H.; Matsuda, H. *Organometallics* **1987**, *6*, 137-140.

(43) Pfeiffer, E.; Lubbe, E.; Tsumaki, T. *Liebigs Ann.* **1933**, *503*, 84-130.

(44) Jacobsen, E. N.; Zhang, W.; Muci, A. R.; Ecker, J. R.; Deng, L. *J. Am. Chem. Soc.* **1991**, *113*, 7063-7064.

(45) Darensbourg, D. J.; Mackiewicz, R. M.; Rodgers, J. L.; Fang, C. C.; Billodeaux, D. R.; Reibenspies, J. H. *Inorg. Chem.* **2004**, *43*, 6024-6034.

(46) Darensbourg, D. J.; Rodgers, J. L.; Mackiewicz, R. M.; Phelps, A. L. *Catal. Today* **2004**, *98*, 485-492.

(47) Darensbourg, D. J.; Ganguly, P.; Choi, W. *Inorg. Chem.* **2006**, *45*, 3831-3833.

(48) Demadis, K.; Meyer, T. J.; White, P. S. *Inorg. Chem.* **1998**, *37*, 3610-3619.

(49) Sheldrick, G. M. *SADABS*, Bruker AXS Inc.: Madison, WI.

(50) Sheldrick, G. M. *SHELXS-97*, Institüt für Anorganische Chemie der Universität: Gottigen, Germany, 1997.

(51) Sheldrick, G. M. *SHELXL-97*, Institüt für Anorganische Chemie der Universität: Gottigen, Germany, 1997.

(52) Sheldrick, G. M. *SHELXTL, v. 6.14*; Bruker-Nonius Inc.: Madison, WI, 2000.

(53) Barbour, L. J. *J. Supramol. Chem* **2001**, *1*, 189-191.

(54) (a) Darensbourg, D. J.; Mackiewicz, R. M. *J. Am. Chem. Soc.* **2005**, *127*, 14026-14038; (b) Darensbourg, D. J.; Mackiewicz, R. M.; Rodgers, J. L. *J. Am. Chem. Soc.* **2005**, *127*, 17565.

(55) (a) Darensbourg, D. J.; Fitch, S. B. *Inorg. Chem.* **2007**, *47*, 5474-5476; (b) Sugimoto, H.; Ohtsuka, H.; Inoue, S. *J. Polym. Sci., Part A: Polym. Chem.* **2005**, *43*, 4172-4186.

(56) Darensbourg, D. J.; Choi, W.; Richers, C. P. *Macromolecules* **2007**, *40*, 3521-3523.

(57) Sawada, H. *Macromol. Sci., Rev. Macromol. Chem.* **1970**, *C5*, 151-174.

(58) Darensbourg, D. J.; Frantz, E. B.; Andreatta, J. R. *Inorg. Chim. Acta* **2007**, *360*, 523-528.

(59) Luger, P.; Buschmann, J. *J. Am. Chem. Soc.* **1984**, *106*, 7118-7121.

(60) (a) Darensbourg, D. J.; Yarbrough, J. C. *J. Am. Chem. Soc.* **2002**, *124*, 6335-6342; (b) Darensbourg, D. J.; Yarbrough, J. C.; Ortiz, C.; Fang, C. C. *J. Am. Chem. Soc.* **2003**, *125*, 7586-7591.

(61) Kricheldorf, H. R.; Weegen-Schulz, B. *Polymer* **1995**, *36*, 4997-5003.

(62) Ling, J.; Shen, Z.; Huang, Q. *Macromolecules* **2001**, *34*, 7613-7616.

(63) (a) Martínez, L. E.; Leighton, J. L.; Carste, D. H.; Jacobsen, E. N. *J. Am. Chem. Soc.* **1995**, *117*, 5897-5898; (b) Hansen, K. B.; Leighton, J. L.; Jacobsen, E. N. *J. Am. Chem. Soc.* **1996**, *118*, 10924-10925.

(64) Darensbourg, D. J.; Mueller, B. L.; Bischoff, C. J.; Chojnacki, S. S.; Reibenspies, J. H. *Inorg. Chem.* **1991**, *30*, 2418-2424.

(65) Darensbourg, D. J.; Frantz, E. B. *Inorg. Chem.* **2008**, *47*, 4977-4987.

(66) *FRAMBO:FRAME Buffer Operation, v.4.1.05*; Bruker AXS Inc.: Madison, WI.

(67) *SMART, v.5.632*; Bruker AXS Inc.: Madison, WI.

(68) *SAINT, v.6.63*; Bruker AXS Inc.: Madison, WI.

(69) (a) Pell, A. S.; Pilcher, G. *Trans. Faraday Soc* **1965**, *61*, 71-77; (b) Yamashita, Y.; Tsuda, T.; Okada, M.; Iwatsuki, S. *J. Polym. Sci., Part A: Polym. Chem.* **1966**, *4*, 2121-2135.

(70) (a) Lu, X. B.; Feng, X. J.; He, R. *Appl. Catal. A* **2002**, *234*, 25-33; (b) Lu, X. B.; He, R.; Bai, C. X. *J. Mol. Catal. A: Chem.* **2002**, *186*, 1-11; (c) Lu, X. B.; Zhang, Y. J.; Jin, K.; Luo, L. M.; Wang, H. *J. Catal.* **2004**, *227*, 537-541; (d) Lu, X. B.; Zhang, Y. J.; Liang, B.; Li, X.; Wang, H. *J. Mol. Catal. A: Chem.* **2004**, *210*, 31-34.

(71) (a) Darensbourg, D. J.; Fang, C. C.; Rodgers, J. L. *Organometallics* **2004**, *23*, 924-927; (b) Paddock, R. L.; Nguyen, S. T. *J. Am. Chem. Soc.* **2001**, *123*, 11498-11499.

(72) (a) Chen, S. W.; Kawthekar, R. B.; Kim, G. J. *Tetrahedron Lett.* **2007**, *48*, 297-300; (b) Lu, X. B.; Liang, B.; Zhang, Y. J.; Tian, J. Z.; Wang, Y. M.; Bai, C. X.; Wang, H.; Zhang, R. *J. Am. Chem. Soc.* **2004**, *126*, 3732-3733; (c) Shen, Y. M.; Duan, W. L.; Shi, M. *J. Org. Chem.* **2003**, *68*, 1559-1562; (d) Tanaka, H.; Kitaichi, Y.; Sato, M.; Ikeno, T.; Yamada, T. *Chem. Lett.* **2004**, *33*, 676-677.

(73) (a) Jutz, F.; Grunwaldt, J. D.; Baiker, A. *J. Mol. Catal. A: Chem.* **2008**, *279*, 94-103; (b) Srivastava, R.; Bennur, T. H.; Srinivas, D. *J. Mol. Catal. A: Chem.* **2005**, *226*, 199-205.

(74) Jing, H.; Edulji, S. K.; Gibbs, J. M.; Stern, C. L.; Zhou, H.; Nguyen, S. T. *Inorg. Chem.* **2004**, *43*, 4315-4327.

(75) (a) Kasuga, K.; Kabata, N.; Kato, T.; Sugimori, T.; Handa, M. *Inorg. Chim. Acta* **1998**, *278*, 223-225; (b) Kasuga, K.; Nagao, S.; Fukumoto, T.; Handa, M. *Polyhedron* **1996**, *15*, 69-72; (c) Sugimoto, H.; Inoue, S. *Pure Appl. Chem* **1998**, *70*, 2365-2369.

(76) (a) Kawanami, H.; Sasaki, A.; Matsui, K.; Ikushima, Y. *Chem. Commun* **2003**, 896-897; (b) Peng, J.; Deng, Y. *New J. Chem.* **2001**, *25*, 639-641.

(77) Caló, V.; Nacci, A.; Monopoli, A.; Fanizzi, A. *Org. Lett.* **2002**, *4*, 2561-2563.

(78) Li, F.; Xia, C.; Xu, L.; Sun, W.; Chen, G. *Chem. Commun* **2003**, 2042-2043.

(79) Man, M. L.; Lam, K. C.; Sit, W. N.; Ng, S. M.; Zhou, Z.; Lin, Z.; Lau, C. P. *Chem. Eur. J.* **2006**, *12*, 1004-1015.

(80) Kim, H. S.; Bae, J. Y.; Lee, J. S.; Kwon, O. S.; Jelliarko, P.; Lee, S. D.; Lee, S. H. *J. Catal.* **2005**, *232*, 80-84.

(81) Shen, Y. M.; Duan, W. L.; Shi, M. *Adv. Synth. Catal.* **2003**, *345*, 337-340.

(82) Shiels, R. A.; Jones, C. W. *J. Mol. Catal. A: Chem.* **2007**, *261*, 160-166.

(83) Zhou, H.; Zhang, W. Z.; Liu, C. H.; Qu, J. P.; Lu, X. B. *J. Org. Chem.* **2008**, *73*, 8039-8044.

(84) Yamaguchi, K.; Ebitani, K.; Yoshida, T.; Yoshida, H.; Kaneda, K. *J. Am. Chem. Soc.* **1999**, *121*, 4526-4527.

(85) Yano, T.; Matsui, H.; Koike, T.; Ishiguro, H.; Fujihara, H.; Masakuni, Y.; Maeshima, T. *Chem. Commun* **1997**, 1129-1130.

(86) Tu, M.; Davis, R. J. *J. Catal.* **2001**, *199*, 85-91.

(87) Leung, W. H.; Chan, E. Y. Y.; Chow, E. K. F.; Williams, I. D.; Peng, S. M. *J. Chem. Soc., Dalton Trans.* **1996**, 1229-1236.

(88) Nielsen, L. P. C.; Stevenson, C. P.; Blackmond, D. G.; Jacobsen, E. N. *J. Am. Chem. Soc.* **2004**, *126*, 1360-1362.

(89) Sudo, A.; Morioka, Y.; Koizumi, E.; Sanda, F.; Endo, T. *Tetrahedron Lett.* **2003**, *44*, 7889-7891.

(90) (a) Paddock, R. L.; Hiyama, Y.; Mackay, J. M.; Nguyen, S. T. *Tetrahedron Lett.* **2004,** *45*, 2023-2026; (b) Paddock, R. L.; Nguyen, S. T. *Chem. Commun* **2004**, 1622-1623.

(91) Kataeva, O. N.; Litvinov, I. A.; Naumov, V. A. *Zh. Strukt. Khim* **1988**, *29*, 186-188.

(92) Loy, R. N.; Jacobsen, E. N. *J. Am. Chem. Soc.* **2009**, *131*, 2789-2787.

(93) North, M.; Pasquale, R. *Angew. Chem., Int. Ed.* **2009**, *48*, 2946-2948.

(94) Keul, H.; Bacher, R.; Hocker, H. *Makromol. Chem.* **1986**, *187*, 2579-2589.

(95) (a) Endo, T.; Suzuki, T.; Sanda, F.; Takata, T. *Macromolecules* **1996**, *29*, 3315-3316; (b) Endo, T.; Suzuki, T.; Sanda, F.; Takata, T. *Macromolecules* **1996**, *29*, 4819; (c) Höcker, H.; Keul, H. *Adv. Mater.* **1994**, *6*, 21-36.

(96) (a) Luinstra, G. A.; Hass, G. R.; Molnar, F.; Bernhart, V.; Eberhardt, R.; Rieger, B. *Chem. Eur. J.* **2005**, *11*, 6298-6314; (b) Nakano, K.; Kamada, T.; Nozaki, K. *Angew. Chem., Int. Ed.* **2006**, *45*, 1-4.

(97) Darensbourg, D. J.; Bottarelli, P.; Andreatta, J. R. *Macromolecules* **2007**, *40*, 7727-7729.

(98) Darensbourg, D. J.; Yarbrough, J. C.; Ortiz, C.; Fang, C. C. *J. Am. Chem. Soc.* **2003,** *125*, 7586-7591.

(99) McAlees, A. J.; McCrindle, R.; Woon-Fat, A. R. *Inorg. Chem.* **1976**, *15*, 1065-1074.

(100) Doherty, S.; Robins, E. G.; Nieuwenhuyzen, M.; Champkin, P. A.; Clegg, W. *Organometallics* **2002**, *21*, 4147-4158.

APPENDIX A

COPYRIGHT INFORMATION

American Chemical Society's Policy on Theses and Dissertations

If your university requires a signed copy of this letter see contact information below.

Thank you for your request for permission to include your paper(s) or portions of text from your paper(s) in your thesis. Permission is now automatically granted; please pay special attention to the implications paragraph below. The Copyright Subcommittee of the Joint Board/Council Committees on Publications approved the following:

> Copyright permission for published and submitted material from theses and dissertations
> ACS extends blanket permission to students to include in their theses and dissertations their own articles, or portions thereof, that have been published in ACS journals or submitted to ACS journals for publication, provided that the ACS copyright credit line is noted on the appropriate page(s).
>
> Publishing implications of electronic publication of theses and dissertation material
> Students and their mentors should be aware that posting of theses and dissertation material on the Web prior to submission of material from that thesis or dissertation to an ACS journal may affect publication in that journal. Whether Web posting is considered prior publication may be evaluated on a case-by-case basis by the journal's editor. If an ACS journal editor considers Web posting to be "prior publication", the paper will not be accepted for publication in that journal. If you intend to submit your unpublished paper to ACS for publication, check with the appropriate editor prior to posting your manuscript electronically.

If your paper has not yet been published by ACS, we have no objection to your including the text or portions of the text in your thesis/dissertation in **print and microfilm formats**; please note, however, that electronic distribution or Web posting of the unpublished paper as part of your thesis in electronic formats might jeopardize publication of your paper by ACS. Please print the following credit line on the first page of your article: "Reproduced (or 'Reproduced in part') with permission from [JOURNAL NAME], in press (or 'submitted for publication'). Unpublished work copyright [CURRENT YEAR] American Chemical Society." Include appropriate information.

If your paper has already been published by ACS and you want to include the text or portions of the text in your thesis/dissertation in **print or microfilm formats**, please print the ACS copyright credit line on the first page of your article: "Reproduced (or 'Reproduced in part') with permission from [FULL REFERENCE CITATION.] Copyright [YEAR] American Chemical Society." Include appropriate information.

Submission to a Dissertation Distributor: If you plan to submit your thesis to UMI or to another dissertation distributor, you should not include the unpublished ACS paper in your thesis if the thesis will be disseminated electronically, until ACS has published your paper. After publication of the paper by ACS, you may release the entire thesis (**not the individual ACS article by itself**) for electronic dissemination through the distributor; ACS's copyright credit line should be printed on the first page of the ACS paper.

Use on an Intranet: The inclusion of your ACS unpublished or published manuscript is permitted in your thesis in print and microfilm formats. If ACS has published your paper you may include the manuscript in your thesis on an intranet that is not publicly available. Your ACS article cannot be posted electronically on a publicly available medium (i.e. one that is not password protected), such as but not limited to, electronic archives, Internet, library server, etc. The only material from your paper that can be posted on a public electronic medium is the article abstract, figures, and tables, and you may link to the article's DOI or post the article's author-directed URL link provided by ACS. This paragraph does not pertain to the dissertation distributor paragraph above.

Questions? Call +1 202/872-4368/4367. Send e-mail to copyright@acs.org or fax to +1 202-776-8112. 10/10/03, 01/15/04, 06/07/06

APPENDIX B

TABLES OF CRYSTALLOGRAPHIC DATA

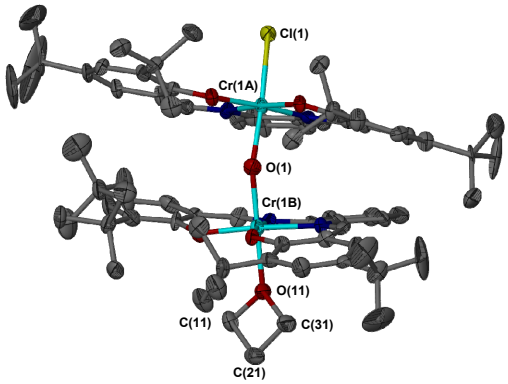

Complex II-5

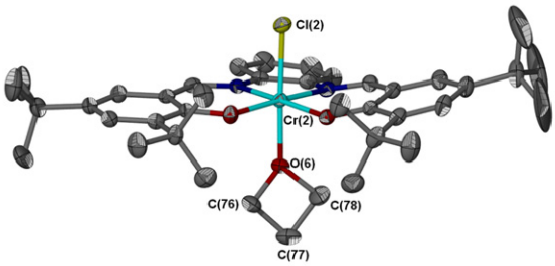

Complex II-6

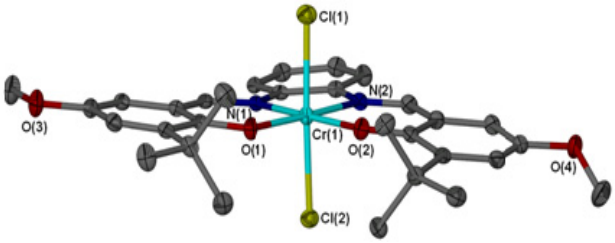

Complex III-3

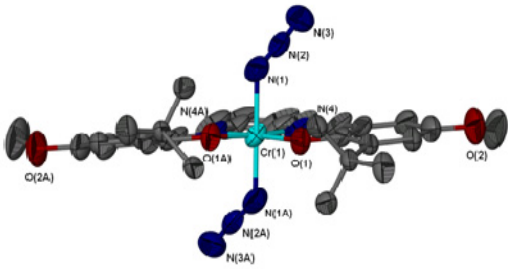

Complex III-4

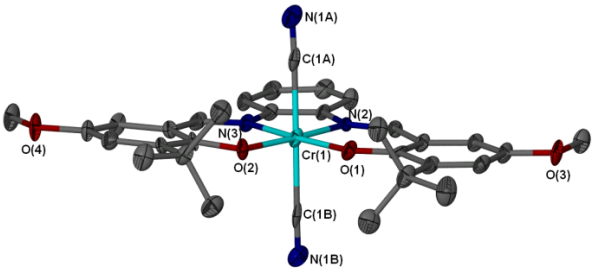

Complex III-5

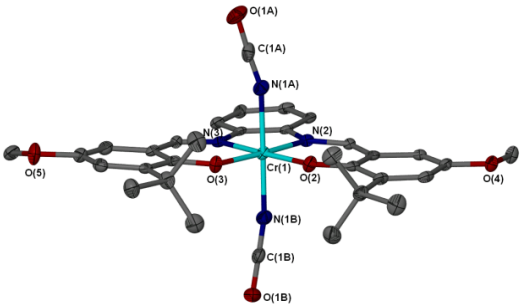

Complex III-6

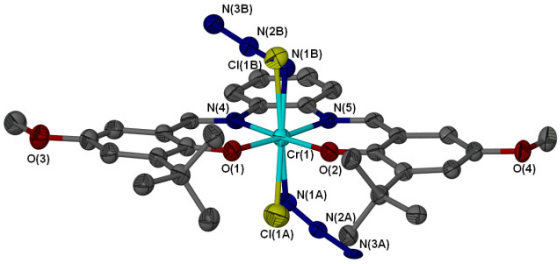

Complex III-7

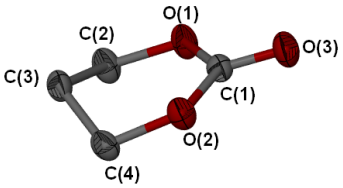

Trimethylene Carbonate

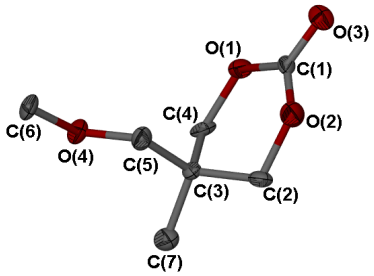

5-Methoxy-methyl-5-methyl-1,3-dioxan-2-one

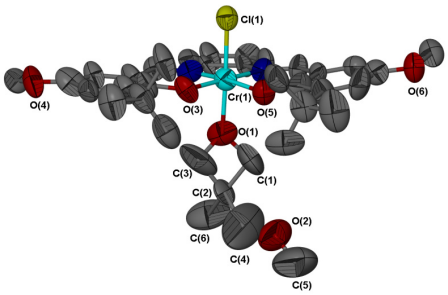

Complex VI-1

Table B-1. Crystal Data and Structure Refinement for Complex **II-5**.

Identification code	dd	
Empirical formula	C80 H110 Cl Cr2 N4 O6	
Formula weight	1363.17	
Temperature	120(2) K	
Wavelength	0.71073 Å	
Crystal system	Triclinic	
Space group	P-1	
Unit cell dimensions	a = 12.266(5) Å	α= 102.839(5)°.
	b = 14.702(5) Å	β= 95.784(5)°.
	c = 21.630(5) Å	γ = 100.245(5)°.
Volume	3702(2) $Å^3$	
Z	2	
Density (calculated)	1.223 Mg/m^3	
Absorption coefficient	0.384 mm^{-1}	
F(000)	1462	
Crystal size	0.20 x 0.20 x 0.10 mm^3	
Theta range for data collection	2.41 to 25.00°.	
Index ranges	-14<=h<=14, -17<=k<=17, 0<=l<=25	
Reflections collected	10087	
Independent reflections	10392 [R(int) = 0.0000]	
Completeness to theta = 25.00°	72.30%	
Absorption correction	Semi-empirical from equivalents	
Max. and min. transmission	0.9627 and 0.9272	
Refinement method	Full-matrix least-squares on F_2	
Data / restraints / parameters	10392 / 51 / 856	
Goodness-of-fit on F_2	1.029	
Final R indices [I>2sigma(I)]	R1 = 0.0755, wR2 = 0.1995	
R indices (all data)	R1 = 0.1239, wR2 = 0.2321	
Largest diff. peak and hole	0.440 and -0.428 $e.Å^{-3}$	

Table B-2. Bond Distances (Å) and Bond Angles (deg) for Complex **II-5**.

Cl(1)-Cr(1A)	2.343(3)	C(10A)-C(7A)-C(8A)	109.4(8)
O(1)-Cr(1B)	1.950(6)	C(3A)-C(7A)-C(8A)	109.4(8)
O(1)-Cr(1A)	2.002(6)	C(10A)-C(7A)-C(9A)	107.5(8)
Cr(1A)-O(1A)	1.909(6)	C(3A)-C(7A)-C(9A)	108.2(9)
Cr(1A)-O(2A)	1.927(6)	C(8A)-C(7A)-C(9A)	106.9(8)
Cr(1A)-N(2A)	1.973(8)	C(13A)-C(11A)-C(12A)	105.9(15)
Cr(1A)-N(1A)	2.021(7)	C(13A)-C(11A)-C(14A)	108.5(15)
O(1A)-C(2A)	1.309(11)	C(12A)-C(11A)-C(14A)	108.2(14)
O(2A)-C(24A)	1.302(11)	C(13A)-C(11A)-C(5A)	112.7(10)
N(1A)-C(15A)	1.300(12)	C(12A)-C(11A)-C(5A)	110.5(11)
N(1A)-C(16A)	1.403(11)	C(14A)-C(11A)-C(5A)	110.9(10)
N(2A)-C(22A)	1.359(11)	N(1A)-C(15A)-C(1A)	127.3(10)
N(2A)-C(17A)	1.422(11)	N(1A)-C(16A)-C(21A)	125.4(9)
C(1A)-C(15A)	1.393(13)	N(1A)-C(16A)-C(17A)	117.1(8)
C(1A)-C(6A)	1.419(12)	C(21A)-C(16A)-C(17A)	117.5(9)
C(1A)-C(2A)	1.441(13)	C(18A)-C(17A)-C(16A)	120.4(9)
C(2A)-C(3A)	1.410(13)	C(18A)-C(17A)-N(2A)	126.2(9)
C(3A)-C(4A)	1.385(13)	C(16A)-C(17A)-N(2A)	113.3(8)
C(3A)-C(7A)	1.518(12)	C(19A)-C(18A)-C(17A)	119.8(10)
C(4A)-C(5A)	1.434(13)	C(18A)-C(19A)-C(20A)	120.4(10)
C(5A)-C(6A)	1.360(13)	C(21A)-C(20A)-C(19A)	119.8(9)
C(5A)-C(11A)	1.520(13)	C(20A)-C(21A)-C(16A)	122.1(10)
C(7A)-C(10A)	1.471(13)	N(2A)-C(22A)-C(23A)	125.2(9)
C(7A)-C(8A)	1.560(12)	C(24A)-C(23A)-C(22A)	123.9(9)
C(7A)-C(9A)	1.577(13)	C(24A)-C(23A)-C(28A)	121.1(9)
C(11A)-C(13A)	1.434(17)	C(22A)-C(23A)-C(28A)	114.9(9)
C(11A)-C(12A)	1.473(18)	O(2A)-C(24A)-C(23A)	123.0(9)
C(11A)-C(14A)	1.493(17)	O(2A)-C(24A)-C(25A)	118.6(9)
C(16A)-C(21A)	1.409(11)	C(23A)-C(24A)-C(25A)	118.4(9)
C(16A)-C(17A)	1.411(13)	C(26A)-C(25A)-C(24A)	116.1(9)
C(17A)-C(18A)	1.390(13)	C(26A)-C(25A)-C(29A)	123.7(9)
C(18A)-C(19A)	1.373(12)	C(24A)-C(25A)-C(29A)	120.2(8)
C(19A)-C(20A)	1.404(13)	C(25A)-C(26A)-C(27A)	127.0(9)
C(20A)-C(21A)	1.341(13)	C(28A)-C(27A)-C(26A)	117.0(9)
C(22A)-C(23A)	1.418(11)	C(28A)-C(27A)-C(33A)	121.2(10)
C(23A)-C(24A)	1.417(13)	C(26A)-C(27A)-C(33A)	121.7(9)
C(23A)-C(28A)	1.438(12)	C(27A)-C(28A)-C(23A)	120.2(9)
C(24A)-C(25A)	1.443(12)	C(25A)-C(29A)-C(32A)	112.0(8)
C(25A)-C(26A)	1.377(12)	C(25A)-C(29A)-C(31A)	110.7(8)

C(25A)-C(29A)	1.493(13)	C(32A)-C(29A)-C(31A)	107.2(8)
C(26A)-C(27A)	1.398(13)	C(25A)-C(29A)-C(30A)	112.2(8)
C(27A)-C(28A)	1.361(12)	C(32A)-C(29A)-C(30A)	105.4(8)
C(27A)-C(33A)	1.521(13)	C(31A)-C(29A)-C(30A)	109.1(8)
C(29A)-C(32A)	1.522(11)	C(35A)-C(33A)-C(34A)	107.5(10)
C(29A)-C(31A)	1.531(12)	C(35A)-C(33A)-C(27A)	113.9(9)
C(29A)-C(30A)	1.552(14)	C(34A)-C(33A)-C(27A)	111.1(9)
C(33A)-C(35A)	1.497(14)	C(35A)-C(33A)-C(36A)	109.5(10)
C(33A)-C(34A)	1.516(13)	C(34A)-C(33A)-C(36A)	105.0(9)
C(33A)-C(36A)	1.528(14)	C(27A)-C(33A)-C(36A)	109.4(9)
Cr(1B)-O(1B)	1.896(7)	O(1B)-Cr(1B)-O(2B)	94.5(3)
Cr(1B)-O(2B)	1.905(6)	O(1B)-Cr(1B)-O(1)	92.3(3)
Cr(1B)-N(2B)	1.990(8)	O(2B)-Cr(1B)-O(1)	90.3(3)
Cr(1B)-N(3B)	2.018(8)	O(1B)-Cr(1B)-N(2B)	91.0(3)
Cr(1B)-O(1O)	2.068(6)	O(2B)-Cr(1B)-N(2B)	173.1(3)
O(1B)-C(2B)	1.331(10)	O(1)-Cr(1B)-N(2B)	93.7(3)
O(2B)-C(24B)	1.310(10)	O(1B)-Cr(1B)-N(3B)	171.6(3)
N(2B)-C(15B)	1.323(11)	O(2B)-Cr(1B)-N(3B)	92.3(3)
N(2B)-C(16B)	1.426(12)	O(1)-Cr(1B)-N(3B)	92.6(3)
N(3B)-C(22B)	1.338(11)	N(2B)-Cr(1B)-N(3B)	81.8(3)
N(3B)-C(17B)	1.410(12)	O(1B)-Cr(1B)-O(1O)	88.0(3)
C(1B)-C(15B)	1.374(13)	O(2B)-Cr(1B)-O(1O)	89.4(3)
C(1B)-C(2B)	1.421(13)	O(1)-Cr(1B)-O(1O)	179.6(3)
C(1B)-C(6B)	1.428(13)	N(2B)-Cr(1B)-O(1O)	86.6(3)
C(2B)-C(3B)	1.418(13)	N(3B)-Cr(1B)-O(1O)	87.1(3)
C(3B)-C(4B)	1.397(12)	C(2B)-O(1B)-Cr(1B)	130.1(6)
C(3B)-C(7B)	1.524(14)	C(24B)-O(2B)-Cr(1B)	129.3(6)
C(4B)-C(5B)	1.407(14)	C(15B)-N(2B)-C(16B)	123.6(8)
C(5B)-C(6B)	1.337(14)	C(15B)-N(2B)-Cr(1B)	123.2(7)
C(5B)-C(11B)	1.545(13)	C(16B)-N(2B)-Cr(1B)	113.3(6)
C(7B)-C(8B)	1.513(13)	C(22B)-N(3B)-C(17B)	123.2(9)
C(7B)-C(10B)	1.549(13)	C(22B)-N(3B)-Cr(1B)	123.6(7)
C(7B)-C(9B)	1.558(13)	C(17B)-N(3B)-Cr(1B)	113.2(6)
C(11B)-C(14B)	1.487(14)	C(15B)-C(1B)-C(2B)	125.0(9)
C(11B)-C(13B)	1.515(15)	C(15B)-C(1B)-C(6B)	117.8(10)
C(11B)-C(12B)	1.559(15)	C(2B)-C(1B)-C(6B)	117.2(10)
C(16B)-C(21B)	1.377(13)	O(1B)-C(2B)-C(1B)	119.6(9)
C(16B)-C(17B)	1.394(13)	O(1B)-C(2B)-C(3B)	119.3(9)
C(17B)-C(18B)	1.374(13)	C(1B)-C(2B)-C(3B)	121.0(9)
C(18B)-C(19B)	1.400(13)	C(4B)-C(3B)-C(2B)	116.2(10)

C(19B)-C(20B)	1.365(13)	C(4B)-C(3B)-C(7B)	121.2(10)
C(20B)-C(21B)	1.365(14)	C(2B)-C(3B)-C(7B)	122.5(9)
C(22B)-C(23B)	1.412(13)	C(3B)-C(4B)-C(5B)	124.7(11)
C(23B)-C(28B)	1.388(12)	C(6B)-C(5B)-C(4B)	116.7(10)
C(23B)-C(24B)	1.422(13)	C(6B)-C(5B)-C(11B)	124.2(10)
C(24B)-C(25B)	1.424(12)	C(4B)-C(5B)-C(11B)	119.0(10)
C(25B)-C(26B)	1.392(13)	C(5B)-C(6B)-C(1B)	124.0(10)
C(25B)-C(29B)	1.532(14)	C(8B)-C(7B)-C(3B)	108.9(9)
C(26B)-C(27B)	1.384(14)	C(8B)-C(7B)-C(10B)	108.5(9)
C(27B)-C(28B)	1.397(13)	C(3B)-C(7B)-C(10B)	111.9(8)
C(27B)-C(33B)	1.565(13)	C(8B)-C(7B)-C(9B)	112.8(9)
C(29B)-C(31B)	1.508(13)	C(3B)-C(7B)-C(9B)	108.3(8)
C(29B)-C(32B)	1.541(13)	C(10B)-C(7B)-C(9B)	106.5(9)
C(29B)-C(30B)	1.582(14)	C(14B)-C(11B)-C(13B)	110.0(10)
C(33B)-C(34B)	1.495(14)	C(14B)-C(11B)-C(5B)	111.5(9)
C(33B)-C(35B)	1.506(15)	C(13B)-C(11B)-C(5B)	109.9(9)
C(33B)-C(36B)	1.511(17)	C(14B)-C(11B)-C(12B)	107.8(10)
O(1O)-C(1O)	1.431(11)	C(13B)-C(11B)-C(12B)	109.8(10)
O(1O)-C(3O)	1.471(10)	C(5B)-C(11B)-C(12B)	107.8(9)
C(1O)-C(2O)	1.505(13)	N(2B)-C(15B)-C(1B)	127.6(9)
C(2O)-C(3O)	1.499(14)	C(21B)-C(16B)-C(17B)	119.2(10)
C(1P)-C(2P)	1.425(16)	C(21B)-C(16B)-N(2B)	124.9(9)
C(2P)-C(3P)	1.356(17)	C(17B)-C(16B)-N(2B)	115.6(8)
C(3P)-C(4P)	1.432(16)	C(18B)-C(17B)-C(16B)	119.8(10)
C(4P)-C(5P)	1.401(15)	C(18B)-C(17B)-N(3B)	124.5(9)
		C(16B)-C(17B)-N(3B)	115.5(9)
Cr(1B)-O(1)-Cr(1A)	156.5(4)	C(17B)-C(18B)-C(19B)	120.2(10)
O(1A)-Cr(1A)-O(2A)	95.1(3)	C(20B)-C(19B)-C(18B)	118.9(11)
O(1A)-Cr(1A)-N(2A)	172.9(3)	C(21B)-C(20B)-C(19B)	121.1(11)
O(2A)-Cr(1A)-N(2A)	91.6(3)	C(20B)-C(21B)-C(16B)	120.6(10)
O(1A)-Cr(1A)-O(1)	85.3(3)	N(3B)-C(22B)-C(23B)	125.5(10)
O(2A)-Cr(1A)-O(1)	88.7(3)	C(28B)-C(23B)-C(22B)	114.9(10)
N(2A)-Cr(1A)-O(1)	92.7(3)	C(28B)-C(23B)-C(24B)	121.0(9)
O(1A)-Cr(1A)-N(1A)	91.3(3)	C(22B)-C(23B)-C(24B)	124.0(9)
O(2A)-Cr(1A)-N(1A)	173.4(3)	O(2B)-C(24B)-C(25B)	117.8(9)
N(2A)-Cr(1A)-N(1A)	81.9(3)	O(2B)-C(24B)-C(23B)	123.9(9)
O(1)-Cr(1A)-N(1A)	90.4(3)	C(25B)-C(24B)-C(23B)	118.3(9)
O(1A)-Cr(1A)-Cl(1)	91.6(2)	C(26B)-C(25B)-C(24B)	117.8(10)
O(2A)-Cr(1A)-Cl(1)	93.0(2)	C(26B)-C(25B)-C(29B)	121.9(9)
N(2A)-Cr(1A)-Cl(1)	90.2(2)	C(24B)-C(25B)-C(29B)	120.3(9)

O(1)-Cr(1A)-Cl(1)	176.6(2)	C(27B)-C(26B)-C(25B)	124.4(10)
N(1A)-Cr(1A)-Cl(1)	88.3(2)	C(26B)-C(27B)-C(28B)	117.4(9)
C(2A)-O(1A)-Cr(1A)	130.8(6)	C(26B)-C(27B)-C(33B)	120.7(10)
C(24A)-O(2A)-Cr(1A)	129.8(6)	C(28B)-C(27B)-C(33B)	121.9(10)
C(15A)-N(1A)-C(16A)	124.1(8)	C(23B)-C(28B)-C(27B)	120.9(10)
C(15A)-N(1A)-Cr(1A)	123.7(7)	C(31B)-C(29B)-C(25B)	109.2(9)
C(16A)-N(1A)-Cr(1A)	112.2(6)	C(31B)-C(29B)-C(32B)	107.3(8)
C(22A)-N(2A)-C(17A)	120.3(8)	C(25B)-C(29B)-C(32B)	112.3(8)
C(22A)-N(2A)-Cr(1A)	124.8(6)	C(31B)-C(29B)-C(30B)	109.7(9)
C(17A)-N(2A)-Cr(1A)	114.9(6)	C(25B)-C(29B)-C(30B)	111.6(8)
C(15A)-C(1A)-C(6A)	115.8(9)	C(32B)-C(29B)-C(30B)	106.6(9)
C(15A)-C(1A)-C(2A)	124.8(9)	C(34B)-C(33B)-C(35B)	110.8(11)
C(6A)-C(1A)-C(2A)	119.2(9)	C(34B)-C(33B)-C(36B)	110.4(11)
O(1A)-C(2A)-C(3A)	121.1(9)	C(35B)-C(33B)-C(36B)	106.9(11)
O(1A)-C(2A)-C(1A)	120.5(9)	C(34B)-C(33B)-C(27B)	110.1(9)
C(3A)-C(2A)-C(1A)	118.4(9)	C(35B)-C(33B)-C(27B)	105.8(9)
C(4A)-C(3A)-C(2A)	119.1(9)	C(36B)-C(33B)-C(27B)	112.7(9)
C(4A)-C(3A)-C(7A)	119.3(9)	C(1O)-O(1O)-C(3O)	91.3(7)
C(2A)-C(3A)-C(7A)	121.5(9)	C(1O)-O(1O)-Cr(1B)	128.3(6)
C(3A)-C(4A)-C(5A)	123.9(10)	C(3O)-O(1O)-Cr(1B)	130.6(6)
C(6A)-C(5A)-C(4A)	115.9(9)	O(1O)-C(1O)-C(2O)	91.2(8)
C(6A)-C(5A)-C(11A)	125.6(10)	C(3O)-C(2O)-C(1O)	87.4(8)
C(4A)-C(5A)-C(11A)	118.4(10)	O(1O)-C(3O)-C(2O)	89.9(8)
C(5A)-C(6A)-C(1A)	123.3(10)	C(3P)-C(2P)-C(1P)	124(2)
C(10A)-C(7A)-C(3A)	115.2(9)	C(2P)-C(3P)-C(4P)	121(2)
		C(5P)-C(4P)-C(3P)	117.2(16)

Table B-3. Crystal Data and Structure Refinement for Complex **II-6**.

Identification code	oxetane3	
Empirical formula	C34.40 H48.80 Cl3.20 Cr0.80 N1.60 O2.40	
Formula weight	678.19	
Temperature	110(2) K	
Wavelength	0.71073 Å	
Crystal system	Triclinic	
Space group	P-1	
Unit cell dimensions	a = 16.175(5) Å	α= 89.781(4)°.
	b = 16.394(5) Å	β= 88.053(4)°.
	c = 17.126(6) Å	γ = 79.249(4)°.
Volume	4459(2) $Å^3$	
Z	5	
Density (calculated)	1.263 Mg/m^3	
Absorption coefficient	0.535 mm^{-1}	
F(000)	1796	
Crystal size	0.30 x 0.10 x 0.10 mm^3	
Theta range for data collection	1.62 to 25.00°.	
Index ranges	-19<=h<=19, -19<=k<=19, -20<=l<=20	
Reflections collected	41341	
Independent reflections	15610 [R(int) = 0.0612]	
Completeness to theta = 25.00°	99.20%	
Absorption correction	None	
Max. and min. transmission	0.9485 and 0.8560	
Refinement method	Full-matrix least-squares on F_2	
Data / restraints / parameters	15610 / 48 / 979	
Goodness-of-fit on F_2	1.077	
Final R indices [I>2sigma(I)]	R1 = 0.0579, wR2 = 0.1433	
R indices (all data)	R1 = 0.0908, wR2 = 0.1643	
Largest diff. peak and hole	0.965 and -0.667 $e.Å^{-3}$	

Table B-4. Bond Distances (Å) and Bond Angles (deg) for Complex **II-6**.

Cr(1)-O(1)	1.9055(10)	C(11)-C(13)-H(13B)	109.5
Cr(1)-O(2)	1.9129(10)	H(13A)-C(13)-H(13B)	109.5
Cr(1)-N(1)	2.0063(12)	C(11)-C(13)-H(13C)	109.5
Cr(1)-N(2)	2.0120(11)	H(13A)-C(13)-H(13C)	109.5
Cr(1)-O(3)	2.0456(10)	H(13B)-C(13)-H(13C)	109.5
Cr(1)-Cl(1)	2.3167(6)	C(11)-C(14)-H(14A)	109.5
Cr(2)-O(4)	1.9053(11)	C(11)-C(14)-H(14B)	109.5
Cr(2)-O(5)	1.9129(10)	H(14A)-C(14)-H(14B)	109.5
Cr(2)-N(3)	2.0070(12)	C(11)-C(14)-H(14C)	109.5
Cr(2)-N(4)	2.0096(13)	H(14A)-C(14)-H(14C)	109.5
Cr(2)-O(6)	2.0528(11)	H(14B)-C(14)-H(14C)	109.5
Cr(2)-Cl(2)	2.3036(7)	N(1)-C(15)-C(1)	125.99(12)
Cl(3)-C(79)	1.7395(19)	N(1)-C(15)-H(15)	117
Cl(4)-C(79)	1.7495(19)	C(1)-C(15)-H(15)	117
Cl(5)-C(81)	1.738(3)	C(21)-C(16)-C(17)	119.39(11)
Cl(6)-C(80)	1.7550(18)	C(21)-C(16)-N(1)	125.27(12)
Cl(7)-C(80)	1.7480(18)	C(17)-C(16)-N(1)	115.33(11)
Cl(9)-C(81)	1.736(3)	C(18)-C(17)-C(16)	119.53(12)
O(1)-C(2)	1.3081(16)	C(18)-C(17)-N(2)	124.75(12)
O(2)-C(24)	1.3160(16)	C(16)-C(17)-N(2)	115.72(10)
O(3)-C(39)	1.4581(17)	C(19)-C(18)-C(17)	120.57(13)
O(3)-C(37)	1.4826(18)	C(19)-C(18)-H(18)	119.7
O(4)-C(41)	1.3091(16)	C(17)-C(18)-H(18)	119.7
O(5)-C(63)	1.3037(15)	C(18)-C(19)-C(20)	119.47(12)
O(6)-C(78)	1.445(2)	C(18)-C(19)-H(19)	120.3
O(6)-C(76)	1.4558(18)	C(20)-C(19)-H(19)	120.3
N(1)-C(15)	1.3034(17)	C(21)-C(20)-C(19)	120.84(13)
N(1)-C(16)	1.4206(15)	C(21)-C(20)-H(20)	119.6
N(2)-C(22)	1.2942(18)	C(19)-C(20)-H(20)	119.6
N(2)-C(17)	1.4112(17)	C(20)-C(21)-C(16)	120.06(13)
N(3)-C(54)	1.3050(18)	C(20)-C(21)-H(21)	120
N(3)-C(55)	1.4203(18)	C(16)-C(21)-H(21)	120
N(4)-C(61)	1.2983(17)	N(2)-C(22)-C(23)	126.55(11)
N(4)-C(56)	1.4259(17)	N(2)-C(22)-H(22)	116.7
C(1)-C(6)	1.4126(19)	C(23)-C(22)-H(22)	116.7
C(1)-C(15)	1.4242(17)	C(28)-C(23)-C(22)	116.12(11)
C(1)-C(2)	1.4265(19)	C(28)-C(23)-C(24)	120.11(12)
C(2)-C(3)	1.4260(18)	C(22)-C(23)-C(24)	123.75(12)
C(3)-C(4)	1.381(2)	O(2)-C(24)-C(25)	120.00(11)

C(3)-C(7)	1.544(2)	O(2)-C(24)-C(23)	121.56(12)
C(4)-C(5)	1.402(2)	C(25)-C(24)-C(23)	118.42(12)
C(4)-H(4)	0.95	C(26)-C(25)-C(24)	117.98(11)
C(5)-C(6)	1.3665(18)	C(26)-C(25)-C(29)	121.73(12)
C(5)-C(11)	1.525(2)	C(24)-C(25)-C(29)	120.23(12)
C(6)-H(6)	0.95	C(25)-C(26)-C(27)	125.27(13)
C(7)-C(10)	1.520(2)	C(25)-C(26)-H(26)	117.4
C(7)-C(8)	1.524(2)	C(27)-C(26)-H(26)	117.4
C(7)-C(9)	1.528(2)	C(28)-C(27)-C(26)	116.06(13)
C(8)-H(8A)	0.98	C(28)-C(27)-C(33)	121.56(12)
C(8)-H(8B)	0.98	C(26)-C(27)-C(33)	122.34(13)
C(8)-H(8C)	0.98	C(27)-C(28)-C(23)	122.14(12)
C(9)-H(9A)	0.98	C(27)-C(28)-H(28)	118.9
C(9)-H(9B)	0.98	C(23)-C(28)-H(28)	118.9
C(9)-H(9C)	0.98	C(31)-C(29)-C(32)	107.66(12)
C(10)-H(10A)	0.98	C(31)-C(29)-C(30)	110.30(12)
C(10)-H(10B)	0.98	C(32)-C(29)-C(30)	107.12(12)
C(10)-H(10C)	0.98	C(31)-C(29)-C(25)	108.90(12)
C(11)-C(12)	1.518(2)	C(32)-C(29)-C(25)	111.70(12)
C(11)-C(13)	1.523(2)	C(30)-C(29)-C(25)	111.10(12)
C(11)-C(14)	1.529(2)	C(29)-C(30)-H(30A)	109.5
C(12)-H(12A)	0.98	C(29)-C(30)-H(30B)	109.5
C(12)-H(12B)	0.98	H(30A)-C(30)-H(30B)	109.5
C(12)-H(12C)	0.98	C(29)-C(30)-H(30C)	109.5
C(13)-H(13A)	0.98	H(30A)-C(30)-H(30C)	109.5
C(13)-H(13B)	0.98	H(30B)-C(30)-H(30C)	109.5
C(13)-H(13C)	0.98	C(29)-C(31)-H(31A)	109.5
C(14)-H(14A)	0.98	C(29)-C(31)-H(31B)	109.5
C(14)-H(14B)	0.98	H(31A)-C(31)-H(31B)	109.5
C(14)-H(14C)	0.98	C(29)-C(31)-H(31C)	109.5
C(15)-H(15)	0.95	H(31A)-C(31)-H(31C)	109.5
C(16)-C(21)	1.3866(19)	H(31B)-C(31)-H(31C)	109.5
C(16)-C(17)	1.4023(18)	C(29)-C(32)-H(32A)	109.5
C(17)-C(18)	1.3922(17)	C(29)-C(32)-H(32B)	109.5
C(18)-C(19)	1.375(2)	H(32A)-C(32)-H(32B)	109.5
C(18)-H(18)	0.95	C(29)-C(32)-H(32C)	109.5
C(19)-C(20)	1.387(2)	H(32A)-C(32)-H(32C)	109.5
C(19)-H(19)	0.95	H(32B)-C(32)-H(32C)	109.5
C(20)-C(21)	1.3779(18)	C(36)-C(33)-C(35)	109.56(14)
C(20)-H(20)	0.95	C(36)-C(33)-C(27)	111.67(13)

C(21)-H(21)	0.95	C(35)-C(33)-C(27)	112.19(12)
C(22)-C(23)	1.4287(19)	C(36)-C(33)-C(34)	107.19(13)
C(22)-H(22)	0.95	C(35)-C(33)-C(34)	108.58(16)
C(23)-C(28)	1.4057(19)	C(27)-C(33)-C(34)	107.46(12)
C(23)-C(24)	1.4298(17)	C(33)-C(34)-H(34A)	109.5
C(24)-C(25)	1.4178(19)	C(33)-C(34)-H(34B)	109.5
C(25)-C(26)	1.377(2)	H(34A)-C(34)-H(34B)	109.5
C(25)-C(29)	1.5353(18)	C(33)-C(34)-H(34C)	109.5
C(26)-C(27)	1.4074(18)	H(34A)-C(34)-H(34C)	109.5
C(26)-H(26)	0.95	H(34B)-C(34)-H(34C)	109.5
C(27)-C(28)	1.377(2)	C(33)-C(35)-H(35A)	109.5
C(27)-C(33)	1.531(2)	C(33)-C(35)-H(35B)	109.5
C(28)-H(28)	0.95	H(35A)-C(35)-H(35B)	109.5
C(29)-C(31)	1.519(2)	C(33)-C(35)-H(35C)	109.5
C(29)-C(32)	1.531(2)	H(35A)-C(35)-H(35C)	109.5
C(29)-C(30)	1.531(2)	H(35B)-C(35)-H(35C)	109.5
C(30)-H(30A)	0.98	C(33)-C(36)-H(36A)	109.5
C(30)-H(30B)	0.98	C(33)-C(36)-H(36B)	109.5
C(30)-H(30C)	0.98	H(36A)-C(36)-H(36B)	109.5
C(31)-H(31A)	0.98	C(33)-C(36)-H(36C)	109.5
C(31)-H(31B)	0.98	H(36A)-C(36)-H(36C)	109.5
C(31)-H(31C)	0.98	H(36B)-C(36)-H(36C)	109.5
C(32)-H(32A)	0.98	O(3)-C(37)-C(38)	90.54(11)
C(32)-H(32B)	0.98	O(3)-C(37)-H(37A)	113.5
C(32)-H(32C)	0.98	C(38)-C(37)-H(37A)	113.5
C(33)-C(36)	1.498(2)	O(3)-C(37)-H(37B)	113.5
C(33)-C(35)	1.515(3)	C(38)-C(37)-H(37B)	113.5
C(33)-C(34)	1.552(3)	H(37A)-C(37)-H(37B)	110.8
C(34)-H(34A)	0.98	C(39)-C(38)-C(37)	86.79(11)
C(34)-H(34B)	0.98	C(39)-C(38)-H(38A)	114.2
C(34)-H(34C)	0.98	C(37)-C(38)-H(38A)	114.2
C(35)-H(35A)	0.98	C(39)-C(38)-H(38B)	114.2
C(35)-H(35B)	0.98	C(37)-C(38)-H(38B)	114.2
C(35)-H(35C)	0.98	H(38A)-C(38)-H(38B)	111.3
C(36)-H(36A)	0.98	O(3)-C(39)-C(38)	91.55(11)
C(36)-H(36B)	0.98	O(3)-C(39)-H(39A)	113.4
C(36)-H(36C)	0.98	C(38)-C(39)-H(39A)	113.4
C(37)-C(38)	1.516(2)	O(3)-C(39)-H(39B)	113.4
C(37)-H(37A)	0.99	C(38)-C(39)-H(39B)	113.4
C(37)-H(37B)	0.99	H(39A)-C(39)-H(39B)	110.7

C(38)-C(39)	1.514(2)	C(54)-C(40)-C(45)	116.23(12)
C(38)-H(38A)	0.99	C(54)-C(40)-C(41)	124.18(12)
C(38)-H(38B)	0.99	C(45)-C(40)-C(41)	119.55(13)
C(39)-H(39A)	0.99	O(4)-C(41)-C(40)	122.12(12)
C(39)-H(39B)	0.99	O(4)-C(41)-C(42)	119.42(12)
C(40)-C(54)	1.417(2)	C(40)-C(41)-C(42)	118.44(12)
C(40)-C(45)	1.4184(19)	C(43)-C(42)-C(41)	118.01(13)
C(40)-C(41)	1.4229(19)	C(43)-C(42)-C(46)	121.73(13)
C(41)-C(42)	1.431(2)	C(41)-C(42)-C(46)	120.25(12)
C(42)-C(43)	1.372(2)	C(42)-C(43)-C(44)	124.81(14)
C(42)-C(46)	1.545(2)	C(42)-C(43)-H(43)	117.6
C(43)-C(44)	1.404(2)	C(44)-C(43)-H(43)	117.6
C(43)-H(43)	0.95	C(45)-C(44)-C(43)	116.88(13)
C(44)-C(45)	1.361(2)	C(45)-C(44)-C(50)	123.90(13)
C(44)-C(50)	1.525(2)	C(43)-C(44)-C(50)	119.16(13)
C(45)-H(45)	0.95	C(44)-C(45)-C(40)	122.26(13)
C(46)-C(49)	1.527(2)	C(44)-C(45)-H(45)	118.9
C(46)-C(48)	1.529(2)	C(40)-C(45)-H(45)	118.9
C(46)-C(47)	1.531(2)	C(49)-C(46)-C(48)	107.82(13)
C(47)-H(47A)	0.98	C(49)-C(46)-C(47)	107.62(12)
C(47)-H(47B)	0.98	C(48)-C(46)-C(47)	109.82(12)
C(47)-H(47C)	0.98	C(49)-C(46)-C(42)	111.42(12)
C(48)-H(48A)	0.98	C(48)-C(46)-C(42)	108.96(12)
C(48)-H(48B)	0.98	C(47)-C(46)-C(42)	111.13(13)
C(48)-H(48C)	0.98	C(46)-C(47)-H(47A)	109.5
C(49)-H(49A)	0.98	C(46)-C(47)-H(47B)	109.5
C(49)-H(49B)	0.98	H(47A)-C(47)-H(47B)	109.5
C(49)-H(49C)	0.98	C(46)-C(47)-H(47C)	109.5
C(50)-C(53)	1.509(3)	H(47A)-C(47)-H(47C)	109.5
C(50)-C(51)	1.521(3)	H(47B)-C(47)-H(47C)	109.5
C(50)-C(52)	1.528(3)	C(46)-C(48)-H(48A)	109.5
C(51)-H(51A)	0.98	C(46)-C(48)-H(48B)	109.5
C(51)-H(51B)	0.98	H(48A)-C(48)-H(48B)	109.5
C(51)-H(51C)	0.98	C(46)-C(48)-H(48C)	109.5
C(52)-H(52A)	0.98	H(48A)-C(48)-H(48C)	109.5
C(52)-H(52B)	0.98	H(48B)-C(48)-H(48C)	109.5
C(52)-H(52C)	0.98	C(46)-C(49)-H(49A)	109.5
C(53)-H(53A)	0.98	C(46)-C(49)-H(49B)	109.5
C(53)-H(53B)	0.98	H(49A)-C(49)-H(49B)	109.5
C(53)-H(53C)	0.98	C(46)-C(49)-H(49C)	109.5

C(54)-H(54)	0.95	H(49A)-C(49)-H(49C)	109.5
C(55)-C(60)	1.3905(19)	H(49B)-C(49)-H(49C)	109.5
C(55)-C(56)	1.3978(19)	C(53)-C(50)-C(51)	107.28(15)
C(56)-C(57)	1.382(2)	C(53)-C(50)-C(44)	111.49(13)
C(57)-C(58)	1.372(2)	C(51)-C(50)-C(44)	111.96(13)
C(57)-H(57)	0.95	C(53)-C(50)-C(52)	109.46(15)
C(58)-C(59)	1.381(2)	C(51)-C(50)-C(52)	108.46(15)
C(58)-H(58)	0.95	C(44)-C(50)-C(52)	108.14(14)
C(59)-C(60)	1.387(2)	C(50)-C(51)-H(51A)	109.5
C(59)-H(59)	0.95	C(50)-C(51)-H(51B)	109.5
C(60)-H(60)	0.95	H(51A)-C(51)-H(51B)	109.5
C(61)-C(62)	1.4197(19)	C(50)-C(51)-H(51C)	109.5
C(61)-H(61)	0.95	H(51A)-C(51)-H(51C)	109.5
C(62)-C(67)	1.4099(19)	H(51B)-C(51)-H(51C)	109.5
C(62)-C(63)	1.4322(19)	C(50)-C(52)-H(52A)	109.5
C(63)-C(64)	1.4185(19)	C(50)-C(52)-H(52B)	109.5
C(64)-C(65)	1.3779(19)	H(52A)-C(52)-H(52B)	109.5
C(64)-C(68)	1.542(2)	C(50)-C(52)-H(52C)	109.5
C(65)-C(66)	1.410(2)	H(52A)-C(52)-H(52C)	109.5
C(65)-H(65)	0.95	H(52B)-C(52)-H(52C)	109.5
C(66)-C(67)	1.370(2)	C(50)-C(53)-H(53A)	109.5
C(66)-C(72)	1.525(2)	C(50)-C(53)-H(53B)	109.5
C(67)-H(67)	0.95	H(53A)-C(53)-H(53B)	109.5
C(68)-C(70)	1.522(2)	C(50)-C(53)-H(53C)	109.5
C(68)-C(71)	1.527(2)	H(53A)-C(53)-H(53C)	109.5
C(68)-C(69)	1.533(2)	H(53B)-C(53)-H(53C)	109.5
C(69)-H(69A)	0.98	N(3)-C(54)-C(40)	126.58(13)
C(69)-H(69B)	0.98	N(3)-C(54)-H(54)	116.7
C(69)-H(69C)	0.98	C(40)-C(54)-H(54)	116.7
C(70)-H(70A)	0.98	C(60)-C(55)-C(56)	118.88(13)
C(70)-H(70B)	0.98	C(60)-C(55)-N(3)	124.74(12)
C(70)-H(70C)	0.98	C(56)-C(55)-N(3)	116.38(12)
C(71)-H(71A)	0.98	C(57)-C(56)-C(55)	120.46(13)
C(71)-H(71B)	0.98	C(57)-C(56)-N(4)	124.47(12)
C(71)-H(71C)	0.98	C(55)-C(56)-N(4)	115.07(12)
C(72)-C(75)	1.469(3)	C(58)-C(57)-C(56)	120.16(14)
C(72)-C(74)	1.469(3)	C(58)-C(57)-H(57)	119.9
C(72)-C(73)	1.499(3)	C(56)-C(57)-H(57)	119.9
C(73)-H(73A)	0.98	C(57)-C(58)-C(59)	119.93(15)
C(73)-H(73B)	0.98	C(57)-C(58)-H(58)	120

C(73)-H(73C)	0.98	C(59)-C(58)-H(58)	120
C(74)-H(74A)	0.98	C(58)-C(59)-C(60)	120.58(14)
C(74)-H(74B)	0.98	C(58)-C(59)-H(59)	119.7
C(74)-H(74C)	0.98	C(60)-C(59)-H(59)	119.7
C(75)-H(75A)	0.98	C(59)-C(60)-C(55)	119.82(14)
C(75)-H(75B)	0.98	C(59)-C(60)-H(60)	120.1
C(75)-H(75C)	0.98	C(55)-C(60)-H(60)	120.1
C(76)-C(77)	1.505(2)	N(4)-C(61)-C(62)	126.08(13)
C(76)-H(76A)	0.99	N(4)-C(61)-H(61)	117
C(76)-H(76B)	0.99	C(62)-C(61)-H(61)	117
C(77)-C(78)	1.512(2)	C(67)-C(62)-C(61)	116.26(13)
C(77)-H(77A)	0.99	C(67)-C(62)-C(63)	119.87(12)
C(77)-H(77B)	0.99	C(61)-C(62)-C(63)	123.84(12)
C(78)-H(78A)	0.99	O(5)-C(63)-C(64)	120.07(12)
C(78)-H(78B)	0.99	O(5)-C(63)-C(62)	121.76(12)
C(79)-H(79A)	0.99	C(64)-C(63)-C(62)	118.14(12)
C(79)-H(79B)	0.99	C(65)-C(64)-C(63)	118.23(13)
C(80)-H(80A)	0.99	C(65)-C(64)-C(68)	122.07(13)
C(80)-H(80B)	0.99	C(63)-C(64)-C(68)	119.69(12)
C(81)-H(81A)	0.99	C(64)-C(65)-C(66)	125.14(14)
C(81)-H(81B)	0.99	C(64)-C(65)-H(65)	117.4
C(83)-C(84)	1.328(5)	C(66)-C(65)-H(65)	117.4
C(83)-H(83A)	0.98	C(67)-C(66)-C(65)	115.96(13)
C(83)-H(83B)	0.98	C(67)-C(66)-C(72)	122.15(14)
C(83)-H(83C)	0.98	C(65)-C(66)-C(72)	121.85(14)
C(84)-C(85)	1.685(6)	C(66)-C(67)-C(62)	122.57(14)
C(84)-H(84A)	0.99	C(66)-C(67)-H(67)	118.7
C(84)-H(84B)	0.99	C(62)-C(67)-H(67)	118.7
C(85)-C(86)	1.295(8)	C(70)-C(68)-C(71)	107.66(14)
C(85)-H(85A)	0.99	C(70)-C(68)-C(69)	109.97(12)
C(85)-H(85B)	0.99	C(71)-C(68)-C(69)	107.08(12)
C(86)-C(87)	1.666(9)	C(70)-C(68)-C(64)	109.58(12)
C(86)-H(86A)	0.99	C(71)-C(68)-C(64)	112.16(12)
C(86)-H(86B)	0.99	C(69)-C(68)-C(64)	110.32(13)
C(87)-H(87A)	0.98	C(68)-C(69)-H(69A)	109.5
C(87)-H(87B)	0.98	C(68)-C(69)-H(69B)	109.5
C(87)-H(87C)	0.98	H(69A)-C(69)-H(69B)	109.5
		C(68)-C(69)-H(69C)	109.5
O(1)-Cr(1)-O(2)	95.58(4)	H(69A)-C(69)-H(69C)	109.5
O(1)-Cr(1)-N(1)	91.43(4)	H(69B)-C(69)-H(69C)	109.5

O(2)-Cr(1)-N(1)	170.39(4)	C(68)-C(70)-H(70A)	109.5
O(1)-Cr(1)-N(2)	171.74(4)	C(68)-C(70)-H(70B)	109.5
O(2)-Cr(1)-N(2)	90.88(4)	H(70A)-C(70)-H(70B)	109.5
N(1)-Cr(1)-N(2)	81.59(4)	C(68)-C(70)-H(70C)	109.5
O(1)-Cr(1)-O(3)	88.80(4)	H(70A)-C(70)-H(70C)	109.5
O(2)-Cr(1)-O(3)	87.23(4)	H(70B)-C(70)-H(70C)	109.5
N(1)-Cr(1)-O(3)	86.33(5)	C(68)-C(71)-H(71A)	109.5
N(2)-Cr(1)-O(3)	86.38(4)	C(68)-C(71)-H(71B)	109.5
O(1)-Cr(1)-Cl(1)	94.82(3)	H(71A)-C(71)-H(71B)	109.5
O(2)-Cr(1)-Cl(1)	93.55(4)	C(68)-C(71)-H(71C)	109.5
N(1)-Cr(1)-Cl(1)	92.42(4)	H(71A)-C(71)-H(71C)	109.5
N(2)-Cr(1)-Cl(1)	89.89(4)	H(71B)-C(71)-H(71C)	109.5
O(3)-Cr(1)-Cl(1)	176.20(3)	C(75)-C(72)-C(74)	108.5(2)
O(4)-Cr(2)-O(5)	95.62(4)	C(75)-C(72)-C(73)	107.6(3)
O(4)-Cr(2)-N(3)	91.49(4)	C(74)-C(72)-C(73)	107.92(19)
O(5)-Cr(2)-N(3)	171.08(5)	C(75)-C(72)-C(66)	110.86(15)
O(4)-Cr(2)-N(4)	171.61(4)	C(74)-C(72)-C(66)	112.73(15)
O(5)-Cr(2)-N(4)	90.36(5)	C(73)-C(72)-C(66)	109.15(16)
N(3)-Cr(2)-N(4)	82.03(5)	C(72)-C(73)-H(73A)	109.5
O(4)-Cr(2)-O(6)	89.11(4)	C(72)-C(73)-H(73B)	109.5
O(5)-Cr(2)-O(6)	87.34(4)	H(73A)-C(73)-H(73B)	109.5
N(3)-Cr(2)-O(6)	87.39(5)	C(72)-C(73)-H(73C)	109.5
N(4)-Cr(2)-O(6)	85.29(4)	H(73A)-C(73)-H(73C)	109.5
O(4)-Cr(2)-Cl(2)	94.88(3)	H(73B)-C(73)-H(73C)	109.5
O(5)-Cr(2)-Cl(2)	93.72(4)	C(72)-C(74)-H(74A)	109.5
N(3)-Cr(2)-Cl(2)	91.04(4)	C(72)-C(74)-H(74B)	109.5
N(4)-Cr(2)-Cl(2)	90.59(3)	H(74A)-C(74)-H(74B)	109.5
O(6)-Cr(2)-Cl(2)	175.75(3)	C(72)-C(74)-H(74C)	109.5
C(2)-O(1)-Cr(1)	131.13(8)	H(74A)-C(74)-H(74C)	109.5
C(24)-O(2)-Cr(1)	128.71(8)	H(74B)-C(74)-H(74C)	109.5
C(39)-O(3)-C(37)	90.13(10)	C(72)-C(75)-H(75A)	109.5
C(39)-O(3)-Cr(1)	128.35(9)	C(72)-C(75)-H(75B)	109.5
C(37)-O(3)-Cr(1)	126.95(7)	H(75A)-C(75)-H(75B)	109.5
C(41)-O(4)-Cr(2)	130.85(9)	C(72)-C(75)-H(75C)	109.5
C(63)-O(5)-Cr(2)	129.90(8)	H(75A)-C(75)-H(75C)	109.5
C(78)-O(6)-C(76)	90.08(11)	H(75B)-C(75)-H(75C)	109.5
C(78)-O(6)-Cr(2)	127.32(8)	O(6)-C(76)-C(77)	90.75(11)
C(76)-O(6)-Cr(2)	130.93(10)	O(6)-C(76)-H(76A)	113.5
C(15)-N(1)-C(16)	121.62(11)	C(77)-C(76)-H(76A)	113.5
C(15)-N(1)-Cr(1)	124.81(8)	O(6)-C(76)-H(76B)	113.5

C(16)-N(1)-Cr(1)	113.57(8)	C(77)-C(76)-H(76B)	113.5
C(22)-N(2)-C(17)	122.61(10)	H(76A)-C(76)-H(76B)	110.8
C(22)-N(2)-Cr(1)	123.74(9)	C(76)-C(77)-C(78)	85.72(12)
C(17)-N(2)-Cr(1)	113.41(8)	C(76)-C(77)-H(77A)	114.4
C(54)-N(3)-C(55)	122.75(11)	C(78)-C(77)-H(77A)	114.4
C(54)-N(3)-Cr(2)	124.30(9)	C(76)-C(77)-H(77B)	114.4
C(55)-N(3)-Cr(2)	112.94(8)	C(78)-C(77)-H(77B)	114.4
C(61)-N(4)-C(56)	122.11(12)	H(77A)-C(77)-H(77B)	111.5
C(61)-N(4)-Cr(2)	124.10(10)	O(6)-C(78)-C(77)	90.88(12)
C(56)-N(4)-Cr(2)	113.20(8)	O(6)-C(78)-H(78A)	113.5
C(6)-C(1)-C(15)	115.77(12)	C(77)-C(78)-H(78A)	113.5
C(6)-C(1)-C(2)	119.80(11)	O(6)-C(78)-H(78B)	113.5
C(15)-C(1)-C(2)	124.22(12)	C(77)-C(78)-H(78B)	113.5
O(1)-C(2)-C(3)	119.67(12)	H(78A)-C(78)-H(78B)	110.8
O(1)-C(2)-C(1)	121.94(11)	Cl(3)-C(79)-Cl(4)	111.74(9)
C(3)-C(2)-C(1)	118.39(12)	Cl(3)-C(79)-H(79A)	109.3
C(4)-C(3)-C(2)	117.65(13)	Cl(4)-C(79)-H(79A)	109.3
C(4)-C(3)-C(7)	122.29(12)	Cl(3)-C(79)-H(79B)	109.3
C(2)-C(3)-C(7)	120.06(12)	Cl(4)-C(79)-H(79B)	109.3
C(3)-C(4)-C(5)	125.44(12)	H(79A)-C(79)-H(79B)	107.9
C(3)-C(4)-H(4)	117.3	Cl(7)-C(80)-Cl(6)	110.63(10)
C(5)-C(4)-H(4)	117.3	Cl(7)-C(80)-H(80A)	109.5
C(6)-C(5)-C(4)	116.16(13)	Cl(6)-C(80)-H(80A)	109.5
C(6)-C(5)-C(11)	123.68(13)	Cl(7)-C(80)-H(80B)	109.5
C(4)-C(5)-C(11)	120.06(12)	Cl(6)-C(80)-H(80B)	109.5
C(5)-C(6)-C(1)	122.55(13)	H(80A)-C(80)-H(80B)	108.1
C(5)-C(6)-H(6)	118.7	Cl(9)-C(81)-Cl(5)	111.48(15)
C(1)-C(6)-H(6)	118.7	Cl(9)-C(81)-H(81A)	109.3
C(10)-C(7)-C(8)	107.31(13)	Cl(5)-C(81)-H(81A)	109.3
C(10)-C(7)-C(9)	108.12(13)	Cl(9)-C(81)-H(81B)	109.3
C(8)-C(7)-C(9)	109.84(13)	Cl(5)-C(81)-H(81B)	109.3
C(10)-C(7)-C(3)	111.65(13)	H(81A)-C(81)-H(81B)	108
C(8)-C(7)-C(3)	111.25(12)	C(84)-C(83)-H(83A)	106.8
C(9)-C(7)-C(3)	108.62(12)	C(84)-C(83)-H(83B)	114.2
C(7)-C(8)-H(8A)	109.5	H(83A)-C(83)-H(83B)	109.5
C(7)-C(8)-H(8B)	109.5	C(84)-C(83)-H(83C)	107.4
H(8A)-C(8)-H(8B)	109.5	H(83A)-C(83)-H(83C)	109.5
C(7)-C(8)-H(8C)	109.5	H(83B)-C(83)-H(83C)	109.5
H(8A)-C(8)-H(8C)	109.5	C(83)-C(84)-C(85)	95.1(3)
H(8B)-C(8)-H(8C)	109.5	C(83)-C(84)-H(84A)	112.7

C(7)-C(9)-H(9A)	109.5	C(85)-C(84)-H(84A)	112.7
C(7)-C(9)-H(9B)	109.5	C(83)-C(84)-H(84B)	112.7
H(9A)-C(9)-H(9B)	109.5	C(85)-C(84)-H(84B)	112.7
C(7)-C(9)-H(9C)	109.5	H(84A)-C(84)-H(84B)	110.2
H(9A)-C(9)-H(9C)	109.5	C(86)-C(85)-C(84)	124.9(5)
H(9B)-C(9)-H(9C)	109.5	C(86)-C(85)-H(85A)	106.1
C(7)-C(10)-H(10A)	109.5	C(84)-C(85)-H(85A)	106.1
C(7)-C(10)-H(10B)	109.5	C(86)-C(85)-H(85B)	106.1
H(10A)-C(10)-H(10B)	109.5	C(84)-C(85)-H(85B)	106.1
C(7)-C(10)-H(10C)	109.5	H(85A)-C(85)-H(85B)	106.3
H(10A)-C(10)-H(10C)	109.5	C(85)-C(86)-C(87)	110.0(5)
H(10B)-C(10)-H(10C)	109.5	C(85)-C(86)-H(86A)	109.7
C(12)-C(11)-C(13)	108.62(13)	C(87)-C(86)-H(86A)	109.7
C(12)-C(11)-C(5)	111.21(13)	C(85)-C(86)-H(86B)	109.7
C(13)-C(11)-C(5)	111.07(12)	C(87)-C(86)-H(86B)	109.7
C(12)-C(11)-C(14)	108.58(12)	H(86A)-C(86)-H(86B)	108.2
C(13)-C(11)-C(14)	108.72(15)	C(86)-C(87)-H(87A)	111.7
C(5)-C(11)-C(14)	108.58(13)	C(86)-C(87)-H(87B)	113.2
C(11)-C(12)-H(12A)	109.5	H(87A)-C(87)-H(87B)	109.5
C(11)-C(12)-H(12B)	109.5	C(86)-C(87)-H(87C)	103.4
H(12A)-C(12)-H(12B)	109.5	H(87A)-C(87)-H(87C)	109.5
C(11)-C(12)-H(12C)	109.5	H(87B)-C(87)-H(87C)	109.5
H(12A)-C(12)-H(12C)	109.5	H(12B)-C(12)-H(12C)	109.5
		C(11)-C(13)-H(13A)	109.5

Table B-5. Crystal Data and Structure Refinement for Complex **III-3**.

Identification code	sadm	
Empirical formula	C47 H72 Cl4 Cr N3 O4	
Formula weight	936.88	
Temperature	110(2) K	
Wavelength	0.71073 Å	
Crystal system	Triclinic	
Space group	P-1	
Unit cell dimensions	a = 13.039(3) Å	α= 93.050(3)°.
	b = 13.372(3) Å	β= 101.587(3)°.
	c = 14.703(3) Å	γ = 104.698(3)°.
Volume	2414.4(9) $Å^3$	
Z	2	
Density (calculated)	1.289 Mg/m^3	
Absorption coefficient	0.502 mm^{-1}	
F(000)	998	
Crystal size	0.14 x 0.08 x 0.06 mm^3	
Theta range for data collection	1.66 to 28.72°.	
Index ranges	-17<=h<=17, -17<=k<=17, -19<=l<=19	
Reflections collected	28288	
Independent reflections	11323 [R(int) = 0.0454]	
Completeness to theta = 28.72°	90.60%	
Absorption correction	Semi-empirical from equivalents	
Max. and min. transmission	0.9705 and 0.9330	
Refinement method	Full-matrix least-squares on F_2	
Data / restraints / parameters	11323 / 0 / 544	
Goodness-of-fit on F_2	1.001	
Final R indices [I>2sigma(I)]	R1 = 0.0452, wR2 = 0.1152	
R indices (all data)	R1 = 0.0706, wR2 = 0.1311	
Largest diff. peak and hole	0.736 and -0.663 $e.Å^{-3}$	

Table B-6. Bond Distances (Å) and Bond Angles (deg) for Complex **III-3**.

Cr(1)-O(1)	1.9145(15)	C(12)-O(1)-Cr(1)	130.03(13)
Cr(1)-O(2)	1.9220(15)	C(21)-O(2)-Cr(1)	129.58(13)
Cr(1)-N(1)	2.0016(17)	C(4)-O(3)-C(5)	115.91(17)
Cr(1)-N(2)	2.0189(17)	C(28)-O(4)-C(29)	116.67(18)
Cr(1)-Cl(1)	2.3236(7)	C(1)-N(1)-C(18)	121.60(17)
Cr(1)-Cl(2)	2.3959(7)	C(1)-N(1)-Cr(1)	124.58(14)
Cl(3)-C(47)	1.749(3)	C(18)-N(1)-Cr(1)	113.68(13)
Cl(4)-C(47)	1.763(3)	C(19)-N(2)-C(13)	122.59(18)
O(1)-C(12)	1.302(2)	C(19)-N(2)-Cr(1)	124.41(14)
O(2)-C(21)	1.293(2)	C(13)-N(2)-Cr(1)	112.98(13)
O(3)-C(4)	1.380(3)	C(31)-N(3)-C(39)	106.83(16)
O(3)-C(5)	1.414(3)	C(31)-N(3)-C(35)	110.14(17)
O(4)-C(28)	1.381(3)	C(39)-N(3)-C(35)	111.01(17)
O(4)-C(29)	1.389(3)	C(31)-N(3)-C(43)	111.46(17)
N(1)-C(1)	1.305(3)	C(39)-N(3)-C(43)	110.31(17)
N(1)-C(18)	1.421(2)	C(35)-N(3)-C(43)	107.15(16)
N(2)-C(19)	1.290(3)	N(1)-C(1)-C(2)	126.32(19)
N(2)-C(13)	1.428(3)	C(1)-C(2)-C(3)	115.37(18)
N(3)-C(31)	1.514(3)	C(1)-C(2)-C(12)	123.91(19)
N(3)-C(39)	1.518(3)	C(3)-C(2)-C(12)	120.72(18)
N(3)-C(35)	1.520(3)	C(4)-C(3)-C(2)	119.83(19)
N(3)-C(43)	1.520(3)	C(3)-C(4)-O(3)	125.45(19)
C(1)-C(2)	1.421(3)	C(3)-C(4)-C(6)	119.6(2)
C(2)-C(3)	1.422(3)	O(3)-C(4)-C(6)	114.92(18)
C(2)-C(12)	1.423(3)	C(7)-C(6)-C(4)	123.20(19)
C(3)-C(4)	1.362(3)	C(6)-C(7)-C(12)	118.38(19)
C(4)-C(6)	1.405(3)	C(6)-C(7)-C(8)	121.60(19)
C(6)-C(7)	1.372(3)	C(12)-C(7)-C(8)	120.01(18)
C(7)-C(12)	1.439(3)	C(7)-C(8)-C(9)	111.87(18)
C(7)-C(8)	1.532(3)	C(7)-C(8)-C(11)	109.03(18)
C(8)-C(9)	1.536(3)	C(9)-C(8)-C(11)	108.48(18)
C(8)-C(11)	1.537(3)	C(7)-C(8)-C(10)	111.18(17)
C(8)-C(10)	1.540(3)	C(9)-C(8)-C(10)	106.91(18)
C(13)-C(14)	1.392(3)	C(11)-C(8)-C(10)	109.29(19)
C(13)-C(18)	1.401(3)	O(1)-C(12)-C(2)	122.92(18)
C(14)-C(15)	1.383(3)	O(1)-C(12)-C(7)	118.85(18)
C(15)-C(16)	1.386(3)	C(2)-C(12)-C(7)	118.21(18)
C(16)-C(17)	1.377(3)	C(14)-C(13)-C(18)	120.14(19)
C(17)-C(18)	1.403(3)	C(14)-C(13)-N(2)	124.40(19)

C(19)-C(20)	1.441(3)	C(18)-C(13)-N(2)	115.44(17)
C(20)-C(30)	1.415(3)	C(15)-C(14)-C(13)	119.8(2)
C(20)-C(21)	1.426(3)	C(14)-C(15)-C(16)	120.2(2)
C(21)-C(22)	1.437(3)	C(17)-C(16)-C(15)	120.7(2)
C(22)-C(27)	1.383(3)	C(16)-C(17)-C(18)	119.8(2)
C(22)-C(23)	1.538(3)	C(13)-C(18)-C(17)	119.20(18)
C(23)-C(26)	1.532(3)	C(13)-C(18)-N(1)	115.80(18)
C(23)-C(24)	1.539(3)	C(17)-C(18)-N(1)	125.00(19)
C(23)-C(25)	1.541(3)	N(2)-C(19)-C(20)	126.0(2)
C(27)-C(28)	1.401(3)	C(30)-C(20)-C(21)	120.45(19)
C(28)-C(30)	1.364(3)	C(30)-C(20)-C(19)	115.13(19)
C(31)-C(32)	1.518(3)	C(21)-C(20)-C(19)	124.27(19)
C(32)-C(33)	1.521(3)	O(2)-C(21)-C(20)	122.87(19)
C(33)-C(34)	1.516(4)	O(2)-C(21)-C(22)	119.18(18)
C(35)-C(36)	1.521(3)	C(20)-C(21)-C(22)	117.95(19)
C(36)-C(37)	1.521(3)	C(27)-C(22)-C(21)	119.00(19)
C(37)-C(38)	1.515(3)	C(27)-C(22)-C(23)	121.55(19)
C(39)-C(40)	1.516(3)	C(21)-C(22)-C(23)	119.39(18)
C(40)-C(41)	1.520(3)	C(26)-C(23)-C(22)	111.74(18)
C(41)-C(42)	1.517(3)	C(26)-C(23)-C(24)	107.00(18)
C(43)-C(44)	1.512(3)	C(22)-C(23)-C(24)	110.51(18)
C(44)-C(45)	1.523(3)	C(26)-C(23)-C(25)	107.97(18)
C(45)-C(46)	1.514(3)	C(22)-C(23)-C(25)	110.00(17)
		C(24)-C(23)-C(25)	109.52(19)
O(1)-Cr(1)-O(2)	94.33(6)	C(22)-C(27)-C(28)	122.4(2)
O(1)-Cr(1)-N(1)	91.69(6)	C(30)-C(28)-O(4)	117.35(19)
O(2)-Cr(1)-N(1)	173.75(6)	C(30)-C(28)-C(27)	119.7(2)
O(1)-Cr(1)-N(2)	173.59(6)	O(4)-C(28)-C(27)	122.88(19)
O(2)-Cr(1)-N(2)	92.05(7)	C(28)-C(30)-C(20)	120.5(2)
N(1)-Cr(1)-N(2)	81.91(7)	N(3)-C(31)-C(32)	115.54(18)
O(1)-Cr(1)-Cl(1)	92.63(5)	C(31)-C(32)-C(33)	111.2(2)
O(2)-Cr(1)-Cl(1)	92.19(5)	C(34)-C(33)-C(32)	113.4(2)
N(1)-Cr(1)-Cl(1)	89.21(5)	N(3)-C(35)-C(36)	116.01(18)
N(2)-Cr(1)-Cl(1)	87.70(5)	C(37)-C(36)-C(35)	110.97(19)
O(1)-Cr(1)-Cl(2)	91.60(5)	C(38)-C(37)-C(36)	112.8(2)
O(2)-Cr(1)-Cl(2)	89.05(5)	C(40)-C(39)-N(3)	116.21(18)
N(1)-Cr(1)-Cl(2)	89.10(5)	C(39)-C(40)-C(41)	110.66(19)
N(2)-Cr(1)-Cl(2)	87.92(5)	C(42)-C(41)-C(40)	114.1(2)
Cl(1)-Cr(1)-Cl(2)	175.49(2)	C(44)-C(43)-N(3)	115.27(18)
C(46)-C(45)-C(44)	110.7(2)	C(43)-C(44)-C(45)	111.0(2)

Cl(3)-C(47)-Cl(4)	111.74(15)

Table B-7. Crystal Data and Structure Refinement for Complex **III-4**.

Identification code	am3	
Empirical formula	C46 H70 Cr N9 O4	
Formula weight	865.11	
Temperature	110(2) K	
Wavelength	0.71073 Å	
Crystal system	Orthorhombic	
Space group	Pnna	
Unit cell dimensions	a = 10.6226(10) Å	α= 90°.
	b = 25.105(2) Å	β= 90°.
	c = 17.2567(17) Å	γ = 90°.
Volume	4602.0(7) $Å^3$	
Z	4	
Density (calculated)	1.249 Mg/m^3	
Absorption coefficient	0.301 mm^{-1}	
F(000)	1860	
Crystal size	0.12 x 0.06 x 0.03 mm^3	
Theta range for data collection	2.39 to 28.34°.	
Index ranges	-14<=h<=13, -33<=k<=33, -21<=l<=23	
Reflections collected	42139	
Independent reflections	5632 [R(int) = 0.0986]	
Completeness to theta = 28.34°	97.90%	
Absorption correction	Semi-empirical from equivalents	
Max. and min. transmission	0.9919 and 0.9648	
Refinement method	Full-matrix least-squares on F_2	
Data / restraints / parameters	5632 / 0 / 278	
Goodness-of-fit on F_2	1	
Final R indices [I>2sigma(I)]	R1 = 0.0822, wR2 = 0.2018	
R indices (all data)	R1 = 0.2139, wR2 = 0.2536	
Largest diff. peak and hole	0.819 and -0.262 $e.Å^{-3}$	

Table B-8. Bond Distances (Å) and Bond Angles (deg) for Complex **III-4**.

Cr(1)-O(1)#1	1.915(3)	N(4)-Cr(1)-N(1)#1	91.24(16)
Cr(1)-O(1)	1.915(3)	O(1)#1-Cr(1)-N(1)	89.49(15)
Cr(1)-N(4)#1	2.007(4)	O(1)-Cr(1)-N(1)	91.86(15)
Cr(1)-N(4)	2.007(4)	N(4)#1-Cr(1)-N(1)	91.24(16)
Cr(1)-N(1)#1	2.050(4)	N(4)-Cr(1)-N(1)	87.24(16)
Cr(1)-N(1)	2.050(4)	N(1)#1-Cr(1)-N(1)	178.0(2)
O(1)-C(12)	1.309(4)	C(12)-O(1)-Cr(1)	130.3(3)
O(2)-C(4)	1.383(5)	C(4)-O(2)-C(5)	117.9(5)
O(2)-C(5)	1.403(7)	N(2)-N(1)-Cr(1)	128.8(3)
N(1)-N(2)	1.174(5)	N(3)-N(2)-N(1)	177.0(4)
N(2)-N(3)	1.168(6)	C(1)-N(4)-C(13)	122.0(4)
N(4)-C(1)	1.294(6)	C(1)-N(4)-Cr(1)	124.5(3)
N(4)-C(13)	1.418(5)	C(13)-N(4)-Cr(1)	113.3(3)
N(5)-C(20)#2	1.509(5)	C(20)#2-N(5)-C(20)	111.1(5)
N(5)-C(20)	1.509(5)	C(20)#2-N(5)-C(16)	112.6(2)
N(5)-C(16)	1.525(5)	C(20)-N(5)-C(16)	105.4(2)
N(5)-C(16)#2	1.525(5)	C(20)#2-N(5)-C(16)#2	105.4(2)
C(1)-C(2)	1.432(6)	C(20)-N(5)-C(16)#2	112.6(2)
C(2)-C(3)	1.405(6)	C(16)-N(5)-C(16)#2	109.8(5)
C(2)-C(12)	1.429(6)	N(4)-C(1)-C(2)	126.3(4)
C(3)-C(4)	1.375(7)	C(3)-C(2)-C(12)	120.5(5)
C(4)-C(6)	1.385(6)	C(3)-C(2)-C(1)	115.4(5)
C(6)-C(7)	1.379(5)	C(12)-C(2)-C(1)	123.9(4)
C(7)-C(12)	1.440(5)	C(4)-C(3)-C(2)	119.5(5)
C(7)-C(8)	1.527(5)	C(3)-C(4)-O(2)	123.2(5)
C(8)-C(9)	1.533(5)	C(3)-C(4)-C(6)	120.4(4)
C(8)-C(10)	1.535(5)	O(2)-C(4)-C(6)	116.3(5)
C(8)-C(11)	1.550(5)	C(7)-C(6)-C(4)	123.2(5)
C(13)-C(13)#1	1.386(9)	C(6)-C(7)-C(12)	117.7(4)
C(13)-C(14)	1.388(6)	C(6)-C(7)-C(8)	122.9(4)
C(14)-C(15)	1.393(7)	C(12)-C(7)-C(8)	119.3(3)
C(15)-C(15)#1	1.314(13)	C(7)-C(8)-C(9)	111.4(3)
C(16)-C(17)	1.499(6)	C(7)-C(8)-C(10)	110.0(3)
C(17)-C(18)	1.529(6)	C(9)-C(8)-C(10)	107.1(4)
C(18)-C(19)	1.497(7)	C(7)-C(8)-C(11)	111.3(3)
C(20)-C(21)	1.511(6)	C(9)-C(8)-C(11)	107.6(3)
C(21)-C(22)	1.432(9)	C(10)-C(8)-C(11)	109.3(3)
C(22)-C(23)	1.393(8)	O(1)-C(12)-C(2)	122.4(4)
		O(1)-C(12)-C(7)	118.8(4)

O(1)#1-Cr(1)-O(1)	95.22(16)	C(2)-C(12)-C(7)	118.7(4)
O(1)#1-Cr(1)-N(4)#1	91.68(14)	C(13)#1-C(13)-C(14)	119.2(3)
O(1)-Cr(1)-N(4)#1	172.46(13)	C(13)#1-C(13)-N(4)	115.8(2)
O(1)#1-Cr(1)-N(4)	172.46(13)	C(14)-C(13)-N(4)	124.9(5)
O(1)-Cr(1)-N(4)	91.67(14)	C(13)-C(14)-C(15)	120.0(6)
N(4)#1-Cr(1)-N(4)	81.6(2)	C(15)#1-C(15)-C(14)	120.7(3)
O(1)#1-Cr(1)-N(1)#1	91.86(15)	C(17)-C(16)-N(5)	117.2(3)
O(1)-Cr(1)-N(1)#1	89.49(15)	C(16)-C(17)-C(18)	109.4(4)
N(4)#1-Cr(1)-N(1)#1	87.24(16)	C(19)-C(18)-C(17)	114.2(4)
C(22)-C(21)-C(20)	112.6(5)	N(5)-C(20)-C(21)	115.0(4)
		C(23)-C(22)-C(21)	113.7(7)

Table B-9. Crystal Data and Structure Refinement for Complex **III-5**.

Identification code	salencrcn2	
Empirical formula	C71 H70 Cl6 Cr N5 O4 P2	
Formula weight	1383.96	
Temperature	110(2) K	
Wavelength	1.54178 Å	
Crystal system	Triclinic	
Space group	P-1	
Unit cell dimensions	a = 12.104(3) Å	α= 66.377(15)°.
	b = 16.019(4) Å	β= 80.31(2)°.
	c = 19.970(7) Å	γ = 79.034(17)°.
Volume	3464.4(18) $Å^3$	
Z	2	
Density (calculated)	1.327 Mg/m^3	
Absorption coefficient	4.330 mm^{-1}	
F(000)	1438	
Crystal size	0.32 x 0.07 x 0.03 mm^3	
Theta range for data collection	2.43 to 58.93°.	
Index ranges	-13<=h<=13, -17<=k<=17, -22<=l<=22	
Reflections collected	24726	
Independent reflections	9069 [R(int) = 0.0606]	
Completeness to theta = 58.93°	91.10%	
Absorption correction	Semi-empirical from equivalents	
Max. and min. transmission	0.8811 and 0.3379	
Refinement method	Full-matrix least-squares on F_2	
Data / restraints / parameters	9069 / 0 / 810	
Goodness-of-fit on F_2	1	
Final R indices [I>2sigma(I)]	R1 = 0.0843, wR2 = 0.2478	
R indices (all data)	R1 = 0.1344, wR2 = 0.3210	
Largest diff. peak and hole	1.346 and -1.077 $e.Å^{-3}$	

Table B-10. Bond Distances (Å) and Bond Angles (deg) for Complex **III-5**.

Cr(1)-O(2)	1.907(5)	N(4)-P(2)-C(38)	111.3(3)
Cr(1)-O(1)	1.919(4)	N(4)-P(2)-C(32)	108.6(3)
Cr(1)-N(2)	2.017(6)	C(38)-P(2)-C(32)	107.1(3)
Cr(1)-N(3)	2.026(5)	N(4)-P(2)-C(44)	113.6(3)
Cr(1)-C(1A)	2.104(9)	C(38)-P(2)-C(44)	109.0(3)
Cr(1)-C(1B)	2.126(10)	C(32)-P(2)-C(44)	107.0(4)
P(1)-N(4)	1.564(6)	C(13)-O(1)-Cr(1)	130.8(5)
P(1)-C(62)	1.786(8)	C(22)-O(2)-Cr(1)	130.1(4)
P(1)-C(50)	1.796(9)	C(5)-O(3)-C(6)	116.5(5)
P(1)-C(56)	1.806(7)	C(29)-O(4)-C(30)	117.1(6)
P(2)-N(4)	1.595(6)	C(2)-N(2)-C(19)	121.9(6)
P(2)-C(38)	1.791(8)	C(2)-N(2)-Cr(1)	124.8(5)
P(2)-C(32)	1.802(9)	C(19)-N(2)-Cr(1)	113.1(4)
P(2)-C(44)	1.808(7)	C(20)-N(3)-C(14)	122.5(6)
Cl(1)-C(69)	1.765(10)	C(20)-N(3)-Cr(1)	123.5(5)
Cl(2)-C(69)	1.775(10)	C(14)-N(3)-Cr(1)	113.9(4)
Cl(3)-C(68)	1.759(9)	P(1)-N(4)-P(2)	140.3(4)
Cl(4)-C(68)	1.738(10)	N(1A)-C(1A)-Cr(1)	177.8(6)
Cl(5)-C(70)	1.767(9)	N(1B)-C(1B)-Cr(1)	176.9(7)
Cl(6)-C(70)	1.756(9)	N(2)-C(2)-C(3)	125.8(7)
O(1)-C(13)	1.308(9)	C(4)-C(3)-C(13)	122.1(6)
O(2)-C(22)	1.313(7)	C(4)-C(3)-C(2)	113.7(7)
O(3)-C(5)	1.377(8)	C(13)-C(3)-C(2)	124.0(6)
O(3)-C(6)	1.420(9)	C(5)-C(4)-C(3)	119.0(7)
O(4)-C(29)	1.385(8)	C(4)-C(5)-O(3)	125.8(7)
O(4)-C(30)	1.426(9)	C(4)-C(5)-C(7)	119.6(7)
N(1A)-C(1A)	1.155(10)	O(3)-C(5)-C(7)	114.6(6)
N(1B)-C(1B)	1.144(10)	C(8)-C(7)-C(5)	123.0(6)
N(2)-C(2)	1.308(8)	C(7)-C(8)-C(13)	118.4(7)
N(2)-C(19)	1.425(9)	C(7)-C(8)-C(9)	121.8(6)
N(3)-C(20)	1.307(9)	C(13)-C(8)-C(9)	119.7(6)
N(3)-C(14)	1.410(9)	C(12)-C(9)-C(10)	108.3(7)
C(2)-C(3)	1.447(10)	C(12)-C(9)-C(11)	110.0(7)
C(3)-C(4)	1.413(10)	C(10)-C(9)-C(11)	107.2(7)
C(3)-C(13)	1.418(11)	C(12)-C(9)-C(8)	109.9(7)
C(4)-C(5)	1.367(10)	C(10)-C(9)-C(8)	111.4(6)
C(5)-C(7)	1.421(11)	C(11)-C(9)-C(8)	110.0(6)
C(7)-C(8)	1.369(10)	O(1)-C(13)-C(3)	122.9(6)
C(8)-C(13)	1.443(10)	O(1)-C(13)-C(8)	119.5(7)

C(8)-C(9)	1.544(11)	C(3)-C(13)-C(8)	117.7(7)
C(9)-C(12)	1.533(11)	C(19)-C(14)-C(15)	119.8(7)
C(9)-C(10)	1.537(10)	C(19)-C(14)-N(3)	115.4(6)
C(9)-C(11)	1.540(12)	C(15)-C(14)-N(3)	124.8(6)
C(14)-C(19)	1.393(9)	C(16)-C(15)-C(14)	118.9(7)
C(14)-C(15)	1.409(9)	C(17)-C(16)-C(15)	120.8(7)
C(15)-C(16)	1.382(11)	C(18)-C(17)-C(16)	121.7(8)
C(16)-C(17)	1.379(10)	C(17)-C(18)-C(19)	118.7(7)
C(17)-C(18)	1.362(10)	C(14)-C(19)-C(18)	120.0(6)
C(18)-C(19)	1.418(11)	C(14)-C(19)-N(2)	116.3(6)
C(20)-C(21)	1.444(11)	C(18)-C(19)-N(2)	123.6(6)
C(21)-C(31)	1.402(10)	N(3)-C(20)-C(21)	127.3(6)
C(21)-C(22)	1.434(10)	C(31)-C(21)-C(22)	122.0(6)
C(22)-C(23)	1.436(10)	C(31)-C(21)-C(20)	115.0(6)
C(23)-C(28)	1.379(9)	C(22)-C(21)-C(20)	123.1(6)
C(23)-C(24)	1.541(10)	O(2)-C(22)-C(21)	123.0(6)
C(24)-C(25)	1.526(11)	O(2)-C(22)-C(23)	119.8(6)
C(24)-C(27)	1.534(11)	C(21)-C(22)-C(23)	117.2(6)
C(24)-C(26)	1.547(11)	C(28)-C(23)-C(22)	118.7(7)
C(28)-C(29)	1.398(10)	C(28)-C(23)-C(24)	121.0(7)
C(29)-C(31)	1.370(11)	C(22)-C(23)-C(24)	120.3(6)
C(32)-C(37)	1.373(11)	C(25)-C(24)-C(27)	108.0(6)
C(32)-C(33)	1.403(10)	C(25)-C(24)-C(23)	109.9(7)
C(33)-C(34)	1.351(11)	C(27)-C(24)-C(23)	111.7(6)
C(34)-C(35)	1.401(11)	C(25)-C(24)-C(26)	110.4(6)
C(35)-C(36)	1.388(11)	C(27)-C(24)-C(26)	107.3(7)
C(36)-C(37)	1.376(12)	C(23)-C(24)-C(26)	109.5(6)
C(38)-C(39)	1.362(11)	C(23)-C(28)-C(29)	122.9(7)
C(38)-C(43)	1.387(12)	C(31)-C(29)-O(4)	123.9(6)
C(39)-C(40)	1.370(14)	C(31)-C(29)-C(28)	120.0(6)
C(40)-C(41)	1.367(14)	O(4)-C(29)-C(28)	116.1(7)
C(41)-C(42)	1.347(12)	C(29)-C(31)-C(21)	119.2(6)
C(42)-C(43)	1.389(12)	C(37)-C(32)-C(33)	119.9(8)
C(44)-C(45)	1.378(11)	C(37)-C(32)-P(2)	121.2(6)
C(44)-C(49)	1.392(10)	C(33)-C(32)-P(2)	118.8(6)
C(45)-C(46)	1.405(11)	C(34)-C(33)-C(32)	119.8(8)
C(46)-C(47)	1.390(12)	C(33)-C(34)-C(35)	121.0(7)
C(47)-C(48)	1.379(13)	C(36)-C(35)-C(34)	118.8(8)
C(48)-C(49)	1.390(11)	C(37)-C(36)-C(35)	120.3(8)
C(50)-C(55)	1.375(12)	C(32)-C(37)-C(36)	120.2(7)

C(50)-C(51)	1.411(11)	C(39)-C(38)-C(43)	118.2(8)
C(51)-C(52)	1.390(12)	C(39)-C(38)-P(2)	122.4(7)
C(52)-C(53)	1.355(13)	C(43)-C(38)-P(2)	119.4(6)
C(53)-C(54)	1.389(13)	C(38)-C(39)-C(40)	120.4(9)
C(54)-C(55)	1.402(12)	C(41)-C(40)-C(39)	120.7(9)
C(56)-C(61)	1.366(11)	C(42)-C(41)-C(40)	120.8(9)
C(56)-C(57)	1.390(10)	C(41)-C(42)-C(43)	118.5(9)
C(57)-C(58)	1.396(11)	C(38)-C(43)-C(42)	121.4(8)
C(58)-C(59)	1.371(13)	C(45)-C(44)-C(49)	121.4(7)
C(59)-C(60)	1.385(12)	C(45)-C(44)-P(2)	117.5(5)
C(60)-C(61)	1.395(11)	C(49)-C(44)-P(2)	121.1(6)
C(62)-C(67)	1.379(11)	C(44)-C(45)-C(46)	119.7(7)
C(62)-C(63)	1.408(11)	C(47)-C(46)-C(45)	118.5(8)
C(63)-C(64)	1.378(12)	C(48)-C(47)-C(46)	121.6(8)
C(64)-C(65)	1.384(13)	C(47)-C(48)-C(49)	119.8(7)
C(65)-C(66)	1.371(12)	C(48)-C(49)-C(44)	119.0(8)
C(66)-C(67)	1.392(12)	C(55)-C(50)-C(51)	118.5(8)
		C(55)-C(50)-P(1)	121.5(6)
O(2)-Cr(1)-O(1)	95.0(2)	C(51)-C(50)-P(1)	119.6(7)
O(2)-Cr(1)-N(2)	173.5(2)	C(52)-C(51)-C(50)	119.5(9)
O(1)-Cr(1)-N(2)	91.5(2)	C(53)-C(52)-C(51)	120.3(8)
O(2)-Cr(1)-N(3)	92.3(2)	C(52)-C(53)-C(54)	122.2(8)
O(1)-Cr(1)-N(3)	172.7(2)	C(53)-C(54)-C(55)	117.1(10)
N(2)-Cr(1)-N(3)	81.2(2)	C(50)-C(55)-C(54)	122.3(8)
O(2)-Cr(1)-C(1A)	90.4(3)	C(61)-C(56)-C(57)	120.6(7)
O(1)-Cr(1)-C(1A)	92.9(2)	C(61)-C(56)-P(1)	119.6(6)
N(2)-Cr(1)-C(1A)	89.6(3)	C(57)-C(56)-P(1)	119.8(6)
N(3)-Cr(1)-C(1A)	87.4(2)	C(56)-C(57)-C(58)	120.0(8)
O(2)-Cr(1)-C(1B)	92.1(2)	C(59)-C(58)-C(57)	119.1(8)
O(1)-Cr(1)-C(1B)	90.3(2)	C(58)-C(59)-C(60)	120.9(7)
N(2)-Cr(1)-C(1B)	87.5(2)	C(59)-C(60)-C(61)	119.9(8)
N(3)-Cr(1)-C(1B)	89.1(2)	C(56)-C(61)-C(60)	119.5(8)
C(1A)-Cr(1)-C(1B)	175.8(3)	C(67)-C(62)-C(63)	119.6(8)
N(4)-P(1)-C(62)	113.0(4)	C(67)-C(62)-P(1)	118.5(6)
N(4)-P(1)-C(50)	114.8(3)	C(63)-C(62)-P(1)	121.6(7)
C(62)-P(1)-C(50)	108.0(4)	C(64)-C(63)-C(62)	119.5(8)
N(4)-P(1)-C(56)	106.1(3)	C(63)-C(64)-C(65)	119.9(8)
C(62)-P(1)-C(56)	105.9(3)	C(66)-C(65)-C(64)	121.4(9)
C(50)-P(1)-C(56)	108.7(4)	C(65)-C(66)-C(67)	118.9(9)
Cl(1)-C(69)-Cl(2)	111.0(5)	C(62)-C(67)-C(66)	120.7(8)

Cl(6)-C(70)-Cl(5)	111.4(5)	Cl(4)-C(68)-Cl(3)	113.0(5)

Table B-11. Crystal Data and Structure Refinement for Complex **III-6**.

Identification code	data0m	
Empirical formula	C70 H68 Cl4 Cr N5 O6 P2	
Formula weight	1331.03	
Temperature	110(2) K	
Wavelength	1.54178 Å	
Crystal system	Triclinic	
Space group	P-1	
Unit cell dimensions	a = 11.961(2) Å	α= 68.179(10)°.
	b = 15.876(3) Å	β= 79.346(12)°.
	c = 18.842(4) Å	γ = 88.643(11)°.
Volume	3260.5(11) $Å^3$	
Z	2	
Density (calculated)	1.356 Mg/m^3	
Absorption coefficient	3.867 mm^{-1}	
F(000)	1386	
Crystal size	0.44 x 0.03 x 0.02 mm^3	
Theta range for data collection	2.57 to 61.32°.	
Index ranges	-13<=h<=12, -17<=k<=17, -21<=l<=21	
Reflections collected	25681	
Independent reflections	9249 [R(int) = 0.0409]	
Completeness to theta = 61.32°	91.80%	
Absorption correction	Semi-empirical from equivalents	
Max. and min. transmission	0.9267 and 0.2810	
Refinement method	Full-matrix least-squares on F_2	
Data / restraints / parameters	9249 / 0 / 801	
Goodness-of-fit on F_2	1	
Final R indices [I>2sigma(I)]	R1 = 0.0504, wR2 = 0.1663	
R indices (all data)	R1 = 0.0657, wR2 = 0.2110	
Largest diff. peak and hole	0.736 and -0.791 $e.Å^{-3}$	

Table B-12. Bond Distances (Å) and Bond Angles (deg) for Complex **III-6**.

Cr(1)-O(2)	1.926(3)	C(56)-P(2)-C(50)	108.47(17)
Cr(1)-O(3)	1.928(3)	N(4)-P(2)-C(62)	111.63(17)
Cr(1)-N(1B)	2.016(4)	C(56)-P(2)-C(62)	106.24(17)
Cr(1)-N(3)	2.020(3)	C(50)-P(2)-C(62)	107.74(17)
Cr(1)-N(2)	2.023(3)	C(13)-O(2)-Cr(1)	129.7(2)
Cr(1)-N(1A)	2.025(3)	C(22)-O(3)-Cr(1)	131.1(2)
P(1)-N(4)	1.586(3)	C(5)-O(4)-C(6)	115.9(3)
P(1)-C(44)	1.802(4)	C(29)-O(5)-C(30)	117.4(3)
P(1)-C(32)	1.804(4)	C(1A)-N(1A)-Cr(1)	162.1(3)
P(1)-C(38)	1.805(4)	C(1B)-N(1B)-Cr(1)	162.4(3)
P(2)-N(4)	1.579(3)	C(2)-N(2)-C(19)	122.0(3)
P(2)-C(56)	1.806(4)	C(2)-N(2)-Cr(1)	124.5(3)
P(2)-C(50)	1.808(4)	C(19)-N(2)-Cr(1)	113.4(2)
P(2)-C(62)	1.813(4)	C(20)-N(3)-C(14)	122.2(3)
Cl(1)-C(68)	1.763(5)	C(20)-N(3)-Cr(1)	124.6(2)
Cl(2)-C(68)	1.755(5)	C(14)-N(3)-Cr(1)	113.2(2)
Cl(3)-C(69)	1.759(6)	P(2)-N(4)-P(1)	139.7(2)
Cl(4)-C(69)	1.775(5)	N(1A)-C(1A)-O(1A)	177.0(5)
O(1A)-C(1A)	1.210(5)	N(1B)-C(1B)-O(1B)	176.6(5)
O(1B)-C(1B)	1.206(5)	N(2)-C(2)-C(3)	126.5(3)
O(2)-C(13)	1.317(4)	C(4)-C(3)-C(2)	114.9(3)
O(3)-C(22)	1.297(4)	C(4)-C(3)-C(13)	120.4(3)
O(4)-C(5)	1.388(4)	C(2)-C(3)-C(13)	124.6(3)
O(4)-C(6)	1.426(5)	C(5)-C(4)-C(3)	120.1(3)
O(5)-C(29)	1.394(5)	C(4)-C(5)-O(4)	124.8(3)
O(5)-C(30)	1.411(5)	C(4)-C(5)-C(7)	119.5(3)
N(1A)-C(1A)	1.173(5)	O(4)-C(5)-C(7)	115.6(3)
N(1B)-C(1B)	1.164(5)	C(8)-C(7)-C(5)	123.2(3)
N(2)-C(2)	1.296(5)	C(7)-C(8)-C(13)	118.1(3)
N(2)-C(19)	1.432(5)	C(7)-C(8)-C(9)	121.2(3)
N(3)-C(20)	1.308(5)	C(13)-C(8)-C(9)	120.7(3)
N(3)-C(14)	1.431(5)	C(10)-C(9)-C(8)	111.7(3)
C(2)-C(3)	1.423(5)	C(10)-C(9)-C(12)	108.0(3)
C(3)-C(4)	1.422(5)	C(8)-C(9)-C(12)	109.1(3)
C(3)-C(13)	1.424(5)	C(10)-C(9)-C(11)	107.0(3)
C(4)-C(5)	1.360(5)	C(8)-C(9)-C(11)	111.2(3)
C(5)-C(7)	1.406(5)	C(12)-C(9)-C(11)	109.8(3)
C(7)-C(8)	1.379(5)	O(2)-C(13)-C(3)	122.6(3)
C(8)-C(13)	1.435(5)	O(2)-C(13)-C(8)	118.8(3)

C(8)-C(9)	1.540(5)	C(3)-C(13)-C(8)	118.5(3)
C(9)-C(10)	1.532(6)	C(15)-C(14)-C(19)	119.3(3)
C(9)-C(12)	1.542(6)	C(15)-C(14)-N(3)	124.6(3)
C(9)-C(11)	1.549(6)	C(19)-C(14)-N(3)	116.1(3)
C(14)-C(15)	1.390(5)	C(16)-C(15)-C(14)	119.9(3)
C(14)-C(19)	1.411(5)	C(15)-C(16)-C(17)	120.7(3)
C(15)-C(16)	1.382(5)	C(16)-C(17)-C(18)	119.9(3)
C(16)-C(17)	1.391(5)	C(19)-C(18)-C(17)	119.5(3)
C(17)-C(18)	1.396(5)	C(18)-C(19)-C(14)	120.6(3)
C(18)-C(19)	1.380(5)	C(18)-C(19)-N(2)	124.1(3)
C(20)-C(21)	1.429(5)	C(14)-C(19)-N(2)	115.3(3)
C(21)-C(31)	1.424(5)	N(3)-C(20)-C(21)	126.7(3)
C(21)-C(22)	1.435(5)	C(31)-C(21)-C(20)	116.0(3)
C(22)-C(23)	1.439(5)	C(31)-C(21)-C(22)	120.4(3)
C(23)-C(28)	1.377(5)	C(20)-C(21)-C(22)	123.6(3)
C(23)-C(24)	1.537(6)	O(3)-C(22)-C(21)	122.6(3)
C(24)-C(27)	1.535(6)	O(3)-C(22)-C(23)	119.0(3)
C(24)-C(26)	1.537(6)	C(21)-C(22)-C(23)	118.3(3)
C(24)-C(25)	1.554(6)	C(28)-C(23)-C(22)	117.9(4)
C(28)-C(29)	1.399(6)	C(28)-C(23)-C(24)	122.6(3)
C(29)-C(31)	1.358(6)	C(22)-C(23)-C(24)	119.4(3)
C(32)-C(37)	1.386(5)	C(27)-C(24)-C(23)	111.2(3)
C(32)-C(33)	1.402(5)	C(27)-C(24)-C(26)	109.2(3)
C(33)-C(34)	1.369(6)	C(23)-C(24)-C(26)	108.5(3)
C(34)-C(35)	1.371(6)	C(27)-C(24)-C(25)	107.3(3)
C(35)-C(36)	1.381(6)	C(23)-C(24)-C(25)	110.9(3)
C(36)-C(37)	1.393(5)	C(26)-C(24)-C(25)	109.8(4)
C(38)-C(43)	1.393(5)	C(23)-C(28)-C(29)	123.6(4)
C(38)-C(39)	1.396(5)	C(31)-C(29)-O(5)	125.5(4)
C(43)-C(42)	1.387(6)	C(31)-C(29)-C(28)	119.9(4)
C(42)-C(41)	1.388(6)	O(5)-C(29)-C(28)	114.5(3)
C(41)-C(40)	1.378(6)	C(29)-C(31)-C(21)	119.9(4)
C(40)-C(39)	1.385(6)	C(37)-C(32)-C(33)	119.4(4)
C(44)-C(45)	1.383(5)	C(37)-C(32)-P(1)	118.3(3)
C(44)-C(49)	1.392(5)	C(33)-C(32)-P(1)	121.6(3)
C(49)-C(48)	1.391(6)	C(34)-C(33)-C(32)	119.9(4)
C(48)-C(47)	1.377(6)	C(33)-C(34)-C(35)	120.8(4)
C(47)-C(46)	1.407(6)	C(34)-C(35)-C(36)	120.2(4)
C(46)-C(45)	1.387(6)	C(35)-C(36)-C(37)	119.9(4)
C(62)-C(63)	1.390(5)	C(32)-C(37)-C(36)	119.8(4)

C(62)-C(67)	1.395(5)	C(43)-C(38)-C(39)	119.4(4)
C(67)-C(66)	1.384(6)	C(43)-C(38)-P(1)	120.0(3)
C(66)-C(65)	1.375(6)	C(39)-C(38)-P(1)	120.5(3)
C(65)-C(64)	1.392(6)	C(42)-C(43)-C(38)	120.2(4)
C(64)-C(63)	1.394(6)	C(43)-C(42)-C(41)	119.5(4)
C(50)-C(55)	1.388(5)	C(40)-C(41)-C(42)	121.0(4)
C(50)-C(51)	1.399(5)	C(41)-C(40)-C(39)	119.5(4)
C(55)-C(54)	1.398(6)	C(40)-C(39)-C(38)	120.4(4)
C(54)-C(53)	1.374(6)	C(45)-C(44)-C(49)	120.8(3)
C(53)-C(52)	1.382(6)	C(45)-C(44)-P(1)	118.4(3)
C(52)-C(51)	1.385(6)	C(49)-C(44)-P(1)	120.4(3)
C(56)-C(61)	1.384(6)	C(48)-C(49)-C(44)	118.8(4)
C(56)-C(57)	1.392(5)	C(47)-C(48)-C(49)	121.5(4)
C(57)-C(58)	1.377(6)	C(48)-C(47)-C(46)	118.9(4)
C(58)-C(59)	1.388(6)	C(45)-C(46)-C(47)	120.2(4)
C(59)-C(60)	1.388(6)	C(44)-C(45)-C(46)	119.7(4)
C(60)-C(61)	1.385(5)	C(63)-C(62)-C(67)	120.7(4)
		C(63)-C(62)-P(2)	120.0(3)
O(2)-Cr(1)-O(3)	95.15(11)	C(67)-C(62)-P(2)	119.4(3)
O(2)-Cr(1)-N(1B)	89.58(12)	C(66)-C(67)-C(62)	119.2(4)
O(3)-Cr(1)-N(1B)	90.73(13)	C(65)-C(66)-C(67)	120.2(4)
O(2)-Cr(1)-N(3)	173.62(11)	C(66)-C(65)-C(64)	121.3(4)
O(3)-Cr(1)-N(3)	91.11(12)	C(65)-C(64)-C(63)	118.8(4)
N(1B)-Cr(1)-N(3)	89.14(12)	C(62)-C(63)-C(64)	119.9(4)
O(2)-Cr(1)-N(2)	91.76(12)	C(55)-C(50)-C(51)	119.8(4)
O(3)-Cr(1)-N(2)	173.08(12)	C(55)-C(50)-P(2)	122.8(3)
N(1B)-Cr(1)-N(2)	88.87(13)	C(51)-C(50)-P(2)	117.1(3)
N(3)-Cr(1)-N(2)	81.98(12)	C(50)-C(55)-C(54)	119.8(4)
O(2)-Cr(1)-N(1A)	92.26(12)	C(53)-C(54)-C(55)	119.6(4)
O(3)-Cr(1)-N(1A)	90.26(12)	C(54)-C(53)-C(52)	121.1(4)
N(1B)-Cr(1)-N(1A)	177.83(13)	C(53)-C(52)-C(51)	119.7(4)
N(3)-Cr(1)-N(1A)	88.90(13)	C(52)-C(51)-C(50)	119.9(4)
N(2)-Cr(1)-N(1A)	89.92(13)	C(61)-C(56)-C(57)	119.7(4)
N(4)-P(1)-C(44)	108.51(17)	C(61)-C(56)-P(2)	118.7(3)
N(4)-P(1)-C(32)	114.84(17)	C(57)-C(56)-P(2)	121.3(3)
C(44)-P(1)-C(32)	110.00(17)	C(58)-C(57)-C(56)	120.6(4)
N(4)-P(1)-C(38)	110.15(17)	C(57)-C(58)-C(59)	119.5(4)
C(44)-P(1)-C(38)	105.97(16)	C(58)-C(59)-C(60)	120.0(4)
C(32)-P(1)-C(38)	107.00(17)	C(61)-C(60)-C(59)	120.3(4)
N(4)-P(2)-C(56)	107.98(17)	C(56)-C(61)-C(60)	119.8(4)

N(4)-P(2)-C(50)	114.43(17)	Cl(2)-C(68)-Cl(1)	110.9(3)
		Cl(3)-C(69)-Cl(4)	111.8(3)

Table B-13. Crystal Data and Structure Refinement for Complex **III-7**.

Identification code	dda	
Empirical formula	C67.50 H67 Cl3 Cr N6 O4 P	
Formula weight	1215.59	
Temperature	110(2) K	
Wavelength	1.54184 Å	
Crystal system	Triclinic	
Space group	P-1	
Unit cell dimensions	a = 12.447(2) Å	α= 70.026(8)°.
	b = 15.076(2) Å	β= 82.558(9)°.
	c = 18.509(3) Å	γ = 79.978(9)°.
Volume	3205.3(9) $Å^3$	
Z	2	
Density (calculated)	1.260 Mg/m^3	
Absorption coefficient	3.261 mm^{-1}	
F(000)	1272	
Crystal size	0.46 x 0.12 x 0.02 mm^3	
Theta range for data collection	4.66 to 59.99°.	
Index ranges	-12<=h<=13, -16<=k<=16, -19<=l<=20	
Reflections collected	21367	
Independent reflections	8449 [R(int) = 0.0965]	
Completeness to theta = 60.00°	89.00%	
Absorption correction	Semi-empirical from equivalents	
Max. and min. transmission	0.9376 and 0.3154	
Refinement method	Full-matrix least-squares on F_2	
Data / restraints / parameters	8449 / 565 / 821	
Goodness-of-fit on F_2	1.001	
Final R indices [I>2sigma(I)]	R1 = 0.0894, wR2 = 0.2131	
R indices (all data)	R1 = 0.1747, wR2 = 0.2716	
Largest diff. peak and hole	1.109 and -0.703 $e.Å^{-3}$	

Table B-14. Bond Distances (Å) and Bond Angles (deg) for Complex **III-7**.

Cr(1)-O(1)	1.906(6)	Cl(1A)-Cr(1)-Cl(1B)	172.9(3)
Cr(1)-O(2)	1.909(5)	N(6)-P(1)-C(61)	110.9(4)
Cr(1)-N(5)	2.001(7)	N(6)-P(1)-C(55)	107.5(4)
Cr(1)-N(1A)	2.01(2)	C(61)-P(1)-C(55)	109.7(4)
Cr(1)-N(4)	2.011(7)	N(6)-P(1)-C(49)	113.7(4)
Cr(1)-N(1B)	2.04(3)	C(61)-P(1)-C(49)	107.9(4)
Cr(1)-Cl(1A)	2.319(8)	C(55)-P(1)-C(49)	107.0(4)
Cr(1)-Cl(1B)	2.363(7)	N(6)-P(2)-C(31)	107.6(4)
P(1)-N(6)	1.565(7)	N(6)-P(2)-C(37)	114.6(4)
P(1)-C(61)	1.793(10)	C(31)-P(2)-C(37)	107.7(4)
P(1)-C(55)	1.796(9)	N(6)-P(2)-C(43)	111.3(4)
P(1)-C(49)	1.806(9)	C(31)-P(2)-C(43)	107.2(4)
P(2)-N(6)	1.574(7)	C(37)-P(2)-C(43)	108.2(4)
P(2)-C(31)	1.777(9)	C(12)-O(1)-Cr(1)	130.4(5)
P(2)-C(37)	1.797(9)	C(21)-O(2)-Cr(1)	130.6(5)
P(2)-C(43)	1.802(9)	C(5)-O(3)-C(4)	117.1(7)
Cl(2)-C(67)	1.73(2)	C(28)-O(4)-C(29)	116.7(6)
Cl(3)-C(67)	1.68(2)	N(2A)-N(1A)-Cr(1)	128.0(19)
Cl(4)-C(68)	1.678(17)	N(2B)-N(1B)-Cr(1)	119(2)
Cl(5)-C(68)	1.54(2)	N(1A)-N(2A)-N(3A)	173.6(16)
O(1)-C(12)	1.304(9)	N(3B)-N(2B)-N(1B)	174(3)
O(2)-C(21)	1.327(9)	C(1)-N(4)-C(18)	123.4(7)
O(3)-C(5)	1.410(10)	C(1)-N(4)-Cr(1)	124.7(6)
O(3)-C(4)	1.412(10)	C(18)-N(4)-Cr(1)	111.8(5)
O(4)-C(28)	1.380(10)	C(19)-N(5)-C(13)	122.5(7)
O(4)-C(29)	1.424(10)	C(19)-N(5)-Cr(1)	125.2(5)
N(1A)-N(2A)	1.212(15)	C(13)-N(5)-Cr(1)	112.2(5)
N(1B)-N(2B)	1.232(15)	P(1)-N(6)-P(2)	142.8(5)
N(2A)-N(3A)	1.218(12)	N(4)-C(1)-C(2)	126.6(8)
N(2B)-N(3B)	1.201(13)	C(12)-C(2)-C(3)	121.5(8)
N(4)-C(1)	1.303(10)	C(12)-C(2)-C(1)	122.1(7)
N(4)-C(18)	1.444(10)	C(3)-C(2)-C(1)	116.4(7)
N(5)-C(19)	1.310(10)	C(4)-C(3)-C(2)	119.1(8)
N(5)-C(13)	1.450(10)	C(3)-C(4)-C(6)	122.0(8)
C(1)-C(2)	1.456(11)	C(3)-C(4)-O(3)	125.7(8)
C(2)-C(12)	1.412(11)	C(6)-C(4)-O(3)	112.2(7)
C(2)-C(3)	1.426(12)	C(7)-C(6)-C(4)	121.5(8)
C(3)-C(4)	1.320(12)	C(6)-C(7)-C(12)	118.2(7)
C(4)-C(6)	1.397(11)	C(6)-C(7)-C(8)	121.2(7)

C(6)-C(7)	1.396(11)	C(12)-C(7)-C(8)	120.6(7)
C(7)-C(12)	1.439(11)	C(9)-C(8)-C(7)	112.1(7)
C(7)-C(8)	1.541(11)	C(9)-C(8)-C(11)	109.4(7)
C(8)-C(9)	1.524(12)	C(7)-C(8)-C(11)	109.7(7)
C(8)-C(11)	1.541(12)	C(9)-C(8)-C(10)	107.0(7)
C(8)-C(10)	1.549(12)	C(7)-C(8)-C(10)	110.1(7)
C(13)-C(18)	1.384(11)	C(11)-C(8)-C(10)	108.4(7)
C(13)-C(14)	1.395(11)	O(1)-C(12)-C(2)	124.5(7)
C(14)-C(15)	1.385(11)	O(1)-C(12)-C(7)	117.8(7)
C(15)-C(16)	1.370(12)	C(2)-C(12)-C(7)	117.7(7)
C(16)-C(17)	1.405(12)	C(18)-C(13)-C(14)	120.2(7)
C(17)-C(18)	1.397(11)	C(18)-C(13)-N(5)	116.0(7)
C(19)-C(20)	1.422(10)	C(14)-C(13)-N(5)	123.7(7)
C(20)-C(21)	1.419(11)	C(15)-C(14)-C(13)	118.7(8)
C(20)-C(30)	1.444(11)	C(16)-C(15)-C(14)	121.8(8)
C(21)-C(22)	1.441(11)	C(15)-C(16)-C(17)	119.8(8)
C(22)-C(27)	1.376(11)	C(18)-C(17)-C(16)	118.7(8)
C(22)-C(23)	1.541(12)	C(13)-C(18)-C(17)	120.7(8)
C(23)-C(25)	1.507(12)	C(13)-C(18)-N(4)	116.7(7)
C(23)-C(24)	1.537(12)	C(17)-C(18)-N(4)	122.7(7)
C(23)-C(26)	1.538(12)	N(5)-C(19)-C(20)	125.5(7)
C(27)-C(28)	1.387(11)	C(21)-C(20)-C(19)	125.0(7)
C(28)-C(30)	1.352(11)	C(21)-C(20)-C(30)	118.4(7)
C(31)-C(32)	1.391(12)	C(19)-C(20)-C(30)	116.6(7)
C(31)-C(36)	1.419(12)	O(2)-C(21)-C(20)	121.6(7)
C(32)-C(33)	1.371(12)	O(2)-C(21)-C(22)	118.6(7)
C(33)-C(34)	1.377(12)	C(20)-C(21)-C(22)	119.7(7)
C(34)-C(35)	1.395(12)	C(27)-C(22)-C(21)	116.9(7)
C(35)-C(36)	1.374(12)	C(27)-C(22)-C(23)	123.3(7)
C(37)-C(38)	1.402(12)	C(21)-C(22)-C(23)	119.8(7)
C(37)-C(42)	1.426(12)	C(25)-C(23)-C(24)	111.2(7)
C(38)-C(39)	1.391(12)	C(25)-C(23)-C(26)	106.9(7)
C(39)-C(40)	1.375(13)	C(24)-C(23)-C(26)	108.4(7)
C(40)-C(41)	1.393(13)	C(25)-C(23)-C(22)	110.5(7)
C(41)-C(42)	1.378(12)	C(24)-C(23)-C(22)	109.5(7)
C(43)-C(48)	1.367(13)	C(26)-C(23)-C(22)	110.3(7)
C(43)-C(44)	1.399(12)	C(22)-C(27)-C(28)	124.7(8)
C(44)-C(45)	1.375(13)	C(30)-C(28)-O(4)	126.1(8)
C(45)-C(46)	1.351(14)	C(30)-C(28)-C(27)	118.8(8)
C(46)-C(47)	1.395(14)	O(4)-C(28)-C(27)	115.1(7)

C(47)-C(48)	1.437(13)	C(28)-C(30)-C(20)	121.3(8)
C(49)-C(54)	1.373(13)	C(32)-C(31)-C(36)	118.0(8)
C(49)-C(50)	1.414(12)	C(32)-C(31)-P(2)	120.5(7)
C(50)-C(51)	1.387(12)	C(36)-C(31)-P(2)	121.3(6)
C(51)-C(52)	1.347(13)	C(33)-C(32)-C(31)	120.8(9)
C(52)-C(53)	1.396(13)	C(32)-C(33)-C(34)	121.0(8)
C(53)-C(54)	1.419(13)	C(33)-C(34)-C(35)	119.6(8)
C(55)-C(60)	1.378(11)	C(36)-C(35)-C(34)	119.9(9)
C(55)-C(56)	1.394(12)	C(35)-C(36)-C(31)	120.7(8)
C(56)-C(57)	1.373(13)	C(38)-C(37)-C(42)	119.9(8)
C(57)-C(58)	1.322(12)	C(38)-C(37)-P(2)	118.1(6)
C(58)-C(59)	1.405(12)	C(42)-C(37)-P(2)	121.7(7)
C(59)-C(60)	1.371(12)	C(39)-C(38)-C(37)	119.8(8)
C(61)-C(66)	1.385(13)	C(40)-C(39)-C(38)	120.7(9)
C(61)-C(62)	1.399(12)	C(39)-C(40)-C(41)	119.4(9)
C(62)-C(63)	1.420(13)	C(42)-C(41)-C(40)	122.3(8)
C(63)-C(64)	1.357(14)	C(41)-C(42)-C(37)	117.9(9)
C(64)-C(65)	1.368(14)	C(48)-C(43)-C(44)	119.2(9)
C(65)-C(66)	1.409(13)	C(48)-C(43)-P(2)	120.0(7)
		C(44)-C(43)-P(2)	120.7(8)
O(1)-Cr(1)-O(2)	93.4(2)	C(45)-C(44)-C(43)	120.9(10)
O(1)-Cr(1)-N(5)	174.8(2)	C(46)-C(45)-C(44)	119.9(10)
O(2)-Cr(1)-N(5)	91.6(2)	C(45)-C(46)-C(47)	122.4(10)
O(1)-Cr(1)-N(1A)	96.8(7)	C(46)-C(47)-C(48)	116.9(10)
O(2)-Cr(1)-N(1A)	90.9(7)	C(43)-C(48)-C(47)	120.6(10)
N(5)-Cr(1)-N(1A)	84.4(7)	C(54)-C(49)-C(50)	119.7(8)
O(1)-Cr(1)-N(4)	91.6(3)	C(54)-C(49)-P(1)	120.7(7)
O(2)-Cr(1)-N(4)	175.0(3)	C(50)-C(49)-P(1)	119.5(7)
N(5)-Cr(1)-N(4)	83.4(3)	C(51)-C(50)-C(49)	119.1(9)
N(1A)-Cr(1)-N(4)	88.7(7)	C(52)-C(51)-C(50)	121.3(9)
O(1)-Cr(1)-N(1B)	93.9(8)	C(51)-C(52)-C(53)	121.1(9)
O(2)-Cr(1)-N(1B)	90.0(9)	C(52)-C(53)-C(54)	118.5(10)
N(5)-Cr(1)-N(1B)	84.8(8)	C(49)-C(54)-C(53)	120.2(9)
N(1A)-Cr(1)-N(1B)	169.2(10)	C(60)-C(55)-C(56)	118.9(8)
N(4)-Cr(1)-N(1B)	89.5(9)	C(60)-C(55)-P(1)	121.7(7)
O(1)-Cr(1)-Cl(1A)	86.8(3)	C(56)-C(55)-P(1)	119.2(7)
O(2)-Cr(1)-Cl(1A)	91.2(3)	C(57)-C(56)-C(55)	119.7(9)
N(5)-Cr(1)-Cl(1A)	94.4(3)	C(58)-C(57)-C(56)	121.6(9)
N(1A)-Cr(1)-Cl(1A)	10.0(7)	C(57)-C(58)-C(59)	120.0(9)
N(4)-Cr(1)-Cl(1A)	89.2(3)	C(60)-C(59)-C(58)	119.4(8)

N(1B)-Cr(1)-Cl(1A)	178.5(10)	C(59)-C(60)-C(55)	120.4(8)
O(1)-Cr(1)-Cl(1B)	87.8(3)	C(66)-C(61)-C(62)	119.2(9)
O(2)-Cr(1)-Cl(1B)	93.6(3)	C(66)-C(61)-P(1)	119.2(7)
N(5)-Cr(1)-Cl(1B)	90.6(3)	C(62)-C(61)-P(1)	121.5(7)
N(1A)-Cr(1)-Cl(1B)	173.4(8)	C(61)-C(62)-C(63)	119.6(10)
N(4)-Cr(1)-Cl(1B)	86.4(3)	C(64)-C(63)-C(62)	119.7(10)
N(1B)-Cr(1)-Cl(1B)	6.9(8)	C(63)-C(64)-C(65)	121.5(10)
Cl(3)-C(67)-Cl(2)	115.3(13)	C(64)-C(65)-C(66)	119.8(10)
Cl(5)-C(68)-Cl(4)	123.7(13)	C(61)-C(66)-C(65)	120.1(10)

Table B-15. Crystal Data and Structure Refinement for Trimethylene Carbonate.

Identification code	d	
Empirical formula	C4 H6 O3	
Formula weight	102.09	
Temperature	110(2) K	
Wavelength	0.71073 Å	
Crystal system	Monoclinic	
Space group	P2(1)/n	
Unit cell dimensions	a = 6.097(6) Å	α= 90°.
	b = 11.306(11) Å	β= 102.259(11)°.
	c = 6.734(7) Å	γ = 90°.
Volume	453.6(8) $Å^3$	
Z	4	
Density (calculated)	1.495 Mg/m^3	
Absorption coefficient	0.130 mm^{-1}	
F(000)	216	
Crystal size	0.20 x 0.10 x 0.05 mm^3	
Theta range for data collection	3.58 to 24.99°.	
Index ranges	-7<=h<=7, -13<=k<=13, -7<=l<=7	
Reflections collected	3668	
Independent reflections	708 [R(int) = 0.0277]	
Completeness to theta = 24.99°	88.90%	
Absorption correction	Semi-empirical from equivalents	
Max. and min. transmission	0.9935 and 0.9745	
Refinement method	Full-matrix least-squares on F_2	
Data / restraints / parameters	708 / 0 / 64	
Goodness-of-fit on F_2	1.017	
Final R indices [I>2sigma(I)]	R1 = 0.0277, wR2 = 0.0752	
R indices (all data)	R1 = 0.0286, wR2 = 0.0761	
Largest diff. peak and hole	0.172 and -0.145 $e.Å^{-3}$	

Table B-16. Bond Distances (Å) and Bond Angles (deg) for Trimethylene Carbonate.

O(1)-C(1)	1.3296(18)	C(1)-O(1)-C(2)	122.39(10)
O(1)-C(2)	1.4545(17)	C(1)-O(2)-C(4)	120.97(10)
O(2)-C(1)	1.3297(18)	O(3)-C(1)-O(1)	119.81(11)
O(2)-C(4)	1.4575(16)	O(3)-C(1)-O(2)	119.73(12)
O(3)-C(1)	1.2056(15)	O(1)-C(1)-O(2)	120.44(9)
C(2)-C(3)	1.4910(19)	O(1)-C(2)-C(3)	110.91(11)
C(2)-H(2A)	0.99	O(1)-C(2)-H(2A)	109.5
C(2)-H(2B)	0.99	C(3)-C(2)-H(2A)	109.5
C(3)-C(4)	1.5073(18)	O(1)-C(2)-H(2B)	109.5
C(3)-H(3A)	0.99	C(3)-C(2)-H(2B)	109.5
C(3)-H(3B)	0.99	H(2A)-C(2)-H(2B)	108
C(4)-H(4A)	0.99	C(2)-C(3)-C(4)	107.47(10)
C(4)-H(4B)	0.99	C(2)-C(3)-H(3A)	110.2
C(2)-C(3)-H(3B)	110.2	C(4)-C(3)-H(3A)	110.2

Table B-17. Crystal Data and Structure Refinement for Complex **VI-1**.

Identification code	dda	
Empirical formula	C36 H46 Cl Cr N2 O6	
Formula weight	690.2	
Temperature	110(2) K	
Wavelength	1.54184 Å	
Crystal system	Monoclinic	
Space group	P2(1)/c	
Unit cell dimensions	a = 17.268(9) Å	α= 90°.
	b = 18.138(10) Å	β= 106.48(2)°.
	c = 11.499(5) Å	γ = 90°.
Volume	3453(3) $Å^3$	
Z	4	
Density (calculated)	1.327 Mg/m^3	
Absorption coefficient	3.820 mm^{-1}	
F(000)	1460	
Crystal size	0.10 x 0.10 x 0.001 mm^3	
Theta range for data collection	2.44 to 60.00°.	
Index ranges	-18<=h<=19, -19<=k<=20, -10<=l<=12	
Reflections collected	16688	
Independent reflections	4447 [R(int) = 0.2681]	
Completeness to theta = 60.00°	86.90%	
Absorption correction	Semi-empirical from equivalents	
Max. and min. transmission	0.9962 and 0.7013	
Refinement method	Full-matrix least-squares on F_2	
Data / restraints / parameters	4447 / 5 / 426	
Goodness-of-fit on F_2	0.782	
Final R indices [I>2sigma(I)]	R1 = 0.0852, wR2 = 0.1070	
R indices (all data)	R1 = 0.2433, wR2 = 0.1445	
Largest diff. peak and hole	0.119 and -0.097 $e.Å^{-3}$	

Table B-18. Bond Distances (Å) and Bond Angles (deg) for Complex **VI-1**.

Cr(1)-O(3)	1.880(5)	O(1)-C(3)-C(1)	45.2(5)
Cr(1)-O(5)	1.920(6)	C(2)-C(3)-C(1)	50.5(5)
Cr(1)-N(2)	2.012(7)	O(1)-C(3)-H(3A)	111.6
Cr(1)-N(1)	2.029(7)	C(2)-C(3)-H(3A)	114
Cr(1)-O(1)	2.056(8)	C(1)-C(3)-H(3A)	133.8
Cr(1)-Cl(1)	2.297(3)	O(1)-C(3)-H(3B)	114.1
O(1)-C(1)	1.397(9)	C(2)-C(3)-H(3B)	111.9
O(1)-C(3)	1.398(8)	C(1)-C(3)-H(3B)	115.9
O(2)-C(5)	1.278(15)	H(3A)-C(3)-H(3B)	110.2
O(2)-C(4)	1.279(15)	O(2)-C(4)-C(2)	116.9(18)
O(3)-C(18)	1.425(9)	O(2)-C(4)-H(4A)	108.1
O(4)-C(10)	1.368(13)	C(2)-C(4)-H(4A)	108.1
O(4)-C(11)	1.373(9)	O(2)-C(4)-H(4B)	108.1
O(5)-C(27)	1.333(10)	C(2)-C(4)-H(4B)	108.1
O(6)-C(34)	1.383(11)	H(4A)-C(4)-H(4B)	107.3
O(6)-C(35)	1.441(10)	O(2)-C(5)-H(5A)	109.5
N(1)-C(7)	1.292(9)	O(2)-C(5)-H(5B)	109.5
N(1)-C(24)	1.413(9)	H(5A)-C(5)-H(5B)	109.5
N(2)-C(25)	1.320(8)	O(2)-C(5)-H(5C)	109.5
N(2)-C(19)	1.392(10)	H(5A)-C(5)-H(5C)	109.5
C(1)-C(2)	1.549(10)	H(5B)-C(5)-H(5C)	109.5
C(1)-C(3)	1.969(18)	C(2)-C(6)-H(6A)	109.5
C(1)-H(1A)	0.9599	C(2)-C(6)-H(6B)	109.5
C(1)-H(1B)	0.9601	H(6A)-C(6)-H(6B)	109.5
C(2)-C(6)	1.518(16)	C(2)-C(6)-H(6C)	109.5
C(2)-C(3)	1.550(10)	H(6A)-C(6)-H(6C)	109.5
C(2)-C(4)	1.551(10)	H(6B)-C(6)-H(6C)	109.5
C(3)-H(3A)	0.9599	N(1)-C(7)-C(8)	127.5(10)
C(3)-H(3B)	0.9601	N(1)-C(7)-H(7)	116.3
C(4)-H(4A)	0.99	C(8)-C(7)-H(7)	116.3
C(4)-H(4B)	0.99	C(18)-C(8)-C(9)	120.3(9)
C(5)-H(5A)	0.98	C(18)-C(8)-C(7)	122.8(9)
C(5)-H(5B)	0.98	C(9)-C(8)-C(7)	116.4(10)
C(5)-H(5C)	0.98	C(10)-C(9)-C(8)	120.5(10)
C(6)-H(6A)	0.98	C(10)-C(9)-H(9)	119.8
C(6)-H(6B)	0.98	C(8)-C(9)-H(9)	119.8
C(6)-H(6C)	0.98	C(9)-C(10)-O(4)	125.0(10)
C(7)-C(8)	1.441(10)	C(9)-C(10)-C(12)	116.8(12)
C(7)-H(7)	0.95	O(4)-C(10)-C(12)	118.1(11)

C(8)-C(18)	1.343(12)	O(4)-C(11)-H(11A)	109.5
C(8)-C(9)	1.406(11)	O(4)-C(11)-H(11B)	109.5
C(9)-C(10)	1.361(12)	H(11A)-C(11)-H(11B)	109.5
C(9)-H(9)	0.95	O(4)-C(11)-H(11C)	109.5
C(10)-C(12)	1.424(13)	H(11A)-C(11)-H(11C)	109.5
C(11)-H(11A)	0.98	H(11B)-C(11)-H(11C)	109.5
C(11)-H(11B)	0.98	C(13)-C(12)-C(10)	124.6(10)
C(11)-H(11C)	0.98	C(13)-C(12)-H(12)	117.7
C(12)-C(13)	1.348(11)	C(10)-C(12)-H(12)	117.7
C(12)-H(12)	0.95	C(12)-C(13)-C(18)	115.0(9)
C(13)-C(18)	1.430(11)	C(12)-C(13)-C(14)	120.5(9)
C(13)-C(14)	1.620(14)	C(18)-C(13)-C(14)	124.0(9)
C(14)-C(17)	1.500(15)	C(17)-C(14)-C(15)	108.0(11)
C(14)-C(15)	1.512(12)	C(17)-C(14)-C(16)	110.6(11)
C(14)-C(16)	1.603(13)	C(15)-C(14)-C(16)	105.4(9)
C(15)-H(15A)	0.98	C(17)-C(14)-C(13)	115.4(10)
C(15)-H(15B)	0.98	C(15)-C(14)-C(13)	113.1(10)
C(15)-H(15C)	0.98	C(16)-C(14)-C(13)	104.0(10)
C(16)-H(16A)	0.98	C(14)-C(15)-H(15A)	109.5
C(16)-H(16B)	0.98	C(14)-C(15)-H(15B)	109.5
C(16)-H(16C)	0.98	H(15A)-C(15)-H(15B)	109.5
C(17)-H(17A)	0.98	C(14)-C(15)-H(15C)	109.5
C(17)-H(17B)	0.98	H(15A)-C(15)-H(15C)	109.5
C(17)-H(17C)	0.98	H(15B)-C(15)-H(15C)	109.5
C(19)-C(24)	1.364(9)	C(14)-C(16)-H(16A)	109.5
C(19)-C(20)	1.456(10)	C(14)-C(16)-H(16B)	109.5
C(20)-C(21)	1.342(12)	H(16A)-C(16)-H(16B)	109.5
C(20)-H(20)	0.95	C(14)-C(16)-H(16C)	109.5
C(21)-C(22)	1.342(11)	H(16A)-C(16)-H(16C)	109.5
C(21)-H(21)	0.95	H(16B)-C(16)-H(16C)	109.5
C(22)-C(23)	1.411(11)	C(14)-C(17)-H(17A)	109.5
C(22)-H(22)	0.95	C(14)-C(17)-H(17B)	109.5
C(23)-C(24)	1.362(11)	H(17A)-C(17)-H(17B)	109.5
C(23)-H(23)	0.95	C(14)-C(17)-H(17C)	109.5
C(25)-C(26)	1.426(11)	H(17A)-C(17)-H(17C)	109.5
C(25)-H(25)	0.95	H(17B)-C(17)-H(17C)	109.5
C(26)-C(36)	1.354(10)	C(8)-C(18)-O(3)	124.3(9)
C(26)-C(27)	1.451(12)	C(8)-C(18)-C(13)	122.0(9)
C(27)-C(28)	1.400(13)	O(3)-C(18)-C(13)	113.7(8)
C(28)-C(33)	1.369(12)	C(24)-C(19)-N(2)	121.1(8)

C(28)-C(29)	1.556(14)	C(24)-C(19)-C(20)	117.4(8)
C(29)-C(30)	1.493(14)	N(2)-C(19)-C(20)	121.6(8)
C(29)-C(31)	1.507(15)	C(21)-C(20)-C(19)	119.6(8)
C(29)-C(32)	1.585(14)	C(21)-C(20)-H(20)	120.2
C(30)-H(30A)	0.98	C(19)-C(20)-H(20)	120.2
C(30)-H(30B)	0.98	C(22)-C(21)-C(20)	122.3(9)
C(30)-H(30C)	0.98	C(22)-C(21)-H(21)	118.8
C(31)-H(31A)	0.98	C(20)-C(21)-H(21)	118.8
C(31)-H(31B)	0.98	C(21)-C(22)-C(23)	119.2(9)
C(31)-H(31C)	0.98	C(21)-C(22)-H(22)	120.4
C(32)-H(32A)	0.98	C(23)-C(22)-H(22)	120.4
C(32)-H(32B)	0.98	C(24)-C(23)-C(22)	120.0(9)
C(32)-H(32C)	0.98	C(24)-C(23)-H(23)	120
C(33)-C(34)	1.369(13)	C(22)-C(23)-H(23)	120
C(33)-H(33)	0.95	C(23)-C(24)-C(19)	121.6(8)
C(34)-C(36)	1.328(12)	C(23)-C(24)-N(1)	126.7(8)
C(35)-H(35A)	0.98	C(19)-C(24)-N(1)	111.7(8)
C(35)-H(35B)	0.98	N(2)-C(25)-C(26)	127.9(9)
C(35)-H(35C)	0.98	N(2)-C(25)-H(25)	116
C(36)-H(36)	0.95	C(26)-C(25)-H(25)	116
		C(36)-C(26)-C(25)	117.2(9)
O(3)-Cr(1)-O(5)	94.5(3)	C(36)-C(26)-C(27)	120.0(8)
O(3)-Cr(1)-N(2)	171.7(3)	C(25)-C(26)-C(27)	122.6(8)
O(5)-Cr(1)-N(2)	92.8(3)	O(5)-C(27)-C(28)	119.8(11)
O(3)-Cr(1)-N(1)	91.9(3)	O(5)-C(27)-C(26)	123.1(8)
O(5)-Cr(1)-N(1)	169.6(3)	C(28)-C(27)-C(26)	117.1(10)
N(2)-Cr(1)-N(1)	80.4(3)	C(33)-C(28)-C(27)	118.1(11)
O(3)-Cr(1)-O(1)	86.2(3)	C(33)-C(28)-C(29)	125.0(11)
O(5)-Cr(1)-O(1)	88.4(3)	C(27)-C(28)-C(29)	116.9(10)
N(2)-Cr(1)-O(1)	89.9(3)	C(30)-C(29)-C(31)	110.4(10)
N(1)-Cr(1)-O(1)	83.9(3)	C(30)-C(29)-C(28)	114.6(10)
O(3)-Cr(1)-Cl(1)	93.9(2)	C(31)-C(29)-C(28)	110.1(10)
O(5)-Cr(1)-Cl(1)	94.5(2)	C(30)-C(29)-C(32)	107.8(11)
N(2)-Cr(1)-Cl(1)	89.7(2)	C(31)-C(29)-C(32)	105.0(10)
N(1)-Cr(1)-Cl(1)	93.3(2)	C(28)-C(29)-C(32)	108.5(10)
O(1)-Cr(1)-Cl(1)	177.2(2)	C(29)-C(30)-H(30A)	109.5
C(1)-O(1)-C(3)	89.6(10)	C(29)-C(30)-H(30B)	109.5
C(1)-O(1)-Cr(1)	129.3(8)	H(30A)-C(30)-H(30B)	109.5
C(3)-O(1)-Cr(1)	127.6(7)	C(29)-C(30)-H(30C)	109.5
C(5)-O(2)-C(4)	127.0(19)	H(30A)-C(30)-H(30C)	109.5

C(18)-O(3)-Cr(1)	127.6(5)	H(30B)-C(30)-H(30C)	109.5
C(10)-O(4)-C(11)	118.8(8)	C(29)-C(31)-H(31A)	109.5
C(27)-O(5)-Cr(1)	128.1(6)	C(29)-C(31)-H(31B)	109.5
C(34)-O(6)-C(35)	113.8(8)	H(31A)-C(31)-H(31B)	109.5
C(7)-N(1)-C(24)	120.8(8)	C(29)-C(31)-H(31C)	109.5
C(7)-N(1)-Cr(1)	123.7(6)	H(31A)-C(31)-H(31C)	109.5
C(24)-N(1)-Cr(1)	115.2(6)	H(31B)-C(31)-H(31C)	109.5
C(25)-N(2)-C(19)	125.5(7)	C(29)-C(32)-H(32A)	109.5
C(25)-N(2)-Cr(1)	122.9(6)	C(29)-C(32)-H(32B)	109.5
C(19)-N(2)-Cr(1)	111.6(6)	H(32A)-C(32)-H(32B)	109.5
O(1)-C(1)-C(2)	94.5(8)	C(29)-C(32)-H(32C)	109.5
O(1)-C(1)-C(3)	45.2(5)	H(32A)-C(32)-H(32C)	109.5
C(2)-C(1)-C(3)	50.6(5)	H(32B)-C(32)-H(32C)	109.5
O(1)-C(1)-H(1A)	111.2	C(34)-C(33)-C(28)	123.8(11)
C(2)-C(1)-H(1A)	109.8	C(34)-C(33)-H(33)	118.1
C(3)-C(1)-H(1A)	111.9	C(28)-C(33)-H(33)	118.1
O(1)-C(1)-H(1B)	113.6	C(36)-C(34)-C(33)	118.6(10)
C(2)-C(1)-H(1B)	116.7	C(36)-C(34)-O(6)	128.5(10)
C(3)-C(1)-H(1B)	137.8	C(33)-C(34)-O(6)	112.8(10)
H(1A)-C(1)-H(1B)	110.2	O(6)-C(35)-H(35A)	109.5
C(6)-C(2)-C(1)	123.5(12)	O(6)-C(35)-H(35B)	109.5
C(6)-C(2)-C(3)	111.8(11)	H(35A)-C(35)-H(35B)	109.5
C(1)-C(2)-C(3)	78.9(9)	O(6)-C(35)-H(35C)	109.5
C(6)-C(2)-C(4)	91.3(12)	H(35A)-C(35)-H(35C)	109.5
C(1)-C(2)-C(4)	114.3(11)	H(35B)-C(35)-H(35C)	109.5
C(3)-C(2)-C(4)	141.5(13)	C(34)-C(36)-C(26)	122.2(9)
O(1)-C(3)-C(2)	94.4(8)	C(34)-C(36)-H(36)	118.9
		C(26)-C(36)-H(36)	118.9

Table B-19. Crystal Data and Structure Refinement for 5-Methoxy-methyl-5-methyl-1,3-dioxan-2-one.

Identification code	dtt-14	
Empirical formula	C7 H12 O4	
Formula weight	160.17	
Temperature	110(2) K	
Wavelength	1.54178 Å	
Crystal system	Monoclinic	
Space group	P2(1)/c	
Unit cell dimensions	a = 6.446(2) Å	α= 90°.
	b = 5.5780(19) Å	β= 101.943(19)°.
	c = 22.186(7) Å	γ = 90°.
Volume	780.4(4) $Å^3$	
Z	4	
Density (calculated)	1.363 Mg/m^3	
Absorption coefficient	0.950 mm^{-1}	
F(000)	344	
Crystal size	0.20 x 0.20 x 0.01 mm^3	
Theta range for data collection	7.02 to 57.98°.	
Index ranges	-7<=h<=7, -6<=k<=5, -24<=l<=23	
Reflections collected	4639	
Independent reflections	1023 [R(int) = 0.0762]	
Completeness to theta = 57.98°	94.00%	
Absorption correction	Semi-empirical from equivalents	
Max. and min. transmission	0.9953 and 0.8328	
Refinement method	Full-matrix least-squares on F_2	
Data / restraints / parameters	1023 / 0 / 101	
Goodness-of-fit on F_2	1.214	
Final R indices [I>2sigma(I)]	R1 = 0.1500, wR2 = 0.3127	
R indices (all data)	R1 = 0.1702, wR2 = 0.3205	
Extinction coefficient	0.019(4)	
Largest diff. peak and hole	0.554 and -0.455 $e.Å^{-3}$	

Table B-20. Bond Distances (Å) and Bond Angles (deg) for 5-Methoxy-methyl-5-methyl-1,3-dioxan-2-one.

O(1)-C(1)	1.357(12)	C(2)-C(3)-C(7)	108.2(9)
O(1)-C(4)	1.460(12)	C(4)-C(3)-C(7)	108.6(8)
O(2)-C(1)	1.322(13)	C(5)-C(3)-C(7)	110.8(8)
O(2)-C(2)	1.481(13)	O(1)-C(4)-C(3)	113.0(8)
O(3)-C(1)	1.187(12)	O(1)-C(4)-H(4A)	109
O(4)-C(5)	1.416(13)	C(3)-C(4)-H(4A)	109
O(4)-C(6)	1.418(13)	O(1)-C(4)-H(4B)	109
C(2)-C(3)	1.510(15)	C(3)-C(4)-H(4B)	109
C(2)-H(2A)	0.99	H(4A)-C(4)-H(4B)	107.8
C(2)-H(2B)	0.99	O(4)-C(5)-C(3)	110.7(9)
C(3)-C(4)	1.516(15)	O(4)-C(5)-H(5A)	109.5
C(3)-C(5)	1.529(14)	C(3)-C(5)-H(5A)	109.5
C(3)-C(7)	1.543(14)	O(4)-C(5)-H(5B)	109.5
C(4)-H(4A)	0.99	C(3)-C(5)-H(5B)	109.5
C(4)-H(4B)	0.99	H(5A)-C(5)-H(5B)	108.1
C(5)-H(5A)	0.99	O(4)-C(6)-H(6A)	109.5
C(5)-H(5B)	0.99	O(4)-C(6)-H(6B)	109.5
C(6)-H(6A)	0.98	H(6A)-C(6)-H(6B)	109.5
C(6)-H(6B)	0.98	O(4)-C(6)-H(6C)	109.5
C(6)-H(6C)	0.98	H(6A)-C(6)-H(6C)	109.5
C(7)-H(7A)	0.98	H(6B)-C(6)-H(6C)	109.5
C(7)-H(7B)	0.98	C(3)-C(7)-H(7A)	109.5
C(7)-H(7C)	0.98	C(3)-C(7)-H(7B)	109.5
C(1)-O(1)-C(4)	121.7(8)	H(7A)-C(7)-H(7B)	109.5
C(1)-O(2)-C(2)	121.2(8)	C(3)-C(7)-H(7C)	109.5
C(5)-O(4)-C(6)	111.4(8)	H(7A)-C(7)-H(7C)	109.5
O(3)-C(1)-O(2)	122.0(10)	H(7B)-C(7)-H(7C)	109.5
O(3)-C(1)-O(1)	118.3(10)	C(3)-C(2)-H(2B)	109.4
O(2)-C(1)-O(1)	119.7(9)	H(2A)-C(2)-H(2B)	108
O(2)-C(2)-C(3)	111.1(8)	C(2)-C(3)-C(4)	105.6(8)
O(2)-C(2)-H(2A)	109.4	C(2)-C(3)-C(5)	111.8(9)
C(3)-C(2)-H(2A)	109.4	C(4)-C(3)-C(5)	111.6(9)
O(2)-C(2)-H(2B)	109.4		

VITA

Adriana Inez Moncada received her Bachelor of Science degree in chemical engineering from La Universidad del Zulia at Maracaibo, Venezuela in 2001. In 2005 she received her masters's degree in chemistry from Oklahoma State University. She entered the chemistry doctoral program at Texas A&M University in August of 2005, and received her Ph.D degree in May 2010. Her research interests include homogeneous catalysis, inorganic, and polymer chemistry.

Questions and comments may be directed to Texas A&M University, Department of Chemistry, MS 3255, College Station, TX 77842-3012.